

**Root-Endophytic *Trichoderma* Fungi: Combinations with  
Rhizobacteria to Enhance Induced Systemic Resistance (ISR)  
against *Verticillium longisporum* in Rapeseed**

Dissertation

for the degree of  
Doctor of Natural Sciences (Dr. rer. nat.)

Submitted to the  
Faculty of Natural Sciences I  
Institute of Biology  
Martin Luther University,  
Halle-Wittenberg

Presented by:  
Fatema Binte Hafiz  
Born on 10.02.1989 in Meherpur (Bangladesh)

The experimental works were performed, and this dissertation was written under the supervision of Dr. Jörg Geistlinger and Prof. Dr. Wilfried Rozhon in Department of Agriculture, Ecotrophology, and Landscape Development, Anhalt University of Applied Sciences, Bernburg, Germany in the frame of Determinants of Plant Performance, International Graduate Schools in Agricultural and Polymer Sciences (AGRIPOLY), Martin Luther University, Halle-Wittenberg.

Supervisor: Prof. Dr. Wilfried Rozhon

Co-supervisor: Prof. Dr. Klaus Humbeck

Reviewer: Prof. Dr. Günter Neumann

Defended on

27.02.2023

All the results of the presented work were obtained during this study and partial results and part of the abstract, introduction and discussion have already been published in the following manuscript:

**Hafiz, F. B.,** Moradtalab, N., Goertz, S., Rietz, S., Dietel, K., Rozhon, W., Humbeck, K., Geistlinger, J., Neumann, G., and Schellenberg, I. 2022. Synergistic effects of a root-endophytic *Trichoderma* fungus and *Bacillus* on early root colonization and defense activation against *Verticillium longisporum* in rapeseed. *Mol. Plant Microbe Interact.* 35:380-392.

## Abstract

Rhizosphere-competent microbes frequently interact with plant roots and exhibit beneficial effects on plant performance. Numerous bacterial and fungal isolates are able to prime host plants for fast adaptive responses against pathogen attacks. Combined action of fungi and bacteria may lead to synergisms exceeding effects of single strains. Individual beneficial fungi and bacteria have been extensively studied in *Arabidopsis thaliana*, but little is known about their concerted actions in the economically important Brassicaceae. Here, an *in-vitro* system with oilseed rape (*Brassica napus*) was established. Roots of two different cultivars were inoculated with well-characterized fungal (*Trichoderma harzianum* OMG16) and bacterial (*Bacillus velezensis* FZB42) isolates individually or in combination. Microscopic analysis confirmed that OMG16 hyphae entered root hairs through root hair tips and formed distinct intracellular structures. Quantitative PCR revealed that root colonization of OMG16 increased up to 10-fold in the presence of FZB42. Effects of OMG16 and FZB42 synergism on root growth and morphology was analysed using the WinRhizo image analysis system. Increased root lengths, dry weight, root volume, and fine-root lengths were documented, mainly at the early timepoints. Relative transcript levels of the ethylene- and jasmonic acid-responsive genes *PDF1.2*, *ERF2*, and *AOC3* were observed in leaves by quantitative reverse transcription PCR to measure induced systemic resistance in tissues distant from the roots. Combined action of OMG16 and FZB42 induced transcript abundances more efficiently than single inoculation. Importantly, microbial priming reduced *Verticillium longisporum* root infection in rapeseed by approximately 100-fold compared with non-primed plants. Systemic induction of JA biosynthesis genes *LOX2*, *AOC3* and *OPR3*; ET biosynthesis and signalling genes *ACS2*, *ACO4* and *ERF2*; JA/ET marker genes *PDF1.2* and *VSP2*; SA biosynthesis and signalling genes *ICS1* and *PRI* were analysed in leaves by qRT-PCR. In addition, the relative expression of *AOC3*, *OPR3*, *ACS2*, *ACO4*, *ICS1* and *PRI* were also analysed separately in leaf, stem and root tissues. To successfully colonize the rapeseed roots, the V143 pathogen suppressed the biosynthesis of JA, ET and SA hormones in the non-primed plants. Priming led to faster and stronger systemic responses of the JA, ET and SA biosynthesis and signalling pathways individually in leaves, stems and roots compared to the non-primed plants. Moreover, the endogenous amounts of JA and SA hormones were quantified in root and shoot (leaf and stem) tissues of both V143 infected primed and non-primed plants with UHPLC-MS. 1.7 and 2.6-fold increase of JA and SA were recorded in shoots of primed plants, respectively. In roots, endogenous JA and SA levels increased up to 3.9 and 2.3-fold in V143 infected primed plants compare to the non-primed plants.

Taken together, this data indicate that microbial priming stimulates rapeseed defence responses against *Verticillium* infection and transduces the defence signals from the root to the upper parts of the plant by phytohormone signalling.

## Table of contents

<b>Abstract</b> .....	<b>III</b>
<b>List of figures</b> .....	<b>IX</b>
<b>List of tables</b> .....	<b>XII</b>
<b>1. Introduction</b> .....	<b>1</b>
1.1.Plant beneficial fungi.....	1
1.2.Plant beneficial rhizobacteria.....	2
1.3.Origin and cultivation of <i>Brassica napus</i> .....	4
1.4.Rapeseed disease caused by plant pathogen <i>Verticillium longisporum</i> .....	5
1.5.Rapeseed response to <i>V. longisporum</i> infection-when plants make a counterattack	6
1.6.Plant immune response mechanism against pathogen attack.....	7
1.7.Phytohormones in plant defence.....	9
1.7.1. ET biosynthesis.....	10
1.7.2. JA biosynthesis.....	12
1.7.3. SA biosynthesis.....	13
1.8.JA, ET and SA signal transduction.....	15
1.8.1. ET signalling.....	15
1.8.2. JA signalling.....	16
1.8.3. SA signalling.....	17
1.9.Crosstalk among JA, ET and SA signalling pathways.....	18
1.10.    Aim of the thesis.....	21
<b>2. Materials and methods</b> .....	<b>22</b>
2.1.Plant materials.....	22
2.1.1. <i>B. napus</i> seed sterilization.....	23
2.1.2. Plant beneficial fungal isolates.....	24
2.1.3. Fungal growth conditions.....	24
2.1.4. Plant beneficial bacteria.....	25
2.1.5. Bacterial culture and growth condition.....	25
2.1.6. Microbial inoculation and plant growth conditions.....	25
2.2.Microscopy.....	26
2.2.1. Root staining with fuchsine red solution.....	26
2.2.2. Transformation of fluorescence genes into <i>Trichoderma</i> protoplasts..	27
2.2.2.1.pBARGPE1-Hygro-EGFP plasmid.....	27
2.2.2.1.1. Stock solution of pBARGPE1-Hygro-EGFP plasmid.....	28

2.2.2.1.2. Working solution of pBARGPE1-Hygro-EGFP plasmid.....	28
2.2.2.1.3. Transformation of competent <i>E. coli</i> cells.....	28
2.2.2.1.4. Colony PCR of <i>E. coli</i> DH5 $\alpha$ /pBARGPE1-Hygro-EGFP transformants	28
2.2.2.1.5. Mini preparation of plasmid DNA.....	30
2.2.2.2.pCAMDsRed plasmid.....	31
2.2.2.2.1. Colony PCR of <i>E. coli</i> K-12/pCAMDsRed.....	31
2.2.2.2.2. Isolation of pCAMDsRed plasmid DNA.....	32
2.2.2.3.Preparation of <i>Trichoderma</i> protoplasts.....	33
2.2.2.4.PEG-mediated transformation of <i>Trichoderma</i> protoplasts.....	34
2.2.2.5.Confirming the stability of the transformants by PCR.....	34
2.3.Molecular-standard techniques.....	35
2.3.1. Isolation of genomic DNA from plants.....	35
2.3.2. Isolation of genomic DNA from fungi.....	35
2.3.3. Isolation of genomic DNA from bacteria.....	37
2.3.4. Agarose gel electrophoresis.....	38
2.3.5. Gel and PCR clean-up.....	38
2.3.6. DNA quantification.....	39
2.4.Primer design.....	39
2.4.1. Primers for <i>FZB42</i> specific, <i>AOC3</i> and <i>ERF2</i> genes.....	39
2.4.2. Primers for <i>BnaUbiquitin11</i> , <i>VSP2</i> , <i>OPR3</i> and <i>ICS1</i> genes.....	39
2.4.3. Molecular marker of OMG16 DNA.....	40
2.5.Quantification of OMG16 and FZB42 root colonization by qPCR.....	40
2.6.Determination of extracellular pH.....	41
2.7.Observation of root morphology.....	42
2.8.Gene expression studies upon beneficial microbial treatments by qRT-PCR...	42
2.8.1. Isolation of RNA.....	42
2.8.2. RNA quantification.....	43
2.8.3. First-strand cDNA synthesis reaction.....	44
2.8.4. Quantification of cDNA concentration.....	44
2.8.5. Touchdown and gradient PCR.....	44
2.8.6. Determination of amplification efficiencies of primers.....	45
2.8.7. Quantitative reverse transcription PCR (qRT-PCR).....	47
2.8.8. Validation of reference genes.....	48
2.8.9. Calculation of relative transcript abundances.....	49

2.9.Challenging rapeseed roots with pathogen.....	49
2.9.1. Fungal pathogen.....	49
2.9.2. Infection of rapeseed roots with V143.....	50
2.9.3. Staining infected rapeseed leaf tissue with royal blue dye.....	51
2.9.4. Quantification of V143 DNA.....	51
2.9.5. Relative expression of defence related genes after V143 infection.....	52
2.10. Determination of phytohormones by UHPLC-MS analysis.....	52
2.11. Statistical analysis.....	53
2.12. Reagents.....	54
2.12.1. Primers.....	54
2.12.2. Buffer and solutions.....	55
2.12.3. Media.....	55
<b>3. Results.....</b>	<b>56</b>
3.1.Chapter I: Inoculation of rapeseed roots with plant beneficial fungi and bacterium and analysis of subsequent defence activation.....	56
3.1.1. Microscopic observation of root/fungus interactions.....	56
3.1.1.1.Interaction of <i>T. harzianum</i> OMG16 and rapeseed.....	56
3.1.1.2.Interaction of <i>T. virens</i> M9B and rapeseed.....	57
3.1.1.3.Expression of fluorescence proteins in <i>Trichoderma</i> fungi.....	58
3.1.2. Synergistic effects of fungus and bacterium.....	59
3.1.2.1.Enhanced fungal root colonization rate in presence of <i>B. velezensis</i> FZB42	60
3.1.2.2.Medium acidification caused by microbes.....	61
3.1.2.3.Enhanced bacterial root colonization rate in presence of <i>T. harzianum</i> OMG16.....	61
3.1.3. Effects of synergism on root morphology and growth.....	62
3.1.4. Relative expression of rapeseed defence-related genes after OMG16 and FZB42 treatments.....	64
3.2.Chapter II: Pathogen challenge and analysis of defence activation upon priming.	67
3.2.1. Infection of rapeseed roots with <i>V. longisporum</i> 43.....	67
3.2.2. Synergism of OMG16 and FZB42 reduced <i>V. longisporum</i> V143 root colonization	
3.2.3. Enhanced rapeseed defence upon priming.....	68
3.2.3.1.Expression of defence related genes in roots.....	69
3.2.3.1.1. JA biosynthesis genes.....	69
3.2.3.1.2. ET biosynthesis genes .....	71



3.2.3.1.3. SA biosynthesis and signalling genes.....	72
3.2.3.2.Expression of defence related genes in stems.....	74
3.2.3.2.1. JA biosynthesis genes.....	74
3.2.3.2.2. ET biosynthesis genes.....	76
3.2.3.2.3. SA biosynthesis and signalling genes.....	77
3.2.3.3.Expression of defence related genes in leaves.....	79
3.2.3.3.1. JA biosynthesis genes.....	79
3.2.3.3.2. ET biosynthesis and signalling genes.....	81
3.2.3.3.3. JA/ET marker genes.....	83
3.2.3.3.4. SA biosynthesis and signalling genes.....	85
3.2.4. Determination of stress-related phytohormonal homeostasis.....	86
3.2.4.1.Phytohormone contents in root tissue.....	86
3.2.4.2.Phytohormone contents in shoot tissue.....	88
<b>4. Discussion.....</b>	<b>90</b>
4.1.Interaction between rapeseed roots and <i>Trichoderma</i> .....	90
4.2.Effects of synergism on <i>Trichoderma</i> root colonization abundance.....	92
4.3.Effects of synergism on root morphology and growth.....	92
4.4.Effects of synergism on the expression of defence-related rapeseed genes in cv. AgP1 and AgP4.....	93
4.5.Priming effects on <i>V. longisporum</i> root infection in cv. AgP4.....	96
4.6.Priming effects on rapeseed enhanced defence activation after V143 pathogen challenge.....	97
4.6.1. Priming effects on roots.....	98
4.6.2. Priming effects on stems.....	100
4.6.3. Priming effects on leaves.....	100
<b>5. Conclusion.....</b>	<b>103</b>
<b>6. References.....</b>	<b>105</b>
<b>7. Appendix.....</b>	<b>136</b>
<b>Acknowledgements.....</b>	<b>154</b>
<b>Curriculum Vitae.....</b>	<b>155</b>
<b>Publications.....</b>	<b>156</b>
<b>Declaration.....</b>	<b>157</b>

## List of figures

Figure 1:	Schematic representation of FZB42 mediated biocontrol activities in plant rhizosphere.....	4
Figure 2:	Life cycle of <i>V. longisporum</i> in rapeseed.....	6
Figure 3:	Schematic representation depicting the mechanisms of SAR and ISR systems.....	9
Figure 4:	Ethylene biosynthesis and regulation pathway in plants.....	11
Figure 5:	Octadecanoid pathway for JA biosynthesis and metabolism.....	13
Figure 6:	The biosynthesis pathway of SA in plants.....	14
Figure 7:	Pathway of ET signalling cascade.....	15
Figure 8:	JA signal transduction pathway.....	17
Figure 9:	SA signal transduction in plants.....	18
Figure 10:	Schematic representation of the crosstalk among ET, JA and SA phytohormones signalling pathways at the transcriptional level.....	20
Figure 11:	Infection of rapeseed varieties AgP1 and AgP4 with <i>V. longisporum</i> 43 in the greenhouse.....	23
Figure 12:	20-day-old <i>T. harzianum</i> OMG16 (a) and <i>T. virens</i> M9B (b) fungal strains grown on PDA plates.....	25
Figure 13:	Experimental setup for inoculation of <i>B. napus</i> plantlets.....	26
Figure 14:	pBARGPE1-Hygro-EGFP plasmid map.....	27
Figure 15:	pCAMDsRed plasmid map.....	31
Figure 16:	Microscopic appearance of <i>in vitro</i> <i>Verticillium longisporum</i> 43 conidia..	50
Figure 17:	Intracellular interactions between <i>T. harzianum</i> OMG16 and rapeseed...	57
Figure 18:	Intracellular interactions between <i>T. virens</i> M9B and rapeseed.....	58
Figure 19:	Quantification of OMG16 in total root DNA.....	60
Figure 20:	Acidification of plant growth medium due to the presence of OMG16, FZB42 and OMG16 plus FZB42.....	61
Figure 21:	Quantification of <i>B. velezensis</i> FZB42 DNA in two-week-old rapeseed roots from AgP1 (left) and AgP4 (right) cultivars inoculated with FZB42 and FZB42 plus OMG16. ....	62
Figure 22:	Effects of OMG16 and FZB42 inoculation on root development.....	64
Figure 23:	Relative expression of rapeseed defence genes <i>PDF1.2</i> , <i>ERF2</i> and <i>AOC3</i> upon OMG16, FZB42 and OMG16 plus FZB42 inoculation.....	66
Figure 24:	Interactions between <i>V. longisporum</i> 43 and rapeseed.....	67

Figure 25:	Priming with OMG16 and FZB42 enhances the resistance of <i>B. napus</i> cv. AgP4 against infection with <i>V. longisporum</i> .....	68
Figure 26:	Relative expression of rapeseed defence genes <i>LOX2</i> (a) and <i>OPR3</i> (b) in roots upon OMG16 plus FZB42 plus V143 and V143 inoculation alone...	70
Figure 27:	Relative expression of rapeseed defence genes <i>ACS2</i> (a) and <i>ACO4</i> (b) in roots upon OMG16 plus FZB42 plus V143 and V143 inoculation alone...	72
Figure 28:	Relative expression of rapeseed defence genes <i>ICS1</i> (a) and <i>PRI</i> (b) in roots upon OMG16 plus FZB42 plus V143 and V143 inoculation alone.....	73
Figure 29:	Relative expression of rapeseed defence genes <i>LOX2</i> (a) and <i>OPR3</i> (b) in stems upon OMG16 plus FZB42 plus V143 and V143 inoculation alone..	75
Figure 30:	Relative expression of rapeseed defence genes <i>ACS2</i> (a) and <i>ACO4</i> (b) in stems upon OMG16 plus FZB42 plus V143 and V143 inoculation alone..	77
Figure 31:	Relative expression of rapeseed defence genes <i>ICS1</i> (a) and <i>PRI</i> (b) in stems upon OMG16 plus FZB42 plus V143 and V143 inoculation alone..	78
Figure 32:	Relative expression of rapeseed defence genes <i>LOX2</i> (a), <i>AOC3</i> (b) and <i>OPR3</i> (c) in leaves upon OMG16 plus FZB42 plus V143 and V143 inoculation alone.....	80
Figure 33:	Relative expression of rapeseed defence genes <i>ACS2</i> (a), <i>ACO4</i> (b) and <i>ERF2</i> (c) in leaves upon OMG16 plus FZB42 plus V143 and V143 inoculation alone.....	82
Figure 34:	Relative expression of rapeseed defence genes <i>PDF1.2</i> (a) and <i>VSP2</i> (b) in leaves upon OMG16 plus FZB42 plus V143 and V143 inoculation alone.....	84
Figure 35:	Relative expression of rapeseed defence genes <i>ICS1</i> (a) and <i>PRI</i> (b) in leaves upon OMG16 plus FZB42 plus V143 and V143 inoculation alone.	85
Figure 36:	Endogenous concentration of JA (a) and SA (b) phytohormones in root tissue of rapeseed plants at different time points upon OMG16 plus FZB42 plus V143 and V143 inoculation alone.....	87
Figure 37:	Endogenous concentration of JA (a) and SA (b) phytohormones in shoot tissue of rapeseed plants at different time points upon OMG16 plus FZB42 plus V143 and V143 inoculation alone.....	88
Figure 38:	Simplified model of molecular mechanisms involved in rapeseed defence signalling modulated by crosstalk between the ET and JA hormonal	

pathways in response to *Trichoderma*-rapeseed interaction and  
*Trichoderma-Bacillus*-rapeseed synergism..... 95

Figure 39: Schematic representation of molecular mechanisms involved in rapeseed  
defence signalling from root-stem-leaf modulated by crosstalk among the  
SA, ET and JA hormonal pathways in response to *Verticillium*-rapeseed  
interaction and *Trichoderma-Bacillus-Verticillium*-rapeseed priming..... 103

## List of tables

Table 1:	Components for colony PCR of <i>E. coli</i> DH5 $\alpha$ /pBARGPE1-Hygro-EGFP.	29
Table 2:	Cycling instructions for colony PCR of <i>E. coli</i> DH5 $\alpha$ /pBARGPE1-Hygro-EGFP.....	29
Table 3:	Components for colony PCR of <i>E. coli</i> K-12/pCAMDsRed.....	31
Table 4:	Cycling instructions for colony PCR of <i>E. coli</i> K-12/pCAMDsRed.....	32
Table 5:	Components for qPCR reaction.....	40
Table 6:	Cycling instructions for qPCR.....	41
Table 7:	Components for annealing primers to template RNA.....	44
Table 8:	Components for preparing reverse transcription reaction mix.....	44
Table 9:	Components for touchdown and gradient PCRs.....	45
Table 10:	Cycling instructions for gradient PCR.....	45
Table 11:	Components for PCR.....	46
Table 12:	Cycling instructions for PCR.....	46
Table 13:	Components for qRT-PCR reaction.....	47
Table 14:	Cycling instructions for qRT-PCR.....	47
Table 15:	List of the primers of reference genes used in this study.....	48
Table 16:	Components for qPCR reaction for V143 quantification.....	51
Table 17:	Cycling instructions for qPCR to quantify V143 DNA.....	52
Table 18:	List of primers used in this study.....	54

## 1. Introduction

Rhizosphere microbiomes play crucial roles in plant growth and health by improving nutrient mobilization and acquisition, exhibiting plant growth-promoting properties, enhancing plant tolerance to biotic and abiotic stresses, possessing antagonistic effects on phytopathogens and inducing plant defence-related genes (Berg et al. 2016; Mendes et al. 2011). Diverse plant growth-promoting fungi (Coleman-Derr et al. 2016; Rodriguez et al. 2009) and bacteria (Kloepper et al. 1980), dwelling in the rhizospheres, can enhance plant yield and protect against a broad spectrum of pathogenic microbes by stimulating plant defence system (Zhang et al. 2018).

### 1.1. Plant beneficial fungi

The root-associated, non-pathogenic fungi possess the ability to colonize the host roots, solubilize phosphates and generate secondary metabolites such as, auxin, siderophore, cellulase and chitinase which directly or indirectly enhance plant growth and development (Coleman-Derr et al. 2016; Jogaiah et al. 2013; Muslim et al. 2019; Rodriguez et al. 2009, Zhang et al. 2018). Many of those plant growth-promoting fungi are known to stimulate the innate plant immune system against a wide range of pathogens (Alkooranee et al. 2015; Heil and Bostock, 2002; Lee et al. 2012; Naznin et al. 2014). To inhibit the pathogen invasion, plants undergo fungal induced cell wall modification and activation of defence related enzymes such as phenylalanine ammonia-lyase (PAL), peroxidases (POX), chitinase and  $\beta$ -1,3 glucanase (Hassan et al. 2014; Hossain et al. 2017; Sindhu et al. 2018; Zhou et al. 2018). Thus, regular application of the beneficial fungi in biological plant protection can be an efficient way to reduce the use of chemical pesticides (Carreras-Villasenor et al. 2012; Harman et al. 2012; Hermosa et al. 2012; Mastouri et al. 2010; Perazzolli et al. 2008; Ryder et al. 2012; Salas-Marina et al. 2011).

*Trichoderma* isolates (Ascomycota) are extensively used as plant beneficial fungi because of their versatile abilities to stimulate induced systemic resistance (ISR) by modulating biosynthesis of numerous signalling molecules and hormones including jasmonic acid (JA), ethylene (ET), and salicylic acid (SA) (Alkooranee et al. 2015; Brotman et al. 2013; Hermosa et al. 2012; Naznin et al. 2014). A number of *Trichoderma* strains have also been shown to enter root cells and develop an avirulent plant endo-symbiotic relationship (Geistlinger et al. 2015; Harman et al. 2004; Tucci et al. 2011). Due to the ability to form intracellular structures, some *Trichoderma* strains are categorized as root-endophytes (Hoyos-Carvajal et al. 2009). Mutualistic characteristics of *Trichoderma* have already been detected in a large number of plants including *A. thaliana* (Alonso-Ramírez et al. 2015), cucumber (Meng et al. 2019), tomato

(Coppola et al. 2019; Khoshmanzar et al. 2020), rapeseed (Poveda et al. 2019) and some woody plants (Carro-Huerga et al. 2020).

*Trichoderma harzianum*, a well-characterized fungus in the genus *Trichoderma*, is able to colonize the plant roots intercellularly and intracellularly. This fungus is widely distributed in nature and can activate the microbe associated molecular patterns (MAMPs)-triggered immunity (MTI) and effector-triggered immunity (ETI) as well as reduce the effector-triggered susceptibility (ETS) in plants (Harman et al. 2004; Lorito et al. 2010; Mukherjee et al. 2013; Sharma et al. 2017). Therefore, *T. harzianum* is extensively used in agriculture as plant disease suppressor against a broad spectrum of fungal and bacterial pathogens (De Palma et al. 2019; Harman et al. 2004; Singh et al. 2019).

## **1.2. Plant beneficial rhizobacteria**

Besides plant-growth-promoting fungi, plant rhizospheres also harbour communities of plant-growth-promoting rhizobacteria (Kloepper et al. 1980; Windisch et al. 2021) with the ability to promote plant growth and suppress pathogens by means of direct antagonism or indirectly affecting pathogens via stimulating ISR (Chowdhury et al. 2015a; Doornbos et al. 2012). Numerous rhizobacteria are able to enhance the root colonization ability of symbiotic fungi by synergistic interactions (Frey-Klett et al. 2007). *Bacillus velezensis* FZB42 syn. *B. amyloliquefaciens* subsp. *plantarum* FZB42, a well-studied gram-positive rhizobacterium, protects the plants against a broad spectrum of phytopathogens through its biocontrol activities and thereby enhances crop yields and productivity (Fan et al. 2018). This aerobic-endospore-forming rhizobacterium (Borriss et al. 2011) can trigger defence responses against *Phytophthora nicotianae* infection in *Nicotiana benthamiana* leaves by activating expression of the JA biosynthesis gene *LOX*, the ethylene-responsive transcription factor *ERF1* and the SA-regulated pathogen-related gene *PR-1a* (Wu et al. 2018). Sarosh et al. (2009) demonstrated enhanced expression of JA/ET marker gene, *plant defencing factor 1.2* (*PDF1.2*) upon *B. velezensis* mediated ISR in oilseed rape against *Botrytis cinerea*. Also, in lettuce plant, FZB42 induced *PDF1.2* expression through the activation of JA/ET pathway and suppressed SA pathway by decreasing *PR1* expression in response to *Rhizoctonia solani* infection (Chowdhury et al. 2015b). The reported responses of plants primed with *Bacillus* include stimulation of resistance gene transcripts, disease suppression as well as increased root biomass.

The root-endophytic nature of FZB42 was confirmed using a GFP-labelled strain (Fan et al. 2011, 2012). Complete genome sequence disclosed that as much as 8.5% FZB42 genome is dedicated in synthesis of antimicrobial metabolites mediated by non-ribosomal pathways and their corresponding immunity genes (Chen et al. 2007; Chowdhury et al. 2015a). Several *in*

*in vitro* studies reported that the cyclic lipopeptide bacillomycin D and fengycin showed antifungal activities (Koumoutsi et al. 2004) while polyketides (Chen et al. 2006), and bacilysin (Chen et al. 2009), and ribosomally synthesized bacteriocins (Scholz et al. 2011, 2014) possessed antibacterial activities. Nine giant gene clusters have been detected that are involved in synthesis of bioactive non-ribosomal peptides (NRPs) and polyketides with biocontrol and plant-growth-promoting activities. Non-ribosomally synthesized lipopeptides utilized by FZB42 to defend against phytopathogens in the plant rhizosphere include surfactin, fengycin, bacillomycin D, dipeptide bacilysin and the Fe<sup>2+</sup> siderophore bacillibactin. Membrane-bound polyketide-megasynthases (PKS-MS) catalyse the synthesis of antibacterial polyketides bacillaene, macrolactin and difficidin. Upon colonizing the plant roots, bacillibactin and the nrs-encoded peptide of FZB42 deprive the essential iron of bacterial and fungal pathogens while antimicrobial lipopeptides and polyketides directly inhibit the growth of these pathogens (Chen et al. 2007). Among them, bacillomycin D and difficidin are respectively reported to be the most effective antifungal and antibacterial metabolites generated by FZB42. For instance, FZB42 produced excessive amount of bacillomycin D in response to *R. solani* in axenic system which indicates to the ability of this bacterium to recognize and response to fungal pathogen by antibiosis effects (Chowdhury et al. 2015b). Gu et al. 2017 reported that bacillomycin D generated by FZB42 suppresses the reactive oxygen species (ROS) scavenging genes, which leads to increased deposition of ROS and results in cell death of *Fusarium graminearum* hyphae and conidia. On the other hand, FZB42 secreted difficidin inhibits the growth of fire blight causing pathogenic bacterium *Erwinia amylovora* in apple trees (Chen et al. 2009). FZB42 showed direct antagonistic effects against *R. solani* by generating fengycin, surfactin and bacillomycin D in the rhizosphere of lettuce plant which in turn activated the plant defence responses by enhancing the expression of *PDF1.2* (Chowdhury et al. 2015a). In *A. thaliana* seedlings, surfactin and microbial volatile organic compounds (mVOCs), particularly 2,3-butanediol and acetoin (3-hydroxy-2-butanone) produced by FZB42 showed plant growth promotion and ISR activities (Ryu et al. 2003).

Taken together, it is demonstrated that antimicrobial metabolites, mVOCs, and secondary metabolites secreted by FZB42 in the rhizosphere trigger the onset of plant ISR priming system, which is reported to be the main mechanism for FZB42 mediated biocontrol actions (Fig. 1) (Chowdhury et al. 2015a).



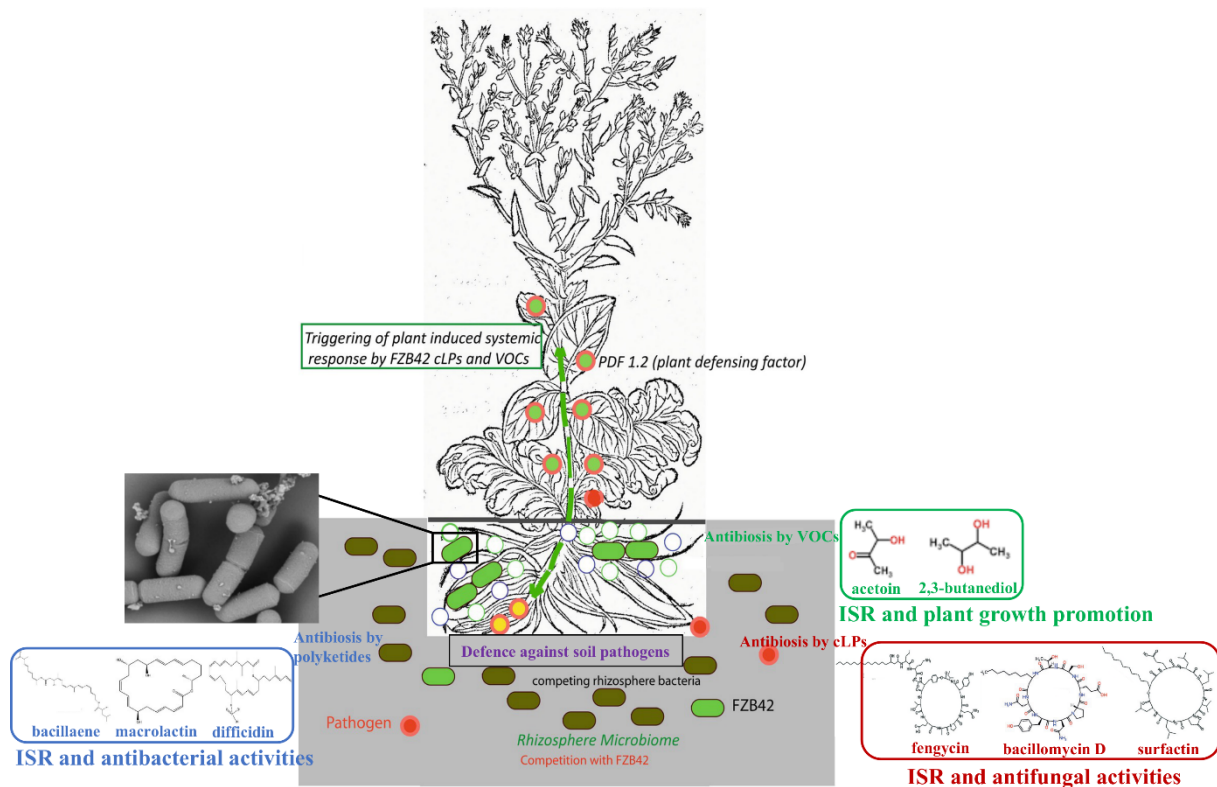


**Fig. 1.** Schematic representation of FZB42 mediated biocontrol activities in plant rhizosphere. After successful colonization of plant roots, FZB42 generates VOCs (e.g., acetoin, 2,3-butanediol) with ISR and plant growth promotion activities (marked in green); cyclic lipopeptides (e.g., fengycin, bacillomycin D, surfactin) with ISR and antifungal activities (marked in red) and polyketides with ISR and antibacterial activities (marked in blue). (Picture modified from Chowdhury et al. 2015a; Mácha et al. 2021; Rabbee et al. 2019).

### 1.3. Origin and cultivation of *Brassica napus*

Originating by spontaneous inter-specific hybridization events between *Brassica rapa* (AA = 20) and *Brassica oleracea* (CC = 18) from ~1910-7180 years ago, *Brassica napus* (AACC = 38) is one of the earliest allotetraploid crops. Rapeseed, belonging to the Brassicaceae plant family, was first cultivated in Europe as winter oilseed rape (An et al. 2019; Chalhoub et al. 2014; Lu et al. 2019). In the last decades, oilseed rape has been extensively cultivated worldwide because of its growing importance as feedstock for edible oil, forage crop and source for renewable energy (Rybakova et al. 2017). In 2022, rapeseed plants are being cultivated in 5.74 million hectares of land in European Union aiming to produce 17.98 million tonnes of rapeseed (European Commission, 2022). Whilst in autumn 2021, Germany sowed winter oilseed rape in 1.1 million hectares of land to produce 3.9 million tonnes of rapeseed for the 2022 harvest ([https://www.destatis.de/EN/Press/2021/12/PE21\\_597\\_41241.html](https://www.destatis.de/EN/Press/2021/12/PE21_597_41241.html)).

#### 1.4. Rapeseed disease caused by plant pathogen *Verticillium longisporum*

The soil-borne fungal pathogen *Verticillium longisporum* (C. Stark) from Ascomycota phylum can cause massive yield losses in rapeseed (Depotter et al. 2016; Karapapa et al. 1997). *V. longisporum* is an amphidiploid hybrid that originated from four different ancestors by interspecific hybridization. It has a very restricted host range that mainly comprises Brassicaceae crops (Leonard et al. 2020; Novakazi et al. 2015). Developing from the clusters of melanised, thick-walled fungal cells called microsclerotia, *V. longisporum* hyphae enter the host root system, preferentially via root hairs (Depotter et al. 2016; Taylor et al. 2022) and subsequently colonize the root cortex and enter the xylem. Afterwards, hyphae spread through the vascular system via the transpiration stream (Eynck et al. 2007) or by penetrating the pit membranes and the adjacent vessel membrane walls (Garber and Houston, 1966). Such colonization of vascular system by *V. longisporum* hyphae results blockage of the vessels which causes obstruction of sap stream in the xylem (Kamble et al. 2013). During senescence, hyphae enter the stem parenchyma from xylem vessel and eventually complete their life cycle by forming microsclerotia on stem cortex beneath the epidermis and foliar tissues (Depotter et al. 2016; Wilhelm, 1955). After decomposition of plant debris, microsclerotia enter the soil and reside to start new infection cycle upon the availability of suitable environmental conditions (Fig. 2). There is no evidence for spreading of *V. longisporum* by seed transmission so far (Depotter et al. 2016).

At the initial disease stage, dark unilateral stripes become visible on the stem of healthy plant at the late growing season due to the cortical tissue necrosis caused by *V. longisporum* (Heale and Karapapa, 1999). While in later stage, microsclerotia are generated in the stem cortex. Disease symptoms develop with the increasing amount of pathogen colonized rapeseed root and shoot tissues (Dunker et al. 2008). Typical wilting symptoms are not visible on rapeseed, rather *V. longisporum* induced stem striping appears upon infection. Although, it is difficult to distinguish the disease symptoms from the natural senescence due to the premature crop ripening caused by *V. longisporum* (Depotter et al. 2016).

The infestation by this soil-borne pathogen is vastly devastating in all Brassicaceae and hard to eradicate by conventional fungicides (Depotter et al. 2016). Resistance breeding is also not possible as no sufficient resistance (R) gene against *V. longisporum* has yet been identified. However, useful genetic resources, responsible in decreasing the susceptibility of brassicaceous plants to *V. longisporum* infection, was found. For example, Enhancer of vascular Wilt Resistance 1 (EWR1) protein, only identified within the Brassicaceae family (Yadeta et al. 2014), increases the resistance of *A. thaliana* against *V. longisporum* infestation (Yadeta et al.

2011, 2014). However, no monogenic resistance has been yet detected against *V. longisporum*. While quantitative resistance exists mainly in the C-genome of parental *B. oleracea* lines where three quantitative trait loci (QTLs) that notably correlate with *V. longisporum* resistance were identified (Obermeier et al. 2013). Therefore, this is in high importance to look for alternative, cost-effective and efficient strategies to control the *V. longisporum* infection in rapeseed.

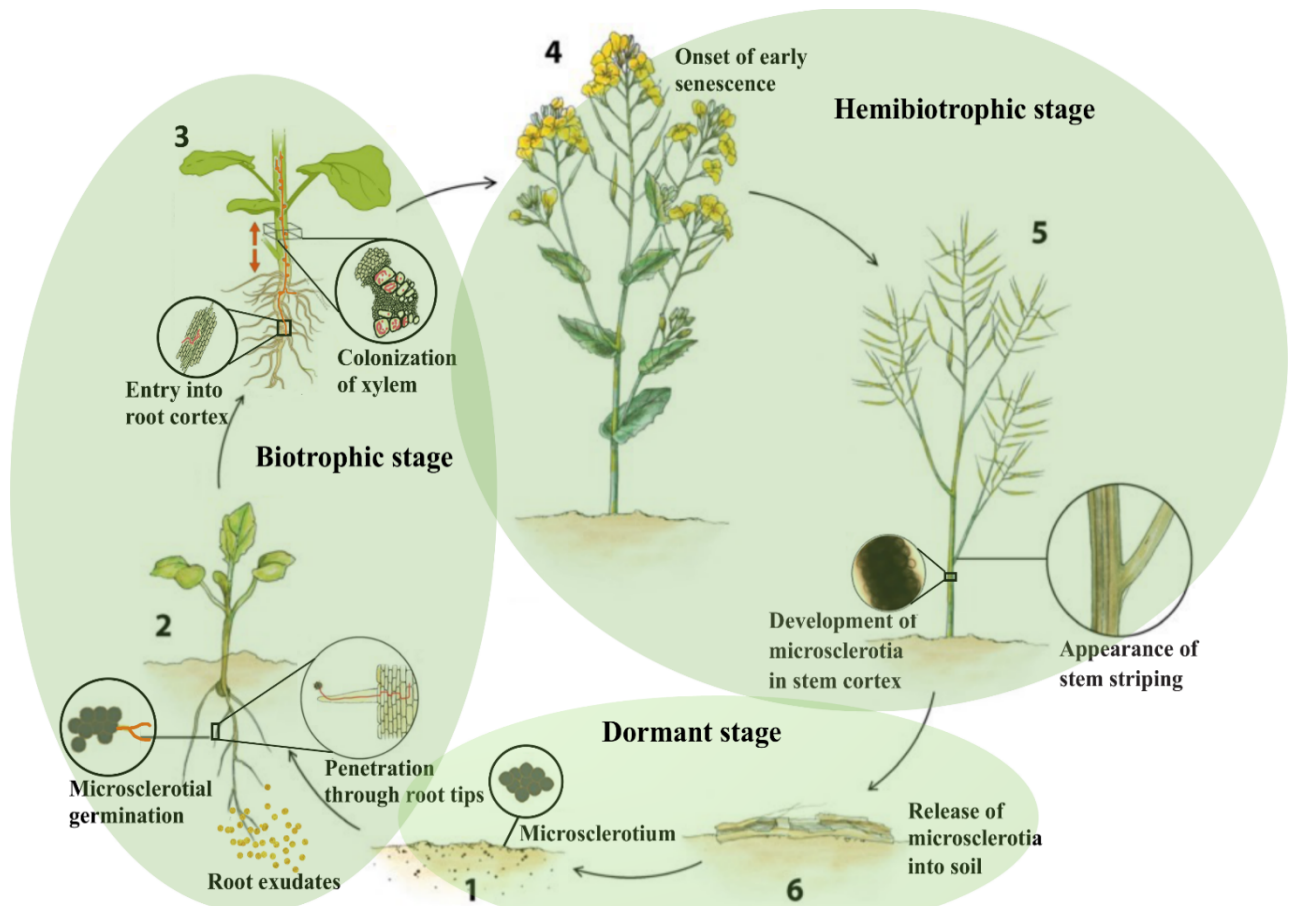


**Fig. 2.** Life cycle of *V. longisporum* in rapeseed. 1. Microsclerotia reside in soil, 2. secreted root exudates initiate the germination of microsclerotia and hyphal growth towards the plant roots, hyphae penetrate the root through root hairs, 3. hyphae colonize root cortex and enter the vascular system through xylem, 4. pathogen triggers early senescence during the growing season, 5. thick cell-walled and highly melanized microsclerotia developed in stem cortex and dark strips are visible on stems during the ripening of rapeseed, 6. after decomposition of plant debris, microsclerotia are released into the soil. (Picture modified from Dhar et al. 2020; Depotter et al. 2016; Rowe and Powelson, 2002).

### 1.5. Rapeseed response to *V. longisporum* infection - when plants make a counterattack

The vascular pathogen *V. longisporum* is highly host specific. It severely infects Brassicaceae plants, particularly rapeseed (Lopisso et al. 2017). In response to pathogen attack, rapeseed develops numerous physical or biochemical defence mechanisms. Root transcriptome analysis

illustrated that in plant-*V. longisporum* interaction, rapid reprogramming of plant gene expression takes place (Iven et al. 2012). Roots of *V. longisporum* infected *A. thaliana* plants produced higher levels of secondary metabolites like glucosinolates (Wittstock and Halkier, 2002) and tryptophan-derived metabolites (Iven et al. 2012) while soluble phenylpropanoids accumulated in leaves (König et al. 2014). Eynck et al. 2009 reported that rapeseed prevents the spread of *V. longisporum* from root to shoots by accumulating phenolics and lignin in the cell wall, which subsequently block the hypocotyl tissue. Moreover, rapeseed generates increased amounts of defence related antifungal proteins, including endochitinase, peroxidase and glucanase, in the xylem and leaf apoplast after *V. longisporum* infection (Floerl et al. 2008; Kehr et al. 2005).

Besides forming physical barriers, in *V. longisporum* infected oilseed rape also the level of membrane-bound plant receptor kinases increases through the activation of pathogen-associated molecular patterns (PAMP), which in turn enhance the synthesis of the plant defence hormones jasmonic acid (JA), ethylene (ET) and salicylic acid (SA) (Kamble et al. 2013; Ralhan et al. 2012; Ratzinger et al. 2009). Enhanced accumulation of such phytohormones can prevent pathogen proliferation and subsequent disease development by activating the defence responses of host plant upon pathogen infection (Lefevre et al. 2020).

Therefore, detailed analysis of phytohormone biosynthesis and signalling pathways, and their respective marker genes can facilitate explicit understanding about plants defence responses against fungal pathogens.

### **1.6. Plant immune response mechanism against pathogen attack**

In response to pathogen attack, plants develop numbers of inducible defence mechanisms for protection (Wu et al. 2018) including induced systemic resistance (ISR), triggered by beneficial fungi e.g., *T. harzianum* (Alkooranee et al. 2017; Yadav et al. 2021) and rhizobacteria e.g., *B. velezensis* (Chowdhury et al. 2015a; Lam et al. 2021); systemic acquired resistance (SAR), triggered by pathogenic fungi e.g., *V. longisporum* (Zheng et al. 2019), bacteria or insects (Van Wees et al. 2008). Although ISR and SAR share several signalling components, these two phenomena are different from each other based on elicitors and the regulatory pathways (Fig. 3). In systemic tissues, initiation of ISR requires the activation of JA and ET regulated pathways. Whilst SAR system comprises of increased SA levels which subsequently enhances the expression of pathogenesis-related (PR)-protein coding genes through the activation of redox-regulated protein non-expressor of PR genes 1 (NPR1) (Choudhary et al. 2007; Pieterse et al. 1998, 2002, 2012, 2014; Romera et al. 2019; Van Loon et al. 1998).

In contrast to SAR, in ISR system, plant beneficial microbes stimulate the defence system of whole plant body for a faster and stronger responses against pathogen attack, instead of directly activating the local defence responses. This phenomenon is called defence priming (Choudhary et al. 2007; Berendsen et al. 2012; Jung et al. 2012; Pieterse et al. 2014; Martinez-Medina et al. 2016). To enter the plant cells and subsequently establish symbiotic relationship, beneficial rhizosphere associated microbes suppress the host defence system by modulating plant hormone signalling pathways (Pieterse et al. 2012).

Jones and Dangl (2006) proposed the ‘zigzag model’ of multi-layer innate immune system including recognition of microbial/pathogen-associated molecular patterns (MAMPs/ PAMPs) developed by plants, through secreted pattern recognition receptors (PRRs) to induce PAMP-triggered immunity (PTI). Pathogens secreted effectors successfully overcome plant PTI and result effector-triggered susceptibility (ETS). *R* genes encoding nucleotide binding site-leucine rich repeat (NBS-LRR) proteins directly recognize the pathogen effectors inside the cells and activate effector-triggered immunity (ETI). NBS-LRR-mediated disease resistance can effectively suppress the obligate biotrophic and hemi-biotrophic pathogens (Glazebrook 2005). Eventually, ETI develops disease resistance and cause a hypersensitive cell death response (HR) at the infection site. Besides MAMPs, plant beneficial rhizosphere microbes also secrete elicitors, e.g., VOCs and siderophore to initiate the onset of ISR. Evidently, ET and JA pathways, the central players of ISR, contribute to enhance plant defence towards necrotrophic pathogens while SA-signalling pathway triggers plant response against biotrophic pathogens through SAR system (Li et al. 2019).

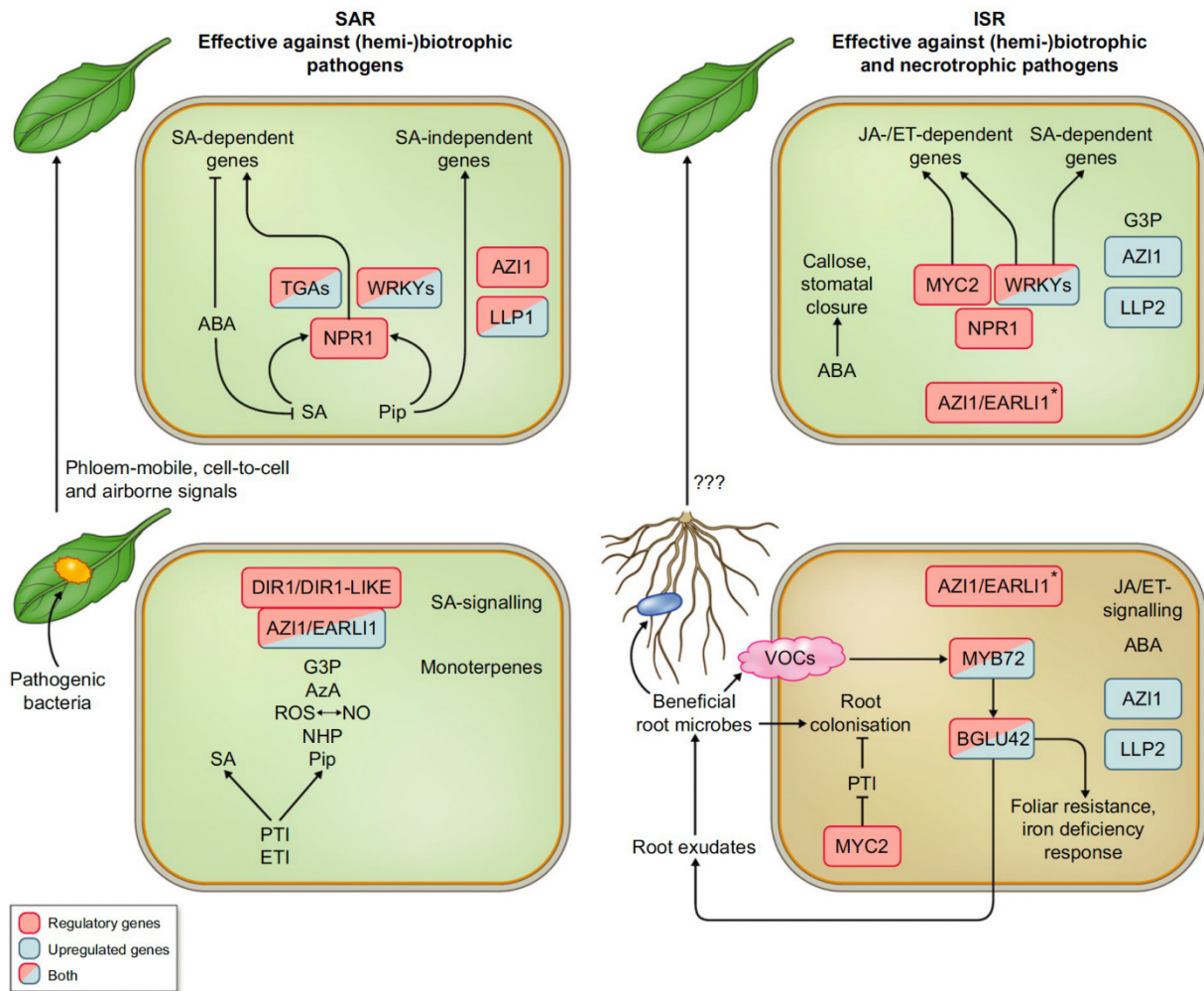


**Fig. 3.** Schematic representation depicting the mechanisms of SAR and ISR systems. SAR and ISR procedures are delineated on the left and right sides, respectively, with responses in local tissue at the bottom and in systemic tissue at the top. AZI1, azelaic acid induced 1; EARLI1, early arabidopsis aluminum induced 1; LLP, legume lectin-like protein; ABA, abscisic acid; AzA, azelaic acid; ROS, reactive oxygen species; NO, nitric oxide; G3P, glycerol-3-phosphate; BGLU42,  $\beta$  glucosidase 42; DIR1, defective in induced resistance 1; NHP, N-hydroxypipicolinic acid; MYB72, MYB domain protein 72; Pip, pipelicolic acid. (Picture taken from Vlot et al. 2021).

### 1.7. Phytohormones in plant defence

Phytohormones are a class of naturally occurring small organic molecules which regulate the plant physiological processes. A minute amount of phytohormones can influence cell division, elongation and differentiation; plant development and stress resistance; dormancy, germination, flower and fruit development and sex determination (Guo et al. 2020; Jiang and Asami, 2018; Xu et al. 2017). In addition, hormones are the fundamental plant components that effectively respond to biotic stresses and act as chemical messengers to coordinate the cellular activities of plants in response to inevitable pathogen attack (Zhao et al. 2021).

### 1.7.1. ET biosynthesis

The phytohormone ET is very important for successful colonization of pathogenic *V. longisporum* fungi in host plants as *etr1-1* receptor mutant *A. thaliana* showed reduced *V. longisporum*-induced symptoms (Johansson et al. 2006; Ralhan et al. 2012; Veronese et al. 2003). This gaseous hormone is synthesized at the site of action and diffuses across the membranes into nearby cells to move within the plant. Therefore, transporter proteins are not needed to carry ET to the target cells (Chang 2016).

Amino acid methionine is the general precursor of ET biosynthesis pathway in plants (Lieberman et al. 1966) which is converted into S-adenosyl-L-methionine (SAM) by SAM synthetase using ATP (Adams and Yang, 1977). The subsequent ET biosynthesis reaction from SAM precursor is carried out in a two-step biochemical pathway (Van de Poel and Van der Straeten, 2014; Pattyn et al. 2021; Xu and Zhang, 2015). In the first step, 1-aminocyclopropane-1-carboxylic acid (ACC) synthase (ACS) enzyme converts SAM to ACC and 5'-methylthioadenosine (MTA) (Adams and Yang, 1977, 1979; Boller et al. 1979). The by-product MTA, a precious sulphur moiety, is recycled back to methionine by Yang cycle to ensure constant supply of methionine during high rates of ethylene production (Murr and Yang, 1975). In the second step, ACC oxidase (ACO) catalyses the formation of ET, CO<sub>2</sub> and cyanide from immediate precursor ACC (Fig. 4) (Hamilton et al. 1991; Ververidis and John, 1991). The side product cyanide is immediately converted to β-cyanoalanine (Yip and Yang, 1988) catalysed by β-cyanoalanine synthases (Hatzfeld et al. 2000) to abolish its toxicity. Multiple gene families encode both ACS and ACO enzymes. Expression of the genes belonging to these families is regulated by internal developmental and environmental stress signals including pathogen attack (Xu and Zhang, 2015).

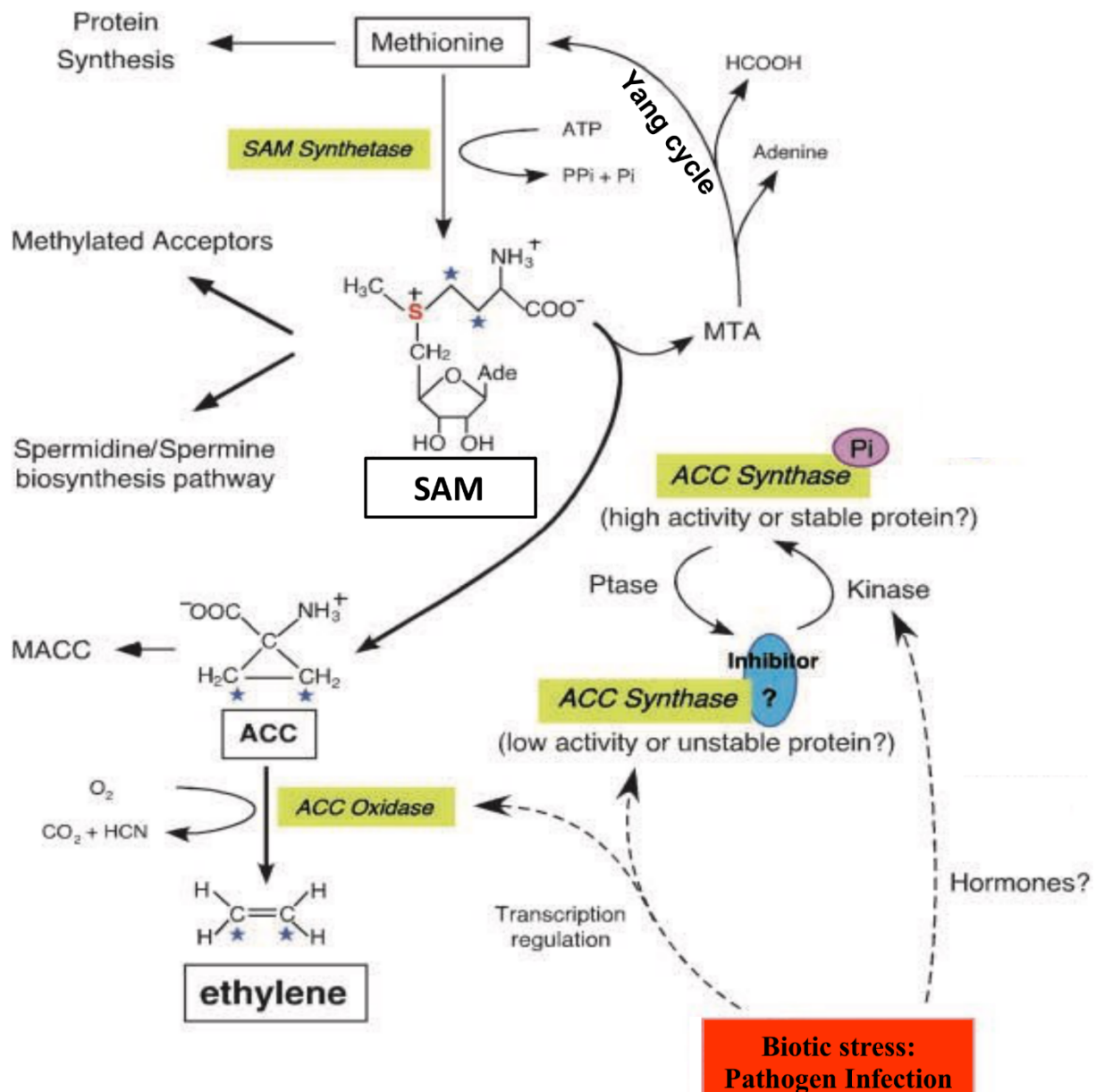


**Fig. 4.** Ethylene biosynthesis and regulation pathway in plants. SAM synthetase catalyses the synthesis of SAM from methionine. One molecule of ATP is consumed in per molecule of SAM generation. SAM donates methyl group to nucleic acids, proteins, and lipid (Methylated Acceptors), and acts as a precursor of Spermidine/Spermine biosynthesis pathway. ACC synthase converts SAM to ACC and generates MTA as a by-product which is again used to generate methionine by Yang cycle. ACC is malonylated to malonyl-ACC (MACC) which can cause ACC deficiency and limit ET production rate. The final step is catalysed by ACC oxidase to synthesize ET from ACC. Dashed arrows indicate the transcriptional regulation of ACC synthase and ACC oxidase. It is hypothesized that ACC synthase may be reversibly phosphorylated and induced by unknown phosphatases (Ptase) and kinases. Biotic stress, including pathogen infection can apparently activate the kinases. The carboxyl end of ACC synthase binds with a hypothetical inhibitor which can be isolated from the enzyme by phosphorylation modification. (Picture modified from Wang et al. 2002).



### 1.7.2. JA biosynthesis

Enhanced production of JA hormone in response to *Verticillium* infection enables *A. thaliana* plants to develop resistance against this pathogen attack (Sun et al. 2014). Jasmonic acid (JA) and its derivatives named jasmonates (JAs) are class of oxidized lipid-derived (oxylipins) signalling molecules. JAs, ubiquitous in higher plants and certain fungi, are synthesized from  $\alpha$ -linolenic acids ( $\alpha$ -LAs) precursors and systematically enhance the expression of defence molecule encoding genes to repair pathogen created damage (Larrieu and Vernoux, 2016). Three subcellular compartments: chloroplast, peroxisome, and cytoplasm are involved in JA biosynthesis through the octadecanoids pathway (Fig. 5).

In the first step, upon the perception of pathogen induced wound signal, chloroplast membrane localized galacto- and phospholipids form  $\alpha$ -LA through the activity of phospholipases (PLAs) enzyme (Ishiguro et al. 2001). 13-lipoxygenase (LOX) oxidizes the polyunsaturated fatty acids,  $\alpha$ -LA to generate 13-hydroperoxy-octadecatrienoic acid (13-HPOT) (Caldelari et al. 2011; Chauvin et al. 2013, 2016). Afterwards, stable *cis*(+)-oxophytodienoic acid (*cis*-OPDA) intermediate is synthesized from 13-HPOT by oxidation of allene oxide synthase (AOS), and allene oxide cyclase (AOC) (Lee et al. 2008; Stenzel et al. 2012; Otto et al. 2016; Laudert et al. 1996).

In the next step, *cis*-OPDA enters subcellular compartment, peroxisome. The transfer process of *cis*-OPDA from chloroplast to peroxisome is mostly unknown. Only one gene encoding a peroxisome-localized protein, COMATOSE, of ATP binding cassette (ABC) transporter has been identified so far, which is evidenced to be involved in JA transport into peroxisome (Laudert et al. 1996; Dave et al. 2011). However, in peroxisome, *cis*-OPDA is reduced to 3-oxo-2(2'-pentenyl)-cyclopentane-1-octanoic acid (OPC-8:0) by 12-oxo-phytodienoate reductase isoenzyme 3 (OPR3). OPC-8:0 subsequently undergoes 3 cycles of  $\beta$ -oxidation by acyl-CoA oxidase (ACX) enzymes and ultimately synthesize JA (Breithaupt et al. 2006; Cruz et al. 2004; Wasternack and Hause, 2013).

JA is then transported to cytoplasm through an unknown manner. Gretchen Hagen 3 (GH3) enzyme conjugates amino acid, isoleucine with JA and produce bioactive (+)-7-isojasmonoyl-L-isoleucine (JA-Ile) molecule (Fonseca et al. 2009; Haroth et al. 2019; Staswick and Tiryaki, 2004). While JA carboxyl methyltransferase (JMT) metabolizes JA to generate methyl jasmonate (MeJA) (Cheong and Choi, 2003; Seo et al. 2001).

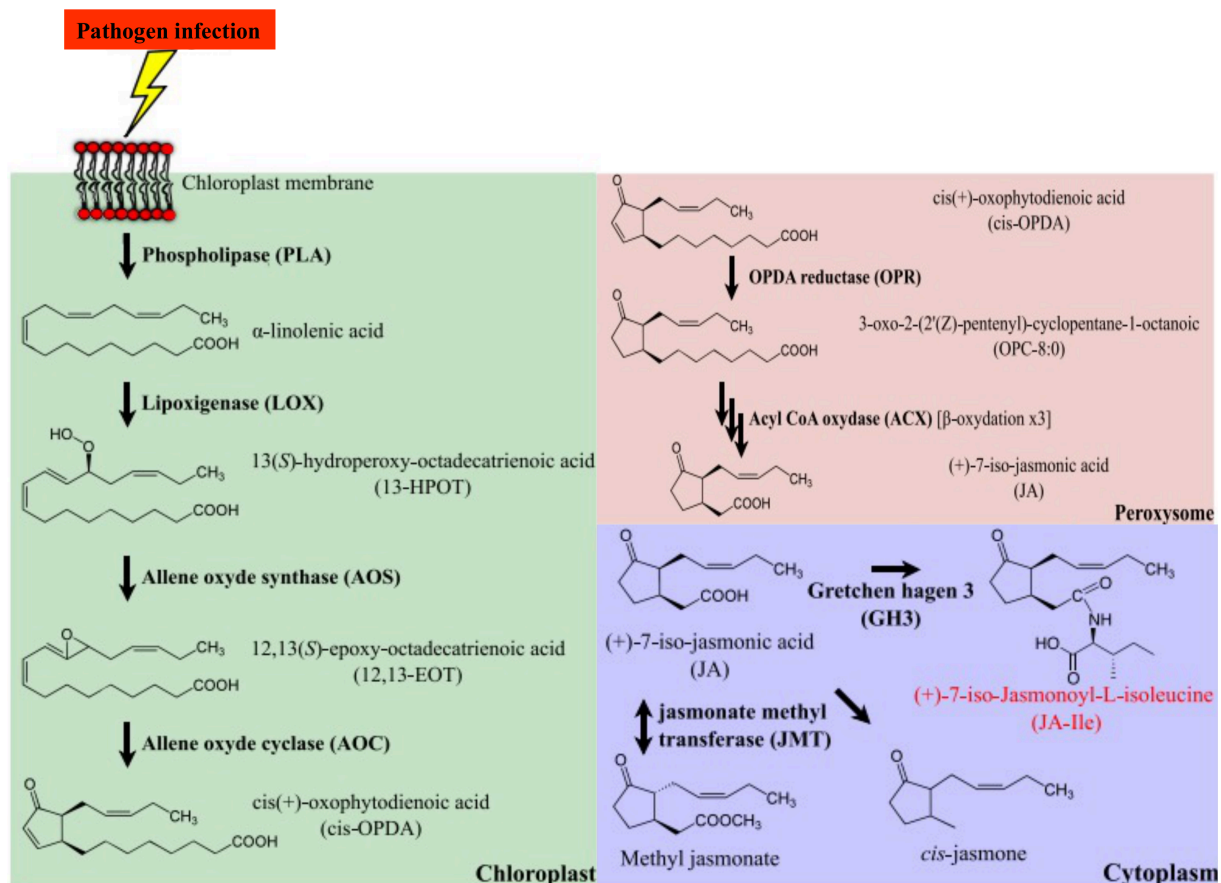


**Fig. 5.** Octadecanoid pathway for JA biosynthesis and metabolism. JA biosynthesis process starts in the chloroplast using  $\alpha$ -LAs as precursor and continues to the formation of 12-oxo-PDA, which is then transported to peroxisomes and undergoes several cycles of reduction and oxidation reactions to synthesize JA. Newly synthesized JA is then immediately exported to cytoplasm where it is metabolized to form bioactive JA compounds including JA-Ile, MeJA and *cis*-jasmone. (Picture taken from Larrieu and Vernoux, 2016 with minor modification).

### 1.7.3. SA biosynthesis

Due to its central role in SAR (Huang et al. 2020), SA hormone contributes to enhanced resistance against *Verticillium* spp. infection in *Arabidopsis*, tomato, and cotton (Dhar et al. 2020; Fradin et al. 2009; Gao et al. 2011; Johansson et al. 2006). Likewise, in *V. longisporum* infected *B. napus* plants, increased accumulation of SA was measured in its root xylem sap, hypocotyl, and shoots (Ratzinger et al. 2009).

SA is synthesized in higher plants by two individual pathways, isochorismate synthase (ICS) pathway and phenylalanine (Phe) ammonia-lyase (PAL) pathway (Fig. 6) (Dempsey et al. 2011; Hartmann and Zeier, 2019; Zhang and Li, 2019). Both pathways begin in plastid, using chorismite (CA), originated from the shikimate pathway, as precursor molecule (Huang et al. 2020).

In *A. thaliana*, the ICS pathway was found to be indispensable in pathogen induced SA production (Nawrath and Metraux, 1999). Two *ICS* homologous genes, *ICS1* and *ICS2* were identified in *A. thaliana* genome (Garcion et al. 2008). *ICS1*, localized in plastid, converts CA to isochorismate (IC) (Garcion et al. 2008; Wildermuth et al. 2001) which was then exported to the cytosol by enhanced disease susceptibility 5 (EDS5) transporter, confined in the chloroplast envelop (Serrano et al. 2013). In the cytosol, *avrPphB* susceptible 3 (PBS3) enzyme catalyses the conjugation of glutamate to IC and formed isochorismate-9-glutamate (IC-9-Glu) (Torrens-Spence et al. 2019). The newly evolved IC-9-Glu is then converted to SA either by catalysation of an acyltransferase, enhanced pseudomonas susceptibility 1 (EPS1) (Torrens-Spence et al. 2019), or by spontaneous decomposition (Rekhter et al. 2019).

The PAL pathway of SA biosynthesis has been characterized by isotope labelling experiments in tobacco (Ribnicky et al. 1998; Yalpani et al. 1993). In the first step, PAL catalyses the conversion of Phe to trans-cinnamic acid (Trans-CA) (Vogt, 2010). While in the second step, Trans-CA is further modified to benzoic acid (BA) through  $\beta$ -oxidation catalysed by abnormal inflorescence meristem 1 (AIM1) enzyme (Richmond and Bleecker, 1999; Xu et al. 2017). BA is then hydroxylated to SA by BA 2-hydroxylase enzyme. (Leon et al. 1993, 1995). BA 2-hydroxylase coding gene has not been yet identified (Huang et al. 2020).

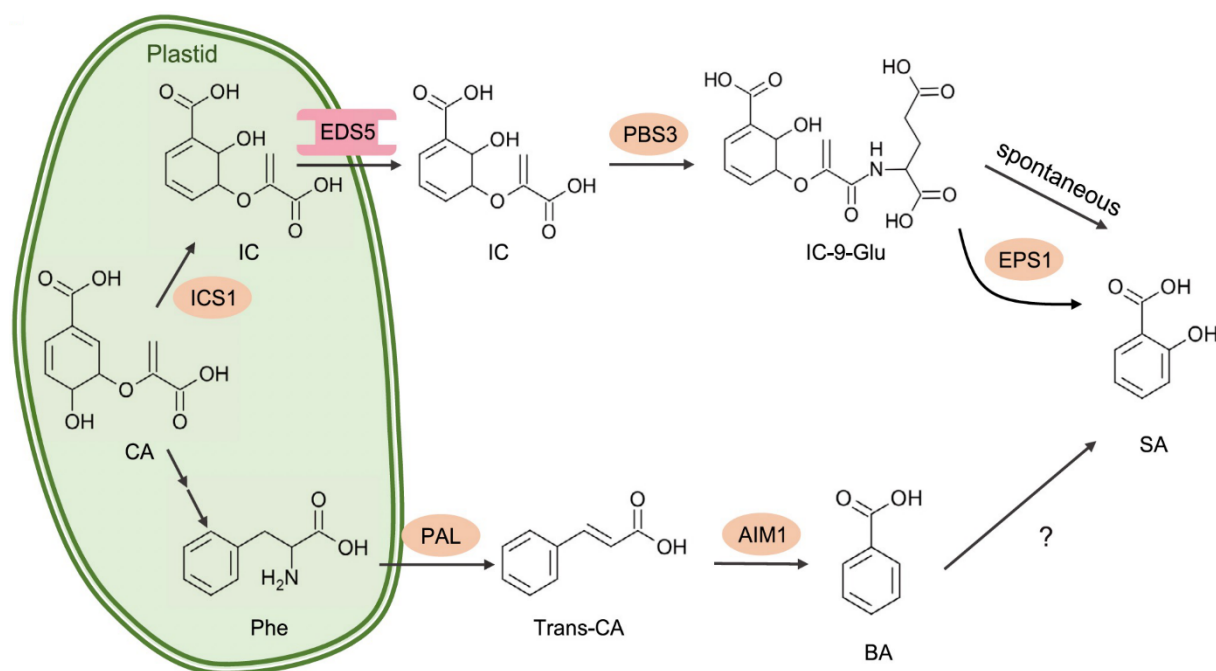


**Fig. 6.** The biosynthesis pathway of SA in plants. In ICS pathway, CA is converted to IC by ICS in the plastid. The MATE transporter EDS5 transports IC from plastid to cytosol, where PBS3 converts IC to IC-9-Glu. EPS1 degrades IC-9-Glu to SA in Brassicaceae. In the PAL pathway, Phe converts to trans-CA by PALs and AIM1 oxidized trans-CA to BA which is then converted to SA by a yet-to-be-identified BA 2-hydroxylase. (Picture taken from Huang et al. 2020).

## 1.8. JA, ET and SA signal transduction

Induced defence responses of plants against pathogenic infection rely on the inception of ET/JA and SA phytohormones mediated signalling pathways (Yang et al. 2019).

### 1.8.1. ET signalling

ET signalling pathway is absolutely conserved in higher plants. The detailed mechanism of ET signalling has been extensively studied in the model plant *A. thaliana* by combined approaches of genetics, cell biology, molecular biology and biochemistry (Guillaume and Sauter, 2008; Klee, 2004). After biosynthesis, ET is perceived by endoplasmic reticulum (ER) membrane bound receptors ETR1, the first known plant hormone receptor (Chang et al. 1993; Ju and Chang, 2015). After ET binding, ER-localized protein, ethylene-insensitive 2 (EIN2) is dephosphorylated because of the receptor associated constitutive triple response 1 (CTR1) protein kinase inactivation. Dephosphorylated EIN2 splits up and releases its soluble C-terminal domain, which shuttles into nucleus and activates EIN3 transcription factor (Alonso et al. 1999; Ju et al. 2012; Qiao et al. 2012). EIN3 directly activates the ET-responsive transcription factors such as ethylene response factors (ERFs) which in turn rapidly induces the ET response (Fig. 7) (Pré et al. 2008; Solano et al. 1998).

The cleaved C-end EIN2 protein is also stabilized by inhibiting the translation of two F-box proteins, EIN3 binding F-box protein 1 (EBF1) and EBF2 in the cytoplasm. This translational repression is a crucial step for ET signalling. Otherwise, in the nucleus, EBF1/2 proteins would proteolytically degrade two master transcription factors, EIN3/ EIL1, indispensably required for ethylene responses (An et al. 2010).

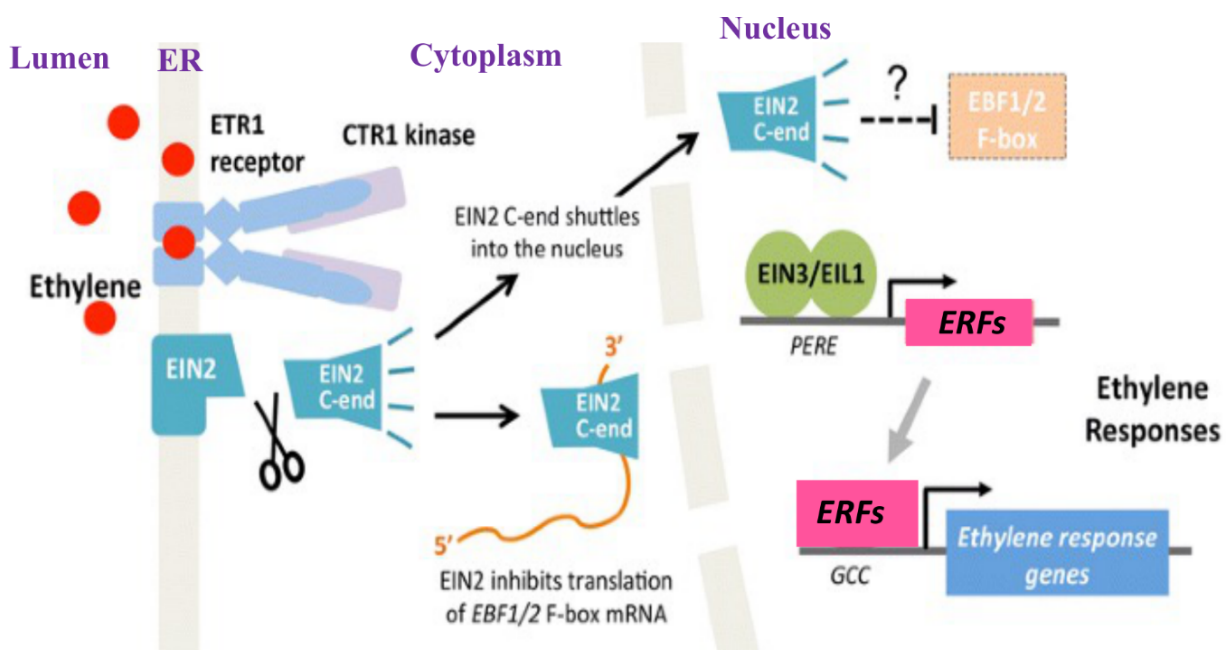


**Fig. 7.** Pathway of ET signalling cascade. In the presence of ET, CTR1 inactivates and releases the EIN2 C-END by proteolytic cleavage. EIN2 C-END suppresses the translation of F-box proteins EBF1/2 as well as stabilizes EIN3 which in turn activates ERF transcription factor to generate ET response. (Picture taken from Chang, 2016).

### **1.8.2. JA signalling**

In *A. thaliana*, extensive studies of JA related transcriptome revealed that JA response in plants largely depends on the context that triggers the onset of JA signalling (De Vos et al. 2005; Pauwels et al. 2009; Pozo et al. 2008). Therefore, in plant-pathogen interaction, JA responsive genes are distinctively activated by different JAs and fine-tune the JA response (Farmer et al. 2003; Gfeller et al. 2010).

Central regulator of JA signalling pathway is the F-box protein coronatine insensitive 1 (COI1) (Chung et al. 2009), which acts as JA-Ile receptor in E3 ubiquitin-ligase Skip-Cullin-F-box complex SCF<sup>COI1</sup> (Fig. 8) (Yan et al. 2009). Attachment of JA-Ile with COI1 causes degradation of transcriptional repressor protein JASMONATE ZIM-domain (JAZ) by 26S proteasome (Chini et al. 2007; Thines et al. 2007). JAZ protein mainly consists of two conserved regions: a ZIM domain, regulating JA signal transduction and a Jas motif, responsible for JA perception and signal transduction (Pauwels and Goossens, 2011). Degradation of JAZ releases downstream transcriptional factors, MYC2 which results in activation of numerous JA responsive marker genes, including *plant defensin 1.2* (*PDF1.2*) and *vegetative storage protein 2* (*VSP2*) (Dubois et al. 2018; Gimenez-Ibanez et al. 2017).

In the absence of JA, ZIM domain recruits the transcriptional co-repressors TOPLESS (TPL) through interaction with a protein, termed NINJA (Novel Interactor of JAZ) (Pauwels et al. 2010). Binding of JAZ with NINJA suppresses the positive transcriptional regulators, MYC2 (Chini et al. 2007) and blocks their interaction with the transcriptional mediator complex subunit, MED25 (Zhang et al. 2015).

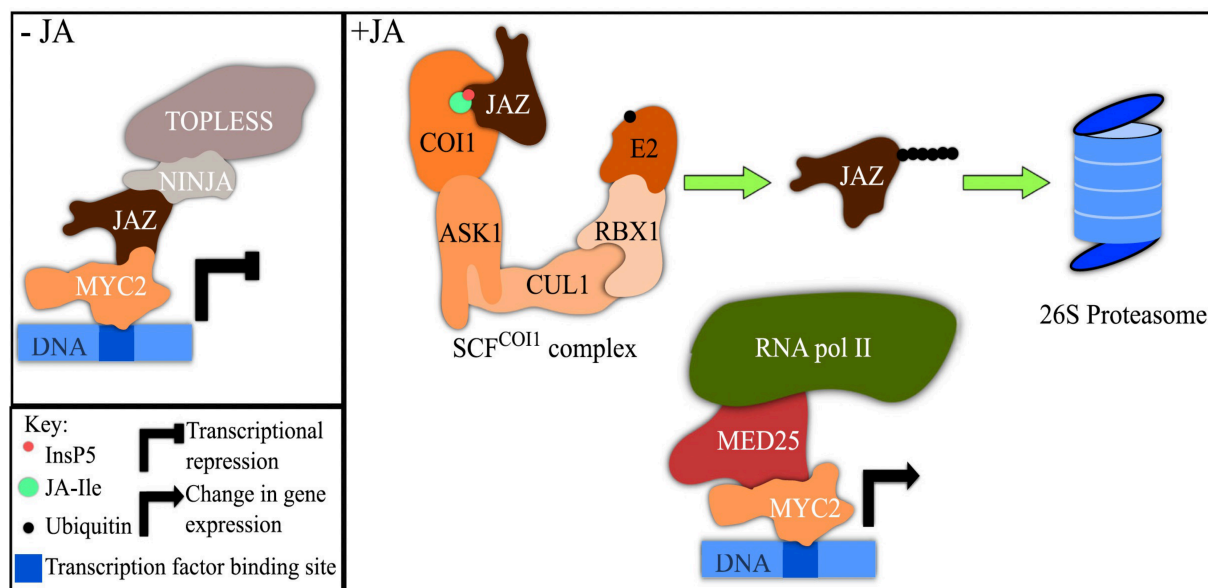


**Fig. 8.** JA signal transduction pathway. In the absence of JA, JAZ protein binds with transcriptional repressors protein TOPLESS (TPL) via NINJA and results suppression of JA transcriptional regulators, MYC2. Whilst in the presence of JA, F-box protein COI1 binds with JA-Ile in the SCF<sup>COI1</sup> protein complex. This interaction facilitates the degradation and release of JAZ protein by 26 S proteasome and mediates the interaction of positive TFs MYC2 with the transcriptional mediator, MED25 and triggers the transcription of downstream JA responsive genes by RNA pol II. (Picture taken from Larrieu and Vernoux, 2016).

### 1.8.3. SA signalling

SA is an internal defence signalling molecule of plants, crucial to protect against pathogen invasion (Klessig et al. 2018; Li et al. 2019). In SA dependent defence response, non-expressor of pathogenesis protein 1 (NPR1) (Cao et al. 1994; Delaney et al. 1995), is the key regulatory protein (Ding and Ding, 2020). In uninfected healthy plants, NPR1 mainly remains in cytosol by forming oligomeric complexes and is incapable of defence gene activation. Following pathogen infection, increased SA production changes the redox state of cytosol and switches the oligomeric NPR1 to its active monomeric form. Monomeric NPR1 is then translocated to the nucleus and acts as a transcriptional co-activator at the target defence gene promoter (Mou et al. 2003). Spoel et al. (2009) reported that, for successfully activating the target genes in the nucleus, NPR1 undergoes Cullin3 (CUL3) E3 ligase mediated ubiquitination and subsequent degradation by 26S proteasome. The activated NPR1 then binds with transcriptional activators of the TGACG-binding factor (TGA) transcription factor family (Saleh et al. 2015).

A comprehensive study by Fu et al. (2012) elucidated that in uninfected plants at low SA concentration, the CUL3 E3 ligase adaptor proteins NPR3 and NPR4, paralogs of NPR1, can specifically degrade NPR1. While after pathogen attack, high concentration of SA enhances the interaction of NPR3 with NPR1 and inhibit the transcriptional repression activity of NPR3. This

interaction leads to NPR1 protein turn-over and subsequent defence-associated programmed cell death (PCD) at the site of pathogen infection (local part). In the uninfected distal tissue of the same plant (systemic part), relative lower concentration of SA accumulates which is sufficient to subsequently activate NPR1. Such induction can enhance the expression of defence genes without triggering PCD and establish systemic acquired resistance (Fig. 9).

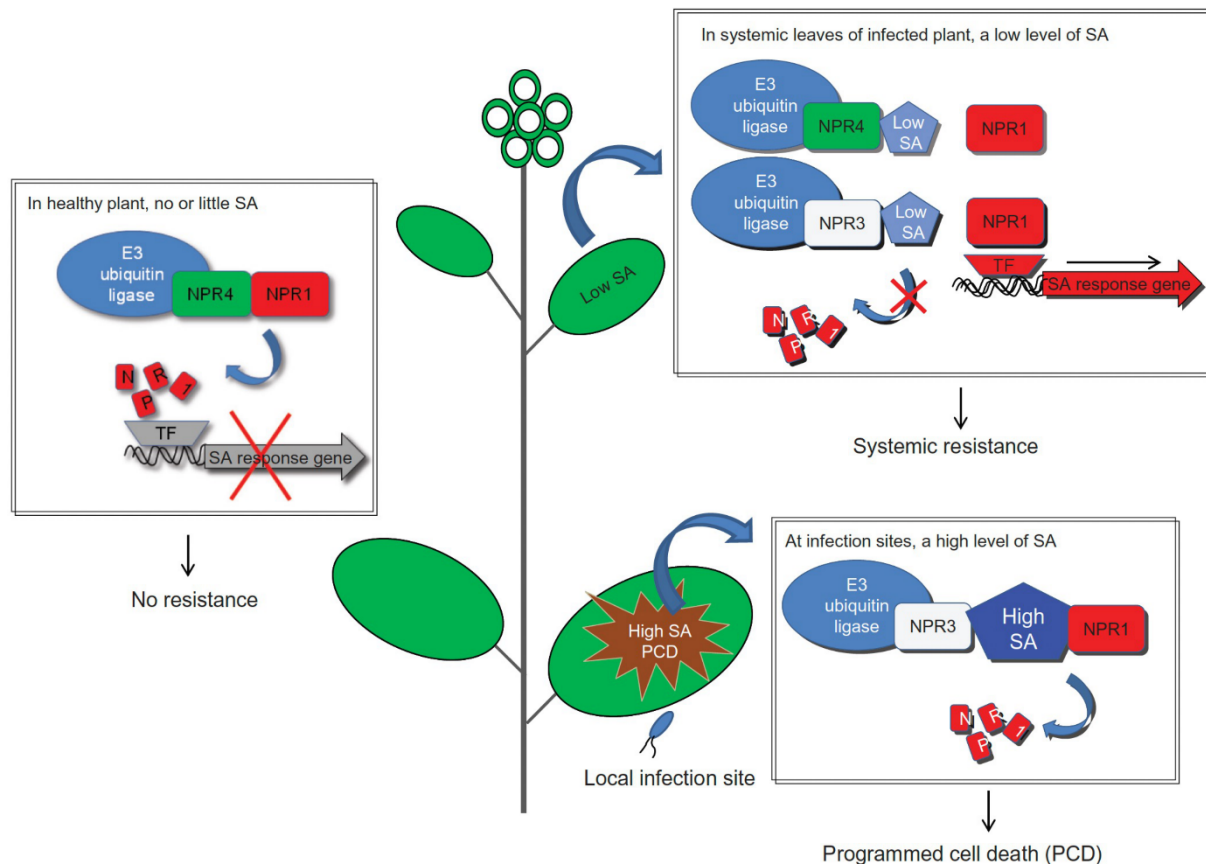


**Fig. 9.** SA signal transduction in plants. In uninfected healthy plants with no or a little SA, NPR1 resides in the cytosol in its oligomeric form. The residual NPR1 binds with NPR3 and NPR4 in the nucleus and remains inactive. After pathogen infection, higher concentration of SA accumulates in the site of infection and binds with NPR3 which leads to turn-over of NPR1 protein and defence-associated PCD. While the systemic distal tissue accumulates relatively lower amount of SA which activate NPR1 to interact with TGA and activate defence related genes. (Picture taken from Attaran and He, 2012).

### 1.9. Crosstalk among JA, ET and SA signalling pathways

In nature, the crosstalk of phytohormones is the backbone of plants defence responses against biotrophic and necrotrophic pathogens (He et al. 2017; Li et al. 2019). Detailed analysis of *A. thaliana* mutants impaired in SA, JA and ET signalling, single or in combination, revealed that defence signalling is not mediated individually, rather orchestrate in a complex network in which SA, ET and JA hormones extensively crosstalk (Hillmer et al. 2007; Kim et al. 2014; Mine et al. 2017; Tsuda et al. 2009, 2013). Studies also reported both synergistic and

antagonistic functions of the SA, ET and JA dependent defence signalling pathways (Fig. 10) (Caarls et al. 2015; De Vleeschauwer et al. 2014; Pieterse et al. 2012; Shigenaga and Argueso, 2016; Shigenaga et al. 2017). For instance, Mur et al. (2006) documented that the SA marker gene *PRI* and the JA marker gene *PDF1.2* act synergistically after treatment with lower concentrations (typically 10-100  $\mu\text{M}$ ) of exogenous SA and JA in tobacco (*Nicotiana tabacum*) plants. Whereas in higher SA and JA concentrations (250  $\mu\text{M}$ ), these two genes act antagonistically. JA and ET signalling pathways also interact with each other in both synergistic and antagonistic manners (Zhu, 2014; Zhu and Lee, 2015).

Molecular compounds including MYC2, TGAs, and PDF1.2 (Gatz, 2013); redox regulators glutathione (GRX) and thioredoxin (TRX); WRKY70 (Shim et al. 2013) and mitogen-activated protein kinase (MAPK) (Rodriguez et al. 2010) are involved in regulation of the JA and SA signalling crosstalk (Yang et al. 2019). In pathogen infected plant, presence of SA activates NPR1 which, in turn, induces the TF WRK70. Transcriptionally activated WRK70 then binds to the *PRI* promoter region and enhance *PRI* expression which ultimately induce the defence responses of plants. At the same time, SA-induced redox state converts NPR1 polymer to its monomeric form such as GRX480 which binds with TGAs in the nucleus and regulates *PRI* expression as well (Fu et al. 2012; Gatz, 2013; Leon-Reyes et al. 2009; Spoel et al. 2009; Zander et al. 2012). Hence, a dual role is revealed through the transformation of NPR1 polymer and monomer in respectively activating and inhibiting the expression of defence-related genes. Similarly, MPK4 activates SA signalling pathway by positively regulating GRX480 and inhibits JA signalling pathway by negatively regulating MYC2, which is essential for the activation of JA responsive genes, such as *PDF1.2* and *THI2.1* (Wasternack and Hause, 2013). Therefore, the crosstalk between JA and SA signalling pathways are co-ordinately regulated by the TFs MYC2 and its upstream MPK4. Indeed, the SA signalling pathway induces the expression of early defence related genes while JA pathway enhances the expression of late defence related genes (Yang et al. 2019).

The crosstalk between JA and ET signalling pathways includes EIN2 and its homologue EIN3-like 1 (EIL1) in the ET signalling pathway and JAZs and MYC2 in the JA signalling pathway (Zhang et al. 2014). Transcriptional activity of EIN3/EIL1 is suppressed by JAZ, by which ERFs are activated to bind to the promoter of *PDF1.2*. Enhanced expression of *PDF1.2* provides increased resistance against hemi-biotrophic and necrotrophic pathogens (Zhu et al. 2011).



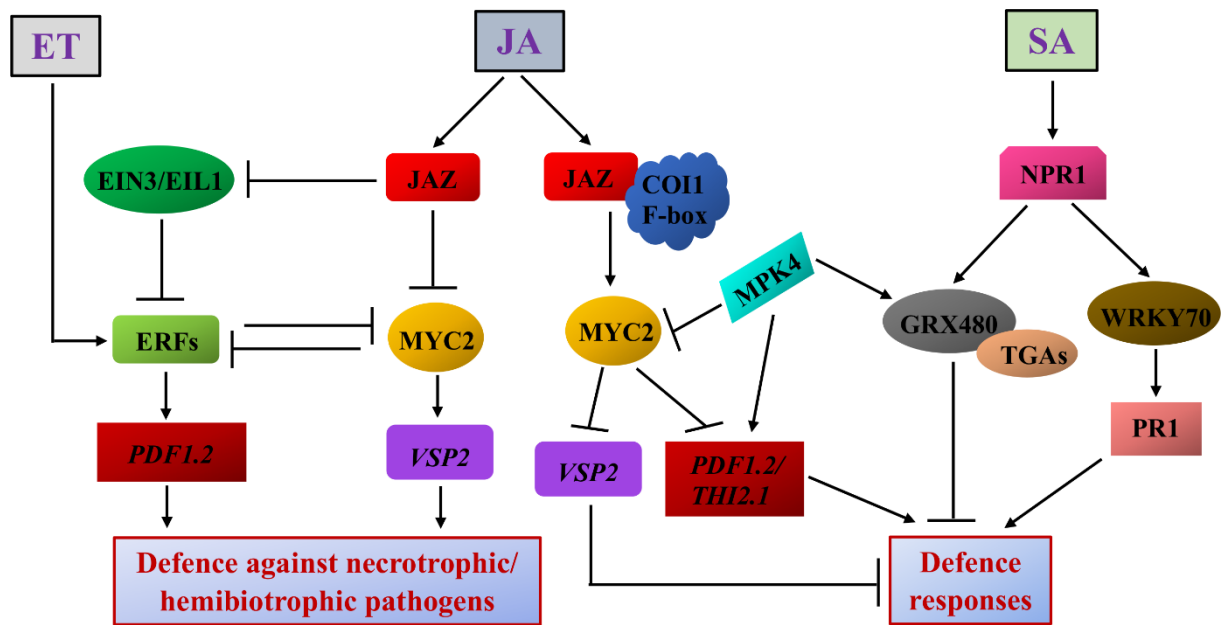


**Fig. 10.** Schematic representation of the crosstalk among ET, JA and SA phytohormone signalling pathways at the transcriptional level. Arrows indicate positive regulation (activation), blunt-ended lines indicate negative regulation (repression). (Picture modified from Yang et al. 2019).

### 1.10. Aim of the thesis

Potential synergistic effects of plant beneficial microorganisms, *Trichoderma* and *Bacillus* species in rapeseed and the underlying physiological mechanisms remain elusive. Therefore, the aim of this study was to analyse the synergistic effects of *T. harzianum* OMG16 and *B. velezensis* FZB42 in colonization of rapeseed roots, to monitor growth responses and changes in root morphology and to achieve induced systemic resistance against *V. longisporum* 43 (Vl43) infection. This major objective was addressed by the following sub-objectives:

1. Confirming the presence of OMG16 fungus inside the root tissue by microscopic analysis.
2. Absolute quantification of root-endophytic OMG16 and FZB42 microbes from *in vitro* grown rapeseed plants of two different cultivars, AgP1 and AgP4 by qPCR technique.
3. Determining the effects of OMG16 and FZB42 synergism on root morphology development of both AgP1 and AgP4 cultivars by WinRhizo image analysis system.
4. Analysing the systemic expression of defence genes, *AOC3*, *ERF2* and *PDF1.2* in leaf tissue of two rapeseed cultivars, AgP1 and AgP4 upon OMG16 and FZB42 synergism by qRT-PCR.
5. Analysis the potency of preventing infection of Vl43 pathogen in *B. napus* seedlings of AgP4 cultivar upon priming with combined application of OMG16 and FZB42 by qPCR.
6. Relative quantification of ET, JA and SA phytohormone biosynthesis as well as signalling genes separately in root, stem and leaf tissues of Vl43 infected primed and non-primed plants of AgP4 rapeseed cultivar by applying qRT-PCR.
7. Quantification of endogenous phytohormones, JA and SA separately in shoot (leaf+stem) and root tissues after Vl43 infection in primed and non-primed rapeseed plants of AgP4 cultivar by UHPLC-MS analysis.

## **2. Materials and methods**

### **2.1. Plant materials**

In this study two different *B. napus* (oilseed rape) genotypes, AgP1 and AgP4 were analysed. *B. napus* seeds were provided by the NPZ Innovation GmbH, Hohenlieth, Germany. According to the classification in *Verticillium* bioassays, performed by the breeder NPZi (personal communication), AgP1 was more susceptible towards the pathogen in the juvenile stages than AgP4 (Fig. 11). Furthermore, the genotypes differ in speed of emergence and root architecture. While AgP4 germinates faster and shows a tap root dominant phenotype with a high proportion of root hairs, AgP1 is slower in germination and has a more pronounced lateral root system. Both genotypes were “00” hybrids.

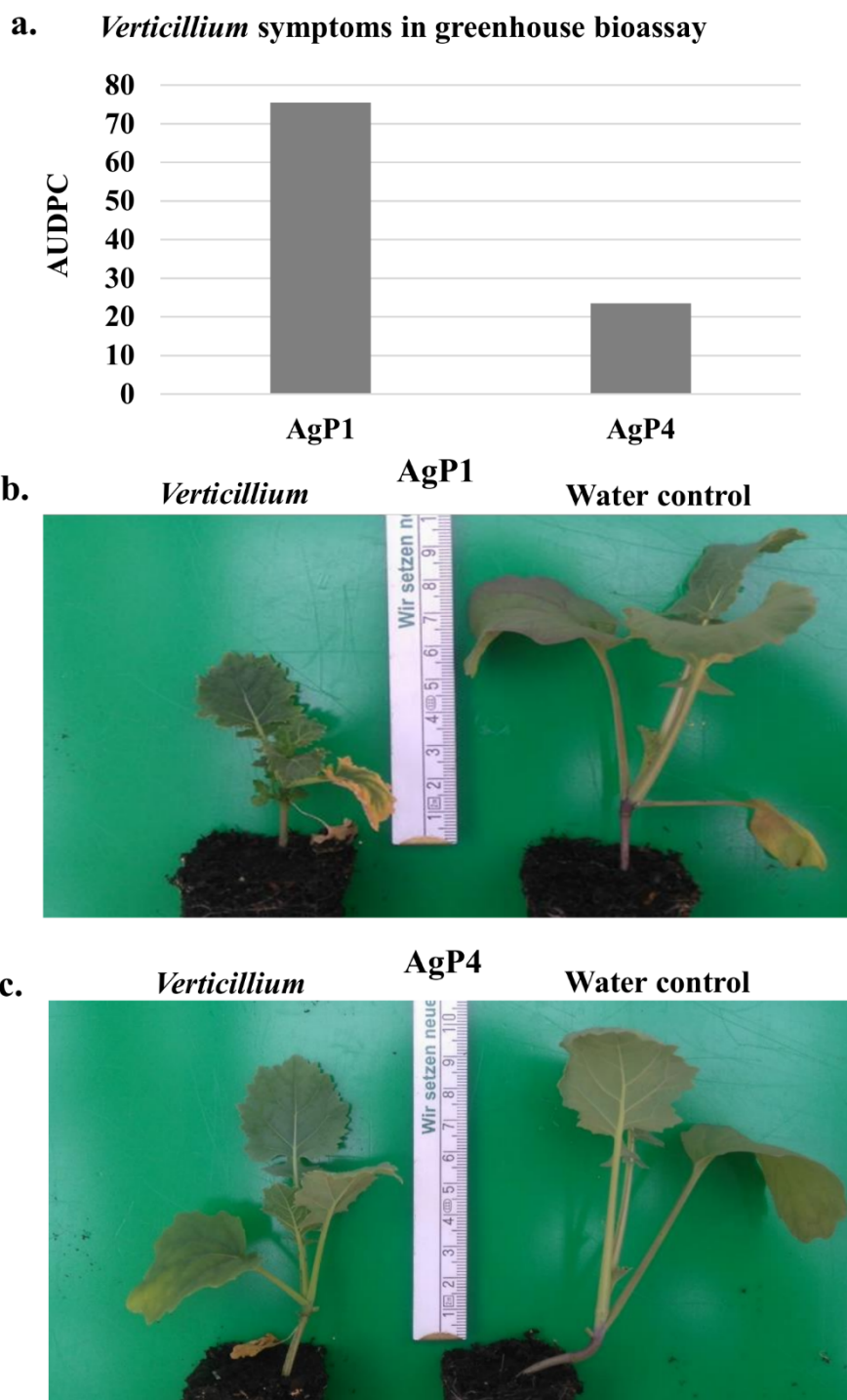


**Fig. 11.** Infection of rapeseed varieties AgP1 and AgP4 with *V. longisporum* 43 in the greenhouse. Symptoms were scored at 21 and 35 days after infection. AUDPC: area under disease progression curve in relation to the water treated control plants. (Data were provided by the breeder, NPZi).

### 2.1.1. *B. napus* seed sterilization

1. For surface sterilization, *B. napus* seeds were placed in 3% sodium hypochlorite solution (Carl Roth, product no. 9062.3) for 15 min with gently shaking.
2. Then the seeds were thoroughly washed three times with sterile deionised water.

3. Surface sterilized seeds were plated on sterile glass Petri dishes fitted with filter papers (grade MN 619 eh; Macherey-Nagel), which were soaked with autoclaved water.
4. The seed plates were incubated for 12 h at 8°C in the dark.
5. Subsequently, the plates were transferred into a growth chamber with 16 h light (80  $\mu\text{mol m}^{-2}\text{s}^{-1}$ ) and 8 h dark, 20°C and 60% relative humidity for germination.
6. Six-day-old single seedlings were transferred into sterile boxes fitted with sterile filter papers soaked with half-strength Murashige and Skoog (MS) medium (Sigma-Aldrich, product no. M5519) supplemented with 0.5% sucrose and 5.4  $\mu\text{M}$  NAA (1-naphthylacetic acid).
7. These plant boxes were placed in an incubator set to the conditions mentioned in step 5.
8. For microbial inoculation, seedlings were grown in the incubator until they were two-week-old.

### **2.1.2. Plant beneficial fungal isolates**

*T. harzianum* OMG16 (Fig. 12a) (Moradtalab et al. 2020; Mpanga et al. 2019a; Mpanga et al. 2019b) and *T. virens* M9B (Fig. 12b) strains were obtained from the strain collection of Anhalt University of Applied Sciences, Bernburg, Germany.

### **2.1.3. Fungal growth conditions**

1. Fungi were grown on potato dextrose agar (PDA) (Carl Roth, product no. CP74.2) at room temperature.
2. Spores were harvested by adding 5 mL of sterile deionised water to the surface of a 20-day-old PDA plate.
3. The obtained spore suspension was filtered through a single layer of Miracloth (Merck) in order to separate mycelial fragments from conidia.
4. The spore concentration was determined with the hemocytometer and adjusted to a final concentration of 20,000 spores  $\text{mL}^{-1}$ .

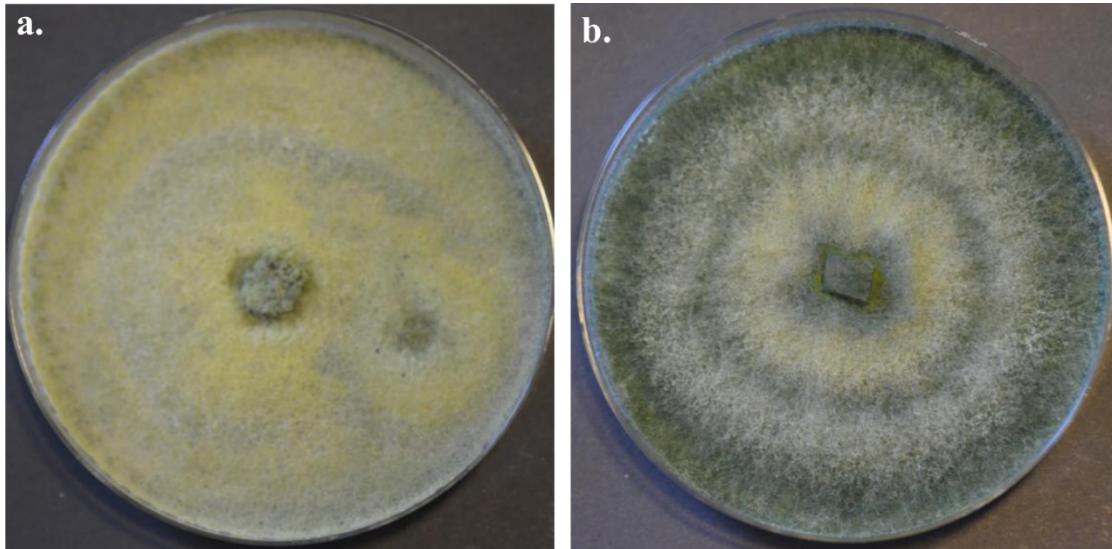


**Fig. 12.** 20-day-old *T. harzianum* OMG16 (a) and *T. virens* M9B (b) fungal strains grown on PDA plates.

#### **2.1.4. Plant beneficial bacteria**

The bacterial strain *B. velezensis* FZB42 syn. *B. amyloliquefaciens* subsp. *plantarum* FZB42 was provided by ABiTEP GmbH, Berlin, Germany.

#### **2.1.5. Bacterial culture and growth condition**

1. A single colony of *B. velezensis* FZB42 was picked to inoculate DEV nutrient medium (meat extract 10.0 g/L, meat peptone 10.0 g/L and sodium chloride 5.0 g/L; adjusted to pH 7.3 with NaOH).
2. The culture was grown overnight at 37°C at 160 rpm to an OD<sub>600</sub> of 0.2 in order to inoculate the rapeseed roots.

#### **2.1.6. Microbial inoculation and plant growth conditions**

1. Prior to inoculation, an approximately 2 cm arch was formed with the roots to prevent spreading of the microorganisms on the filter paper (Fig. 13).
2. Roots of 14-day-old seedlings were directly treated on filter paper with deionised water (control), OMG16, FZB42 or OMG16 plus FZB42.
  - a. For single fungal inoculation, plants were treated with 10 µL fungal spore suspensions (200 spores/root) directly dropped onto each arch of roots (drop inoculation).
  - b. For single bacterial inoculation, roots were inoculated with 10 µL FZB42 culture with an OD<sub>600</sub> of 0.23 (corresponding to approximately  $1.8 \times 10^8$  cells mL<sup>-1</sup>, as estimated by using <https://www.chem.agilent.com/store/biocalculators/calcODBacterial.jsp>).
  - c. For co-inoculation, single roots were inoculated with 20 µL mixture of OMG16 and FZB42 solution.

3. Five biological replicates were collected for each treatment.

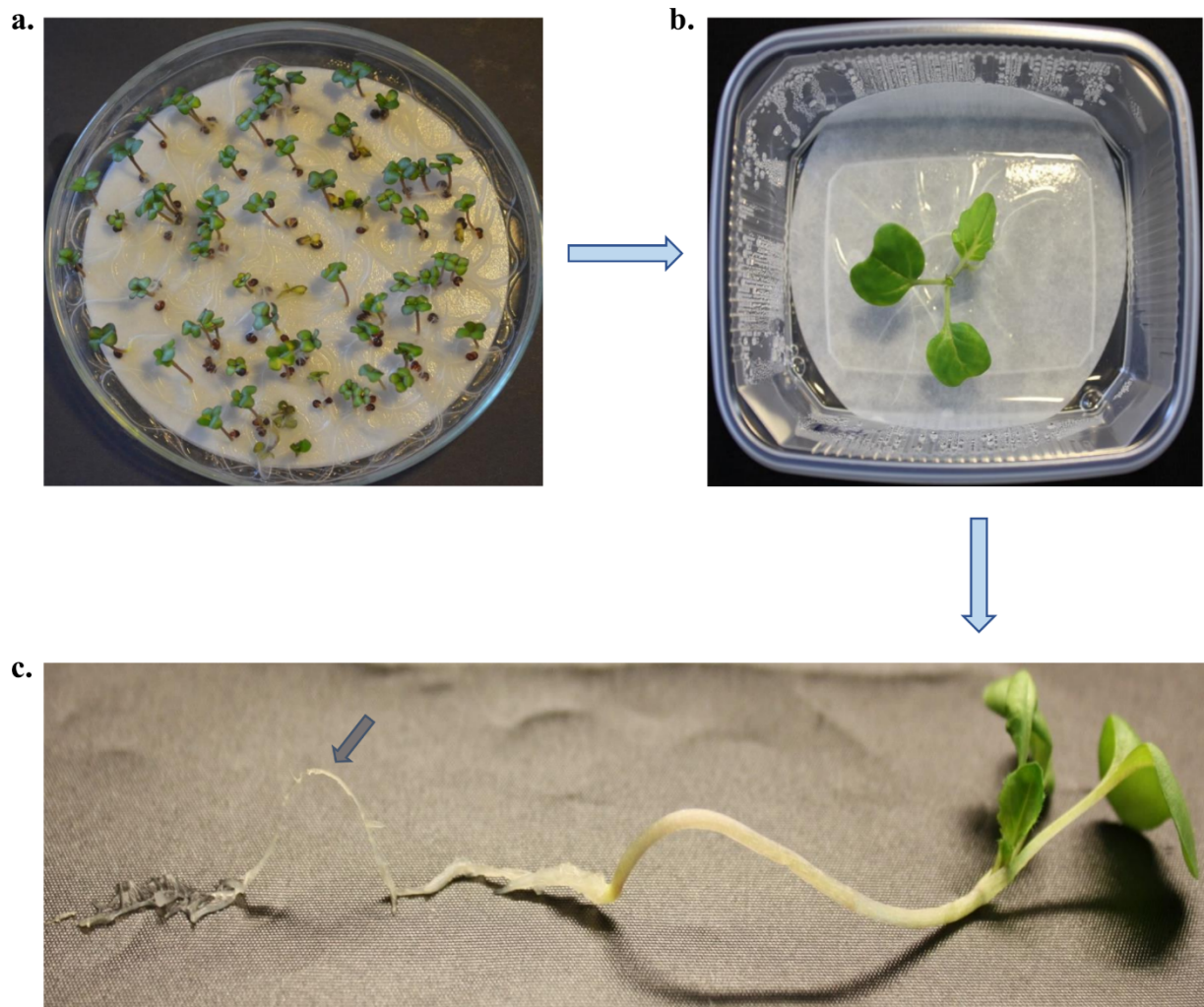


**Fig. 13.** Experimental setup for inoculation of *B. napus* plantlets. (a) Surface sterilized seeds were plated on filter paper wetted with deionized water and placed in sterile glass petri dishes for germination. (b) After 6 days, single seedlings were transferred into sterile boxes fitted with sterile filter paper soaked with half-strength Murashige and Skoog (MS) medium supplemented with 0.5% sucrose and 5.4  $\mu\text{M}$  NAA (1-naphthylacetic acid). The plant boxes were placed in an incubator and the plantlets were grown until they were two weeks old. (c) An arch was formed with the roots to inoculate the microbial cultures directly on the roots by drop inoculation.

## 2.2. Microscopy

To analyse rapeseed root colonization by *Trichoderma*, 14-day-old rapeseed seedlings were inoculated with OMG16 and M9B.

### 2.2.1. Root staining with fuchsine red solution

1. Prior staining, roots were separated from the stem with a sharp scalpel and thoroughly washed with tap water.
2. Then the roots were heated in 10% KOH for 3 min at 121°C.

3. After heating, roots were washed repeatedly in tap water.
4. Afterwards, roots were soaked in 1% HCl for 1 h.
5. Then the roots were incubated with fuchsin red solution (0.01% acidic fuchsin, 87.5% lactic acid and 6.3% glycerol in H<sub>2</sub>O) for 3 min at 121°C.
6. Lastly, stained roots were stored in 50% glycerol and visualized under a Zeiss Axio Observer 7 inverse microscope using the ZEN 2.0 Imaging Software (Carl Zeiss).

### 2.2.2. Transformation of fluorescence genes into *Trichoderma* protoplasts

To improve the visualization of root colonization mechanism by microscopic analysis, fluorescence proteins, enhanced green fluorescent protein, EGFP-coding gene *gfp* and red fluorescent protein, DsRed-coding gene *dsred* were separately transformed into the protoplast of *T. harzianum* OMG16 and *T. virens* M9B fungal strains.

#### 2.2.2.1. pBARGPE1-Hygro-EGFP plasmid

Plasmid pBARGPE1-Hygro-EGFP (Life Science Market, Hong Kong; product no. PVT5307) contains *egfp* gene under the control of the constitutive *Aspergillus nidulans* glyceraldehyde 3-phosphate promoter (PgpdA), the *A. nidulans* *trpC* transcriptional terminator (TrpC) and hygromycin B resistance gene for the selection of transformants (Fig. 14). The plasmid was transformed into OMG16 and M9B protoplast by a PEG-mediated transformation process.

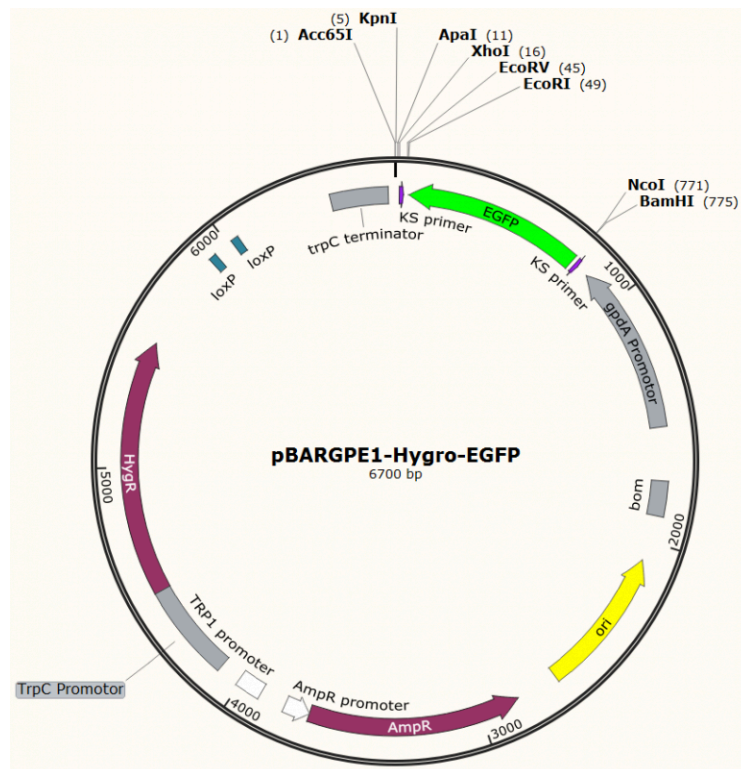


**Fig. 14.** pBARGPE1-Hygro-EGFP plasmid map. (Picture taken from Life Science Market, 2018).



#### **2.2.2.1.1. Stock solution of pBARGPE1-Hygro-EGFP plasmid**

1. The vial of pBARGPE1-Hygro-EGFP plasmid stock solution (2  $\mu\text{g}$ ) purchased from the commercial distributor was centrifuged at  $6,000 \times g$  for 1 min at  $4^\circ\text{C}$ .
2. Lyophilized plasmid (2  $\mu\text{g}$ ) was reconstituted in 20  $\mu\text{L}$  of sterile TE buffer to a final concentration 100  $\text{ng } \mu\text{L}^{-1}$ .
3. The lid was closed, and the vial was vortexed for 1 min.

#### **2.2.2.1.2. Working solution of pBARGPE1-Hygro-EGFP plasmid**

To prepare the working solution, a 1:10 dilution of the stock solution was performed using nuclease-free water to a final concentration of 10  $\text{ng } \mu\text{L}^{-1}$ . Transformation of the plasmid DNA performed directly after completion of this step.

#### **2.2.2.1.3. Transformation of competent *E. coli* cells (adapted from the protocol of Thermo Fisher Scientific)**

1. *E. coli* DH5 $\alpha$  competent cells (Fisher Scientific, product no. 18258012) were thawed on ice. 1.5 mL microcentrifuge tubes were placed on ice.
2. The cells were mixed gently, then 20  $\mu\text{L}$  of competent cells were aliquoted into chilled polypropylene tubes.
3. 1  $\mu\text{L}$  of the plasmid DNA (10  $\text{ng DNA}$ ) was added to 20  $\mu\text{L}$  competent cell, the pipette was being moved through the cells while dispensing. Tubes were gently tapped to mix.
4. The mixture was incubated on ice for 30 min.
5. The tubes were transferred to a heating block preheated at  $42^\circ\text{C}$  for 45 s.
6. The tubes were transferred back to ice and incubated for another 2 min.
7. 0.9 mL room temperature S.O.C. Medium was added to the experimental reactions and incubated for 10 min at room temperature.
8. The tubes were then incubated at  $37^\circ\text{C}$  for 1 h on a shaker at 225 rpm.
9. 250  $\mu\text{L}$  cells were plated with 100  $\mu\text{L}$  ampicillin on an MLB plate.
10. The plate was incubated at  $37^\circ\text{C}$  overnight.

#### **2.2.2.1.4. Colony PCR of *E. coli* DH5 $\alpha$ /pBARGPE1-Hygro-EGFP transformants**

Transformed *E. coli* DH5 $\alpha$ /pBARGPE1-Hygro-EGFP colonies were analysed by colony PCR to confirm the transformation.

1. Single colonies were taken in PCR tubes with a sterile inoculation loop and dissolved each of them very well in 6  $\mu\text{L}$  nuclease free water.
2. The tubes were incubated at  $99^\circ\text{C}$  for 10 min in a thermocycler.
3. The following components were added into a PCR tube:

**Table 1: Components for colony PCR of *E. coli* DH5 $\alpha$ /pBARGPE1-Hygro-EGFP**

Components	Conc. of stock solution	Volume
DreamTaq Green PCR Master Mix (2 X) (Thermo Fisher Scientific)	2 X	10 $\mu$ L
Primer EGFP forw.	10 $\mu$ mol L <sup>-1</sup>	2 $\mu$ L
Primer EGFP rev.	10 $\mu$ mol L <sup>-1</sup>	2 $\mu$ L
Nuclease free H <sub>2</sub> O		4 $\mu$ L
Template (dissolved colony)		2 $\mu$ L

\*pBARGPE1-Hygro-EGFP plasmid DNA obtained from the commercial distributor was included in the reaction as a positive control.

4. The tubes were placed in the thermocycler, and the following PCR program was used:

**Table 2: Cycling instructions for colony PCR of *E. coli* DH5 $\alpha$ /pBARGPE1-Hygro-EGFP**

Step	Temperature	Time	Cycle
Initial Denaturation	94°C	3 min	1
Denaturation	94°C	30 s	} 3
Annealing	65°C	30 s	
Extension	72°C	30 s	
Denaturation	94°C	30 s	} 3
Annealing	64°C	30 s	
Extension	72°C	30 s	
Denaturation	94°C	30 s	} 3
Annealing	63°C	30 s	
Extension	72°C	30 s	
Denaturation	94°C	30 s	} 3
Annealing	62°C	30 s	
Extension	72°C	30 s	
Denaturation	94°C	30 s	} 3
Annealing	61°C	30 s	
Extension	72°C	30 s	
Denaturation	94°C	30 s	} 30
Annealing	60°C	30 s	
Extension	72°C	30 s	
Final Extension	72°C	10 min	1

5. The fragments were separated by 0.8% agarose gel electrophoresis and the transformed colony was selected. Length of the amplified fragment of *egfp* gene was 787 bp.
6. 10 mL of LB medium was inoculated with the selected transformed colony and incubated overnight at 37°C on a rotary shaker at 150 rpm.
7. After overnight incubation, the culture was used to isolate plasmid DNA with QIAprep® Spin Miniprep Kit (Qiagen) according to the following protocol.

**2.2.2.1.5. Mini preparation of plasmid DNA (modified from the protocol of Qiagen)**

1. 5 mL bacterial overnight culture was pelleted by centrifugation at >8000 rpm (6800 × g) for 3 min at room temperature.
2. Pelleted bacterial cells were resuspended in 250 µL buffer P1 and transfer to a microcentrifuge tube.
3. 250 µL buffer P2 was added and mixed thoroughly by inverting the tube 4-6 times until the solution became clear. The lysis reaction should not be allowed to proceed for more than 5 min.
4. 350 µL buffer N3 was added and mixed immediately and thoroughly by inverting the tube 4-6 times.
5. The mixture was centrifuged for 10 min at 13,000 rpm (~17,900 × g) in a table-top microcentrifuge.
6. 800 µL supernatant was applied from step 5 to the QIAprep 2.0 spin column by pipetting.
7. The column was centrifuged for 45 s and the flow-through was discarded.
8. The QIAprep 2.0 spin column was washed by adding 0.5 mL buffer PB, centrifuged for 45 s and the flow-through was discarded.
9. The QIAprep 2.0 spin column was washed by adding 0.75 mL buffer PE, centrifuged for 45 s and the flow-through was discarded.
10. The QIAprep 2.0 spin column was transferred to the collection tube, centrifuged for 1 min to remove residual wash buffer.
11. The QIAprep 2.0 column was placed in a clean 1.5 mL microcentrifuge tube.
12. To elute DNA, 40 µL buffer EB (10 mM TrisCl, pH 8.5) was added to the centre of the QIAprep 2.0 spin column, incubated for 1 min, and centrifuged for 1 min.
13. To analyse the extracted DNA on a gel, 1 volume of loading dye (provided) was added to 5 volumes of purified DNA. The solution was mixed by pipetting and load into 0.8% agarose gel.

### 2.2.2.2. pCAMDsRed plasmid

The pCAMDsRed plasmid (Eckert et al. 2005) transformed into *E. coli* K-12 was obtained from Fungal Genetic Stock Centre (FGSC), Kansas State University, Manhattan, USA. The plasmid contained *dsred-express* gene under the control of PgpdA promoter and TrpC terminator and hygromycin resistance gene (*hph*) (Fig. 15).

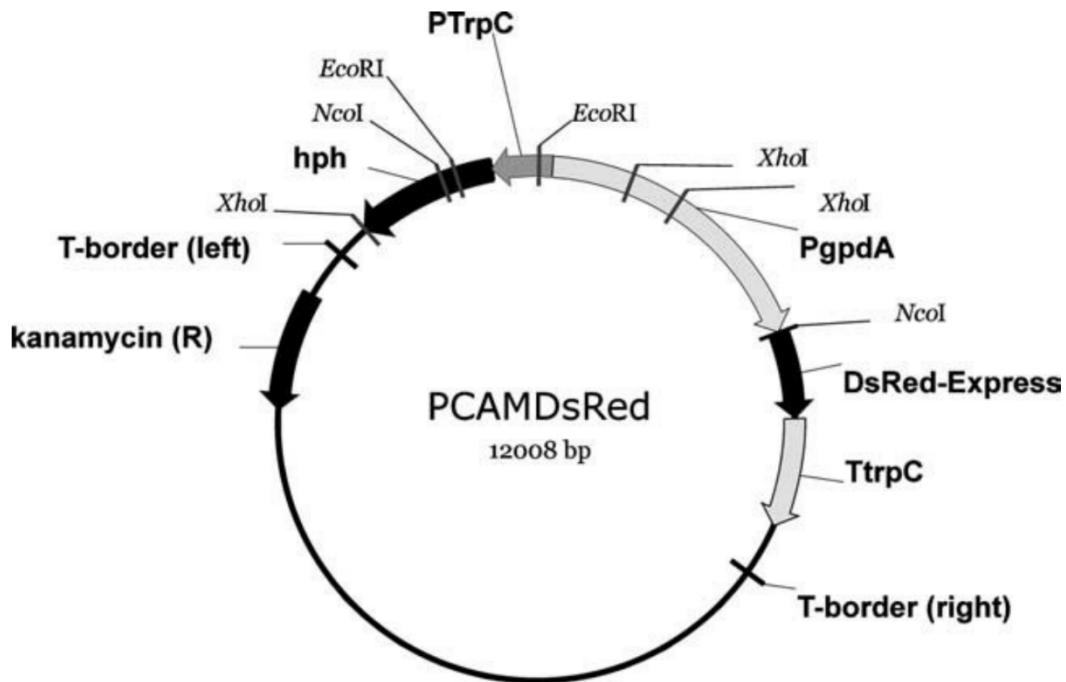


Fig. 15. pCAMDsRed plasmid map. (Picture taken from Eckert et al. 2005).

1. 20 mL of LB medium was inoculated with *E. coli* K-12/pCAMDsRed and incubated overnight at 37°C at 120 rpm.
2. LB agar plate containing 100 µg mL<sup>-1</sup> of kanamycin was inoculated with the overnight culture by streak plate technique and the plate was incubated overnight at 37°C.

Moreover, *B. velezensis* FZB42 strains transformed with the *gfp* gene was obtained from AbiTep Ltd., Berlin.

#### 2.2.2.2.1. Colony PCR of *E. coli* K-12/pCAMDsRed

*E. coli* K-12/pCAMDsRed colonies were analysed by colony PCR to select the transformants.

1. Single colonies were taken in PCR tubes with a sterile inoculation loop and dissolved each of them very well in 10 µL nuclease free water.
2. The tubes were incubated at 99°C for 10 min in a thermocycler.
3. The following components were added into a PCR tube:

Table 3: Components for colony PCR of *E. coli* K-12/pCAMDsRed

Components	Conc. of stock solution	Volume
DreamTaq Green PCR Master Mix (2 X) (Thermo Fisher Scientific)	2 X	10 µL
Primer DsRed forw.	10 µmol L <sup>-1</sup>	2 µL
Primer DsRed rev.	10 µmol L <sup>-1</sup>	2 µL
Nuclease free H <sub>2</sub> O		4 µL
Template (dissolved colony)		2 µL

\* pCAMDsRed Plasmid DNA obtained from the FGSC was included in the reaction as a positive control.

4. The tubes were placed in the thermocycler, and the following PCR program was used:

**Table 4: Cycling instructions for colony PCR of *E. coli* K-12/pCAMDsRed**

Step	Temperature	Time	Cycle
Initial Denaturation	94°C	3 min	1
Denaturation	94°C	30 s	} 3
Annealing	70°C	30 s	
Extension	72°C	30 s	
Denaturation	94°C	30 s	} 3
Annealing	69°C	30 s	
Extension	72°C	30 s	
Denaturation	94°C	30 s	} 3
Annealing	68°C	30 s	
Extension	72°C	30 s	
Denaturation	94°C	30 s	} 30
Annealing	67°C	30 s	
Extension	72°C	30 s	
Final Extension	72°C	10 min	1

- The fragments were separated by 0.8% agarose gel electrophoresis and the transformed colony was selected. Length of targeted *dsred* gene fragment was 579 bp.
- 10 mL of LB medium was inoculated with a single colony of *E. coli* K-12/pCAMDsRed and incubated overnight at 37°C on a rotary shaker at 150 rpm.

#### 2.2.2.2.2. Isolation of pCAMDsRed plasmid DNA

pCAMDsRed plasmid DNA was isolated from the overnight culture using QIAprep® Spin Miniprep Kit (Qiagen) according to the protocol mentioned in section 2.2.2.1.5.

### 2.2.2.3. Preparation of *Trichoderma* protoplasts

1. *T. harzianum* OMG16 and *T. virens* M9B strains were grown separately on PDA plates at room temperature.
2. Spore suspension was prepared by flooding 20-day-old plates with sterile distilled water and filtering the suspension through single layers of sterile Miracloth (Merck).
3. The amount of spores mL<sup>-1</sup> in the spore suspension was counted by hemocytometer and added an equal amount of double strength potato dextrose broth (PDB).
4. ~100 mL of the spore suspension was germinated overnight in a 500 mL Erlenmeyer flask by incubating at 28°C and 150 rpm.
5. The germinated spores that form a mycelial mat overnight were harvested by filtration through Miracloth, washed with 0.8 M mannitol (Sigma Aldrich).
6. The mycelia (~500 mg) were transferred into sterile 50 mL Falcon tubes containing 20 mL enzyme buffer (0.4 M mannitol, 20 mM KCl, 20 mM MES pH 5.7, 10 mM CaCl<sub>2</sub>) and 40 mg mL<sup>-1</sup> driselase (Sigma Aldrich), 30 mg mL<sup>-1</sup> lysing enzyme from *T. harzianum* (Sigma Aldrich), and 15 mg mL<sup>-1</sup> cellulose (Sigma Aldrich).
7. Prior to dissolving the enzymes in the buffer, the starch carrier was removed from driselase by incubating driselase mixed with 20 mL of 0.7 M NaCl on ice for 15 min, followed by centrifugation at 652 × g for 5 min.
8. The decanted driselase-NaCl suspension was added to other enzymes.
9. The protoplasts were released from mycelia through incubation at 28°C for 1 h on a shaker at 60 rpm and until enough protoplasts would release.
10. Protoplasts were separated from the mycelial residues by filtration through single layers of Miracloth into 50 mL Falcon tubes.
11. The protoplast solutions were centrifuged for 4 min at 652 × g at 20°C in a swing bucket centrifuge to pellet protoplasts.
12. Supernatants were removed and the protoplasts were washed with 20 mL of W5 buffer (154 mM NaCl, 125 mM CaCl<sub>2</sub>, 2 mM 2-morpholinoethanesulfonic (MES) pH 5.7 and 5 mM KCl).
13. The protoplast suspensions were centrifuged again at 652 × g for 4 min at 20°C.
14. Supernatants were removed and W5 buffer was added to adjust the protoplast concentrations to ~1 × 10<sup>6</sup> protoplasts mL<sup>-1</sup>.
15. The protoplasts were incubated on ice for 20 min.
16. Protoplast suspensions were centrifuged at 652 × g for 4 min at 20°C and the supernatants were removed.

17. The protoplast pellets were resuspended in MMg solution (0.4 M mannitol, 15 mM MgCl<sub>2</sub> and 200 mM MES pH 5.7) to a final concentration of  $2 \times 10^7$  protoplasts mL<sup>-1</sup>.
18. The protoplast solutions were incubated at room temperature for 10 min, before transformation.

#### **2.2.2.4. PEG-mediated transformation of *Trichoderma* protoplasts**

1. Each of 1 mL protoplast suspension isolated separately from *T. harzianum* OMG16 and *T. virens* M9B strains was aliquoted into four different 15 mL Falcon tubes on ice.
2. 2.5 µg of isolated plasmid DNA (pBARGPE1-Hygro-EGFP or pCAMDsRed) was added in two tubes, mixed well by slowly pipetting and incubated on ice for 30 min.
3. 1 mL of PEG buffer (Carl Roth) was added, mixed well by slowly pipetting and incubated at room temperature for 20 min.
4. 10 mL of melted PDA (55°C) was added to each Falcon tube, the solution was immediately mixed by inverting 4-5 times, and poured into 90-mm Petri dishes.
5. The solidified plates were overlaid with 15 mL of 1% water agar solution containing hygromycin B (Thermo Fisher Scientific) to a final concentration of 100 µg mL<sup>-1</sup>.
6. The transformation plates were incubated for 5 days at 25°C in the dark.
7. The transient transformants that show EGFP and DsRed fluorescence signals under microscope were transferred to fresh PDA plates containing 100 µg mL<sup>-1</sup> hygromycin for selection of stable transformants.
8. Transformants were continuously cultured for five consecutive generations on fresh PDA plates containing 100 µg mL<sup>-1</sup> hygromycin to obtain stable resistance against hygromycin B.

#### **2.2.2.5. Confirming the stability of the transformants by PCR**

1. 50 mL of PDB media was separately inoculated with agar blocks (2 cm<sup>2</sup>) containing the mycelia of *T. harzianum* OMG16/pCAMDsRed, *T. virens* M9B/pCAMDsRed and *T. virens* M9B/pBARGPE1-Hygro-EGFP respectively and incubated on a shaker in 25°C for 48 h.
2. Plasmid DNAs were isolated from the growing mycelia using QIAprep<sup>®</sup> Spin Miniprep Kit (Qiagen) according to the protocol mentioned in section 2.2.2.1.5.
3. Targeted sequences of *egfp* and *dsred* genes have been amplified by touchdown PCR mentioned in Tables 2 and 4.
4. Amplified fragments were separated by 0.8% agarose gel electrophoresis to examine the presence of *egfp* and *dsred* genes in the transformed colonies.

## **2.3. Molecular-standard techniques**

### **2.3.1. Isolation of genomic DNA from plants**

Total DNA was isolated from fresh plant materials with the DNeasy Plant Mini Kit (Qiagen) according to manufacturer's instruction

1. 60-80 mg of plant materials were weighted in a 2 mL tube. 400  $\mu$ L lysis buffer AP1 was added to the tube and mechanically homogenized in a FastPrep24 instrument (MP Biomedicals, Heidelberg, Germany) three times for 30 s at a speed of 6 m/s with 1.0 mm silica spheres and an additional 0.25-inch ceramic bead. Samples were incubated on ice for 1 min after each homogenization cycle.
2. 4  $\mu$ L RNase A (100 mg mL<sup>-1</sup>) was added, vortexed and incubated for 10 min at 65°C. The tube was inverted 2-3 times during incubation.
3. 130  $\mu$ L buffer P3 was added in the tube, briefly mixed and incubated for 5 min on ice.
4. The lysate was centrifuged for 5 min at 16,000  $\times$  g (14,000 rpm) and pipetted into a QIAshredder spin column placed in a 2 mL collection tube.
5. Tube was centrifuged for 2 min at 16,000  $\times$  g.
6. The flow-through was transferred into a new tube without disturbing the pellet if present. 1.5 volumes of buffer AW1 was added into the tube and mixed by pipetting.
7. 650  $\mu$ L of the mixture was transferred into a DNeasy Mini spin column placed in a 2 mL collection tube and centrifuged for 1 min at  $\geq 6000 \times$  g ( $\geq 8000$  rpm). The flow-through was discarded.
8. Step 7 was repeated with the remaining sample.
9. The spin column was placed into a new 2 mL collection tube. 500  $\mu$ L buffer AW2 was added onto the column, and centrifuged for 1 min at  $\geq 6000 \times$  g. The flow-through was discarded.
10. Another 500  $\mu$ L buffer AW2 was added and centrifuged for 2 min at 20,000  $\times$  g.
11. The spin column was transferred to a new 1.5 mL microcentrifuge tube. The spin column was removed from the collection tube carefully so that the column did not come into contact with the flow-through.
12. 100  $\mu$ L buffer AE was added onto the column for elution. The tube was incubated for 5 min at room temperature and centrifuged 1 min at  $\geq 6000 \times$  g.

### **2.3.2. Isolation of genomic DNA from fungus**

Genomic DNA of OMG16 fungus was isolated with the peqGOLD Fungal DNA Mini Kit (VWR) according to manufacturer's instruction.



1. 50 mL of PDB medium was inoculated with a piece of fungal mycelia containing agar block (2 cm<sup>2</sup>) and incubated at room temperature on a rotary shaker at 120 rpm.
2. 3-day-old mycelia was taken and briefly dried with soft tissue papers.
3. 60 mg of mycelia were weighted in a 2 mL tube. 400  $\mu$ L lysis buffer PL1 was added to the tube and mechanically homogenized in a FastPrep24 instrument (MP Biomedicals, Heidelberg, Germany) three times for 30 s at a speed of 6 m/s with 1.0 mm silica spheres and an additional 0.25-inch ceramic bead. Samples were incubated on ice for 1 min after each homogenization cycle.
4. 15  $\mu$ L RNase A (20 mg mL<sup>-1</sup>) was added to the tube and vortexed for 10 s to mix.
5. The mixture was incubated at 65°C for 30 min on a shaker at 650 rpm.
6. 100  $\mu$ L lysis buffer PL2 was added and vortexed for 5 s to mix.
7. The mixture was incubated on ice for 5 min.
8. Tube was centrifuged at maximum speed for 10 min.
9. A microfilter was placed into a fresh 2.0 mL collection tube. The supernatant was applied thoroughly to the microfilter and centrifuged for 1 min at 10,000  $\times$  g.
10. The microfilter and collection tube were discarded, and the flow-through liquid was placed in a new 1.5 mL microfuge tube.
11. 0.5 volumes (approx. 225  $\mu$ L) of DNA binding buffer was added to the cleared lysate and mixed well by pipetting.
12. The entire sample (including any precipitate that may have formed) was applied to a PerfectBind DNA column placed in a new 2.0 mL collection tube.
13. The column was centrifuged at 10,000  $\times$  g for 1 min to bind DNA.
14. Collection tube and the flow-through liquid were discarded.
15. The column was placed into a new 2.0 mL collection tube and 650  $\mu$ L of DNA wash buffer (completed with 1.5 volumes of absolute ethanol) was added.
16. The tube was centrifuged at 10,000  $\times$  g for 1 min. Collection tube and the flow-through liquid were discarded.
17. A new collection tube was taken, and the washing step described in step 15-16 was repeated with 650  $\mu$ L of DNA wash buffer.
18. The collection tube was centrifuged at 10,000  $\times$  g for 2 min to completely dry the column.
19. The column was placed into a sterile 1.5 mL microfuge tube and 50  $\mu$ L of elution buffer was added. The tube was incubated for 1 min at room temperature.

20. To elute DNA from the column, tube was centrifuged at  $6,000 \times g$  for 1 min at room temperature.

### 2.3.3. Isolation of genomic DNA from bacteria

Genomic DNA of *B. velezensis* FZB42 was isolated with the peqGOLD Bacterial DNA Mini Kit (VWR) according to manufacturer's instruction.

1. 10 mL of DEV nutrient media was inoculated with a single colony of *B. velezensis* FZB42 and incubated overnight at  $37^{\circ}\text{C}$  on a shaker at 130 rpm.
2. 2 mL of overnight culture was taken in a 2 mL tube and centrifuged for 10 min at  $4000 \times g$ .
3. The pellet was re-suspended in 100  $\mu\text{L}$  of TE buffer and 100  $\mu\text{L}$  of lysozyme solution ( $10 \text{ mg mL}^{-1}$ ) was added.
4. Cells were incubated for 45 min at  $30^{\circ}\text{C}$  on a shaker at 700 rpm.
5. Digested cells were centrifuged for 5 min at  $4000 \times g$  at room temperature.
6. Cell pellet was resuspended in 400  $\mu\text{L}$  DNA lysis buffer T, 20  $\mu\text{L}$  of a Proteinase K solution ( $10 \text{ mg mL}^{-1}$ ) and 15  $\mu\text{L}$  RNase A ( $20 \text{ mg mL}^{-1}$ ) was added.
7. Mixture was vortexed for 10 s to mix well and incubated at  $70^{\circ}\text{C}$  in 45 min on a shaker at 700 rpm for complete lysis.
8. 200  $\mu\text{L}$  DNA binding buffer was added and mixed well by pipetting.
9. A PerfectBind DNA column was assembled in a 2.0 mL collection tube.
10. The entire lysate was transferred into the column including any precipitate that may have formed to the PerfectBind DNA column and centrifuged at  $10,000 \times g$  for 1 min to bind DNA.
11. The flow-through and collection tube were discarded.
12. The column was placed into a fresh 2.0 mL collection tube and washed by adding 650  $\mu\text{L}$  of DNA wash buffer (completed with 1.5 volumes of 100% ethanol) and centrifuged at  $10,000 \times g$  for 1 min. Flow-through and collection tube was discarded.
13. The washing step was repeated as described in step 12 with another 650  $\mu\text{L}$  of DNA wash buffer.
14. The PerfectBind DNA column containing DNA was placed in the 2.0 mL collection tube and centrifuged for 2 min at  $10,000 \times g$  to dry the column matrix.
15. The column was placed into a sterile 1.5 mL microfuge tube and 50  $\mu\text{L}$  of elution buffer was added.
16. Tubes were incubated for 3 min at room temperature and centrifuged at  $6,000 \times g$  for 1 min to elute DNA from the column.

#### **2.3.4. Agarose gel electrophoresis**

1. 0.96 g agarose (0.9%) was weighted and transferred into a flask, 120 mL of 1X TAE buffer was added and the agarose was dissolved by heating in a microwave; the lid of the flask was kept partially opened.
2. The mixture was allowed cool to about 50°C then 5 µL of Rotisafe (Carl Roth) was added and mixed gently. The gel was poured, and the combs were inserted.
3. After the gel had solidified, the combs were removed, the gel was transferred into an electrophoresis chamber and 1X TAE buffer was added so that the gel was just covered.
4. A mixture of 10 µL DNA and 2 µL 6 X loading dye was loaded into the slots; 10 µL of GeneRuler 1 Kb DNA Ladder (Thermo Fisher Scientific) was also loaded.
5. A voltage of 6 V/cm was applied for 40-45 min.
6. The DNA was visualized with a UV transilluminator or a gel documentation system (Bio-Rad).

#### **2.3.5. Gel and PCR clean-up according to Wizard® SV Gel and PCR Clean-Up System (Promega)**

##### **1. Gel slice and PCR product preparation**

###### **A. Dissolving the gel slice**

- a. Following electrophoresis, PCR fragment was excised from gel and gel slice was placed in a 1.5 mL microcentrifuge tube.
- b. 10 µL membrane binding solution was added per 10 mg of gel slice. The tube was vortexed and incubated at 50-65°C until gel slice was completely dissolved.

###### **B. Processing PCR amplifications**

- a. An equal volume of membrane binding solution was added to the PCR amplification.

##### **2. Binding of DNA**

- a. SV Minicolumn was inserted into collection tube.
- b. Dissolved gel mixture or prepared PCR product was transferred to the Minicolumn assembly and incubated at room temperature for 1 min.
- c. The column was centrifuged at  $16,000 \times g$  for 1 min. Flow-through was discarded and Minicolumn was reinserted into collection tube.

##### **3. Washing**

- d. 700 µl membrane wash solution (70% ethanol added) was added to Minicolumn and centrifuged at  $16,000 \times g$  for 1 min. Flow-through was discarded and Minicolumn was reinserted into collection tube.

- e. Step d was repeated with 500  $\mu$ L membrane wash solution and centrifuged at 16,000  $\times$  g for 5 min.
- f. Flow-through was discarded and the column assembly was re-centrifuged for 1 min with the microcentrifuge lid open (or off) to allow evaporation of any residual ethanol.

#### 4. Elution

- g. Minicolumn was carefully transferred to a clean 1.5 mL microcentrifuge tube.
- h. 50  $\mu$ L of nuclease-free water was added to the Minicolumn and incubated at room temperature for 1 min. The column was centrifuged at 16,000  $\times$  g for 1 min.
- i. Minicolumn was discarded and DNA was stored at -20°C.

#### 2.3.6. DNA quantification

DNA was quantified using Qubit 3.0 Fluorometer with Qubit<sup>TM</sup> dsDNA Assay Kit (Thermo Fisher Scientific).

1. 1  $\mu$ L of Qubit<sup>®</sup> reagent and 199  $\mu$ L of Qubit<sup>®</sup> buffer was mixed by vortexing to prepare the working solution.
2. 10  $\mu$ L of standards from kit (standard A or B) were mixed separately with 190  $\mu$ L working solution in two new tubes.
3. 199  $\mu$ L working solution was added with 1  $\mu$ L sample and vortexed for 2-3 s.
4. Steps 1, 2 and 3 were performed under laminar flow hood.
5. The tubes (both standards and samples) were incubated at room temperature for 2 min.
6. Tubes containing the standard solution were first inserted in the Qubit<sup>®</sup> 3.0 Fluorometer and readings were taken. Same procedures were repeated for samples.
7. Data were recorded twice for each sample.

#### 2.4. Primer design

##### 2.4.1. Primers specific for *FZB42*, *AOC3* and *ERF2* genes

1. Initially, the primer sequences of *B. velezensis* FZB42 strain specific marker were taken from Maheshwari, (2011).
2. Primer sequences of two ISR genes, *AOC3* and *ERF2*, were obtained from Alkooranee et al. (2017).
3. The targets were amplified by PCR, sequenced (Microsynth Seqlab) and internal primer sequences were designed using the Primer 3 software (Rozen and Skaletsky, 2000).

##### 2.4.2. Primers for *BnaUbiquitin11*, *VSP2*, *OPR3* and *ICS1* genes

1. In order to design the primer pairs of *BnaUbiquitin11*, *VSP2*, *OPR3* and *ICSI* genes, a total of 5 sequences of *BnaUbiquitin11* gene transcripts, 2 sequences of *VSP2* transcripts, 4 sequences of *OPR3* transcripts and 12 sequences of *ICSI* gene transcripts were taken from NCBI database (<https://www.ncbi.nlm.nih.gov/>).
2. Consensus sequences were generated from 5, 2, 4 and 12 entries, respectively, using BioEdit Sequence Editor, version 7.0.5 (Ibis Biosciences: Carlsbad, CA, USA)
3. The consensus sequences were used to design primer pairs using the Primer 3 software.

#### 2.4.3. Molecular marker of OMG16 DNA

1. OMG16 strain specific primers were designed from a distinct *T. harzianum* OMG16 single-locus microsatellite region (AGT)<sub>13</sub> obtained from a draft genome sequence of OMG16 (unpublished) and used as a molecular marker for quantification of OMG16 DNA in root tissues. Its sequence is shown in Appendix 1.

#### 2.5. Quantification of OMG16 and FZB42 root colonization by qPCR

The relative amount of root-endophytic OMG16 fungal and FZB42 bacterial DNA inside rapeseed roots of both AgP1 and AgP4 cultivars were determined in total root DNA by qPCR using the absolute quantification approach based on standard curves.

1. An approximately 3 cm root section (root arch) was cut from drop-inoculated samples with a sharp scalpel, washed with sterile deionised water by vortexing for 30 s, rinsed with water, dried between soft tissue papers, and cut into small pieces.
2. Total DNA was isolated from approximately 50 mg of root segments of OMG16, FZB42 and OMG16 plus FZB42 inoculated plants with the DNeasy Plant Mini Kit (Qiagen) according to the procedure mentioned in section 2.3.1.
3. DNA quality was assayed on 0.9% agarose gels and concentrations were determined with the Qubit 3.0 Fluorometer using the Qubit<sup>TM</sup> dsDNA Assay Kit (Thermo Fisher Scientific).
4. For absolute quantification of OMG16 and FZB42 DNA present inside the rapeseed roots, qPCR was carried out. The following components were added into a PCR tube:

**Table 5: Components for qPCR reaction**

Components	Conc. of stock solution	Volume
PowerUp <sup>TM</sup> SYBR <sup>TM</sup> Green Master Mix (Applied Biosystems)	2 X	10 µL
Forward primer	5 µmol L <sup>-1</sup>	2 µL
Reverse primer	5 µmol L <sup>-1</sup>	2 µL

- |                               |                          |                        |
|-------------------------------|--------------------------|------------------------|
| Template (extracted root DNA) | 15 ng $\mu\text{L}^{-1}$ | 1.5 $\mu\text{L}$      |
| H <sub>2</sub> O              |                          | up to 20 $\mu\text{L}$ |
- Strain-specific markers for OMG16 (T.harz.SSRAGT13-F/R) and FZB42 (FZB42-F/R) were applied for absolute quantification of the resulting amplicons.
  - Amplifications were performed in a QuantStudio™ 5 Real-Time PCR System (Applied Biosystems) under the following conditions:

**Table 6: Cycling instructions for qPCR**

Step	Temperature	Time	Cycle
UGD activation	50°C	2 min	Hold
Dual-Lock™ DNA polymerase	95°C	2 min	Hold
Denaturation	95°C	1 s	} 40
Annealing/elongation	60°C for OMG16 / 63°C for FZB42	20 s	

- A melting curve was recorded with initial denaturation at 95°C for 1 s, annealing at 60°C for 20 s and finally a linear increase of the temperature from 60°C to 95°C with a rate of 0.1°C/s.
- qPCR was performed in technical quadruplicate for each biological replicate.
- Standard curves were determined with dilution series of pure OMG16 and FZB42 DNAs in the range of 10 ng to 1 pg.
- The absolute amount of OMG16 and FZB42 DNA in total root DNA was calculated from quantification cycles (Cq) using the standard curves.
- Copy numbers of OMG16 strain-specific genomic region were calculated from the absolute amount of OMG16 DNA.
- There were no cross reactions with any of the bacterial and/or plant DNAs used.

## 2.6. Determination of the pH of the medium

- 50 mL of ½ MS liquid medium (supplemented with 0.5% sucrose and 5.4  $\mu\text{M}$  NAA) was separately inoculated with 100  $\mu\text{L}$  FZB42 ( $\text{OD}_{600} = 0.22$ ), 2000 spores  $\text{mL}^{-1}$  OMG16 and mixture of OMG16 plus FZB42.
- The cultures were incubated at 20°C and 16 h light on a rotary shaker at 160 rpm.
- The pH of the media was measured with a pH meter on 1 day, 2 days and 3 days after inoculation.

## **2.7. Observation of root morphology**

Roots of two-week-old rapeseed seedlings were inoculated with OMG16, FZB42 and OMG16 plus FZB42 strains by drop inoculation or treated with distilled water for control according to the procedure described in section 2.1.6.

1. Five biological replicates were assigned for each treatment and cultivar and care was taken that seedlings of identical developmental stage and size were used for the experiment.
2. Root sections were separated from the green plant parts with a sharp scalpel.
3. Roots were harvested on three consecutive days after inoculation and stored in 30% (v/v) ethanol until further use.
4. The root systems were spread in a film of water in transparent Perspex trays and images were taken with a flat-bed scanner (Epson Expression 10000 XL, Tokyo, Japan).
5. Root morphological characteristics were measured with the WinRHIZO Pro V.2009c image analysis system (Reagent Instruments, Quebec, QC, Canada; WinRHIZO software release, 2009).
6. Afterwards, the roots were oven dried at 65°C for 48 h in order to assess the dry weights.

## **2.8. Gene expression studies upon beneficial microbial treatments by qRT-PCR**

### **2.8.1. Isolation of RNA (modified from the protocol of Qiagen)**

The green plant parts from root colonization experiments mentioned in section 2.5 were immediately transferred to -80°C on 1 h after inoculation (hai), and 1 day, 2 days and 3 days after inoculation (dai). Total RNA was isolated from leaves using the RNeasy® Plant Mini Kit (Qiagen) according to the following procedure:

1. Approximately 60 mg of plant materials was weighted.
2. 450 µL of RLT Qiagen lysis buffer and 1% β-Mercaptoethanol (Carl Roth) was added.
3. The plant material was ground in a speed mill (FastPrep 24, MP Biomedicals) two times for 30 s at a speed of 6 ms<sup>-1</sup> with 1.0 mm silica spheres and an additional 0.25-inch ceramic bead. Samples were incubated on ice for 1 min after each homogenization cycle.
4. The tube was centrifuged at maximum speed for 2 min and lysates were transferred into a QIAshredder spin column.
5. The column was centrifuged for 2 min at maximum speed
6. Approximately 350 µL clear lysates were obtained and DNase treatment was performed.
7. DNase digestion:

- a. ~350  $\mu\text{L}$  lysate was aliquoted into 7 tubes with 50  $\mu\text{L}$  each for DNase digestion.
- b. For 1 aliquot, 5  $\mu\text{L}$  10X Turbo DNase buffer and 1  $\mu\text{L}$  Turbo DNase (2 U  $\mu\text{L}^{-1}$ ) (TURBO DNA-free™ Kit, Thermo Fisher Scientific) was mixed.
- c. 6  $\mu\text{L}$  of this mixture was added to each aliquot (50  $\mu\text{L}$ ) and incubated 20 min at 37°C.
- d. 1  $\mu\text{L}$  Turbo DNase was added to each tube and incubated again for 10 min at 37°C.
8. All the 7 aliquots were mixed in a single tube (~400  $\mu\text{L}$ ) and 0.1 X volume of DNase Inactivation Reagent was added to stop the enzymatic reaction and to remove divalent cations.
9. The mixture was incubated at room temperature for 5 min and centrifuged for 1.5 min at 10,000 rpm.
10. The supernatant was taken and centrifuged again at 10,000 rpm for 1.5 min.
11. The supernatant was taken into a new microfuge tube.
12. 0.5 volume of 96% ethanol was added, mixed well by pipetting, and transferred to a RNeasy Mini spin column in a 2 mL collection tube.
13. The column was centrifuged for 15 s at  $8000 \times g$ .
14. The flow-through was discarded.
15. 700  $\mu\text{L}$  RW1 buffer was added to the RNeasy spin column
16. The column was centrifuged for 15 s at  $8000 \times g$
17. The flow-through was discarded
18. 500  $\mu\text{L}$  buffer RPE was added to the RNeasy spin column.
19. The column was centrifuged for 15 s at  $8000 \times g$ .
20. The flow-through was discarded
21. 500  $\mu\text{L}$  buffer RPE was added again to the RNeasy spin column.
22. Centrifuged for 2 min at  $8000 \times g$
23. The RNeasy spin column was placed in a new 2 mL collection tube (supplied) and centrifuged at full speed for 1 min to dry the membrane.
24. The RNeasy spin column was placed in a new 1.5 mL collection tube (supplied).
25. 40  $\mu\text{L}$  RNase-free water was directly added to the spin column membrane and incubated 2 min in room temperature.
26. The column was centrifuged for 1 min at  $8000 \times g$  to elute the RNA.
27. The RNA was immediately used for cDNA preparation or stored in -80°C.

### **2.8.2. RNA quantification**

RNA concentrations were quantified with a Qubit 3.0 Fluorometer using the Qubit RNA HS Assay Kit (Thermo Fisher Scientific) according to the protocol mentioned in section 2.3.6.



### 2.8.3. First-strand cDNA synthesis reaction

cDNA was synthesized from 1.2 µg total RNA using SuperScript™ IV First-Strand Synthesis System (Thermo Fisher Scientific) according to the following protocol:

1. Following components were combined in a PCR reaction tube

**Table 7: Components for annealing primers to template RNA**

Components	Volume (for 1 X)
50 µM Oligo d(T) <sub>20</sub> primer	1 µL
50 ng µL <sup>-1</sup> random hexamers	1 µL
10 mM dNTP mix	1 µL
Template RNA	1.2 µg
Nuclease free water	up to 13 µL

2. The components were mixed and briefly centrifuged.
3. The RNA-primer mix was heated at 65°C for 5 min, and then incubated on ice for at least 1 min.
4. Then the following components were combined in a reaction tube.

**Table 8: Components for preparing reverse transcription (RT) reaction mix**

Components	Volume (for 1X)
5 × SSIV buffer	1 µL
100 mM DTT	1 µL
Ribonuclease Inhibitor	4 µL

5. Components were mixed and briefly centrifuged.
6. This RT reaction mix was added to the annealed RNA reaction.
7. 1 µL (200 U µL<sup>-1</sup>) SuperScript RT IV enzyme was added to the tube.
8. The combined reaction mixture was incubated at 50°C for 10 min.
9. The reaction was inactivated by incubating it at 80°C for 10 min.
10. The RT reaction was immediately used for PCR amplification or stored at -20°C.

### 2.8.4. Quantification of cDNA concentration

cDNA concentrations were measured with a Qubit 3.0 Fluorometer using the Qubit ssDNA Assay Kit (Thermo Fisher Scientific) according to the protocol mentioned in section 2.3.6.

### 2.8.5. Touchdown and gradient PCR

1. The ideal annealing temperature (Table 18) of each primer pair was determined by performing touchdown PCR followed by a gradient PCR and adopted in qRT-PCR.

**Table 9: Components for touchdown and gradient PCRs**

Components		Conc. of stock solution	Volume
Phusion™ High-Fidelity Polymerase (Thermo Fisher Scientific)	DNA	2 U $\mu\text{L}^{-1}$	10 $\mu\text{L}$
Forward primer		5 $\mu\text{mol L}^{-1}$	2 $\mu\text{L}$
Reverse primer		5 $\mu\text{mol L}^{-1}$	2 $\mu\text{L}$
Template (cDNA)		10 ng $\mu\text{L}^{-1}$	1 $\mu\text{L}$
Nuclease free H <sub>2</sub> O			5 $\mu\text{L}$

2. Touchdown PCR was performed with the annealing temperature calculated from the melting temperatures ( $T_m$ ) of primers ( $\pm 2^\circ\text{C}$  of the  $T_m$  value).
3. Upon visualization of the amplified products after gel electrophoresis, a gradient PCR was performed to optimize the annealing temperature.

**Table 10: Cycling instructions for gradient PCR**

Step	Temperature	Time	Cycle	Grad ( $^\circ\text{C}$ )
Initial Denaturation	94 $^\circ\text{C}$	4 min	1	
Denaturation	94 $^\circ\text{C}$	30 s	} 35	( $\pm 2^\circ\text{C}$ )
Annealing	60 $^\circ\text{C}$	30 s		
Extension	72 $^\circ\text{C}$	30 s		
Final Extension	72 $^\circ\text{C}$	5 min	1	

4. The ideal annealing temperatures (Table 18) were selected for respective genes by visualizing strong, single bands on 1.7% agarose gel.

### 2.8.6. Determination of amplification efficiencies of primers

Relative standard curves with the amplification efficiencies of each primer pairs and melting curves of generated PCR products were determined and shown in Appendix 2.

#### 1. Determination of primer efficiencies by using genomic DNAs as template

- a. The amplification efficiencies of OMG16, FZB42 and VI43 specific T.harz.SSRAGT13-F/R, FZB42-F/R and OLG70/OLG71 primer pairs, respectively, were determined by preparing standard curves with dilution series of pure OMG16, FZB42 and VI43 DNAs in the range of 10 ng to 1 pg.

#### 2. Determination of primer efficiencies by using combined cDNAs as template

- a. The amplification efficiencies of *VSP2*, *LOX2* and *OPR3* primers were determined by preparing relative standard curves with dilution series of combined cDNA.

- b. cDNA was isolated from leaf, stem and root tissues of microbial inoculated plants as well as from non-inoculated control plants. 1  $\mu\text{L}$  of cDNA was taken from each sample and mixed in a microfuge tube.
- c. The concentration of the combined cDNA sample was measured with a Qubit 3.0 Fluorometer using the Qubit ssDNA Assay Kit (Thermo Fisher Scientific) according to the protocol mentioned in section 2.3.6.
- d. This combined cDNA was diluted in the range of 100 ng to 1 ng and used as templates to prepare the relative standard curves.

### 3. Determination of primer efficiencies by using PCR products as template

- a. Amplification efficiencies of *BnaUBQ11*, *BnaActin*, *BnaTubulin*, *PDF1.2*, *ERF2*, *AOC3*, *ACS2*, *ACO4*, *ICS1*, *PR1* primer pairs were determined by using amplified PCR products as templates.
- b. The following components were placed in a PCR tube:

**Table 11: Components for PCR**

Components			Conc. of stock solution	Volume
Phusion™	High-Fidelity	DNA	2 U $\mu\text{L}^{-1}$	10 $\mu\text{L}$
Polymerase (Thermo Fisher Scientific)				
Forward primer			5 $\mu\text{mol L}^{-1}$	2 $\mu\text{L}$
Reverse primer			5 $\mu\text{mol L}^{-1}$	2 $\mu\text{L}$
Template (combined cDNA)			20 ng $\mu\text{L}^{-1}$	1 $\mu\text{L}$
Nuclease free H <sub>2</sub> O				5 $\mu\text{L}$

- c. The tubes were placed in the thermocycler and the following PCR program was used:

**Table 12: Cycling instructions for PCR**

Step	Temperature	Time	Cycle
Initial Denaturation	94°C	4 min	1
Denaturation	94°C	30 s	} 35
Annealing	60°C	30 s	
Extension	72°C	30 s	
Final Extension	72°C	5 min	1

- d. The fragments were separated by 1.7% agarose gel electrophoresis.
- e. Upon visualization of single band, the PCR products were purified.
- f. In case of multiple bands, appropriate bands were excised from the gel based on the expected length of the fragments.

- g. Both Gel and PCR products were purified by using Gel and PCR clean-up according to Wizard® SV Gel and PCR Clean-Up System (Promega) according to the protocol mentioned in section 2.3.5.
- h. Concentrations of the purified PCR products were measured with using Qubit 3.0 Fluorometer with Qubit dsDNA Assay Kit (Thermo Fisher Scientific) as mentioned in section 2.3.6.
- i. The PCR products were diluted in the range of 1 pg to 1 ag and used as templates to prepare the relative standard curves to access PCR efficiencies of primers in qRT-PCR.

### 2.8.7. Quantitative reverse transcription PCR (qRT-PCR)

Gene expression was analysed by qRT-PCR based on relative transcript abundances.

1. The following components were added into a PCR tube:

**Table 13: Components for qRT-PCR reaction**

Components	Conc. of stock solution	Volume
PowerUp™ SYBR™ Green Master Mix (Applied Biosystems)	2 X	10 µL
Forward primer	5 µmol L <sup>-1</sup>	2 µL
Reverse primer	5 µmol L <sup>-1</sup>	2 µL
Template (cDNA)	65 ng µL <sup>-1</sup>	1 µL
H <sub>2</sub> O		up to 20 µL

2. qRT-PCR reactions were performed in a QuantStudio™ 5 Real-Time PCR System (Applied Biosystems) and carried out in quadruplicate in 20 µL total volume under the following conditions:

**Table 14: Cycling instructions for qRT-PCR**

Step	Temperature	Time	Cycle
UGD activation	50°C	2 min	Hold
Dual-Lock™ DNA polymerase	95°C	2 min	Hold
Denaturation	95°C	1 s	} 40
Annealing/elongation	60°C		

3. After amplification, a melting curve was recorded with initial denaturation at 95°C for 15 s, annealing at 60°C for 1 min and finally a linear increase of the temperature from 60°C to 95°C with a rate of 0.1°C s<sup>-1</sup>.

### 2.8.8. Validation of reference genes

1. The expressions of the following reference genes in rapeseed were analysed by qRT-PCR to determine the steady state expression of these genes in current experimental conditions.

**Table 15: List of the primers of reference genes used in this study.**

Code	Sequence (5'-3')	Annealing Temp.	References
At1g17210_F	CTGCTTCATATGAATCACGAG	56°C	Working group of IBAS
At1g17210_R	TCAACACTATCTGCACGTTGT		
At2g19980_F	AATATTCACCGACGGAACG	58°C	Working group of IBAS
At2g19980_R	TAAGGCTTCTCCGTAAACCAA		
At2g20000_F	GTATAGTCCACCACCTT	58°C	Working group of IBAS
At2g20000_R	TCTTCTAGGTGCTTGAAGAGT		
AtUbiquitin11_F	GATGCAGATCTTCGTTAAGACT	60°C	Working group of IBAS
AtUbiquitin11_R	CCTTCCTTATCCTGGATCTTG		
AtEF1- $\alpha$ _F	TGAGCACGCTCTTCTTGCT	58°C	Working group of IBAS
AtEF1- $\alpha$ _R	GTGGCATCCATCTTGTTACA		
AtCyp1_F	GGATCCTGTCGATGGCGAAC	58°C	Working group of IBAS
AtCyp1_R	TCCACGACCTGCCCAAACAC		
AtCyp5_F	CTTCAGAGCTTTGTGCACAGG	58°C	Working group of IBAS
AtCyp5_R	AAGCTGGGAATGATTTCGATG		
AtActin7/8_F	GGTCGTACAACCGGTATTGT	58°C	Working group of IBAS
AtActin7_R	GATAGCATGTGGAAGTGAGAA		
AtActin8_R	GAAGAGCATACCCCTCGTA		
BnaActin7_1_F	GGAGCTGAGAGATTCCGTTG	61°C	Wu et al. 2019
BnaActin7_1_R	GAACCACCACTGAGGACGAT		
BnaActin7_2_F	TGGGTTTGCTGGTGACGAT	59°C	This study
BnaActin7_2_R	TGCCTAGGACGACCAACAATACT		
BnaActin_3_F	ATTCAGCCCCTTGTTTG TG	58°C	Yang et al. 2019
BnaActin_3_R	GTAAGCGTCTTTTGGACCCAT		
BnaActin_4_F	TGCTGGATTCTGGTGATGGTGTGT	58°C	Haddadi et al. 2019
BnaActin_4_R	CAGTGGTCGTA C TACTGGTATTG		
BnaActin_5_F	CCCTGGAATTGCTGACCGTA	60°C	Poveda et al. 2019
BnaActin_5_R	TGGAAAGTGCTGAGGGATGC		
BnaActin_6_F	ACGACAGCAGAGCGGGAAAT		

BnaActin_6_R	GGCTGGAACAGGACCTCTGG	60°C	Li et al. 2019
BnaEF1- $\alpha$ _F	GCCTGGTATGGTTGTGACCT	60°C	Feng et al. 2020
BnaEF1- $\alpha$ _R	GAAGTTAGCAGCACCTTGG		
BnaTubulin_F	CAGCAATACAGTGCCTTGAGTG	60°C	Feng et al. 2020
BnaTubulin_R	CCTGTGTACCAATGAAGGAAAGCC		
BnaPP2A_F	CAATGACGATGACGATGAGGTG	60°C	Behrens et al. 2019
BnaPP2A_R	ATGCTCAACCAAGTCACTCTCC		
BnaTMA7_F	TTCCTGTGTTTTATCCATGTAGCC	60°C	Zhao et al. 2019
BnaTMA7_R	CAGTCACTCTCCTACGAACATGATAG		
BnaCyp1_F	TGGAGCTGTACACCGACAAG	59°C	This study
BnaCyp1_R	CCTGGCACATGAAGTTAGGG		

2. *BnaUbiquitin11*, *BnaActin* and *BnaTubulin* (Table 18) were selected to serve as endogenous controls for normalization.

### 2.8.9. Calculation of relative transcript abundances

1. Relative transcript abundances of genes were calculated using the Pfaffl and Vandesompele methods (Pfaffl, 2001 and Vandesompele et al. 2002) and MIQE guidelines for qRT-PCR (Bustin et al. 2009).
2. Efficiency corrected Cq of three endogenous controls were averaged.
3.  $\Delta Cq$  was calculated as follows:

$$\Delta Cq = Cq \text{ reference genes} - Cq \text{ target gene}$$

## 2.9. Challenging rapeseed roots with pathogen

### 2.9.1. Fungal pathogen

1. Fresh spore suspension of *V. longisporum* 43 strain (V143) (Fig. 16) with a concentration of  $10^6$  spores  $\text{mL}^{-1}$  was provided by NPZ Innovation GmbH, Hohenlieth, Germany.
2. To prepare the spore suspension, V143 fungus was grown in potato dextrose broth for 7 days at 23°C on a rotary shaker at 100 rpm.
3. The spore suspension was harvested by filtering through sterile gauze.
4. Spore concentration was counted with a hemocytometer and adjusted to  $10^6$  spores  $\text{mL}^{-1}$ .



**Fig. 16.** Microscopic appearance of *in vitro* grown *V. longisporum* 43 conidia. Scale bar, 10  $\mu\text{m}$ .

### **2.9.2. Infection of rapeseed roots with VI43**

1. *B. napus* seeds of the AgP4 cultivar were grown following the procedure mentioned in section 2.1.1.
2. Two-week-old rapeseed seedlings were taken from the sterile boxes and incubated by root dipping for 30 min in a mixed suspension of OMG16 (2,000 spores  $\text{mL}^{-1}$ ) plus FZB42 ( $\text{OD}_{600} = 0.275$ , corresponding to approximately  $2.2 \times 10^8$  cells  $\text{mL}^{-1}$ ) or in sterile deionised water (control).
3. Subsequently, inoculated seedlings were placed back in the sterile boxes and incubated in a growth chamber with 16 h light ( $80 \mu\text{mol m}^{-2}\text{s}^{-1}$ ) and 8 h dark,  $20^\circ\text{C}$  and 60% relative humidity.
4. Two days after OMG16 plus FZB42 treatment, roots of the primed plants were infected by dipping into VI43 spore suspension ( $10^6$  spores  $\text{mL}^{-1}$ ) for 30 min or into deionised water (control). As positive controls, roots of non-primed AgP4 seedlings were infected by dipping in VI43 spores for 30 min.
5. For each treatment, three individual plants were pooled to obtain one biological replicate and five biological replicates were collected for each treatment.

### **2.9.3. Staining of VI43 infected rapeseed leaf tissue with royal blue dye**

1. Prior staining, leaves were separated from the stem with a sharp scalpel and thoroughly washed with tap water.
2. Then the leaves were dipped in blue staining solution (25% acetic acid and 10% royal blue ink from Rohrer and Klingner Leipzig-Co.) for 1 min.
3. Stained leaves were briefly washed with sterilize deionized water and examined under microscope.

#### 2.9.4. Quantification of VI43 DNA

1. Roots of VI43 infected primed and non-primed plants of AgP4 cultivar were harvested on 1 day, 2 days, 3 days and 5 days after infection (dai).
2. Roots were harvested by separating from the shoots with a sharp scalpel, washed in sterile deionized water by vortexing for 30 s and briefly dried with a soft tissue paper.
3. Cleaned roots were cut into small pieces and weighted to 60 mg.
4. Genomic DNA was isolated from roots using DNeasy Plant Mini Kit (Qiagen) as mentioned in section 2.3.1.
5. Prior to qPCR analysis, the following components were added into a PCR tube:

**Table 16: Components for qPCR reaction for VI43 quantification**

Components	Conc. of stock solution	Volume
PowerUp™ SYBR™ Green Master Mix (Applied Biosystems)	2 X	10 µL
OLG70 forward primer	5 µmol L <sup>-1</sup>	2 µL
OLG71 reverse primer	5 µmol L <sup>-1</sup>	2 µL
Template (root DNA)	15 ng µL <sup>-1</sup>	1 µL
H <sub>2</sub> O		up to 20 µL

6. qPCR reactions were performed in a QuantStudio™ 5 Real-Time PCR System (Applied Biosystems) and carried out in quadruplicate in 20 µL total volume under the following conditions:

**Table 17: Cycling instructions for qPCR to quantify VI43 DNA**

Step	Temperature	Time	Cycle
UGD activation	50°C	2 min	Hold
Dual-Lock™ DNA polymerase	95°C	2 min	Hold
Denaturation	95°C	20 s	} 36
Annealing	59°C	30 s	
Elongation	72°C	30 s	

7. After amplification, a melting curve was recorded with initial denaturation at 95°C for 15 s, annealing at 60°C for 1 min and finally a linear increase of the temperature from 60°C to 95°C with a rate of 0.1°C s<sup>-1</sup>.
8. Standard curve was determined with dilution series of pure VI43 DNA in the range of 10 ng to 1 pg.



9. The absolute amount of VI43 DNA in total root DNA was calculated from quantification cycles (Cq) using the standard curves.
10. There was no cross reaction of the VI43 primers with any of the fungal, bacterial and/or plant DNAs used.

#### **2.9.5. Relative expression of defence related genes after VI43 infection**

Relative expression of rapeseed defence genes upon VI43 pathogen challenge was analysed by qRT-PCR.

1. Total RNA was isolated separately from leaves, stems and roots of AgP4 cultivar by using the RNeasy® Plant Mini Kit (Qiagen) according to the procedure mentioned in section 2.8.1.
2. cDNA was synthesized from 1.5 µg total RNA using SuperScript™ IV First-Strand Synthesis System (Thermo Fisher Scientific) according to the protocol described in section 2.8.3.
3. qRT-PCR analysis was performed with 15 ng cDNA according to the protocol described in section 2.8.7.

#### **2.10. Determination of phytohormones by UHPLC-MS analysis (modified from Moradtalab et al. 2018)**

1. After microbial inoculation onto rapeseed roots of AgP4 genotype as mentioned in section 2.9.2, roots and shoots were harvested by cutting with a sharp scalpel and tissues were frozen separately into liquid nitrogen. There were 4 biological replicates, and 3 plants were pooled for each biological replicate.
2. 1 g of frozen tissue samples (shoot, roots) were ground to fine powder with liquid N<sub>2</sub> and extracted with 80% methanol (5 mL) using Falcon tubes.
3. Afterwards, the grounded tissues were further homogenized by ultrasonication (Micra D-9 homogenizer, Art, Müllheim Germany) for 1 min and 15 s at 10,000 rpm and then 2 mL methanol extracts were added to microtubes and centrifuged at 14,000 × g for 10 min.
4. Later, the supernatant (400 µL) was mixed with same amount of ultra-pure water and again centrifuged at 14,000 × g for 5 min.
5. The supernatant was cleaned by membrane filtration (Chromafil R O20/15 MS) and transferred to HPLC vials.
6. UHPLC-MS analysis was conducted in a Velos LTQ System (Thermo Fisher Scientific, Waltham, Massachusetts, USA) fitted with a Synergi Polar column, 4µL, 150 \* 3.0 mm,

(Phenomenex, Torrance, California, USA) for the measurement of JA and SA phytohormones.

7. 3  $\mu\text{L}$  volume was injected. The flow rate was adjusted to  $0.5 \text{ mL min}^{-1}$  for gradient elution with mobile phase (A): water and 5% acetonitrile; mobile phase (B): acetonitrile and a gradient profile of: 0-1 min, 95% A, 5% B, 11-13 min, 10% A, 90% B, 13.1 min, 95% A, 5% B, 16 min 95% A, 5% B.
8. All standard reference substances were purchased from Sigma Aldrich, (Sigma Aldrich, St. Louis, Missouri, USA) including (+/-)-jasmonic acid, salicylic acid.

### 2.11. Statistical analysis

All calculations were carried out with R software, version 4.0.2 (R Development Core Team, 2019).

In the root colonization experiment with OMG16, a Shapiro-Wilk normality test was performed. All data sets were normally distributed except the copy number of OMG16 at 1 dai in AgP4 cultivar. Thus, Wilcoxon Rank-Sum test was employed at  $P < 0.05$  at 1 dai in AgP4 cultivar and the rest of the data were analysed with Welch's t-test at  $P < 0.05$ .

Root colonization rate of FZB42 was also calculated by Wilcoxon Rank-Sum test at  $P < 0.05$ .

Observation of root morphology was analysed by Dunnett's test with multivariate testing (mvt) adjustment at  $P < 0.05$ .

Significant differences in transcript abundances in rapeseed leaves upon OMG16 and FZB42 root colonization were also calculated by Dunnett's test with mvt adjustment at  $P < 0.05$ . The differences in gene expression upon single and combined microbial treatments were analysed by one-way ANOVA with post-hoc Tukey's HSD tests.

Unpaired t-test was performed at  $P < 0.05$  for analysing the amount of VI43 in rapeseed roots. Significance of rapeseed defence gene expression after VI43 pathogen challenge was calculated by Dunnett's test with mvt adjustment at  $P < 0.05$  compared to the untreated control plants. Relative expression of genes between VI43 challenged primed and non-primed treatments was calculated by unpaired t-test at  $P < 0.05$ .

Significance of endogenous plant hormone concentrations was calculated by Dunnett's test with mvt adjustment at  $P < 0.05$  compared to the untreated controls. Phytohormone amount between VI43 challenged primed and non-primed plants was calculated by employing unpaired t-test at  $P < 0.05$ .

Significant differences were denoted using asterisks as follows: \*  $P < 0.05$ ; \*\*  $P < 0.01$ ; \*\*\*  $P < 0.001$ ; \*\*\*\*  $P < 0.0001$ .

## 2.12. Reagents

### 2.12.1. Primers

All primer sequences used in this study are given in Table 18.

**Table 18: List of primers used in this study.**

Code	Sequence (5'-3')	Amplicon length (bp)	Annealing Temp.	R <sup>2</sup>	Slope	Efficiency	References
EGFP_F	CGAGGTCGACGGTATCG	787	65-60°C	-	-	-	Life Science Market, 2018
EGFP_R	CGATACCGTCGACCTCG						
DsRed_F	CTCCTCCGAGGACGTCATCAA	579	70-67°C	-	-	-	Eckert et al. 2005
DsRed_R	ACGTAGTAGTAGCCGGGCAGCT						
T.harz.SSRA GT13-F	GCCACAGAGAGAAGCCAGTC	205	60°C	0.999	-3.303	100.8	Mpanga et al. 2019b
T.harz.SSRA GT13-R	GCGTCATGTCCCCATCTATC						
FZB42-F	TTGGATTAACAAGCGGTACCC	175	63°C	0.999	-3.458	94.6	This study
FZB42-R	CCTAGACCCGAAAGCCAAATG						
OLG70	CAGCGAAACGCGATATGTAG	261	59°C	0.998	-3.232	103.9	Eynck et al. 2007
OLG71	GGCTTGTAGGGGGTTTAGA						
BnaUbiquitin 11-F	AGGCCAAGATCCAAGACAAG	154	60°C	1.0	-3.402	96.8	This study
BnaUbiquitin 11-R	TAGAAACCTCCACGGAGACG						
BnaActin-F	ACGACAGCAGAGCGGGAAAT	188	60°C	0.999	-3.403	96.7	Li et al. 2019
BnaActin-R	GGCTGGAACAGGACCTCTGG						
BnaTubulin-F	CAGCAATACAGTGCCTTGAGTG	204	60°C	0.999	-3.367	98.2	Feng et al. 2020
BnaTubulin-R	CCTGTGTACCAATGAAGGAAAGCC						
PDF1.2-F	TCCATCATCACCCCTTCTCTTCGC	268	60°C	1.0	-3.356	98.6	Alkoorane et al. 2017
PDF1.2-R	CCATGTTGTGCTCCTTCAAGTCG						
ERF2-F	GTCCGACTTGAGTTGTATCACC	250	60°C	1.0	-3.419	96.1	This study
ERF2-R	CGTCTCAAACGTCCCTAACC						
AOC3-F	CTGACGAAGCTTCACTTGTC	230	60°C	0.999	-3.349	98.9	This study
AOC3-R	CCGGCGATCTCAAAAAGC						
VSP2-F	AAGGAGAGGAAGAAGCTGGTG	178	59°C	0.991	-3.222	104.3	This study
VSP2-R	GTGGATGCATGGGAACAAC						
LOX2_F	GTGGGTGCCATCAGAGTTTT	218	60°C	0.999	-3.476	93.95	Mamun et al. 2020
LOX2_R	GTCTCCAGCTCCTGTTTTCG						
OPR3_F	GGCAGTGATGAGGAAGAAGC	195	63°C	0.993	-3.467	94.3	This study
OPR3_R	CTTCGCACCAACCTTAAACC						
ACS2_F	AGGTGGTCAAAGACTTAGATAG	128	60°C	0.997	-3.302	100.8	Šašek et al. 2012
ACS2_R	ACCGAGTCGTTGTAAGAATA						
ACO4_F	CATTCTACAACCCTGGAAGCGAC	204	59°C	1.0	-3.387	97.3	

ACO4_R	ATGGTCCAACATTGTTGGCCAC						Zhao et al. 2009
ICS1_F	ACAGAGTGAAGGGCATGATG	236	60°C	1.0	-3.31	100.5	This study
ICS1_R	TCGAGGCCTAGTTGCAGC						
PR1_F	AAAGCTACGCCGACCGACTACGAG	97	59°C	0.999	-3.265	102.4	Alkoorancee et al. 2017
PR1_R	CCAGAAAAGTCGGCGCTACTCCA						

### 2.12.2. Buffer and solutions

**Enzyme buffer:** 0.4 M mannitol; 20 mM KCl; 20 mM MES (2-morpholinoethanesulfonic acid), pH 5.7; 10 mM CaCl<sub>2</sub>

**W5 buffer:** 154 mM NaCl; 125 mM CaCl<sub>2</sub>; 2 mM MES, pH 5.7; 5 mM KCl

**PEG solutions:** 40% PEG4000; 10 mM Tris-HCl, pH 8; 0.6 M KCl; 50 mM CaCl<sub>2</sub>

### 2.12.3. Media

**DEV nutrient medium:** 10 g L<sup>-1</sup> meat extract; 10 g L<sup>-1</sup> meat peptone; 5.0 g L<sup>-1</sup> NaCl, pH 7.3.

### **3. Results**

#### **3.1. Chapter I: Inoculation of rapeseed roots with plant beneficial fungi and bacterium and analysis of subsequent defence gene activation**

##### **3.1.1. Microscopic observation of root/fungus interactions**

Root-endophytic *Trichoderma* fungi often enter the plant cells and colonize the roots to establish an endosymbiotic relationship with various plant species which leads to growth promotion and enhanced immune response against pathogens (Tseng et al. 2020). In this study, two species of *Trichoderma* fungi were investigated to analyse the intracellular interactions between *Trichoderma* and rapeseed roots. Two-weeks-old rapeseed roots were inoculated separately with *T. harzianum* OMG16 and *T. virens* M9B strains and microscopic analysis was performed to confirm their presence in root cells.

##### **3.1.1.1. Interaction of *T. harzianum* OMG16 and rapeseed**

In order to elucidate the physical interactions between *T. harzianum* and rapeseed roots, microscopic analysis was conducted 24 h after inoculation and on the next two days, which revealed that OMG16 spores germinated, and hyphae were able to penetrate rapeseed root hairs. Chitin-specific staining revealed fungal coil-like structures inside the root hairs (Fig. 17b, c and d), which confirmed that hyphae were formed inside the colonised plant cells. The micrographs shown in Fig. 17 provide evidence that the OMG16 fungus used the root hair tips as entry point in root cells. With respect to that it is important to note that it was recently shown that fungi occasionally use root hair tips to enter plant cells (White et al. 2018). Taken together, these data confirmed the endophytic nature of OMG16 in rapeseed roots and its ability to develop distinct intracellular structures.

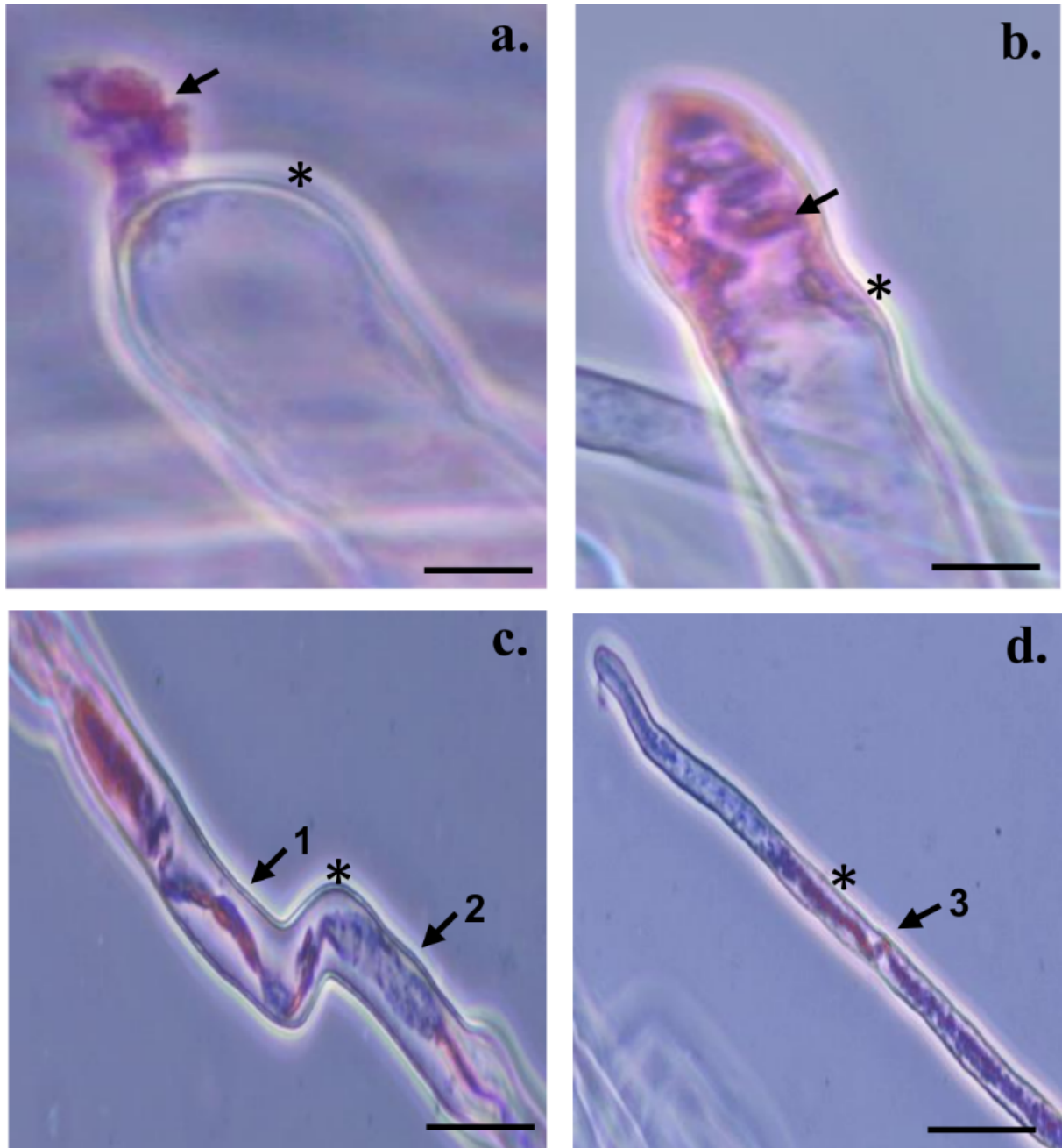


**Fig. 17.** Intracellular interactions between *T. harzianum* OMG16 and rapeseed. (a, b) OMG16 penetrating root hair tips. (c, d) Root hairs endophytically colonized with OMG16; 1. dense fungal cell wall, 2. loosened fungal cell wall, 3. coil-like structure. Arrows point to hyphae stained with acid fuchsin; asterisks indicate cell walls of root hairs. Roots of two-week-old plants were stained with acid fuchsin on 1 day (a, b), 2 days (c) and 3 days (d) after inoculation. Scale bars, 10  $\mu\text{m}$  (a-c) and 50  $\mu\text{m}$  (d).

### 3.1.1.2. Interaction of *T. virens* M9B and rapeseed

Alike *T. harzianum*, *T. virens* is also the opportunistic plant endophytic fungus, which possesses the abilities to colonize the inter- and intracellular spaces of both primary and secondary roots of numerous host plants. Such interactions result into induction of plant immune pathways which protect them against a broad spectrum of biotic and abiotic stresses (Illescas et al. 2021;

Nogueira-Lopez et al. 2018). Therefore, microscopic analysis was conducted in this study to confirm the intracellular interactions between *T. virens* and rapeseed roots on 2 days and 3 days after inoculation. Similar to OMG16, chitin-specific staining confirmed that spores of M9B fungus germinated, and the hyphae thrived to colonize the rapeseed roots on 2 days after inoculation (Fig. 18a). Micrographs presented in Fig. 18 also revealed that hyphae penetrated the root hairs and notably formed coil-like structures inside the root hairs (Fig. 18b). M9B hyphae also endophytically colonized the root epidermal cell layers by forming papilla-like structure on 3 dai (Fig. 18c). Papilla-like structure formation by *Trichoderma* hyphal tip in case of tomato root colonization was previously reported by Chacón et al. 2007.

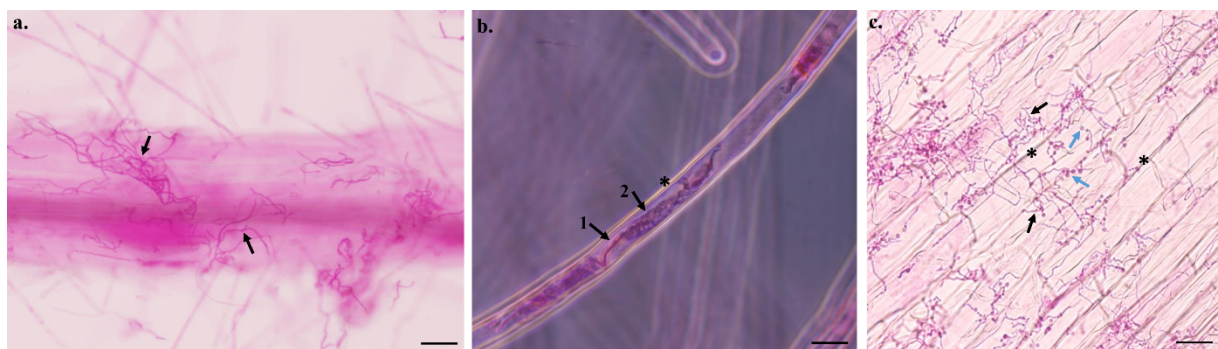


**Fig. 18.** Intracellular interactions between *T. virens* M9B and rapeseed. (a) M9B hyphae colonized the rapeseed roots. (b) Root hairs endophytically colonized with M9B. (c) M9B hyphae resided in root epidermal cell layer. 1. dense fungal cell wall, 2. loosened fungal cell wall. Black arrows point to hyphae stained with acid fuchsin, blue arrows point to papilla-like hyphal tips and asterisks indicate root cell walls. Roots of two-week-old plants were stained with acid fuchsin on 2 days (a, b) and 3 days (c) after inoculation. Scale bars, 100  $\mu\text{m}$  (a), 20  $\mu\text{m}$  (b) and 50  $\mu\text{m}$  (c).

### 3.1.1.3. Expression of fluorescence proteins in *Trichoderma* fungi

In plant-microbe interaction studies, transformation and expression of different fluorescent reporter genes into endophytic fungi have provided an excellent tool to identify the localization of microbes in plant cells (Bae and Knudsen, 2000; Lu et al. 2004). Constitutively expressed enhanced green fluorescent protein, EGFP and red fluorescent protein, DsRed are extensively used in molecular biology to easily detect the presence of living cells (Mikkelsen et al. 2003). Therefore, EGFP-encoding gene *gfp* and DsRed-encoding gene *dsred* were separately transformed into the protoplast of OMG16 and M9B fungal strains to improve the in-depth visualization of their rapeseed root colonization mechanism by microscopic analysis. *egfp* gene was cloned in *E. coli* DH5 $\alpha$  cells containing the pBARGPE1-Hygro-EGFP construct. While *dsred* gene was cloned in *E. coli* K-12 cells containing pCAMDsRed plasmid. Transformed *E. coli* DH5 $\alpha$ /pBARGPE1-Hygro-EGFP and *E. coli* K-12/pCAMDsRed cells were separately

grown in LB medium containing ampicillin and kanamycin, respectively for selecting transformants. Plasmid DNAs were isolated from both constructs. Both pBARGPE1-Hygro-EGFP and pCAMDsRed plasmids were separately transformed into either of the freshly prepared protoplast of OMG16 and M9B fungal strains by PEG-mediated transient transformation process. Transformed fungi were grown on PDA plates containing hygromycin B as a selection marker. Four different transformation was performed including *T. harzianum* OMG16+EGFP, *T. harzianum* OMG16+Ds-Red, *T. virens* M9B+EGFP and *T. virens* M9B+Ds-Red. Among them, mycelia of *T. harzianum* OMG16+EGFP, *T. virens* M9B+EGFP and *T. virens* M9B+Ds-Red fungi grew on hygromycin B containing PDA plates indicating successful transformation of *gfp* and *dsred* gene constructs into *Trichoderma*. Microscopic analysis was conducted to visualize the transformed hyphae *in vitro* on 2 days after transformation. Micrographs presented in Appendix 3a and b confirm that both EGFP and DsRed protein coding genes were individually transformed and expressed in M9B fungus. Both M9B and OMG16 transformants continuously grew on PDA media containing selection marker hygromycin B for five consecutive generations to obtain long-lasting transformation and substantially strong fluorescence signals under microscope. Nevertheless, after four generations of subculture, the drug resistance of both plasmids greatly lost activity and no stable transformants were detected neither in microscopic nor in colony PCR analysis.

Afterwards, two weeks old rapeseed roots were inoculated with the first generation EGFP transformed *T. harzianum* OMG16 fungus. Expression of EGFP in the colonized root cells was observed under fluorescence microscope on 7 days after root inoculation. Green fluorescence signals were detected in the root cells particularly in root hairs of rapeseed seedlings (Appendix 3c). However, high autofluorescence of rapeseed roots was detected as well, which severely impaired the detection of fluorescence signals obtained from EGFP transformed fungi.

### **3.1.2. Synergistic effects of fungus and bacterium**

Communities of rhizobacteria can synergistically interact with plant beneficial fungi to establish symbiotic association and develop the plant metabolic processes. Such bacterial association can enhance fungal spore germination, hyphal growth and root colonization ability (Sangwan and Prasanna, 2022). Moreover, together with fungi, these helper bacteria are able to activate plant defence genes more efficiently than single microbes (Karuppiyah et al. 2019a). At this point of the study, the root colonization rate and root development abilities of endophytic OMG16 fungal and FZB42 bacterial strains and their function in systemic activation of rapeseed defence genes were analysed.



### 3.1.2.1. Enhanced fungal root colonization rate in presence of *B. velezensis* FZB42

To assess synergistic interactions between *Trichoderma* and *Bacillus*, two-week-old rapeseed roots from *in vitro* cultivated plants were inoculated with either OMG16 or FZB42 alone or with both microorganisms in combination. Subsequently, the relative amount of the two microbes was quantified by qPCR at the same time points where root colonization was observed by microscopic analysis. To investigate the impact of co-colonization on different cultivars, the *Verticillium* susceptible cultivar AgP1 and the tolerant cultivar AgP4 were included in this experiment. In comparison with single inoculation, the presence of FZB42 increased the amount of OMG16 that entered root cells of both cultivars (Fig. 19). The difference was highly pronounced on the first day, where the copy number of OMG16 was increased more than 10-fold in the co-cultivation experiment compared to inoculation with *Trichoderma* alone. However, also on the next two days approximately 3-times more fungal DNA could be detected in co-inoculated plants than in seedlings treated only with OMG16.

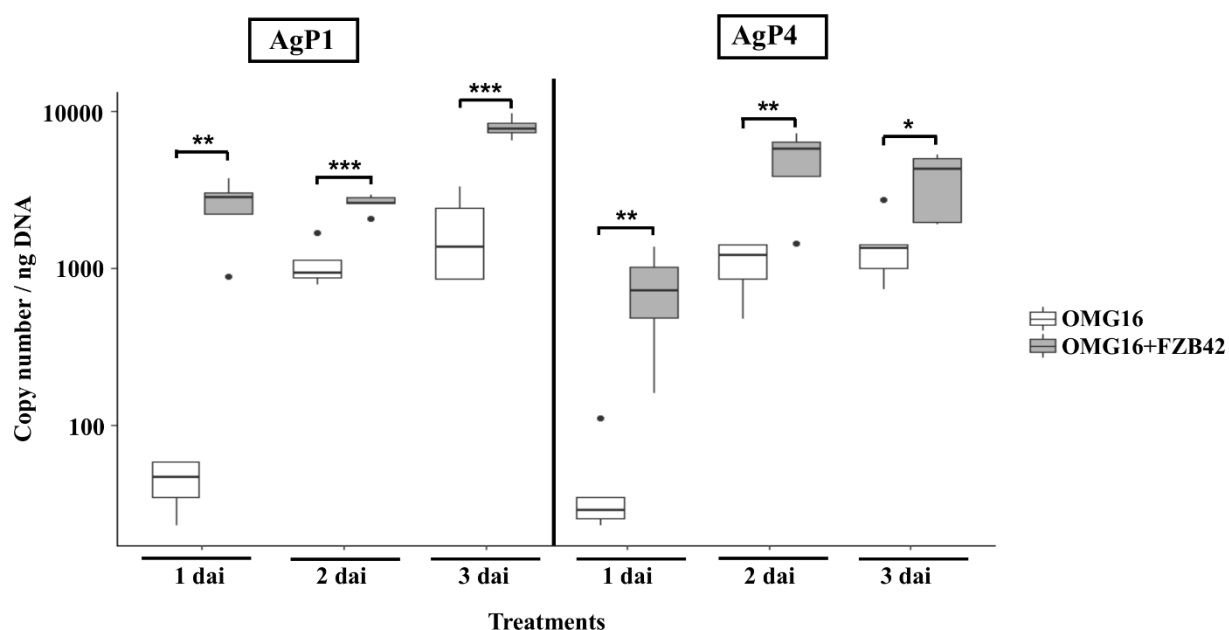


**Fig. 19.** Quantification of OMG16 in total root DNA. Two-week-old rapeseed roots of two cultivars (AgP1, left; AgP4, right) were inoculated with OMG16 and OMG16 plus FZB42. Copy numbers of OMG16 were determined by qPCR using the absolute quantification method. Welch's t-test was employed at  $P < 0.05$  after performing the Shapiro-Wilk normality test ( $n = 5$  plants in quadruplicate qPCRs; except OMG16 at 2 dai and 3 dai, OMG16+FZB42 at 3 dai in AgP1 and OMG16 at 2 dai in AgP4, where  $n = 4$  plants). All data sets were normally distributed except the copy number of OMG16 at 1 dai in AgP4. Therefore, Wilcoxon Rank-Sum test was employed at  $P < 0.05$  in this sample. \*  $P < 0.05$ ; \*\*  $P < 0.01$ ; \*\*\*  $P < 0.001$ . OMG16, *T. harzianum* OMG16; FZB42, *B. velezensis* FZB42; dai, days after inoculation.

### 3.1.2.2. Medium acidification caused by microbes

To assess whether acidification/alkalinisation of the medium changed due to single and dual inoculation, OMG16, FZB42 and OMG16 plus FZB42 were grown separately in half-strength MS medium and the pH was measured. We observed that FZB42 could acidify the growth medium by lowering the pH from 5.8 to 3.6 within 3 days. Also, in cultures co-inoculated with OMG16 and FZB42 the pH declined rapidly while in cultures inoculated with the fungus alone decrease of the pH-value was delayed (Fig. 20). This might, at least partially, explain FZB42-mediated growth enhancement of OMG16 since, as reported previously, *Trichoderma* growth optimal in the acidic pH range (Pelagio-Flores et al. 2017).

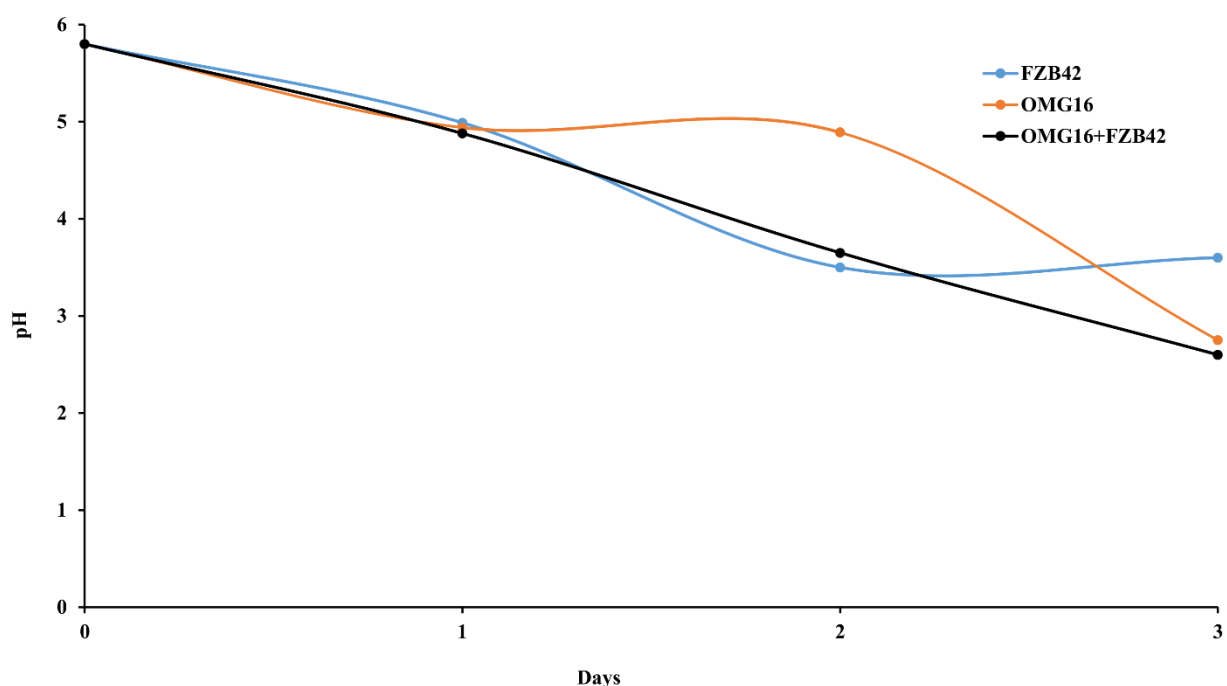


**Fig. 20.** Acidification of plant growth medium due to the presence of OMG16, FZB42 and OMG16 plus FZB42. Each of 50 mL half-strength MS liquid medium at pH 5.8 was separately inoculated with OMG16 ( $2,000 \text{ spores mL}^{-1}$ ), 100  $\mu\text{L}$  FZB42 culture at  $\text{OD}_{600}$  of 0.22 and OMG16 plus FZB42 inocula. The cultures were incubated at  $20^\circ\text{C}$  on a rotary shaker at 160 rpm with 16 h light. pH of the media was measured with a pH meter on 1 day, 2 days and 3 days after OMG16, FZB42 and OMG16 plus FZB42 inoculations. OMG16, *T. harzianum* OMG16; FZB42, *B. velezensis* FZB42.

### 3.1.2.3. Enhanced bacterial root colonization rate in presence of *T. harzianum* OMG16

In addition, the presence of OMG16 increased the root colonization rate of FZB42 significantly (Fig. 21). In AgP1 cultivar, the copy numbers of FZB42 were higher ( $P < 0.05$  on the first day, and  $P < 0.0001$  on the second and third day) in co-inoculated plants than in single FZB42 inoculation. Moreover, in AgP4, the FZB42 copy number increased in co-inoculated plants on

2 dai ( $P < 0.01$ ). This indicates that both microorganisms act synergistically to colonize the root system of *B. napus*.

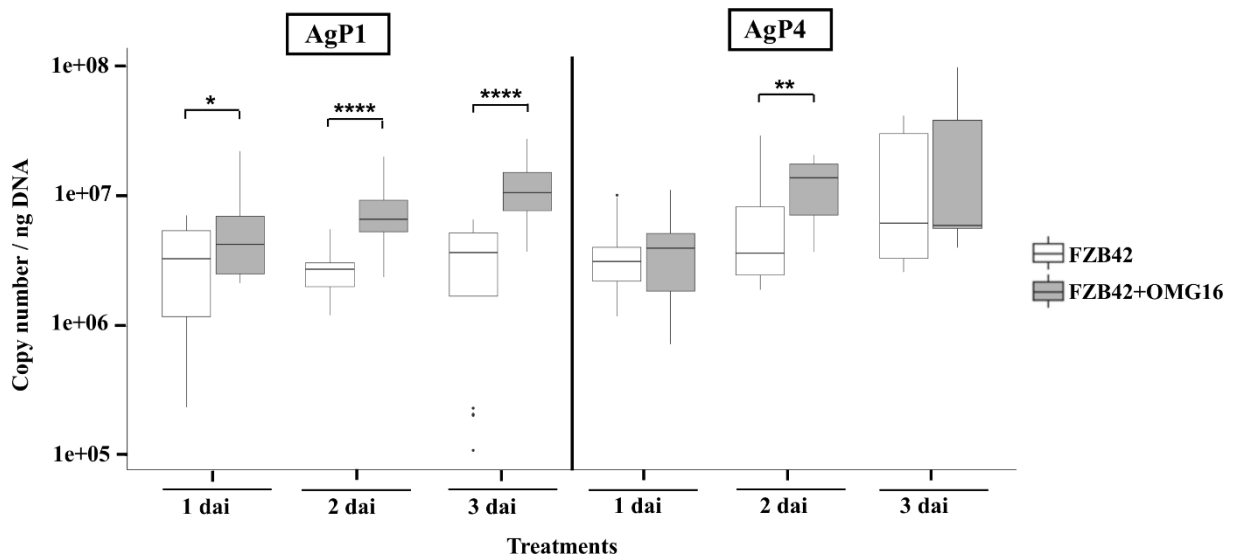
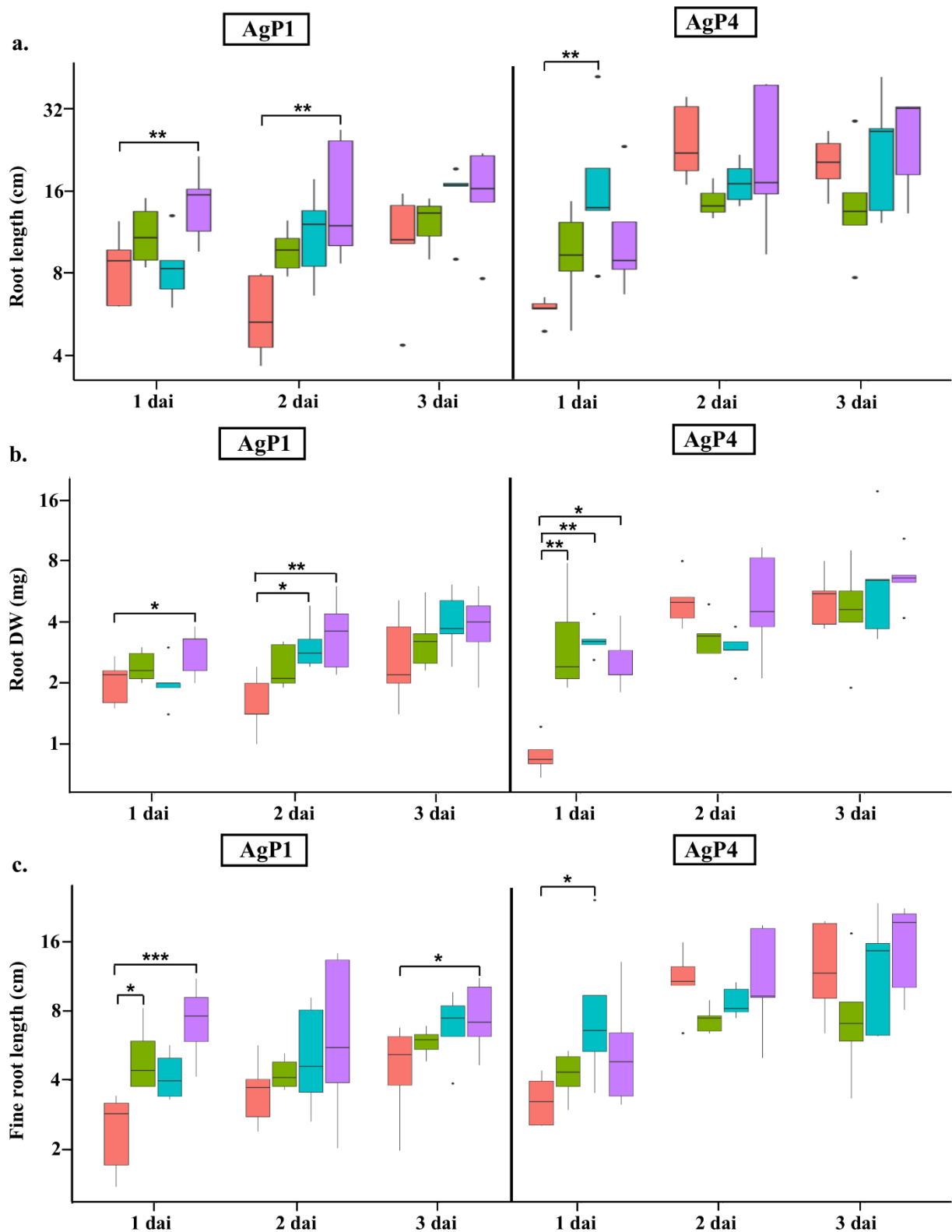


**Fig. 21.** Quantification of *B. velezensis* FZB42 DNA in two-week-old rapeseed roots from AgP1 (left) and AgP4 (right) cultivars inoculated with FZB42 and FZB42 plus OMG16. The absolute amount of FZB42 DNA present in total root DNA was quantified by qPCR using a single locus genomic region of FZB42 as target. Wilcoxon Rank-Sum test was employed at  $P < 0.05$ . Copy number values of FZB42 followed by asterisks (\*) were significantly higher (\*  $P < 0.05$ ; \*\*  $P < 0.01$ ; \*\*\*\*  $P < 0.0001$ ) in FZB42 plus OMG16 co-inoculation than in single FZB42 inoculation. FZB42, *B. velezensis* FZB42; OMG16, *T. harzianum* OMG16; dai, days after inoculation.

### 3.1.3. Effects of synergism on root morphology and growth

Several studies have reported that microorganisms can affect root growth and morphology. Thus, the effects of OMG16 and FZB42 were investigated in this study. Roots of two-week-old rapeseed seedlings of equal sizes were treated with combined and single inoculation or just treated with water as control and the subsequent changes in root morphology were digitised after optical scanning and evaluated with the WinRHIZO software. The total root length was higher in AgP1 cultivar co-inoculated with OMG16 and FZB42 in contrast to the untreated controls ( $P < 0.01$  in 1 and 2 dai) while in the AgP4 single OMG16 increased ( $P < 0.01$ ) the root length on 1 dai (Fig. 22a). Root dry weights increased in single OMG16 inoculated AgP1 plants on 2 dai ( $P < 0.05$ ) and in co-inoculated plants on 1 dai ( $P < 0.05$ ) and 2 dai ( $P < 0.01$ ). In AgP4 plants, root dry weights were higher in single OMG16 ( $P < 0.01$ ) and FZB42 ( $P < 0.01$ ) inoculated and in co-inoculated ( $P < 0.05$ ) plants on 1 dai compared to the control plants (Fig. 22b). Fine root length of AgP1 enhanced on 1 dai after FZB42 ( $P < 0.05$ ) treatment, while in co-inoculation, fine roots were longer on 1 dai ( $P < 0.001$ ) and 3 dai ( $P < 0.05$ ) compared to the control plants. In the AgP4 cultivar, fine roots were longer only in single OMG16 ( $P < 0.05$ )

inoculated plants (Fig. 22c). Moreover, in AgP1 plants, root volumes were higher in single OMG16 ( $P < 0.05$ ) and OMG16 plus FZB42 co-inoculated ( $P < 0.05$ ) plants on 2 dai. In AgP4, the root volumes were increased in single OMG16 ( $P < 0.05$ ) and FZB42 ( $P < 0.01$ ) treated plants on 1 dai (Fig. 22d).



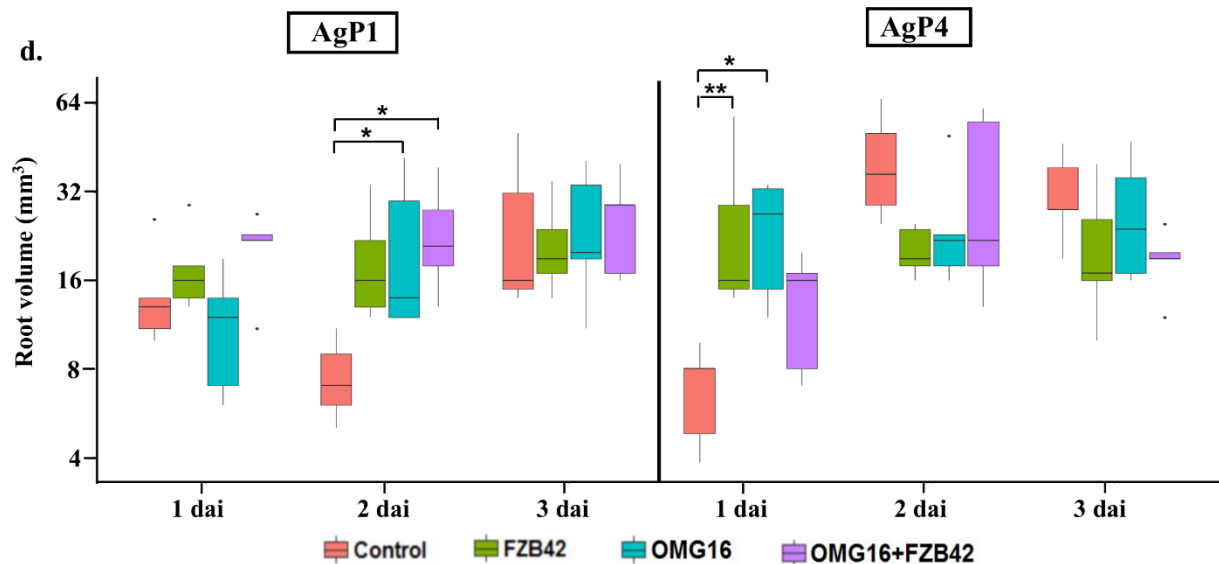


**Fig. 22.** Effects of OMG16 and FZB42 inoculation on root development. Two-week-old rapeseed roots from two different cultivars (AgP1 and AgP4) were treated with OMG16, FZB42 and OMG16 plus FZB42. Box and whisker plots show results of five biological replicates where statistical significance was calculated by Dunnett's test with multivariate testing (mvt) adjustment at  $P < 0.05$  compared to the untreated control plants; \*  $P < 0.05$ ; \*\*  $P < 0.01$ ; \*\*\*  $P < 0.001$ . OMG16, *T. harzianum* OMG16; FZB42, *B. velezensis* FZB42; dai, days after inoculation. Please mind the logarithmic scales of the y-axes.

### 3.1.4. Relative expression of rapeseed defence-related genes after OMG16 and FZB42 treatments

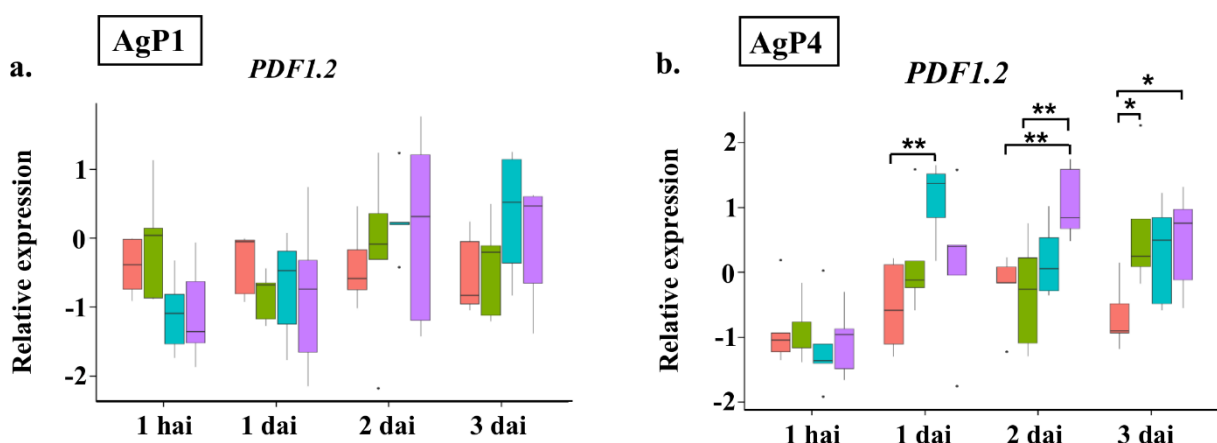
Rhizosphere associated beneficial fungi and bacteria systematically enhance plant defence mechanism through ISR system (Choudhary et al. 2007; Pieterse et al. 2014). Upon successful colonization of plant roots, microbes enhance JA and ET dependent signal transduction in host plants which is crucial for initiation of ISR pathway (Yu et al. 2022; Van Wees et al. 2008). Therefore, to assess the molecular mechanism of plant defence responses, the systemic induction of JA and ET responsive genes is to be in utmost importance to investigate.

To analyse whether synergistic effects of OMG16 and FZB42 co-inoculation might induce plant systemic resistance more efficiently than single microbe inoculation, 14-day-old rapeseed roots of both cultivars were treated with OMG16, FZB42 and OMG16 plus FZB42. The expression of JA/ET-responsive genes was measured in the leaves to confirm systemic responses in distant tissue from the microbial colonization site. This was performed at four different time points according to microscopic and root colonization observations: directly after inoculation (1 hour after inoculation, hai) and 1, 2 and 3 days after inoculation (dai) by qRT-PCR. *Allen oxide cyclase 3 (AOC3)* was selected as a marker of the JA pathway, *ethylene response factor 2 (ERF2)* as marker for ET signalling and *plant defensin 1.2 (PDF1.2)* as a combined marker for both pathways.

There was no change in the expression of *PDF1.2* in the AgP1 cultivar (Fig. 23a), whereas in AgP4, single application of OMG16 enhanced *PDF1.2* expression at 1 dai ( $P < 0.01$ ) compared to the untreated control plants (Fig. 23b). Relative expression of *PDF1.2* increased ( $P < 0.05$ ) as well in solely FZB42 treated plants on 3 dai. Transcript abundances were upregulated in OMG16 plus FZB42 treated plants on 2 dai ( $P < 0.01$ ) and 3 dai ( $P < 0.05$ ). Moreover, *PDF1.2* expression was enhanced on 2 dai ( $P < 0.01$ ) in OMG16 plus FZB42 co-inoculated plants compared to single FZB42 inoculation.

*ERF2* transcript levels increased in the AgP1 plants on day 2 after combined OMG16 and FZB42 treatment ( $P < 0.01$ ) compared to the untreated plants (Fig. 23c). On the other hand, in the AgP4 cultivar, relative transcript abundances of *ERF2* increased in solely OMG16-treated plants on 1 hai ( $P < 0.05$ ), 1 dai ( $P < 0.01$ ) and 3 dai ( $P < 0.01$ ). Inoculation with FZB42 alone enhanced the expression of *ERF2* on 1 hai ( $P < 0.05$ ) and 1 dai ( $P < 0.01$ ). *ERF2* expression was upregulated on 1 hai ( $P < 0.001$ ), 1 dai ( $P < 0.0001$ ) and 2 dai ( $P < 0.01$ ) in co-inoculated plants. Combined treatment of OMG16 and FZB42 enhanced *ERF2* expression on 2 dai ( $P < 0.05$ ) compared to single FZB42 application (Fig. 23d).

There were no significant differences in *AOC3* expression in the AgP1 cultivar (Fig. 23e). In contrast, in AgP4 single fungal inoculation upregulated *AOC3* expression at 1 dai, 2 dai and 3 dai ( $P < 0.01$  each) compared to the untreated plants. *AOC3* expression also enhanced in single OMG16 treated plants at 2 dai ( $P < 0.05$ ) compared to FZB42 treatment (Fig. 23f). Relative expression of *AOC3* increased in co-inoculated plants on 1 hai ( $P < 0.05$ ), 2 dai and 3 dai ( $P < 0.01$  each) compared to the untreated plants.



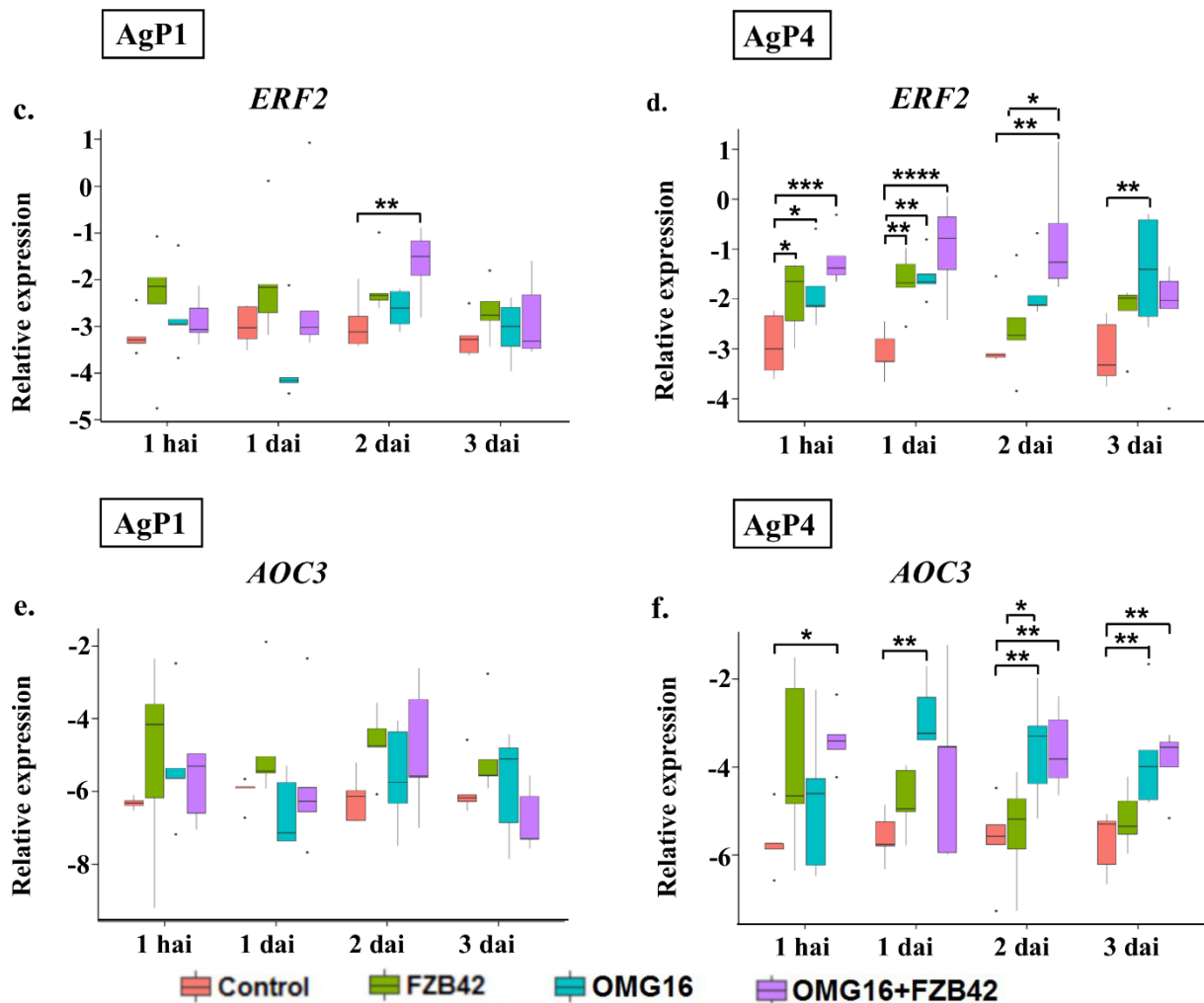


**Fig. 23.** Relative expression of rapeseed defence genes *PDF1.2*, *ERF2* and *AOC3* upon OMG16, FZB42 and OMG16 plus FZB42 inoculation. Roots of two-week-old plants were inoculated, and relative transcript abundances were analysed by qRT-PCR in leaves at 1 h (hai) and three consecutive days after root inoculation (dai). *BnaUbiquitin11*, *BnaActin* and *BnaTubulin* were used as endogenous controls for normalization. Box and whisker plots show  $\Delta Cq$  values of five plants with quadruplicate qRT-PCRs where significance of gene expression was calculated by Dunnett's test with multivariate testing (mvt) adjustment at  $P < 0.05$  compared to the control plants. To compare the differences in gene expression upon OMG16, FZB42 and OMF16 plus FZB42 treatments one-way ANOVA with post-hoc Tukey's HSD tests were performed. \*  $P < 0.05$ ; \*\*  $P < 0.01$ ; \*\*\*  $P < 0.001$ ; \*\*\*\*  $P < 0.0001$ . OMG16, *T. harzianum* OMG16; FZB42, *B. velezensis* FZB42, hai, hour after inoculation; dai, days after inoculation.

## 3.2. Chapter II: Pathogen challenge and analysis of defence activation upon priming

### 3.2.1. Infection of rapeseed roots with *V. longisporum* 43

The hemi-biotrophic pathogen *V. longisporum* infects rapeseed roots through wounds or by direct penetration of root hairs and intercellularly colonize the vascular system for successful disease establishment (Depotter et al. 2016).

To determine the substantial interactions between *Verticillium* and rapeseed, two-week-old rapeseed roots were infected with the spores of pathogenic fungus *V. longisporum* 43 strain. Microscopic analysis was carried out in leaves on 8 days after root infection with V143. Micrograph shown in Fig. 24 revealed the web of hyphae, sufficiently stained with blue ink, colonized the surface of rapeseed leaf. This confirmed that the used V143 spores were vital and virulent. Spores germinated and hyphae were able to penetrate rapeseed roots, colonized xylem and grew into the leaves via vascular system.

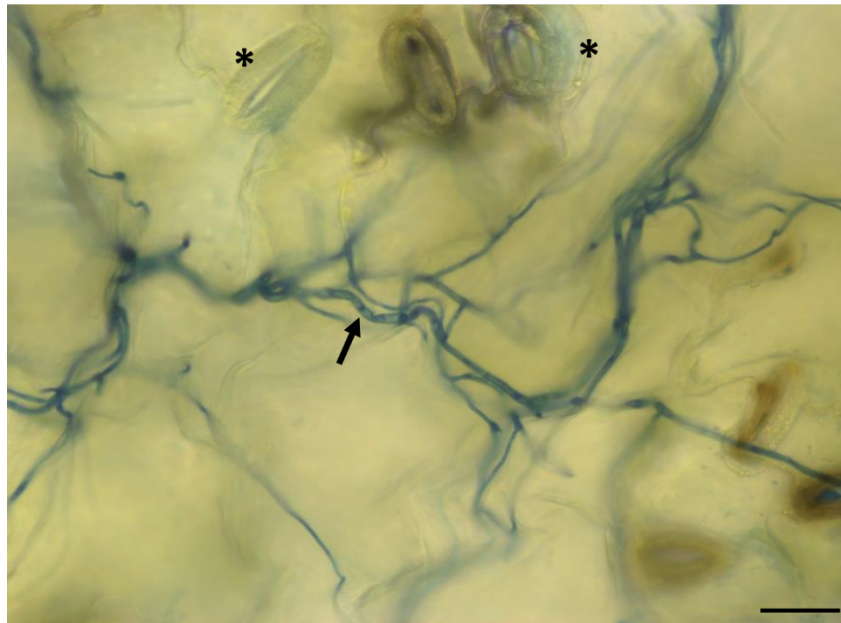


**Fig. 24.** Interactions between *V. longisporum* 43 and rapeseed. V143 hyphae endophytically colonized the rapeseed leaves. Arrows point to hyphae stained with blue ink; asterisks indicate stomata on leaf surface. Roots of two-week-old plants were infected with V143 spores and leaves were stained with royal blue ink on 8 days after infection. Scale bar, 20  $\mu$ m.

### 3.2.2. Synergism of OMG16 and FZB42 reduced *V. longisporum* 43 root colonization

To this end results demonstrated that defence-related genes were induced in the *B. napus* AgP4 cultivar by inoculation with OMG16 and FZB42 while only a weak response was observed in the AgP1 variety. Thus, the reaction in the AgP4 cultivar is investigated in more detail,



particularly whether priming may reduce the root infection rates caused by *Verticillium*. Roots of 14-day-old *B. napus* cv. AgP4 seedlings were primed with OMG16 plus FZB42. Two days after priming, roots were infected with pathogenic *V. longisporum* 43. The absolute amount of VI43 DNA present in total root DNA of primed plants was quantified by qPCR and compared with the amount present in non-primed plants. This indicated that the presence of VI43 DNA was drastically reduced in primed plants compared to the non-primed controls on 1 dai, 2 dai, 3 dai and 5 dai ( $P < 0.0001$  each) (Fig. 25). Disease symptoms could not be observed due to the short growth period of the *in-vitro* plantlets.

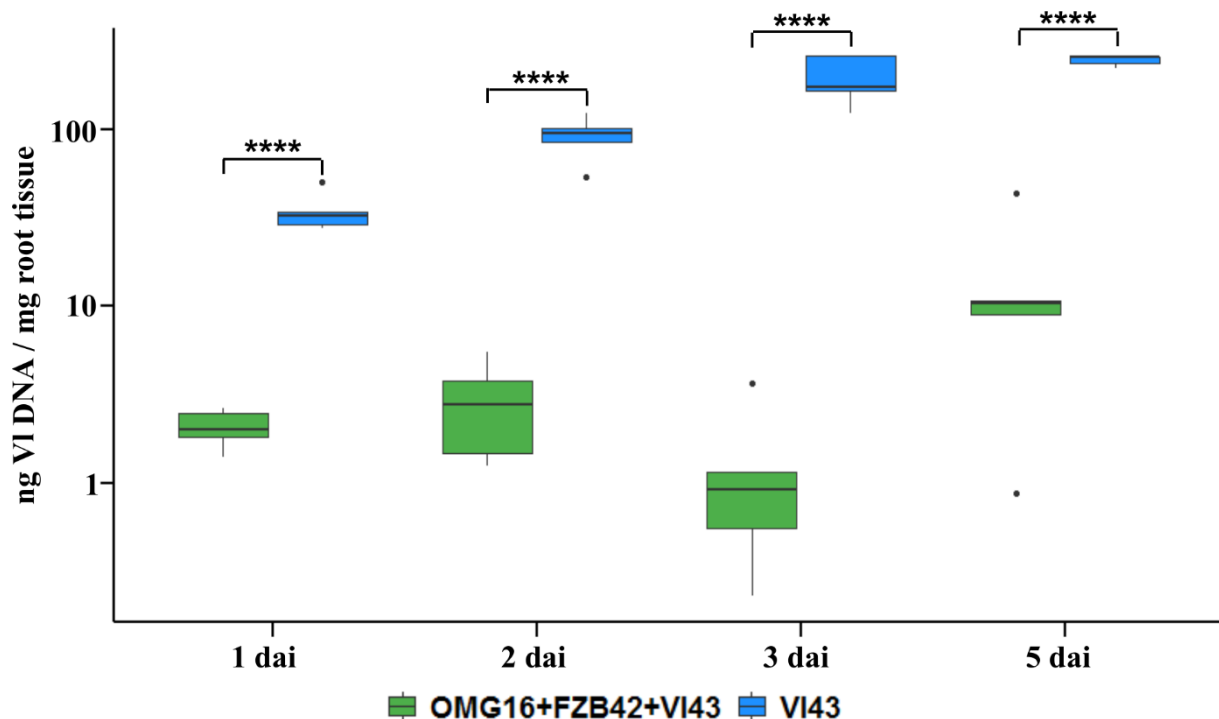


**Fig. 25.** Priming with OMG16 and FZB42 enhances the resistance of *B. napus* cv. AgP4 against infection with *V. longisporum*. Quantification of VI43 DNA in total roots upon OMG16 plus FZB42 plus VI43 and VI43 inoculation alone. Roots of two-week-old rapeseed plantlets of the AgP4 cultivar were primed with OMG16 plus FZB42. Two days after priming, roots were infected with VI43. The absolute amount of VI43 DNA in root samples was quantified by qPCR using a single locus genomic region of VI43. An unpaired t-test was performed at  $P < 0.05$  between OMG16 plus FZB42 plus VI43 and VI43 alone. \*  $P < 0.05$ ; \*\*  $P < 0.01$ ; \*\*\*  $P < 0.001$ ; \*\*\*\*  $P < 0.0001$ . OMG16, *T. harzianum* OMG16; FZB42, *B. velezensis* FZB42; VI43, *V. longisporum* 43; dai, days after infection.

### 3.2.3. Enhanced rapeseed defence upon priming

Transcriptome analyses showed that rapid reprogramming in plant defence gene expression undergoes in rapeseed-*Verticillium* interaction (Shen et al. 2014). Expression of these defence-related genes in pathogen-challenged plants is regulated by JA, ET and SA dependent systemic signalling molecules (Wang et al. 2012). Therefore, relative expression of rapeseed defence

genes involved in JA, ET and SA biosynthesis and signalling pathways was separately analysed by qRT-PCR in leaf, stem and root tissues of V143 pathogen challenged primed and non-primed plants.

### **3.2.3.1. Expression of defence related genes in roots**

To investigate the local defence responses of the plants, the relative transcript abundances of the JA biosynthesis genes *Lipoxygenase 2 (LOX2)* and *12-oxophytodienoic acid reductase 3 (OPR3)*, ET biosynthesis genes *1-aminocyclopropane-1-carboxylate (ACC) synthase 2 (ACS2)* and *ACC oxidase 4 (ACO4)*, SA biosynthesis gene *isochorismate synthase 1 (ICS1)* and SA-specific marker *pathogenesis-related gene 1 (PR1)* were analysed in root tissue by qRT-PCR. Prior to the pathogen infection, there was no significant induction of these defence genes in roots of OMG16 and FZB42 primed plants compared to the untreated controls (Appendix 4).

#### **3.2.3.1.1. JA biosynthesis genes**

There was no induction of *LOX2* in roots of V143 infected primed plants compared to the untreated controls. While in V143 infected non-primed plants, *LOX2* expression was downregulated on 1 dai ( $P < 0.05$ ), 2 dai, 3 dai ( $P < 0.001$  each) and 5 dai ( $P < 0.0001$ ). However, the expression of *LOX2* was higher in V143 infected primed plants on 1 dai, 2 dai ( $P < 0.05$  each), 3 dai and 5 dai ( $P < 0.01$  each) than V143 infected non-primed plants (Fig. 26a).

Expression of *OPR3* was suppressed in the roots of V143 infected primed plants on 1 dai ( $P < 0.01$ ), 2 dai ( $P < 0.001$ ) and 5 dai ( $P < 0.01$ ). Similarly, in V143 infected non-primed plants *OPR3* expression was also suppressed on 1 dai ( $P < 0.001$ ), 2 dai, 3 dai and 5 dai ( $P < 0.0001$  each) compared to the untreated controls. However, enhanced expression of *OPR3* was recorded in roots of V143 infected primed plants on 1 dai ( $P < 0.05$ ), 2 dai, 3 dai ( $P < 0.01$  each) and 5 dai ( $P < 0.001$ ) than V143 infected non-primed plants (Fig. 26b).

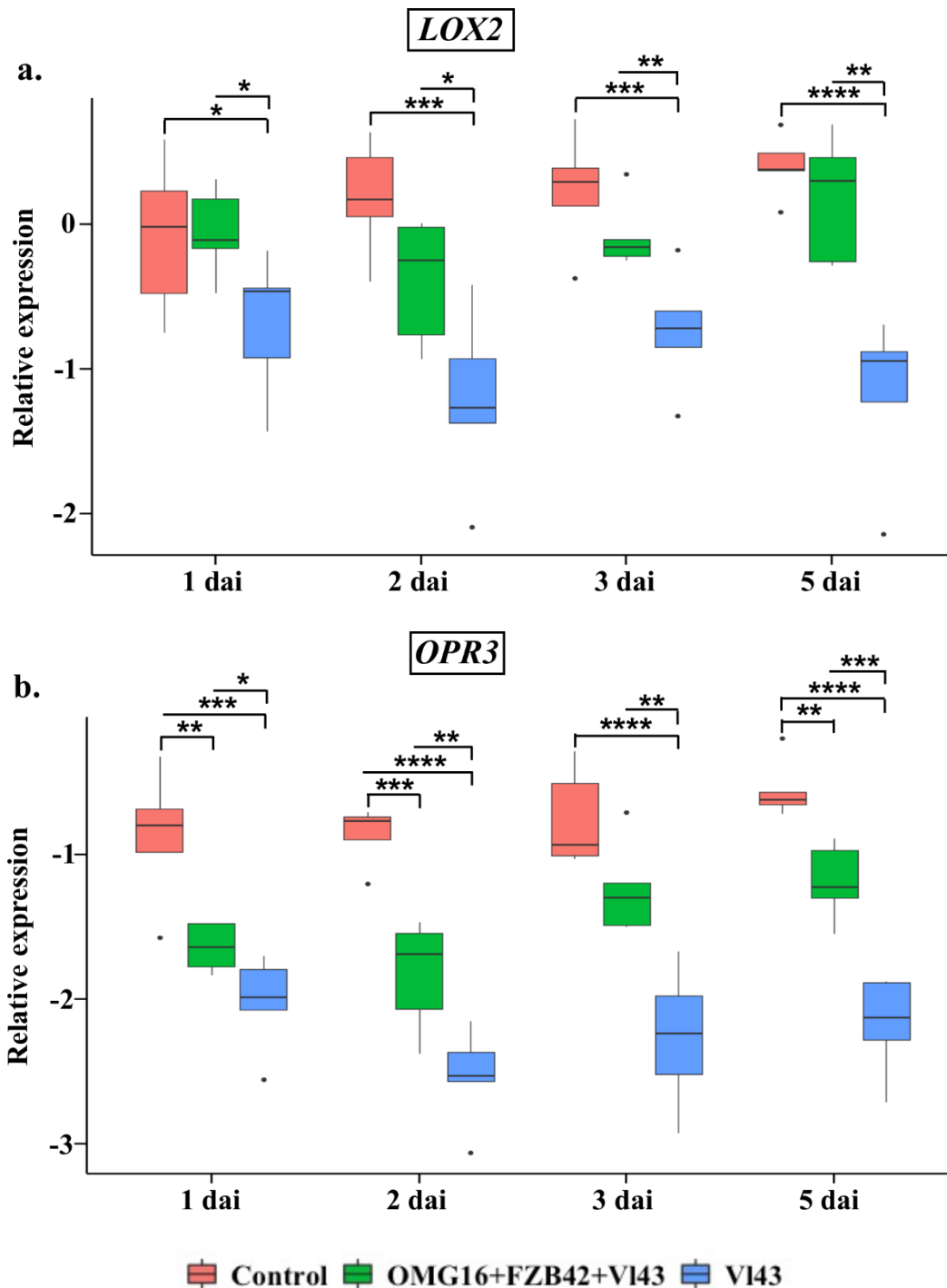


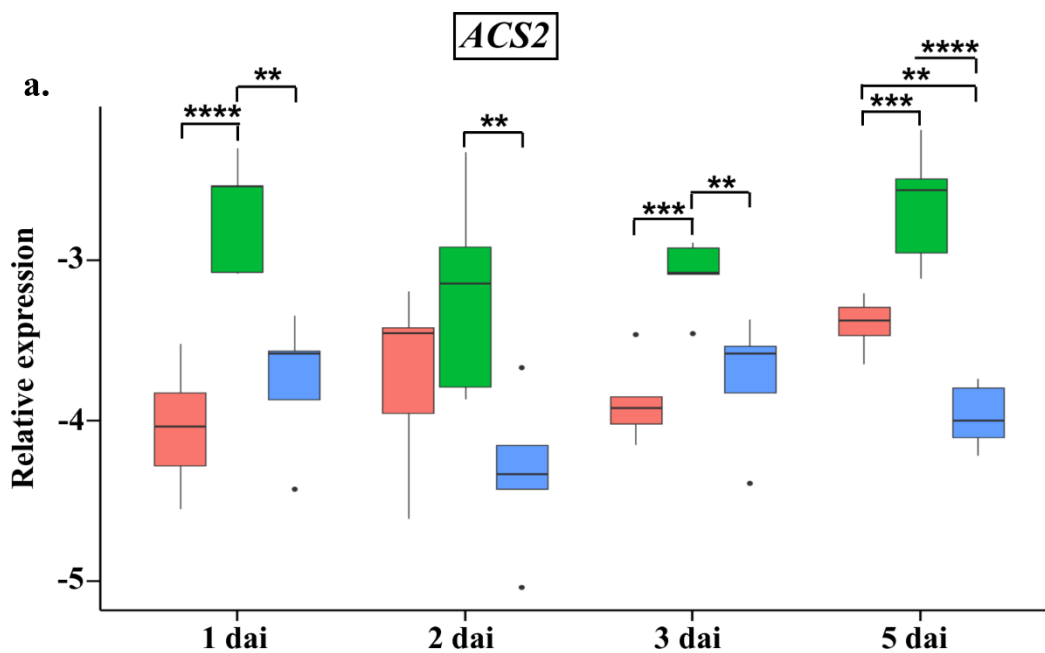
**Fig. 26.** Relative expression of rapeseed defence genes *LOX2* (a) and *OPR3* (b) in roots upon OMG16 plus FZB42 plus VI43 and VI43 inoculation alone. Roots of two-week-old rapeseed plantlets of the AgP4 cultivar were primed with OMG16 plus FZB42. Two days after priming, roots were infected with VI43. To assess local responses, the relative transcript abundances of the rapeseed defence genes were analysed by qRT-PCR in roots of the same plants tested in section 3.2.2. *BnaUbiquitin11*, *BnaActin* and *BnaTubulin* were used as endogenous controls for normalization. Box and whisker plots show  $\Delta Cq$  values of five biological replicates with quadruplicate qRT-PCRs. Significance of changes in gene expression compared to the control plants was calculated by Dunnett's test with mvt adjustment at  $P < 0.05$ . Significances of differences in relative expression of genes between OMG16 plus FZB42 plus VI43 and single VI43 treatments were calculated

using an unpaired t-test at  $P < 0.05$ . \*  $P < 0.05$ ; \*\*  $P < 0.01$ ; \*\*\*  $P < 0.001$ ; \*\*\*\*  $P < 0.0001$ . OMG16, *T. harzianum* OMG16; FZB42, *B. velezensis* FZB42; V143, *V. longisporum* 43; dai, days after infection.

### 3.2.3.1.2. ET biosynthesis genes

In the roots of primed plants *ACS2* expression was increased on 1 dai ( $P < 0.0001$ ), 3 dai and 5 dai ( $P < 0.001$ ) after V143 infection. In non-primed plants the expression of *ACS2* was down-regulated only as late as on 5 dai ( $P < 0.01$ ) compared to the untreated controls. *ACS2* expression increased on 1 dai, 2 dai, 3 dai ( $P < 0.01$  each) and 5 dai ( $P < 0.0001$ ) in V143 infected primed plants than non-primed plants (Fig. 27a).

*ACO4* expression enhanced on 1 dai ( $P < 0.0001$ ), 2 dai ( $P < 0.001$ ), 3 dai and 5 dai ( $P < 0.0001$  each) in roots of V143 infected primed plants. In contrast, the expression of *ACO4* was downregulated on 2 dai, 3 dai and 5 dai ( $P < 0.01$  each) in V143 infected non-primed plants compared to the untreated controls. *ACO4* expression increased on 1 dai, 2 dai, 3 dai and 5 dai ( $P < 0.0001$  each) in V143 infected primed plants than V143 infected non-primed plants (Fig. 27b).



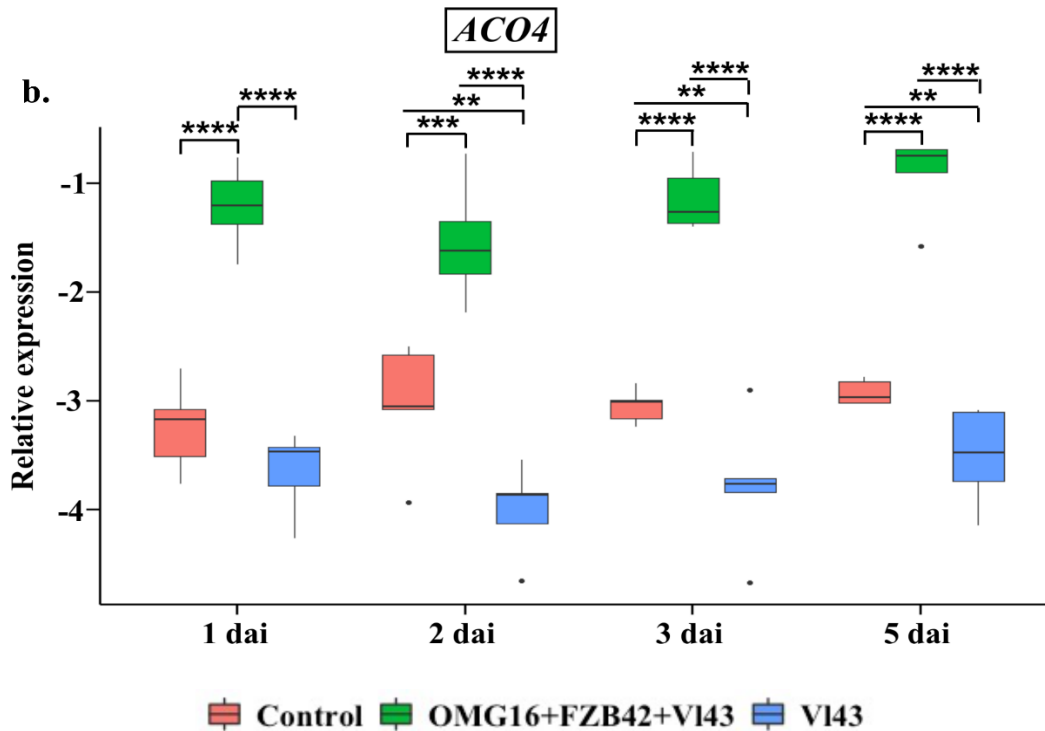


**Fig. 27.** Relative expression of rapeseed defence genes *ACS2* (a) and *ACO4* (b) in roots upon OMG16 plus FZB42 plus VI43 and VI43 inoculation alone. Roots of two-week-old rapeseed plantlets of the AgP4 cultivar were primed with OMG16 plus FZB42. Two days after priming, roots were infected with VI43. To assess local responses, the relative transcript abundances of the rapeseed defence genes were analysed by qRT-PCR in roots of the same plants tested in section 3.2.2. *BnaUbiquitin11*, *BnaActin* and *BnaTubulin* were used as endogenous controls for normalization. Box and whisker plots show  $\Delta Cq$  values of five biological replicates with quadruplicate qRT-PCRs. Significance of changes in gene expression compared to the control plants was calculated by Dunnett's test with mvt adjustment at  $P < 0.05$ . Significances of differences in relative expression of genes between OMG16 plus FZB42 plus VI43 and single VI43 treatments were calculated using an unpaired t-test at  $P < 0.05$ . \*  $P < 0.05$ ; \*\*  $P < 0.01$ ; \*\*\*  $P < 0.001$ ; \*\*\*\*  $P < 0.0001$ . OMG16, *T. harzianum* OMG16; FZB42, *B. velezensis* FZB42; VI43, *V. longisporum* 43; dai, days after infection.

### 3.2.3.1.3. SA biosynthesis and signalling genes

There was no induction of *ICS1* in roots of VI43 infected primed plants. While in VI43 infected non-primed plants, *ICS1* expression was downregulated on 1 dai ( $P < 0.05$ ), 2 dai ( $P < 0.001$ ), 3 dai and 5 dai ( $P < 0.01$  each) compared to the untreated controls. The expression of *ICS1* increased in VI43 infected primed plants on 1 dai ( $P < 0.01$ ), 2 dai, 3 dai ( $P < 0.05$  each) and 5 dai ( $P < 0.01$ ) than VI43 infected non-primed plants (Fig. 28a).

Again, there was no induction of *PR1* in roots of VI43 infected primed plants. In contrast, *PR1* expression suppressed on 2 dai, 3 dai ( $P < 0.01$  each) and 5 dai ( $P < 0.0001$ ) in VI43 infected non-primed plants compared to the untreated control plants. The expression of *PR1* was higher

in V143 infected primed plants on 1 dai ( $P < 0.05$ ) and 5 dai ( $P < 0.01$ ) than the V143 infected non-primed plants (Fig. 28b).

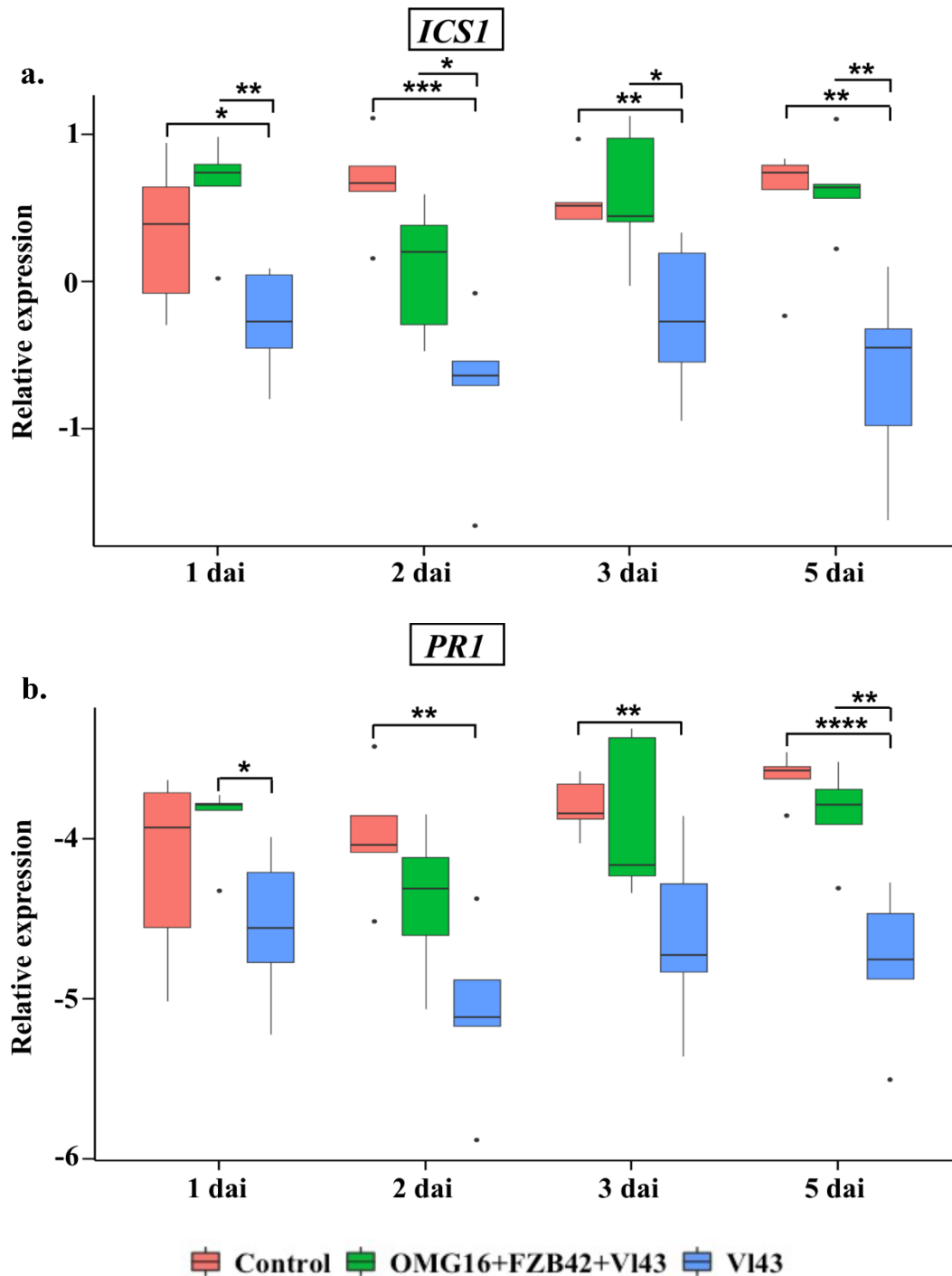


**Fig. 28.** Relative expression of rapeseed defence genes *ICSI* (a) and *PRI* (b) in roots upon OMG16 plus FZB42 plus V143 and V143 inoculation alone. Roots of two-week-old rapeseed plantlets of the AgP4 cultivar were primed with OMG16 plus FZB42. Two days after priming, roots were infected with V143. To assess local responses, the relative transcript abundances of the rapeseed defence genes were analysed by qRT-PCR in roots of the same plants tested in section 3.2.2. *BnaUbiquitin11*, *BnaActin* and *BnaTubulin* were used as endogenous controls for normalization. Box and whisker plots show  $\Delta Cq$  values of five biological replicates

with quadruplicate qRT-PCRs. Significance of changes in gene expression compared to the control plants was calculated by Dunnett's test with mvt adjustment at  $P < 0.05$ . Significances of differences in relative expression of genes between OMG16 plus FZB42 plus VI43 and single VI43 treatments were calculated using an unpaired t-test at  $P < 0.05$ . \*  $P < 0.05$ ; \*\*  $P < 0.01$ ; \*\*\*  $P < 0.001$ ; \*\*\*\*  $P < 0.0001$ . OMG16, *T. harzianum* OMG16; FZB42, *B. velezensis* FZB42; VI43, *V. longisporum* 43; dai, days after infection.

### 3.2.3.2. Expression of defence related genes in stems

In addition, to investigate the systemic defence responses the relative transcript abundances of the previously used JA biosynthesis genes *LOX2* and *OPR3*, ET biosynthesis genes *ACS2* and *ACO4*, SA biosynthesis gene *ICS1* and SA-specific marker gene *PR1* were analysed in stem tissue by qRT-PCR. Prior infection, OMG16 and FZB42 priming significantly increased the relative expression of *LOX2*, *OPR3* and *ICS1* in stems compared to the untreated controls (Appendix 5).

#### 3.2.3.2.1. JA biosynthesis genes

Unlike in leaves, the expression of *LOX2* highly enhanced in stems of VI43 infected primed plants on 1 dai, 2 dai, 3 dai and 5 dai ( $P < 0.0001$  each). *LOX2* expression was also increased in VI43 infected non-primed plants on 1 dai ( $P < 0.001$ ), 2 dai ( $P < 0.0001$ ), 3 dai ( $P < 0.01$ ) and 5 dai ( $P < 0.001$ ) compared to the untreated controls. Moreover, *LOX2* expression increased on 1 dai ( $P < 0.01$ ) and 3 dai ( $P < 0.001$ ) in stems of VI43 infected primed plants than VI43 infected non-primed plants (Fig. 29a).

Relative expression of *OPR3* increased on 3 dai and 5 dai ( $P < 0.01$  each) in stems of VI43 infected primed plants compared to the untreated controls. In VI43 infected non-primed plants *OPR3* expression increased on 2 dai ( $P < 0.05$ ). *OPR3* expression also enhanced on 3 dai and 5 dai ( $P < 0.05$  each) in VI43 infected primed plants compared to the VI43 infected non-primed plants (Fig. 29b).

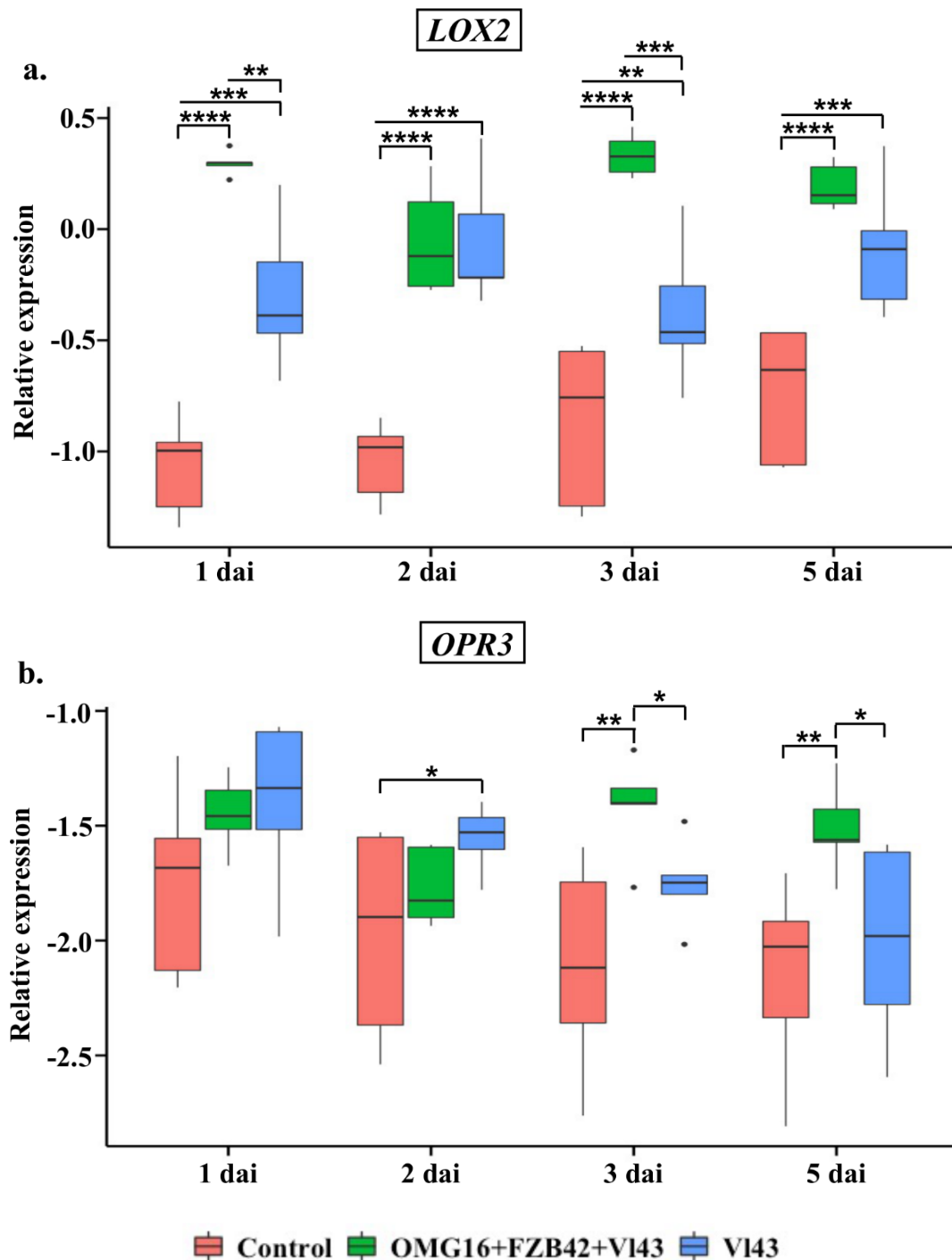


**Fig. 29.** Relative expression of rapeseed defence genes *LOX2* (a) and *OPR3* (b) in stems upon OMG16 plus FZB42 plus VI43 and VI43 inoculation alone. Roots of two-week-old rapeseed plantlets of the AgP4 cultivar were primed with OMG16 plus FZB42. Two days after priming, roots were infected with VI43. To assess systemic responses, the relative transcript abundances of the rapeseed defence genes were analysed by qRT-PCR in stems of the same plants tested in section 3.2.2. *BnaUbiquitin11*, *BnaActin* and *BnaTubulin* were used as endogenous controls for normalization. Box and whisker plots show  $\Delta Cq$  values of five biological replicates with quadruplicate qRT-PCRs. Significance of changes in gene expression compared to the control plants was calculated by Dunnett's test with mvt adjustment at  $P < 0.05$ . Significances of differences in relative expression of genes between OMG16 plus FZB42 plus VI43 and single VI43 treatments were

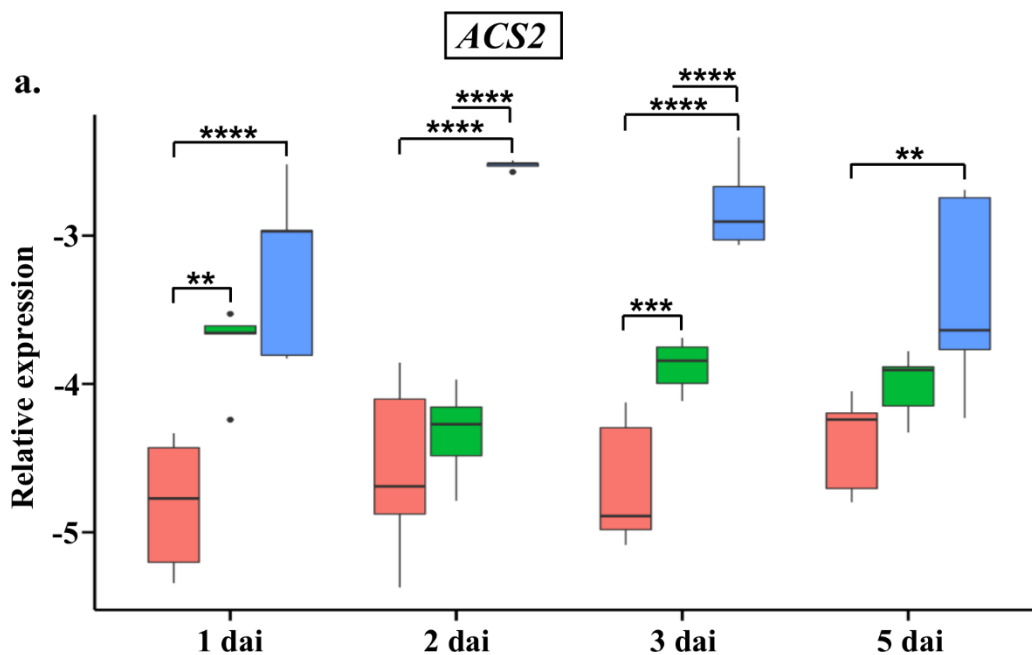


calculated using an unpaired t-test at  $P < 0.05$ . \*  $P < 0.05$ ; \*\*  $P < 0.01$ ; \*\*\*  $P < 0.001$ ; \*\*\*\*  $P < 0.0001$ . OMG16, *T. harzianum* OMG16; FZB42, *B. velezensis* FZB42; V143, *V. longisporum* 43; dai, days after infection.

### 3.2.3.2.2. ET biosynthesis genes

In the stems of primed plants, *ACS2* expression was already elevated on 1 dai ( $P < 0.01$ ) and 3 dai ( $P < 0.001$ ) after V143 infection. While, in non-primed V143 infected plants expression of *ACS2* started to increase on as early as 1 dai and continued to 2 dai, 3 dai ( $P < 0.0001$  each) and 5 dai ( $P < 0.01$ ). Notably, higher expression of *ACS2* was detected on 2 dai and 3 dai ( $P < 0.0001$  each) in stems of V143 infected non-primed plants than the V143 infected primed plants (Fig. 30a).

*ACO4* expression elevated on 1 dai, 2 dai, 3 dai ( $P < 0.0001$  each) and 5 dai ( $P < 0.001$ ) in stems of V143 infected primed plants. In non-primed plants, expression of *ACO4* increased on 1 dai ( $P < 0.05$ ), 2 dai ( $P < 0.0001$ ) and 3 dai ( $P < 0.01$ ) after V143 infection compared to the untreated control plants. *ACO4* expression also increased on 1 dai, 2 dai ( $P < 0.001$  each), 3 dai ( $P < 0.0001$ ) and 5 dai ( $P < 0.001$ ) in V143 infected primed plants than the V143 infected non-primed plants (Fig. 30b).



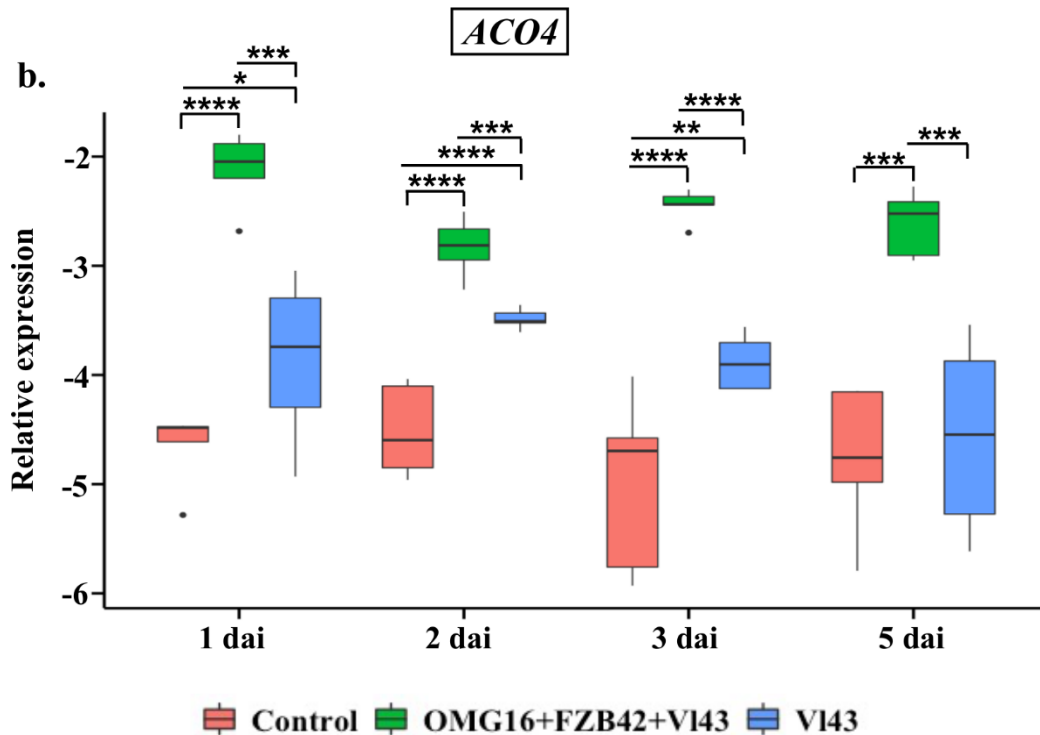


**Fig. 30.** Relative expression of rapeseed defence genes *ACS2* (a) and *ACO4* (b) in stems upon OMG16 plus FZB42 plus VI43 and VI43 inoculation alone. Roots of two-week-old rapeseed plantlets of the AgP4 cultivar were primed with OMG16 plus FZB42. Two days after priming, roots were infected with VI43. To assess systemic responses, the relative transcript abundances of the rapeseed defence genes were analysed by qRT-PCR in stems of the same plants tested in section 3.2.2. *BnaUbiquitin11*, *BnaActin* and *BnaTubulin* were used as endogenous controls for normalization. Box and whisker plots show  $\Delta Cq$  values of five biological replicates with quadruplicate qRT-PCRs. Significance of changes in gene expression compared to the control plants was calculated by Dunnett's test with mvt adjustment at  $P < 0.05$ . Significances of differences in relative expression of genes between OMG16 plus FZB42 plus VI43 and single VI43 treatments were calculated using an unpaired t-test at  $P < 0.05$ . \*  $P < 0.05$ ; \*\*  $P < 0.01$ ; \*\*\*  $P < 0.001$ ; \*\*\*\*  $P < 0.0001$ . OMG16, *T. harzianum* OMG16; FZB42, *B. velezensis* FZB42; VI43, *V. longisporum* 43; dai, days after infection.

### 3.2.3.2.3. SA biosynthesis and signalling genes

Both in primed and non-primed plants, *ICS1* expression only increased on 3 dai ( $P < 0.01$  each) after infection. Interestingly the expression of *ICS1* was higher on 2 dai ( $P < 0.01$ ) in VI43 infected non-primed compared to the primed plants (Fig. 31a).

Expression of *PR1* in stems of VI43 infected primed plants elevated on 1 dai, 2 dai, 3 dai ( $P < 0.0001$  each) and 5 dai ( $P < 0.001$ ). In VI43 infected non-primed plants *PR1* expression also increased on 1 dai, 2 dai, 3 dai ( $P < 0.01$  each) and 5 dai ( $P < 0.0001$ ) than the untreated controls. *PR1* expression enhanced on 1 dai and 2 dai, ( $P < 0.01$  each) in VI43 infected primed plants compared to the non-primed ones. In contrast, on 5 dai *PR1* was higher ( $P < 0.05$ ) in VI43 infected non-primed plants than the primed plants (Fig. 31b).

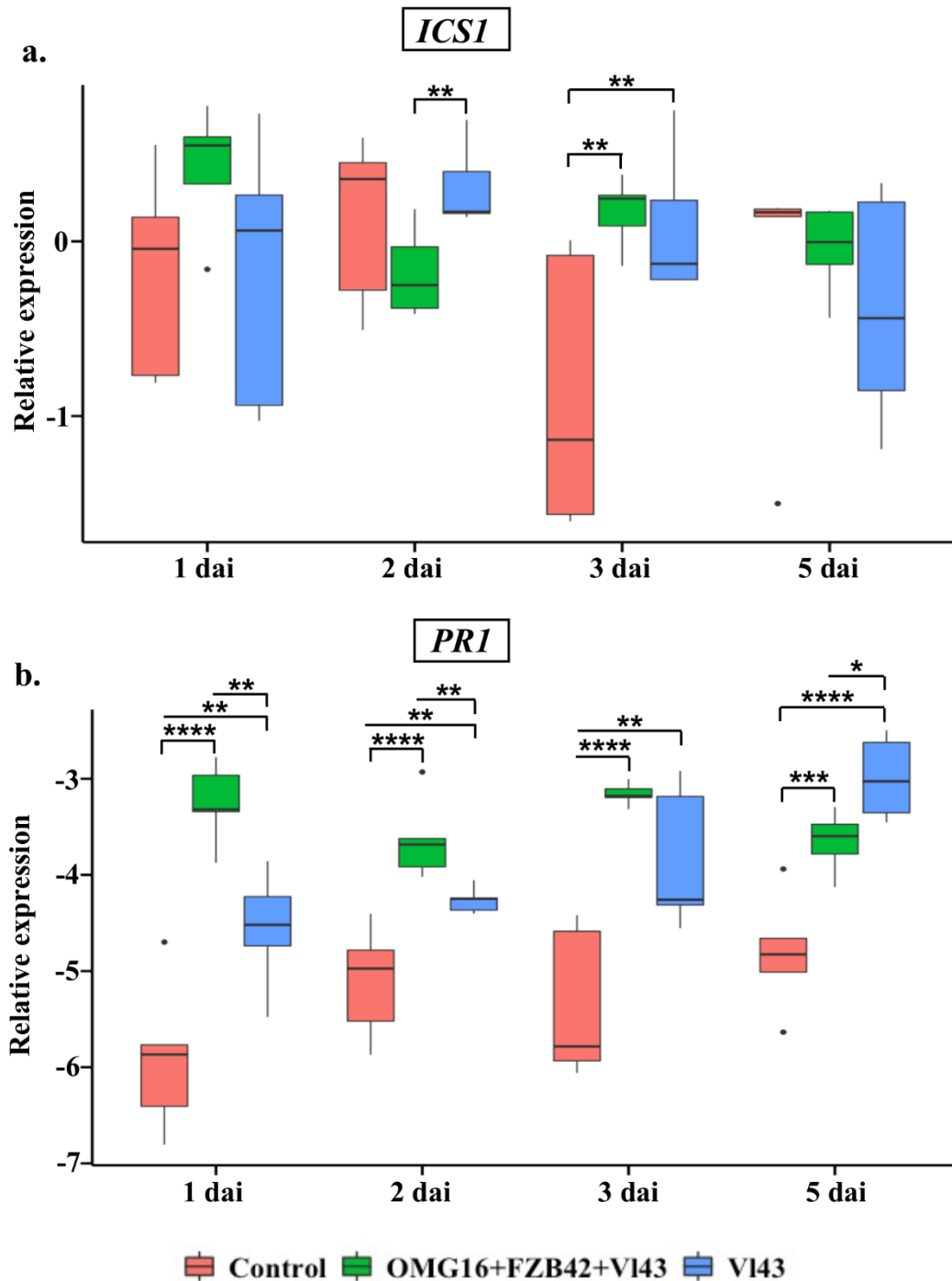


**Fig. 31.** Relative expression of rapeseed defence genes *ICSI* (a) and *PRI* (b) in stems upon OMG16 plus FZB42 plus VI43 and VI43 inoculation alone. Roots of two-week-old rapeseed plantlets of the AgP4 cultivar were primed with OMG16 plus FZB42. Two days after priming, roots were infected with VI43. To assess systemic responses, the relative transcript abundances of the rapeseed defence genes were analysed by qRT-PCR in stems of the same plants tested in section 3.2.2. *BnaUbiquitin11*, *BnaActin* and *BnaTubulin* were used as endogenous controls for normalization. Box and whisker plots show  $\Delta Cq$  values of five biological replicates with quadruplicate qRT-PCRs. Significance of changes in gene expression compared to the control plants was calculated by Dunnett's test with mvt adjustment at  $P < 0.05$ . Significances of differences in relative expression of genes between OMG16 plus FZB42 plus VI43 and single VI43 treatments were

calculated using an unpaired t-test at  $P < 0.05$ . \*  $P < 0.05$ ; \*\*  $P < 0.01$ ; \*\*\*  $P < 0.001$ ; \*\*\*\*  $P < 0.0001$ . OMG16, *T. harzianum* OMG16; FZB42, *B. velezensis* FZB42; V143, *V. longisporum* 43; dai, days after infection.

### 3.2.3.3. Expression of defence related genes in leaves

To investigate the systemic defence responses of the plants, the relative transcript abundances of the previously studied JA/ET marker genes *PDF1.2*, *ERF2*, and *AOC3* were analysed in leaf tissue by qRT-PCR. In addition, expressions of the JA biosynthesis genes *LOX2* and *OPR3*, ET biosynthesis genes *ACS2* and *ACO4*, and SA biosynthesis gene *ICS1* were measured. Moreover, the expressions of JA-specific marker gene *vegetative storage protein 2 (VSP2)* and SA-specific marker *PRI* were measured.

Upon priming, the relative expression of *OPR3*, *ACO4*, *PDF1.2*, *VSP2* and *PRI* significantly enhanced in leaves of OMG16 and FZB42 primed plants prior to V143 infection compared to the untreated controls (Appendix 6).

#### 3.2.3.3.1. JA biosynthesis genes

In V143 infected primed plants *LOX2* showed delayed expression on 3 dai ( $P < 0.05$ ) and 5 dai ( $P < 0.001$ ) compared to the untreated controls. While, in V143 infected non-primed plants expression of *LOX2* increased only as late as on 5 dai ( $P < 0.001$ ). Higher expression of *LOX2* was detected on 3 dai ( $P < 0.05$ ) in V143 infected primed plants than the V143 infected non-primed plants (Fig. 32a).

In primed plants, *AOC3* expression was already elevated on 2 dai ( $P < 0.01$ ) and 5 dai ( $P < 0.05$ ) after V143 infection. While, in non-primed V143 infected plants expression of *AOC3* started to increase only as late as on 5 dai ( $P < 0.05$ ) compared to the untreated controls. *AOC3* expression also enhanced on 3 dai ( $P < 0.05$ ) in V143 infected primed plants than V143 infected non-primed plants (Fig. 32b).

Relative expression of *OPR3* enhanced on 2 dai ( $P < 0.01$ ), 3 dai ( $P < 0.01$ ) and 5 dai ( $P < 0.0001$ ) in V143 infected primed plants compared to the untreated controls. In V143 infected non-primed plants *OPR3* expression increased on 3 dai ( $P < 0.05$ ) and 5 dai ( $P < 0.0001$ ) (Fig. 32c).

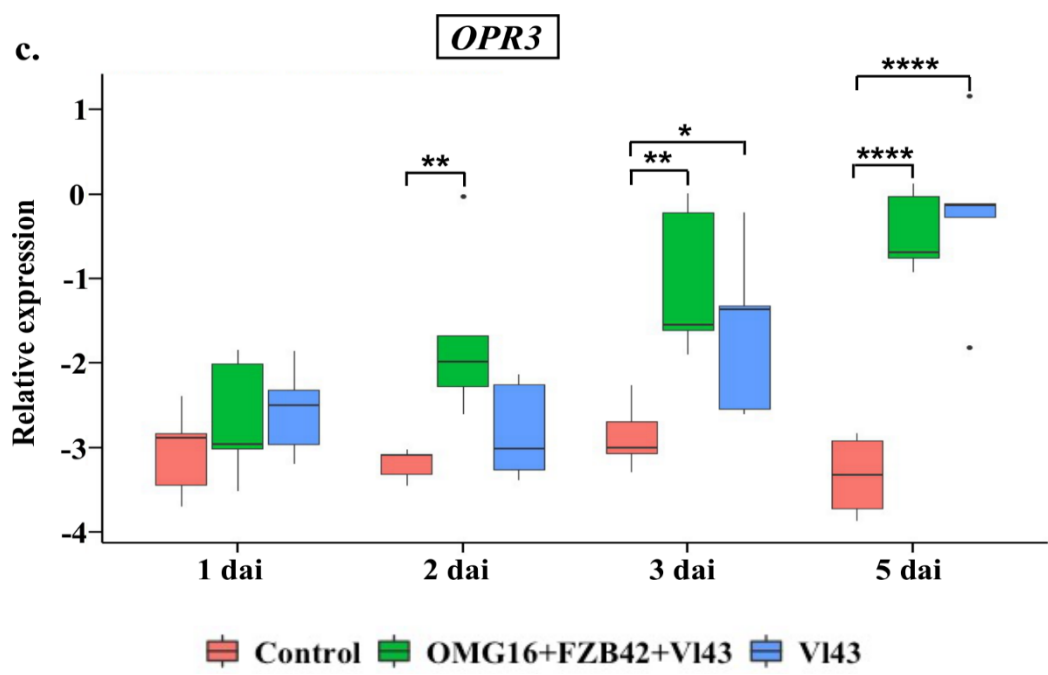
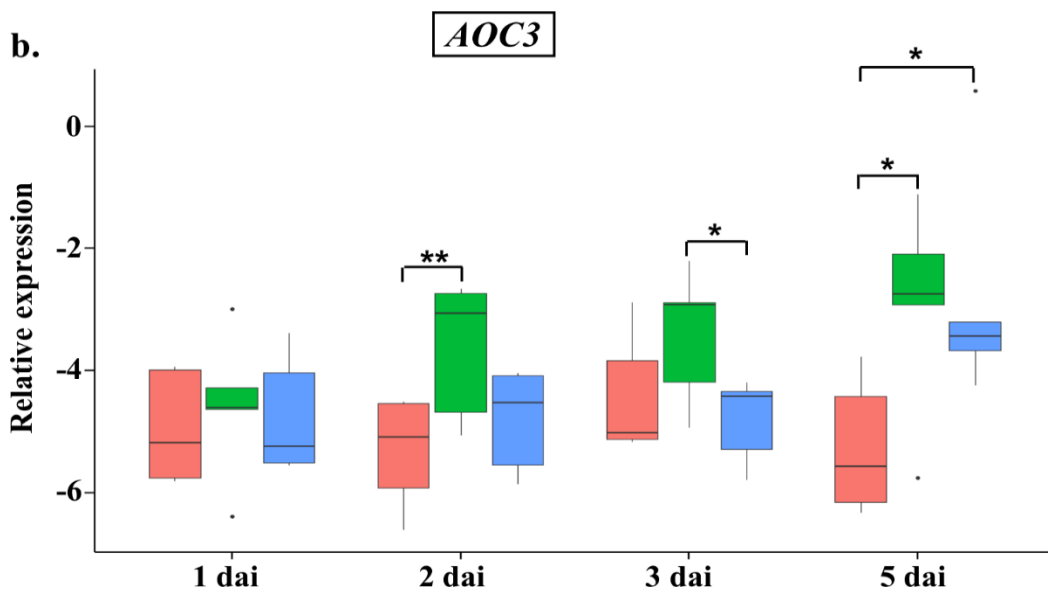
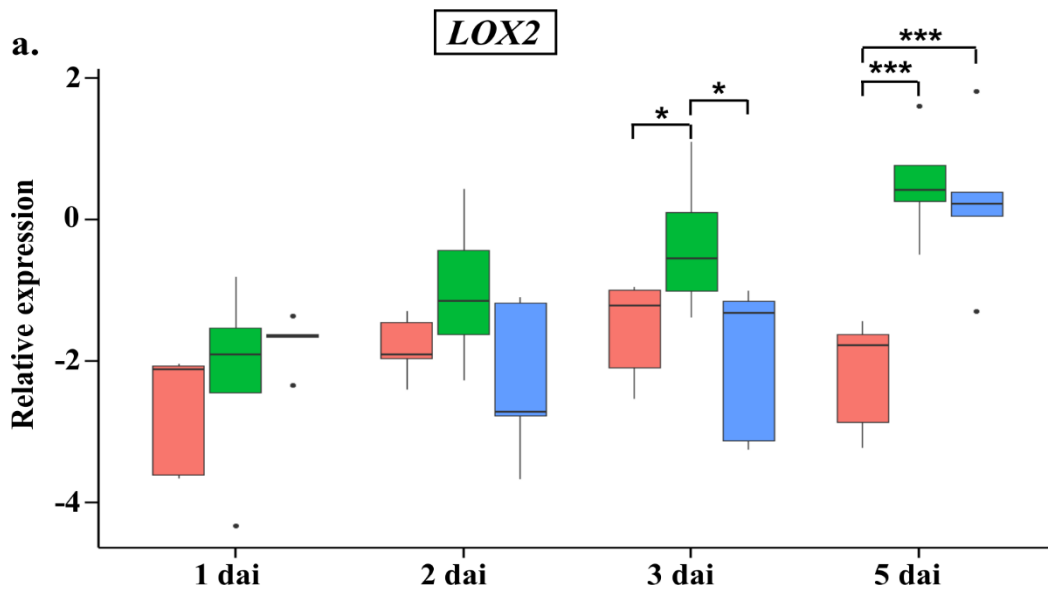


**Fig. 32.** Relative expression of rapeseed defence genes *LOX2* (a), *AOC3* (b) and *OPR3* (c) in leaves upon OMG16 plus FZB42 plus V143 and V143 inoculation alone. Roots of two-week-old rapeseed plantlets of the AgP4 cultivar were primed with OMG16 plus FZB42. Two days after priming, roots were infected with V143. To assess systemic responses, the relative transcript abundances of the rapeseed defence genes were analysed by qRT-PCR in leaves of the same plants tested in section 3.2.2. *BnaUbiquitin11*, *BnaActin* and *BnaTubulin* were used as endogenous controls for normalization. Box and whisker plots show  $\Delta Cq$  values of five biological replicates with quadruplicate qRT-PCRs. Significance of changes in gene expression compared to the control plants was calculated by Dunnett's test with mvt adjustment at  $P < 0.05$ . Significances of differences in relative expression of genes between OMG16 plus FZB42 plus V143 and single V143 treatments were calculated using an unpaired t-test at  $P < 0.05$ . \*  $P < 0.05$ ; \*\*  $P < 0.01$ ; \*\*\*  $P < 0.001$ ; \*\*\*\*  $P < 0.0001$ . OMG16, *T. harzianum* OMG16; FZB42, *B. velezensis* FZB42; V143, *V. longisporum* 43; dai, days after infection.

### 3.2.3.3.2. ET biosynthesis and signalling genes

*ACS2* expression increased in V143 infected primed plants on 2 dai ( $P < 0.001$ ), 3 dai ( $P < 0.05$ ) and 5 dai ( $P < 0.001$ ). While in V143 infected non-primed plants showed late induction of *ACS2* on 5 dai ( $P < 0.001$ ) compared to the untreated controls. *ACS2* expression also increased on 2 dai ( $P < 0.01$ ) in V143 infected primed plants than the V143 infected non-primed plants (Fig. 33a).

In primed plants, *ACO4* expression was elevated on 1 dai, 2 dai, 3 dai and 5 dai ( $P < 0.0001$  each) after V143 infection. While, in non-primed V143 infected plants expression of *ACO4* increased on 1 dai ( $P < 0.001$ ), 2 dai, 3 dai and 5 dai ( $P < 0.0001$  each) compared to the untreated controls. *ACO4* expression also increased as early as on 1 dai ( $P < 0.001$ ) in V143 infected primed plants than the V143 infected non-primed controls (Fig. 33b).

Relative transcript abundances of *ERF2* were significantly increased on 2 dai ( $P < 0.05$ ) and 5 dai ( $P < 0.01$ ) in primed plants compared to untreated controls. In contrast, in V143 infected, non-primed plants *ERF2* expression was enhanced only on 5 days ( $P < 0.01$ ) after treatment (Fig. 33c).

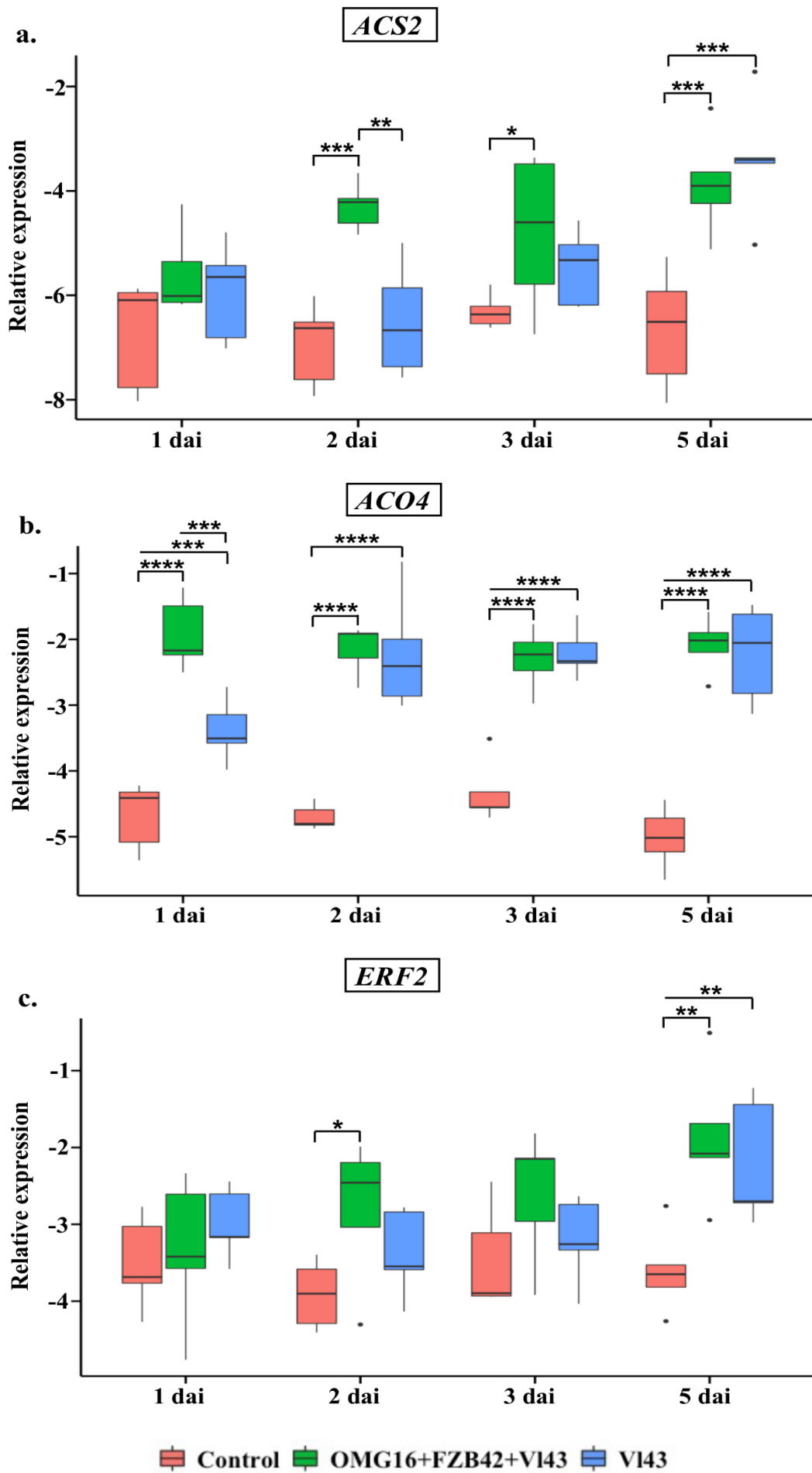


**Fig. 33.** Relative expression of rapeseed defence genes *ACS2* (a), *ACO4* (b) and *ERF2* (c) in leaves upon OMG16 plus FZB42 plus V143 and V143 inoculation alone. Roots of two-week-old rapeseed plantlets of the AgP4 cultivar were primed with OMG16 plus FZB42. Two days after priming, roots were infected with V143. To assess systemic responses, the relative transcript abundances of the rapeseed defence genes were analysed by qRT-PCR in leaves of the same plants tested in section 3.2.2. *BnaUbiquitin11*, *BnaActin* and *BnaTubulin* were used as endogenous controls for normalization. Box and whisker plots show  $\Delta Cq$  values of five biological replicates with quadruplicate qRT-PCRs. Significance of changes in gene expression compared to the control plants was calculated by Dunnett's test with mvt adjustment at  $P < 0.05$ . Significances of differences in relative expression of genes between OMG16 plus FZB42 plus V143 and single V143 treatments were calculated using an unpaired t-test at  $P < 0.05$ . \*  $P < 0.05$ ; \*\*  $P < 0.01$ ; \*\*\*  $P < 0.001$ ; \*\*\*\*  $P < 0.0001$ . OMG16, *T. harzianum* OMG16; FZB42, *B. velezensis* FZB42; V143, *V. longisporum* 43; dai, days after infection.

#### 3.2.3.3.3. JA/ET marker genes

Among the previously employed marker genes, *PDF1.2* showed again the strongest response. *PDF1.2* expression was higher on 1 dai ( $P < 0.01$ ) in V143 infected primed plants than in the V143 infected non-primed plants. In non-primed V143 infected plants, *PDF1.2* expression was enhanced on 1 dai ( $P < 0.01$ ), 2 dai, 3 dai and 5 dai ( $P < 0.0001$  each) compared to the untreated control plants. *PDF1.2* expression also enhanced in V143 infected primed plants on 1 dai, 2 dai, 3 dai and 5 dai ( $P < 0.0001$  each) (Fig. 34a).

To investigate activation of the JA pathway in more detail the *VSP2* marker gene was also included in this experiment, which showed enhanced expression on 1 dai, 2 dai, 3 dai and 5 dai ( $P < 0.0001$  each) in V143 infected primed plants compared to the untreated controls. *VSP2* expression increased likewise on 1 dai, 2 dai, 3 dai and 5 dai ( $P < 0.0001$  each) in non-primed V143 infected plants. Moreover, higher expression of *VSP2* was detected on 2 dai ( $P < 0.01$ ) in V143 infected primed plants than the V143 infected non-primed plants (Fig. 34b).



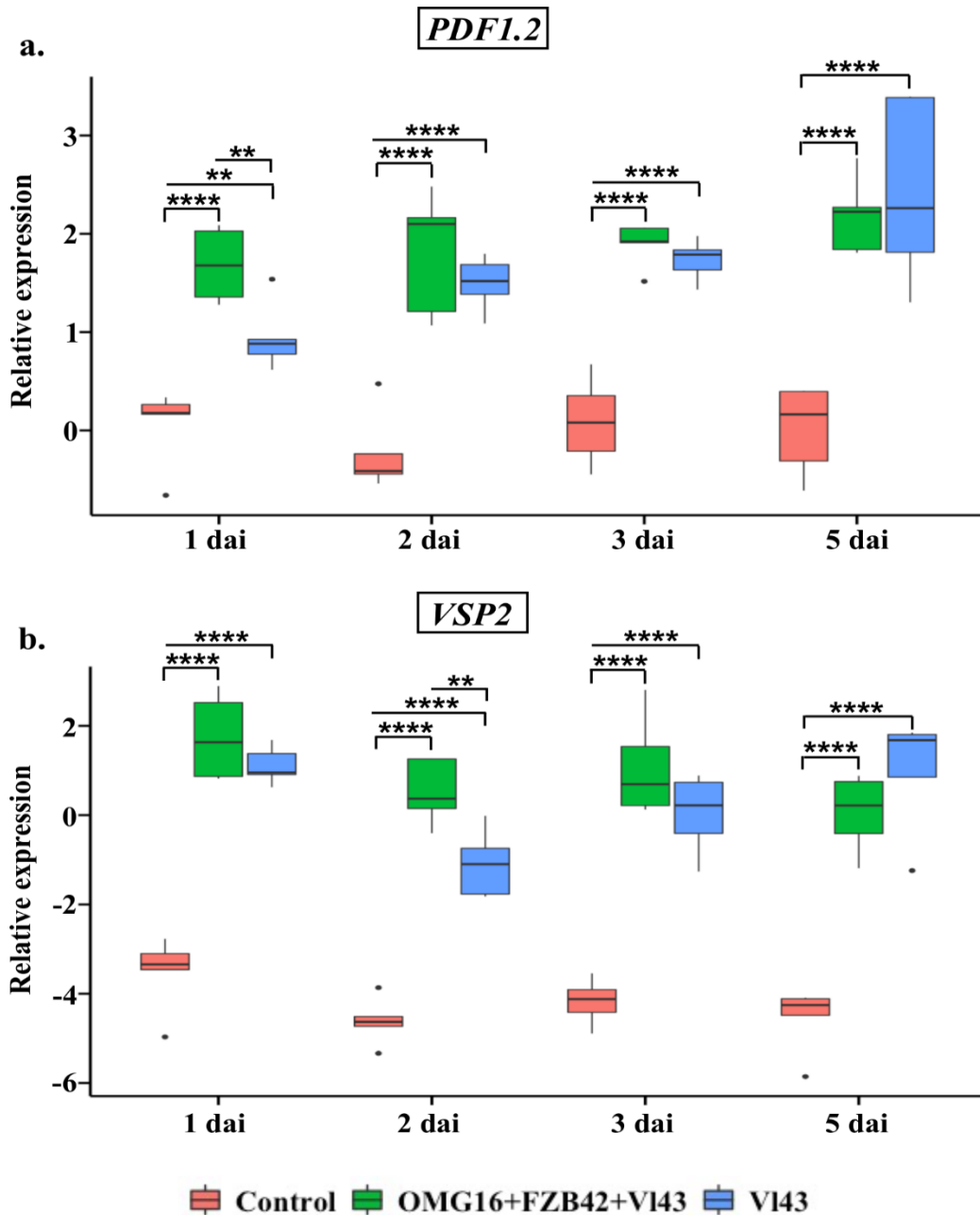


**Fig. 34.** Relative expression of rapeseed defence genes *PDF1.2* (a) and *VSP2* (b) in leaves upon OMG16 plus FZB42 plus VI43 and VI43 inoculation alone. Roots of two-week-old rapeseed plantlets of the AgP4 cultivar were primed with OMG16 plus FZB42. Two days after priming, roots were infected with VI43. To assess systemic responses, the relative transcript abundances of the rapeseed defence genes were analysed by qRT-PCR in leaves of the same plants tested in section 3.2.2. *BnaUbiquitin11*, *BnaActin* and *BnaTubulin* were used as endogenous controls for normalization. Box and whisker plots show  $\Delta$ Cq values of five biological replicates with quadruplicate qRT-PCRs. Significance of changes in gene expression compared to the control plants was calculated by Dunnett's test with mvt adjustment at  $P < 0.05$ . Significances of differences in relative expression of genes between OMG16 plus FZB42 plus VI43 and single VI43 treatments were calculated using an unpaired t-test at  $P < 0.05$ . \*  $P < 0.05$ ; \*\*  $P < 0.01$ ; \*\*\*  $P < 0.001$ ; \*\*\*\*  $P < 0.0001$ . OMG16, *T. harzianum* OMG16; FZB42, *B. velezensis* FZB42; VI43, *V. longisporum* 43; dai, days after infection.

#### 3.2.3.3.4. SA biosynthesis and signalling genes

The expression of *ICS1* was enhanced on 2 dai ( $P < 0.01$ ) and 5 dai ( $P < 0.0001$ ) in V143 infected primed plants. *ICS1* expression only enhanced as late as on 5 dai ( $P < 0.001$ ) in V143 infected non-primed plants compared to the untreated controls. Increased expression of *ICS1* was recorded on 2 dai ( $P < 0.05$ ) in V143 infected primed plants than the V143 infected non-primed plants (Fig. 35a).

In primed plants *PR1* expression increased on 2 dai ( $P < 0.01$ ), 3 dai ( $P < 0.001$ ) and 5 dai ( $P < 0.0001$ ) after V143 infection. In V143 infected non-primed plants late expression of *PR1* was recorded on 5 dai ( $P < 0.0001$ ) than the untreated controls. *PR1* expression was enhanced in V143 infected primed plants on 2 dai and 3 dai ( $P < 0.01$  each) compared to the V143 infected non-primed plants (Fig. 35b).

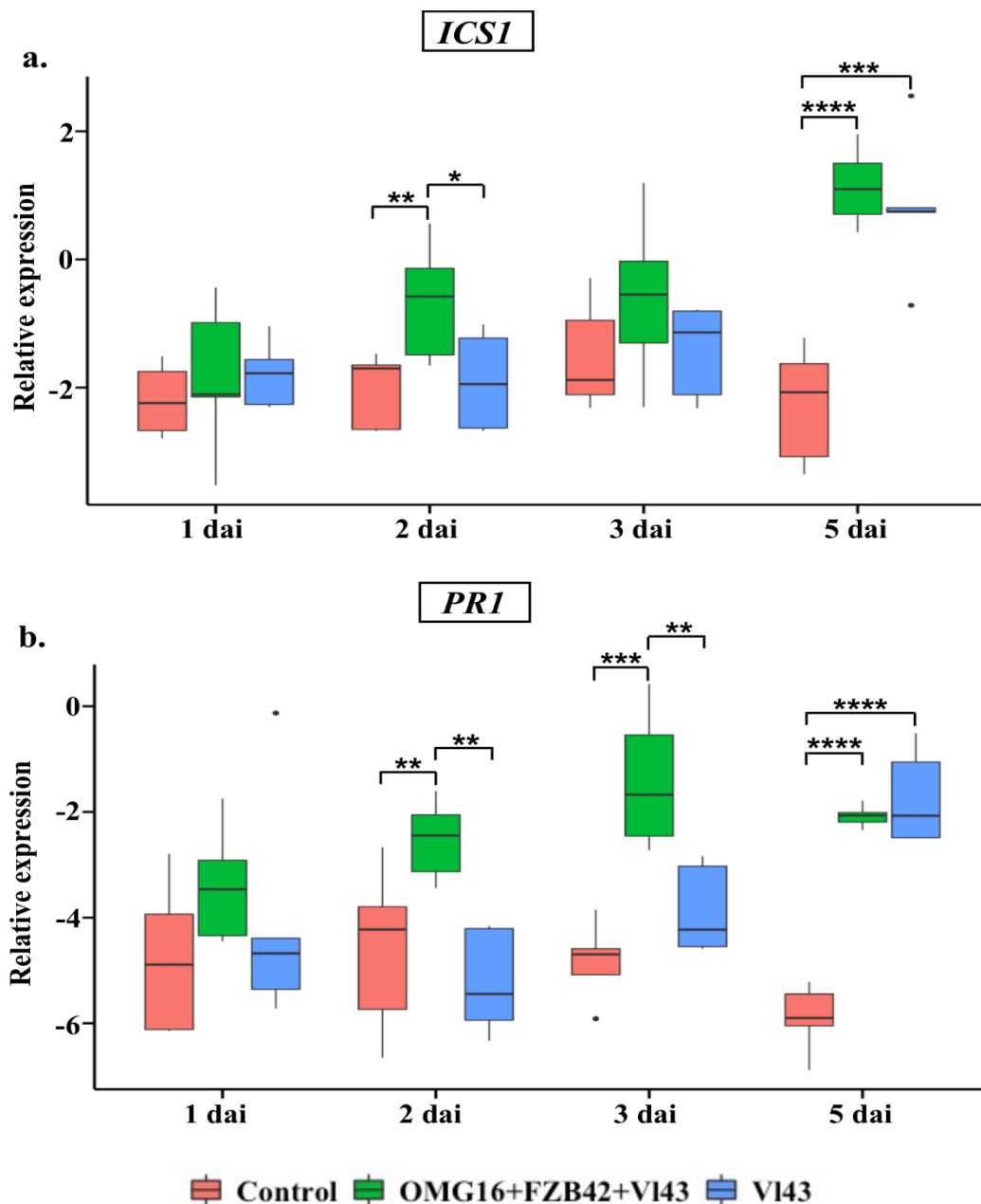


**Fig. 35.** Relative expression of rapeseed defence genes *ICS1* (a) and *PRI* (b) in leaves upon OMG16 plus FZB42 plus V143 and V143 inoculation alone. Roots of two-week-old rapeseed plantlets of the AgP4 cultivar were primed with OMG16 plus FZB42. Two days after priming, roots were infected with V143. To assess systemic responses, the relative transcript abundances of the rapeseed defence genes were analysed by qRT-PCR in leaves of the same plants tested in section 3.2.2. *BnaUbiquitin11*, *BnaActin* and *BnaTubulin* were used as endogenous controls for normalization. Box and whisker plots show  $\Delta Cq$  values of five biological replicates with quadruplicate qRT-PCRs. Significance of changes in gene expression compared to the control plants was calculated by Dunnett's test with mvt adjustment at  $P < 0.05$ . Significances of differences in relative expression of genes between OMG16 plus FZB42 plus V143 and single V143 treatments were calculated using an unpaired t-test at  $P < 0.05$ . \*  $P < 0.05$ ; \*\*  $P < 0.01$ ; \*\*\*  $P < 0.001$ ; \*\*\*\*  $P < 0.0001$ . OMG16, *T. harzianum* OMG16; FZB42, *B. velezensis* FZB42; V143, *V. longisporum* 43; dai, days after infection.

### 3.2.4. Determination of stress-related phytohormonal homeostasis

To analyse the variation in endogenous phytohormone content after priming, amounts of hormones were estimated separately in shoots (both leaves and stems) and roots. 14-day-old *B. napus* cv. AgP4 seedlings were primed with OMG16 plus FZB42. Two days after priming, roots were infected with pathogenic *V. longisporum* 43. Amounts of endogenous plant hormones, JA and SA were measured with UHPLC-MS.

#### 3.2.4.1. Phytohormone contents in root tissue

In root tissue, JA amount decreased on 5 dai ( $P < 0.05$ ) in V143 infected primed plants compared to the untreated controls. While in V143 infected non-primed plants, JA production reduced on 1 dai, 2 dai, 3 dai and 5 dai ( $P < 0.05$  each) than the untreated controls. Nevertheless, JA amount highly increased in roots of V143 infected primed plants on 1 dai ( $P < 0.001$ ) and 2 dai ( $P < 0.0001$ ) compared to the non-primed ones (Fig. 36a).

The amount of SA hormone increased on 2 dai ( $P < 0.001$ ), 3 dai ( $P < 0.01$ ) and 5 dai ( $P < 0.05$ ) in V143 infected primed plants. In contrast, there was no induction of SA amount in V143 infected non-primed plants compared to the untreated controls. Endogenous SA amount enhanced in roots of V143 infected primed plants on 2 dai ( $P < 0.01$ ), 3 dai ( $P < 0.05$ ) and 5 dai ( $P < 0.05$ ) compared to the non-primed controls (Fig. 36b).

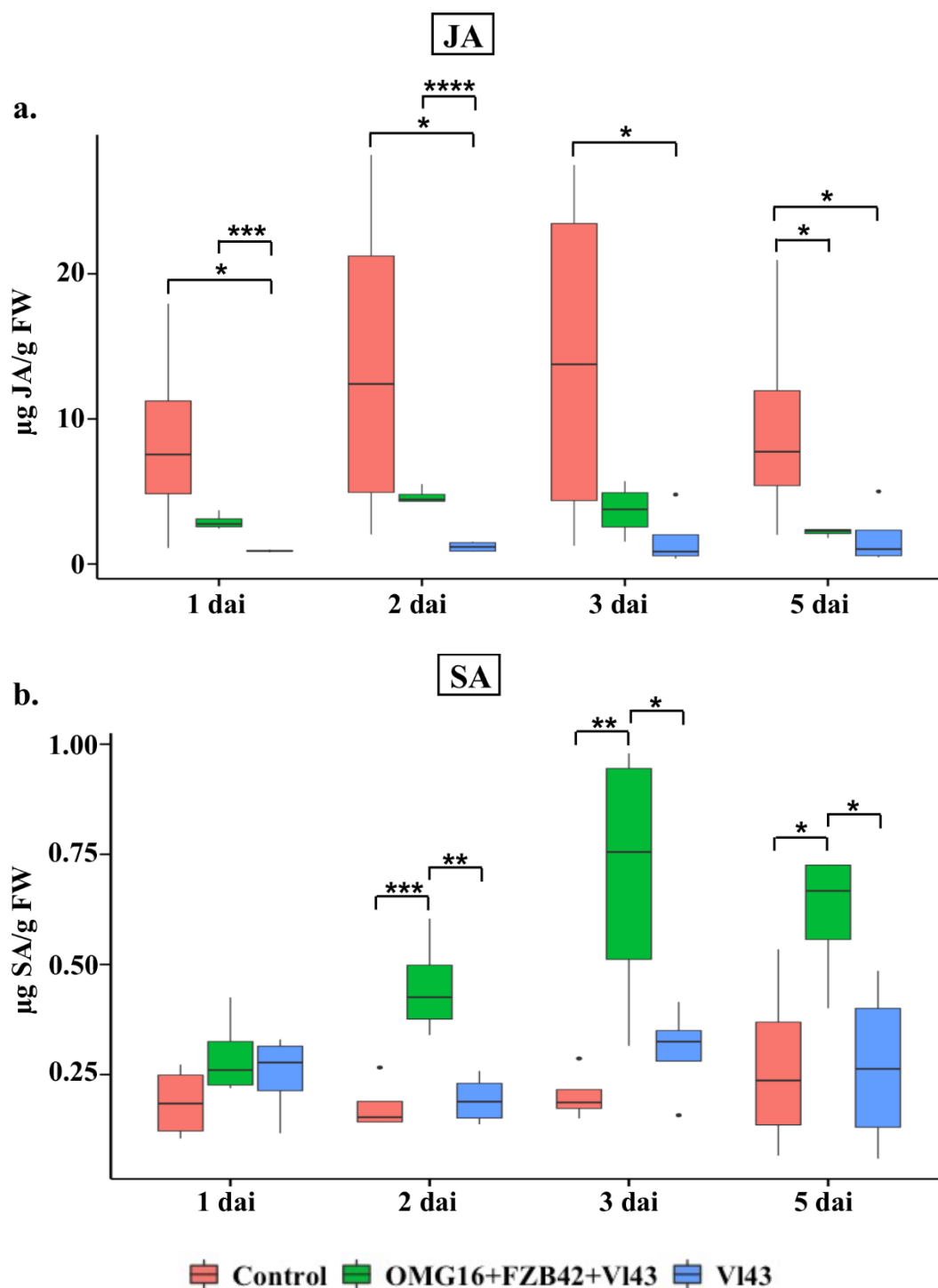


**Fig. 36.** Endogenous concentration of JA (a) and SA (b) phytohormones in root tissue of rapeseed plants at different time points upon OMG16 plus FZB42 plus VI43 and VI43 inoculation alone. Roots of two-week-old rapeseed plantlets of the AgP4 cultivar were primed with OMG16 plus FZB42. Two days after priming, roots were infected with VI43. To assess the phytohormone amounts, roots were analysed by UHPLC-MS. Box and whisker plots show the phytohormone values of five biological replicates where significance was calculated by Dunnett's test with mvt adjustment at  $P < 0.05$  compared to the control plants. Phytohormone amount between OMG16 plus FZB42 plus VI43 and single VI43 treatments was calculated by unpaired t-test at  $P < 0.05$ . \*  $P < 0.05$ ; \*\*  $P < 0.01$ ; \*\*\*  $P < 0.001$ ; \*\*\*\*  $P < 0.0001$ . OMG16, *T. harzianum* OMG16; FZB42, *B. velezensis* FZB42; VI43, *V. longisporum* 43; dai, days after infection.

### 3.2.4.2. Phytohormone contents in shoot tissue

The concentration of JA hormone increased as late as on 5 dai ( $P < 0.05$  each) in shoots of both V143 infected primed and non-primed plants compared to the untreated controls. JA amount also increased in V143 infected primed plants on 2 dai ( $P < 0.05$ ) than the V143 infected non-primed plants (Fig. 37a).

Endogenous concentration of SA hormone enhanced only on 1 dai ( $P < 0.05$ ) in shoots of V143 infected primed plants compared to the untreated controls (Fig. 37b). There was no induction of SA amount in V143 infected primed plants compared to the non-primed ones.

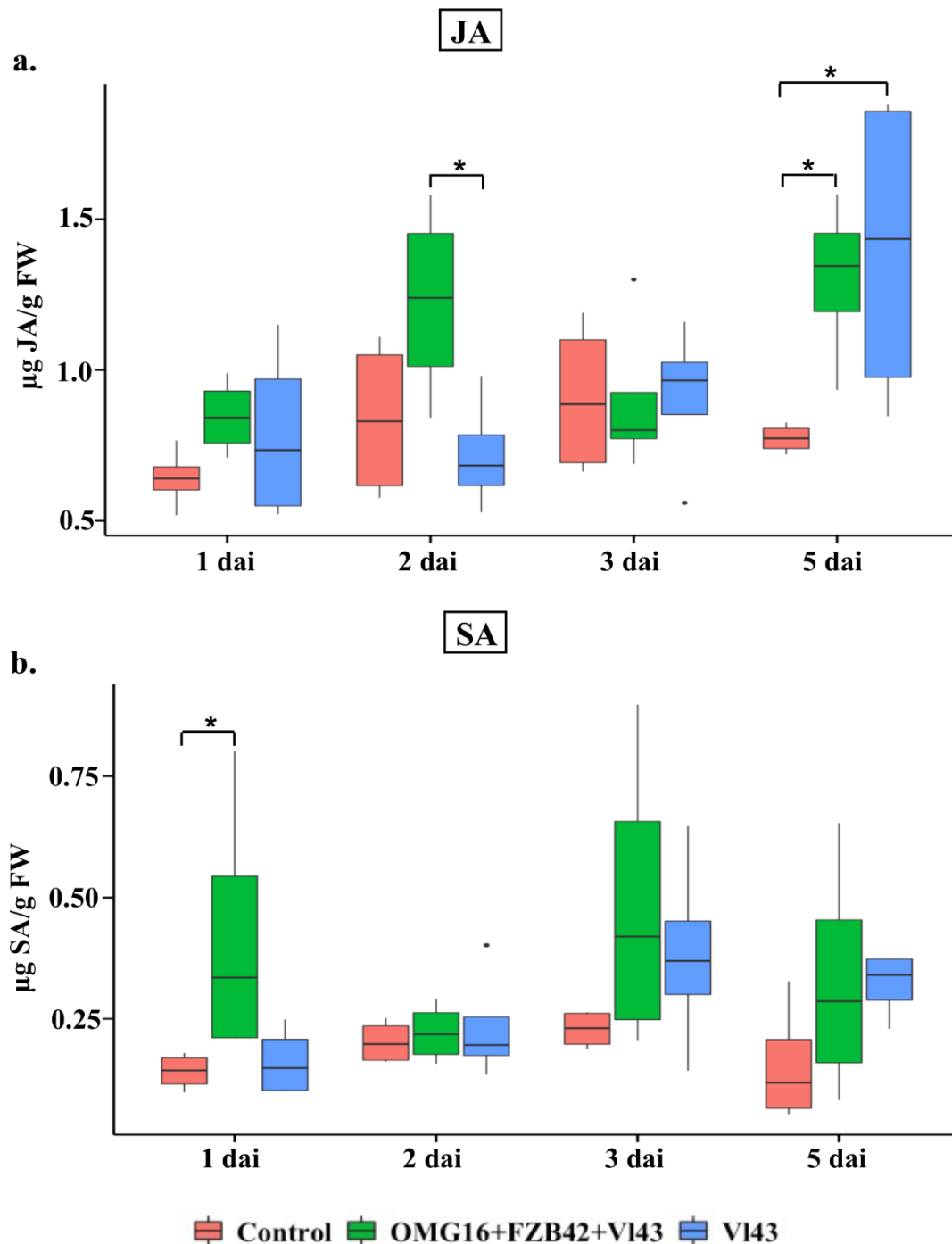


**Fig. 37.** Endogenous concentration of JA (a) and SA (b) phytohormones in shoot tissue of rapeseed plants at different time points upon OMG16 plus FZB42 plus V143 and V143 inoculation alone. Roots of two-week-old rapeseed plantlets of the AgP4 cultivar were primed with OMG16 plus FZB42. Two days after priming, roots were infected with V143. To assess the phytohormone amounts, shoots (both leaves and stems) of the same plants tested in section 3.2.4.1. were analysed by UHPLC-MS. Box and whisker plots show the phytohormone values of five biological replicates where significance was calculated by Dunnett's test with mvt adjustment at  $P < 0.05$  compared to the control plants. Phytohormone amount between OMG16 plus FZB42 plus V143 and single V143 treatments was calculated by unpaired t-test at  $P < 0.05$ . \*  $P < 0.05$ ; \*\*  $P < 0.01$ ; \*\*\*  $P < 0.001$ ; \*\*\*\*  $P < 0.0001$ . OMG16, *T. harzianum* OMG16; FZB42, *B. velezensis* FZB42; V143, *V. longisporum* 43; dai, days after infection.

## 4. Discussion

### 4.1. Interaction between rapeseed roots and *Trichoderma*

In this study, it is confirmed that *T. harzianum* OMG16 exhibits an intracellular endophytic lifestyle in rapeseed roots of *in vitro* grown plantlets as visualized by microscopic analyses. OMG16 possessed the ability to penetrate root hairs shortly after inoculation, notably within 24 h. In a previous study, microscopic observations detected *T. harzianum* CECT 2413 hyphae on tomato root surface at 24 h after inoculation (Samolski et al. 2012). CECT 2413 can also colonize the intercellular spaces of tomato roots without disrupting cell integrity and subsequently enters root epidermal cells and the cortex (Chacón et al. 2007; Velázquez-Robledo et al. 2011; Yedidia et al. 1999). *T. harzianum* T-203 attached to the root epidermis, but not root hair tips in cucumber, by forming appressoria-like structures mediated by *TasHyd1* encoded hydrophobin proteins (Yedidia et al. 1999; Viterbo and Chet, 2006). In this study, OMG16 bound high amounts of fuchsine red in the cell walls, which enabled us to distinguish densely compacted hyphae from hyphal cell wall structures of lower density (Fig. 17). These regions of lower cell wall density may be considered as potential sites of molecular crosstalk (Harman et al. 2004; Yedidia et al. 2000) between the fungus and plant, which possibly led to transcriptional responses of the rapeseed defence-related genes. Appressoria-like structures on the root epidermis or cortex were not found, which provided further evidence that root hair tips were the main entering sites of OMG16 into the rapeseed root system.

Microscopic analyses evinced that *T. virens* M9B fungus is also able to endophytically colonize the rapeseed roots. M9B attached to the root surface and penetrated the root hair cells as early as 2 days after root inoculation of *in-vitro* generated rapeseed seedlings (Fig 18). A previous study performed in maize demonstrated that *T. virens* Gv29.8 accomplished its endophytic characteristics by colonizing both inter and intracellular spaces of epidermal cells of primary and secondary roots (Nogueira-Lopez et al. 2018), which is in line with this study. Accumulation of fuchsine red dye by M9B hyphal cell wall enabled the detection of the fungus forming coiled-like structure inside the root hairs (Fig. 18b). Transcriptional analysis revealed that during root colonization, *T. virens* Gv29-8 suppresses host immune responses by secreting numerous cell wall degrading enzymes, reactive oxygen scavengers, secondary metabolites and effector-like protein molecules (Malinich et al. 2019; Schweiger et al. 2021; Taylor et al. 2021). Initiation of M9B hyphal penetration and expansion inside the root hair cells begins within 2 dai, indicating an early colonization of rapeseed roots. In a previous study, colonization of tomato roots by *T. virens* Gv29-8 was observed as early as 36 hours after inoculation (Malinich et al. 2019). Micrograph presented in Fig. 18c demonstrates that M9B hyphae resided inside

the epidermal cell layers by forming papilla-like structures in hyphal tips. In a previous study, such distinct structure was also observed in *T. harzianum* CECT 2413. After intercellularly colonizing tomato root, this fungus undergoes morphological changes such as formation of papilla-like swollen hyphal tips and yeast-like cells (Chacón et al. 2007).

In this study, it was also intended to separately transform the fluorescence proteins EGFP and DsRed encoding genes, *gfp* and *dsred*, in the protoplast of *T. harzianum* OMG16 and *T. virens* M9B fungal strains in order to achieve improved insights of their colonization mechanism of rapeseed roots under microscope. Both *gfp* and *dsred* containing plasmids were individually transformed in OMG16 and M9B protoplasts by transient transformation. *In vitro* grown transformed OMG16 and M9B hyphae emitted fluorescence signals on 2 days after transformation. Micrographs of Appendix 3a and b indicated successful transformation and expression of EGFP and DsRed proteins into *Trichoderma*. The transient transformants, OMG16 and M9B were cultured on hygromycin containing PDA plates for five generation to obtain stable resistance against hygromycin B. Although after four generations, no transformants was visualized on the screening plates. This observation indicates that either the plasmids drastically lost their resistance against hygromycin, or the plasmids themselves were lost during the repeated transfer process. In PEG mediated transient transformation process, recombinant plasmids containing, hygromycin phosphotransferase (*hph*) selectable marker harbour extrachromosomally in the filamentous fungi. *hph* transcribes in an extrachromosomal manner with a very low possibility of integrating to the host chromosome. These free plasmids are not able to replicate inside the fungi which makes it feasible to dilute the plasmid DNA during cell division and mycelial growth (Honda et al. 2019). Therefore, it is assumed that the OMG16 and M9B transformants lost their inserted extrachromosomal plasmids containing *gfp* and *dsred* during the periodical screening process. Hence, for the successful transformation, the fluorescence genes could be integrated into the host chromosome by stable transformation, for instance homologous recombination. Moreover, EGFP transformed OMG16 fungal hyphae from the first-generation transformation were detected to densely colonize the rapeseed root hairs on 7 dai (Appendix 3c). Nevertheless, analysis of root colonization by OMG16 was extremely impeded by high autofluorescence signals of the rapeseed root tissues. The micrograph appeared just green without the possibility for discrimination of plant tissue and fungal structures. To reduce or eliminate the background autofluorescence for this *in vivo* study applying EGFP fluorescent protein, recently developed novel techniques, such as Förster Resonant Energy Transfer (FRET) (Müller et al. 2013), Fluorescence Lifetime Imaging (FLIM)



(Kodama, 2016) or high-resolution 3D imaging (Dumur et al. 2019) could alternatively be applied.

#### **4.2. Effects of synergism on *Trichoderma* root colonization abundance**

Quantification of OMG16 DNA in roots using established protocols (Geistlinger et al. 2015; Poveda et al. 2019) demonstrated that the presence of FZB42 together with the fungus exhibited synergistic effects and significantly enhanced *Trichoderma* root colonization rate (Fig 19). Medium acidification caused by *B. velezensis* FZB42 might be a factor for improved root colonization frequency of *T. harzianum* OMG16 (Fig. 20). In addition, other mechanisms might also be relevant. For instance, *B. amyloliquefaciens* enhances the expression of cellulase and xylanase encoding genes (Karuppiyah et al. 2021) as well as plant defence response suppressors (Karuppiyah et al. 2019b), which prepare the cell walls of the roots in favour for beneficial fungi to penetrate. In soil-grown maize, the root colonization rate of OMG16 successfully increased by 210% in presence of a consortium of five *Bacillus* strains (Mpanga et al. 2019b). However, this effect depended largely on preferential ammonium supply together with the nitrification inhibitor DMPP (3,4-dimethylpyrazole-phosphate) (Mpanga et al. 2019a). This resembles the conditions in this study where Murashige and Skoog medium was used under sterile conditions, which avoids ammonium nitrification. Another important factor might be increased fine root growth. Importantly, data of this study demonstrated that inoculation of *B. napus* with FZB42 stimulated fine root growth (Fig. 22c), which provided a larger root surface area for quicker and better OMG16 root colonization. With respect to that it is important to mention that particularly at early time points significantly more fungal DNA could be detected in co-treated roots than in roots treated with OMG16 alone (Fig. 19), which substantiates the large surface area hypothesis. Indeed, it has been previously shown that rhizosphere competent bacteria can stimulate fine root formation, which subsequently provides increased potential sites for plants and fungi to interact (Frey-Klett et al. 2007). Such effects have also been described for FZB42 (Thonar et al. 2017; Yusran et al. 2009).

#### **4.3. Effects of synergism on root morphology and growth**

The presented data indicated that AgP4 cultivar had longer roots, prolonged fine roots, and a higher root mass and volume than the AgP1 cultivar (Fig. 22). In the AgP4 cultivar, the development of root morphology was faster after single inoculation with OMG16 or FZB42 than in dual inoculation but only at the early timepoints. Co-inoculation increased root lengths, dry weight, root volume, and fine-root lengths in early and late timepoints in the AgP1 cultivar. In this case, single inoculation had only minor effects on root morphology (Fig. 22). Similar

effects were observed in soil-grown tomato where root length development has been increased by 60-100% due to combined application of the respective microbial inoculants (Mpanga et al. 2018) and such effects were detected in maize after combined inoculation of OMG16 with a consortium of five *Bacillus* strains (Moradtalab et al. 2020). The observed benefits of the investigated OMG16-*Bacillus* combinations also resulted in improved field performance of maize (Mpanga et al. 2019b).

#### **4.4. Effects of synergism on the expression of defence-related rapeseed genes in cv. AgP1 and AgP4**

Based on the hypothesis, a potential systemic synergistic effect of *Trichoderma* and *Bacillus* root colonization on ISR gene expression was evaluated by qRT-PCR and normalized in rapeseed leaf tissue with three different reference genes. Fig. 23 could provide compelling evidence for synergistic effects of *Trichoderma* and *Bacillus* in colonization of *B. napus* roots. Analysis of gene expression by qRT-PCR revealed a very slow and weak induction of the selected defence-related genes *PDF1.2*, *ERF2* and *AOC3* in the AgP1 cultivar. In sharp contrast, expression of the analysed genes was much faster and higher in the AgP4 cultivar pointing also to genotypic differences in responsiveness of the selected rapeseed hybrids. Expression of the ET marker gene *ERF2* was increased at 1 hai and remained activated till 2 dai in dual inoculated plants compared to the untreated controls. Moreover, *ERF2* expression was higher in co-inoculated plants than single bacterial inoculation on 2 dai. In a previous study, ethylene responsive transcription factors (ERFs) belonging to a subfamily of the AP2/ERF superfamily (Yang et al. 2016) were shown to directly regulate the activation of JA/ET-dependent defence genes and to play a vital role in *A. thaliana* resistance against necrotrophic pathogens. Overexpression of *ERF2* gene involved in ET signalling mediated broad-spectrum resistance against pathogens was documented in *A. thaliana* (Bent et al. 1992; Nakano et al. 2006), rice (Nakano et al. 2006), tomato (He et al. 2001; Wilkinson et al. 1995) and tobacco (Ogata et al. 2012).

*AOC3*, which represents a JA biosynthesis gene (Stenzel et al. 2012), was expressed at 1 hai and remained activated till 3 dai (except 1 dai) in co-inoculated plants. *AOC3* catalyses the formation of 12-oxo-phytodienoic acid, the first biologically active intermediate in jasmonate biosynthesis (Schaller et al. 2008). The crosstalk between AP2/ERF TFs and the JA signalling pathway was first discovered in *Catharanthus roseus* by van der Fits and Memelink, (2001) and was also found in *A. thaliana* (Pré et al. 2008). Tolerance against different biotic and abiotic stresses induced by the JA hormonal pathway through the activation of *AOC* genes was

achieved in *A. thaliana* (Stenzel et al. 2012), barley (Jacquard et al. 2009), wheat (Habora et al. 2013; Zhao et al. 2014), soybean (Wu et al. 2011) and *Jatropha curcas* (Liu et al. 2010).

*PDF1.2* is well known to be involved in both ET and JA defence pathways (Penninckx et al. 1998; Zimmerli et al. 2001). The expression of *PDF1.2* also was significantly upregulated in OMG16 plus FZB42 co-inoculated plants at 2 and 3 dai, as compared with the controls. Besides, *PDF1.2* expression was higher at 2 days after dual inoculation than after single bacterial inoculation. Previous study reported that *Bacillus velezensis* treatment in oilseed rape roots induced ISR in leaves by increasing JA/ET-dependent *PDF1.2* expression (Sarosh et al. 2009) which was in line with this study where the expression of *PDF1.2* was significantly upregulated on 3 days upon single FZB42 inoculation (Fig. 23b). Taken together, these data suggest that the JA and ET signalling pathways were activated in AgP4 plantlets shortly after combined microbial treatment (1 hai) and remained activated at least until 3 dai (Fig. 23b, d, f), the end point of this experiment.

Both physical and chemical interactions are involved in underlying molecular mechanism of fungal-bacterial synergism (Frey-Klett et al. 2011). During fungal-bacterial interaction, filamentous Ascomycete fungus *Podospora anserina* can recognize bacteria by using its putative Nod-like immune receptors (NLRs) (Dyrka et al. 2014; Uehling et al. 2017). Several NLRs can directly detect the presence of MAMP and trigger fast transcriptomic responses by inducing the innate immune system of fungi (Ipcho et al. 2016; Paoletti and Saupe 2009; Salvioli et al. 2016). Such synergism also reported in culture conditions when *Trichoderma virens*-secreted cell wall degrading enzymes such as endochitinase or 1,3- $\beta$ -glucosidase can enhance the efficacy of *Pseudomonas syringae* B359 rhizobacterium-produced membrane-disrupting lipodepsipeptides such as syringotoxins and syringomycins by facilitating their entry to the cell membranes. Syringomycins possess the antimicrobial activity while syringotoxins shows phytotoxicity against the fungal pathogen *Botrytis cinerea*. These lipodepsipeptides can be absorbed by the fungal cell wall by binding to chitin and  $\beta$ -1,3-glucans. Appropriate cell wall degrading enzymes can impair this interaction and release the free lipodepsipeptides to reach the nearby plasmalemma (De Lucca et al. 1999; Woo et al. 2002). In a similar context, B359-secreted syringomycin E and syringopeptin 25A synergistically interacted with *Trichoderma atroviride* P1-secreted chitinolytic and gluconolytic enzymes against *Fusarium oxysporum*, *B. cinerea* and *Phytophthora infestans* (Fogliano et al. 2002). Dialysis experiments and electron microscopy analysis demonstrated that intimate physical interaction between the model fungus *Aspergillus nidulans* and *Streptomyces hygroscopicus* bacteria elicited specific signals to communicate among these microorganisms. Both microarray and qRT-PCR analyses

confirmed that such fungal-bacterial interaction induced the production of novel metabolites by activating the silent biosynthesis genes in fungus (Netzker et al. 2015; Schroeckh et al. 2009). Co-cultivation of *B. amyloliquefaciens* and *T. asperellum* was reported to enhance new secondary metabolites through the activation of signalling molecules (Wakefield et al. 2017). Transcriptome analysis of tomato roots revealed that *T. harzianum* T22 initiated the transcriptional reprogramming of genes involved in defence, metabolism and transport during early root colonization. Activation of defence genes induced priming in tomato plants through enhanced ET signal transduction within 72 hours post inoculation of *T. harzianum* T22 (De Palma et al. 2019). Moreover, *T. harzianum* TH12 significantly induced systemic resistance through the JA/ET pathways by increasing the *ERF2*, *PDF1.2* and *AOC3* gene expression levels at 1 and 2 dai in oilseed rape and thereby, established resistance in systemic oilseed rape tissues against *Sclerotinia sclerotiorum* (Alkoorane et al. 2017). In line to these previously published results, this study revealed that individual OMG16 inoculation induced *PDF1.2* on 1 dai while *ERF2* gene activation was observed shortly after inoculation (1 hai), on 1 dai and 3 dai. On the other hand, single rhizobacterium FZB42 mediated ISR gene activation was observed in *PDF1.2* only at 3 dai and in *ERF2* at 1 hai and 1 dai. Therefore, the gene expression data of this study suggest that combined application of root-endophytic OMG16 and FZB42 can activate the rapeseed defence pathways more efficiently than inoculation with the fungus or bacterium alone (Fig. 38). Such induction of rapeseed defence system was potentially activated through the induction of JA/ET signalling pathways.

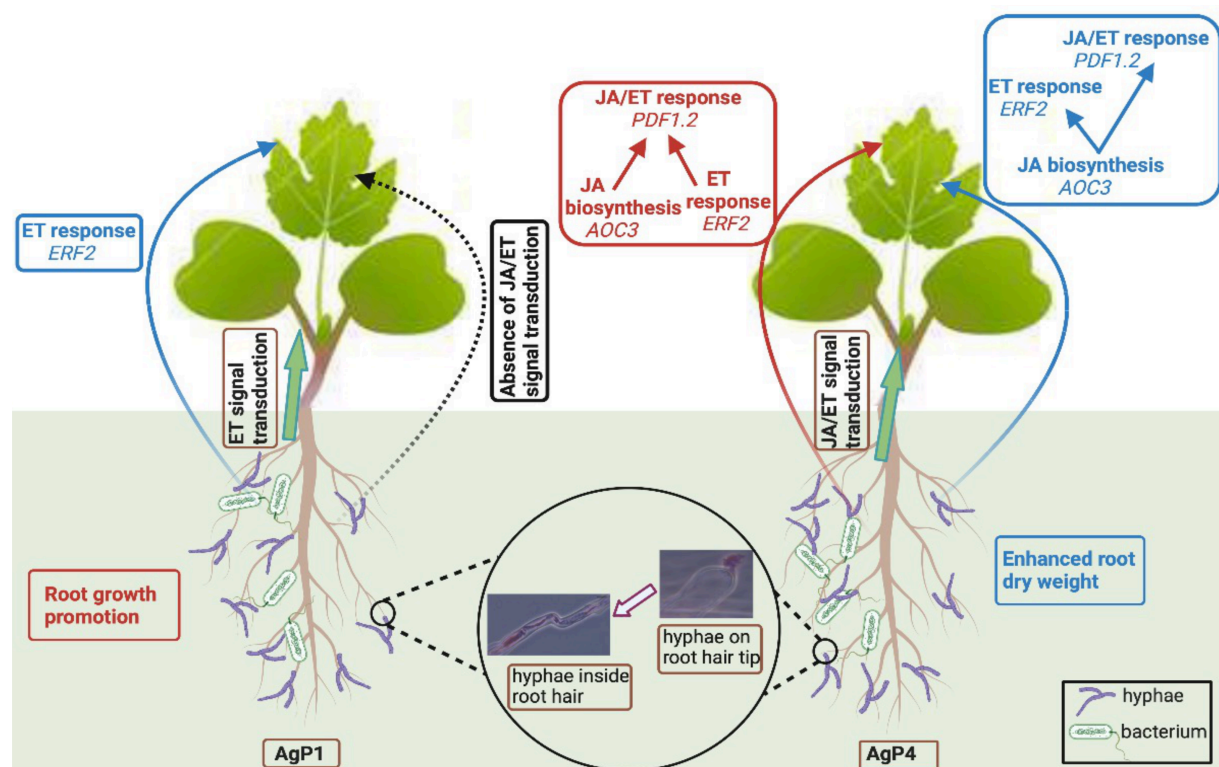


**Fig. 38.** Simplified model of molecular mechanisms involved in rapeseed defence signalling modulated by crosstalk between the ET and JA hormonal pathways in response to *Trichoderma*-rapeseed interaction and *Trichoderma*-*Bacillus*-rapeseed synergism. Red colour represents faster and stronger while blue represents slower and weaker responses. In both cultivars, OMG16 hyphae attached to the top of root hair tips and after penetration developed distinct intracellular structures. Also root development was enhanced in co-inoculated plants of both cultivars. In OMG16 and FZB42 co-inoculated AgP1 plants, the ET signal was transduced from the root system to leaves, where it induced expression of the ET responsive gene *ERF2*. JA/ET signal transduction was absent after single OMG16 inoculation. In the AgP4 cultivar, combined treatment of OMG16 and FZB42 in roots transduced strong JA and ET signals, which induced expression of the JA/ET marker gene *PDF1.2*, the JA biosynthesis gene *AOC3* and the ET responsive *ERF2* gene in leaves. In single OMG16 inoculated plant, weaker and slower JA/ET signal has transduced from root to the shoot and induced JA biosynthesis *AOC3* gene which simultaneously upregulated ET responsive *ERF2* and JA/ET responsive *PDF1.2* genes.

#### 4.5. Priming effects on *V. longisporum* root infection in cv. AgP4

To investigate whether priming may reduce the susceptibility of rapeseed roots for infection with *V. longisporum* 43, plants were primed with OMG16 plus FZB42 two days prior to V143 infection. Subsequent quantification of V143 DNA by qPCR demonstrated that primed plants were approximately 100-times less infected than non-primed plants (Fig. 25). As shown by microscopic studies (Fig. 17), OMG16 forms endophytic hyphae in *B. napus* root hairs, which may act as physical barriers for V143 hyphae to grow and penetrate the roots. A similar mechanism may also account for the FZB42 bacterial cells that had colonized the roots. Moreover, competition of OMG16 and FZB42 with V143 hyphae for micro and macronutrients might be an additional factor for V143 growth suppression. Previous studies showed that *Trichoderma asperellum* T34 protected tomato plants from *Fusarium* wilt by iron competition (Segarra et al. 2010). *Pichia guilliermondii* suppressed *B. cinerea* in apple (Zhang et al. 2011) and *Colletotrichum* spp. in chilli (Chanchaichaovivat et al. 2008) by competition for sugars and nitrate. Furthermore, hydrolytic enzymes produced by many *Trichoderma* strains may permeabilize and degrade the cell wall of fungal pathogens to facilitate the subsequent entry of secondary antimicrobial metabolites (Karlsson et al. 2017; Köhl et al. 2019). Recently, it was shown that an effective biocontrol activity was achieved *in vitro* by a *Trichoderma virens* strain that produced bio-active siderophores (Angel et al. 2016) and membrane-attacking peptaibols (Palyzová et al. 2019). Similarly, *B. velezensis* PGPBacCA1 was shown to secrete antifungal compounds including surfactin, iturin, fengycin and bacillomycins into the interaction zones with the pathogens *Macrophomina phaseolina* (Torres et al. 2016), *F. oxysporum* (Palyzová et al. 2019) and *Verticillium dahliae* (Han et al. 2015). Similar mechanisms may also be thought

for the antifungal effect of combined OMG16 and FZB42 application to inhibit V143 growth as observed in this study.

#### **4.6. Priming effects on rapeseed enhanced defence activation after V143 pathogen challenge**

Besides reducing V143 growth in root tissue, priming of rapeseed cv. 'AgP4' with OMG16 and FZB42 also enhanced the plant systemic defence responses against V143 infection (Fig. 26-37). Rapeseed seedlings were inoculated with OMG16 and FZB42 two days before V143 infection and the expression of JA, ET and SA biosynthesis and signalling genes were analysed separately in roots, stems and leaves by qRT-PCR analysis. Priming of rapeseed roots significantly enhanced the JA and ET biosynthesis as well as JA/ET and SA signalling pathways in leaves by inducing the corresponding biosynthesis and signalling genes (Appendix 6). Previously conducted studies postulated that *T. virens* and *T. atroviride* activated the JA/ET pathway by inducing the expression of *LOX-1* and *PDF1.2* in *A. thaliana*. Same fungi also induced the expression of *PRI*, thereby activating the SAR pathway (Contreras-Cornejo et al. 2011; Salas-Marina et al. 2011).

Similarly, in stems, priming also showed fast and strong induction of JA biosynthesis pathway and relatively slower and weaker induction of SA biosynthesis (Appendix 5). There was no significant induction of JA, ET and SA biosynthesis or signalling in roots (Appendix 4). These data indicate that beneficiary fungal and bacterial strains can prime the whole rapeseed plant body and transduce the ISR defence signal into the upper part of plants through JA and ET phytohormone biosynthesis and signalling pathways. Subsequently, when the rapeseed roots were infected with V143 spores on 2 days after priming, such molecular memory of immunization enhanced rapeseed defence against the pathogen challenge. Similar effects were previously observed after combined application of *T. harzianum* Tr6 and *Pseudomonas* sp. Ps14, which significantly increased the resistance level in cucumber against *Fusarium oxysporum* infection through elevated expression of a set of defence-related genes (Alizadeh et al. 2013).

Priming is associated with substantial reprogramming of the host transcriptome. To establish a successful symbiotic relationship between the plant roots and beneficiary microbes, host plant secretes strigolactones and flavonoids. These metabolites trigger the microbes to produce symbiotic Sym and Nod factors, which eventually initiate the symbiosis signalling pathway in roots of host plants (Oldroyd et al. 2009). Although ISR priming is mainly induced by JA and ET-dependent pathways, *Paenibacillus alvei* K165 rhizobacterium primes the plants through enhanced SA-dependent defence pathway (Tjamos et al. 2005) while endophytic actinobacteria,

can induce both SA and JA/ET pathways in *A. thaliana* during priming (Conn et al. 2008). *Trichoderma* generated MAMP and effector molecules bind to intracellular receptors PRRs. Activated PRRs in turn trigger mitogen-activated protein kinase (MAPK) cascades, leading to the reprogramming of defence related ISR pathway (Alfiky and Weisskopf, 2021). Plant hormone SA was reported to prevent the entry of *T. harzianum* T34 into the vascular system of *A. thaliana* roots and its subsequent spread into aerial parts of plants (Alonso-Ramírez et al. 2014).

Analysis of gene expression by qRT-PCR revealed a fast and strong induction of JA, ET and SA biosynthesis and signalling genes separately in root, stem and leaf tissues of the OMG16 plus FZB42 primed plants. Moreover, non-primed V143 infection also induced rapeseed defence through SAR pathway by enhancing the expression of SA, JA and ET biosynthesis and signalling genes. Such *Verticillium*-mediated defence activation was relatively weaker and slower.

#### 4.6.1. Priming effects on roots

qRT-PCR analysis showed that the expression of *LOX2* and *OPR3* was downregulated in the roots of V143 infected non-primed plants (Fig. 26a, b). This indicates that for successful colonization of rapeseed roots, V143 suppressed the JA biosynthesis pathway shortly after infection (1 dai) and remained attenuated at least until 5 dai, the end point of this experiment. A previous study demonstrated that V143 requires the functional activity of JA receptor, coronatine insensitive 1 (COI1) in the roots of *A. thaliana* to efficiently colonize its roots and elicit disease symptoms in the shoots (Ralhan et al. 2012).

In contrast, rapeseed plants primed with OMG16 and FZB42 were able to successfully overcome the suppression of JA biosynthesis in the roots after V143 infection. Upregulation of both *LOX2* and *OPR3* in the primed plants was identified as fast as 1 dai and remained activated until 5 dai compared to the non-primed plants. Nevertheless, the expression of *OPR3* still remained downregulated in V143 infected primed plants compared to the untreated controls. However, *OPR3* expression was at least remarkably higher in the V143 infected primed plants than the non-primed plants.

In addition, endogenous JA content in rapeseed roots were measured by UHPLC-MS. After synthesizing from  $\alpha$ -LA, JA conjugates with isoleucine amino acid to produce the bioactive JA-Ile (Fonseca et al. 2009; Haroth et al. 2019; Staswick and Tiriyaki, 2004). UHPLC-MS analysis only measured the free endogenous JA present in the leaf tissues. The JA amount was approximately 10-fold less in the roots of V143 infected non-primed plants than the untreated controls. V143 repressed JA production in rapeseed roots as early as 1 dai and continued until

5 dai. Such observation again demonstrated that V143 infection impaired JA biosynthesis during early root colonization process. In V143 infected primed plants the JA content was 3.9-fold higher within 1 dai and 2 dai than in V143 infected non-primed plants (Fig. 36a). This points to the evidence that priming with OMG16 and FZB42 enables the plants to immediately overcome suppression of JA biosynthesis caused by V143.

V143 infection also inhibited ET biosynthesis pathway at the site of infection by downregulating the expression of *ACS2* and *ACO4* in non-primed plants (Fig. 27a, b). Compared to the untreated controls, *ACS2* expression was suppressed as late as on 5 dai while the downregulation of *ACO4* was detected as early as on 2 dai and remained suppressed until 5 dai. Phytohormone ET was reported earlier to be necessary for *V. longisporum* to efficiently colonize the plant roots. *A. thaliana* mutants, *ein2-1*, *ein4-1* and *ein6-1* impaired in ET signalling pathways, displayed an enhanced susceptibility to *V. longisporum* than the wild-types (Johansson et al. 2006; Veronese et al. 2003). In this study, rapeseed roots previously treated with OMG16 and FZB42 suspensions showed a fast and strong induction of ET biosynthesis pathway by enhancing the expression of *ACS2* and *ACO4* in root tissues after V143 infection. In addition, also expression of the ET biosynthesis genes *ACS2* and *ACO4* reacted faster and stronger to V143 infection in primed compared to the non-primed plants. This points to the fact that priming with beneficial microbes enabled rapeseed roots to overcome the adverse effects on ET biosynthesis caused by V143 infection and enhanced the generation of ET.

The expression of *ICS1* and *PRI* was drastically reduced after V143 infection in the non-primed roots, indicating that V143 pathogen suppressed both SA biosynthesis and signalling pathways to successfully colonize the rapeseed roots (Fig. 28a, b). In accordance with this result, no induction of *PRI* was reported earlier in V143 infected rapeseed roots at 3 dai (Behrens et al. 2019). In a COI1-dependent manner, *V. longisporum* suppresses SA dependent defence in rapeseed by generating the JA-isoleucine-mimic coronatine (Ralhan et al. 2012). In this study, primed plants were able to quickly enhance the expression of both *ICS1* and *PRI*, thus mitigating the negative regulation of SA biosynthesis and signalling caused by V143 infection. Moreover, the endogenous SA content was also enhanced in V143 infected primed roots compared to both V143 infected non-primed plants and untreated control plants (Fig. 36b). To facilitate its transport and storage, small hydrophilic molecules are often added to SA, for instance SA is frequently conjugated with glucose to form SA-glucoside (SAG). However, these derivatives have no hormonal activity. Therefore, only free, bioactive SA was measured in root tissue by UHPLC-MS. Synthesis of SA in the roots of primed rapeseed increased to 2.3-fold on 2 dai and remained induced till 5 dai. Ratzinger et al. (2009) reported that SA is involved



in the susceptibility of *B. napus* to *V. longisporum* infection. Priming may reduce the susceptibility by increasing SA accumulation in rapeseed roots.

Taken together, these results suggest that V143 pathogen hijacks the defence system of rapeseed by inhibiting the biosynthesis of JA, ET and SA phytohormones and successfully entered into the roots to establish a long-lasting compatible interaction with the host. Rapeseed roots primed with OMG16 and FZB42 microbes revealed a rapid reprogramming of gene expression to activate the biosynthetic pathways of JA, ET and SA hormones and restricted the entry of V143 pathogen into the root cells.

#### **4.6.2. Priming effects on stems**

After penetrating the root, the vascular pathogen V143 systemically spreads through the xylem and generates microsclerotia in the stem of oil seed rape to develop “Verticillium stem striping” disease (Depotter et al. 2016; Eynck et al. 2007). Gene expression analysis by qRT-PCR revealed a fast and strong induction of *LOX2* and *OPR3* in stem tissue. Expression of these two JA biosynthesis genes indicated the enhanced production of JA hormone both in V143 infected primed and non-primed plants. Notably, the expression of *LOX2* and *OPR3* was higher in stems of V143 infected primed plants than the non-primed controls (Fig. 29a, b).

Similarly, ET production also increased in stem as the expression of ET biosynthesis genes *ACS2* and *ACO4* highly enhanced both in V143 infected primed and non-primed plants (Fig. 30a, b). *ACO4* expression was higher in V143 infected primed plants than non-primed plants. Interestingly, after V143 challenge, *ACS2* expression increased in the non-primed plants compared to the primed ones.

In V143 infected stem, SA biosynthesis and signalling increased both in primed and non-primed plants. Nevertheless, the expression of *ICS1* increased in stem of V143 infected non-primed plants than the primed plants (Fig. 31a). However, *PR1* expression was higher in the primed stems for first 2 days after infection, while the expression increased on 5 dai in the non-primed plants (Fig. 31b). This indicates that SA signalling in stem tissue elevated with the gradual increase of V143 infection. In line with this result, previous study documented an elevated level of SA and its metabolite, salicylic acid glucoside (SAG) in the xylem sap of rapeseed shoots after *V. longisporum* infection. A strong correlation was also reported between *V. longisporum* DNA content in hypocotyls and SAG levels in the shoot (Ratzinger et al. 2009).

#### **4.6.3. Priming effects on leaves**

The micrograph presented in Fig. 24 showed the hyphal net of V143 endophytically colonizing the rapeseed leaves on 8 days after root infection. After entering the rapeseed roots, V143

hyphae was moved to the leaves through vascular system. This hyphal migration process was previously described by Eynck et al. 2007.

Analysis of gene expression by qRT-PCR revealed the faster and stronger induction of *LOX2*, *AOC3* and *OPR3* in leaves of V143 infected primed plants compared to non-primed plants (Fig. 32a, b, c). Expression of these three biosynthesis genes in leaves indicated the activation of the JA biosynthesis pathway both in V143 infected primed and non-primed plants. Moreover, endogenous JA levels increased up to 1.7-fold higher in the shoots of V143 infected primed plants than non-primed plants (Fig. 37a). Such induction in JA level in leaves points to an efficient flux flowing through the JA pathway in the presence of OMG16 and FZB42 in roots. The expression of ET biosynthesis genes *ACS2* and *ACO4* was highly enhanced in the leaves of primed plants after V143 infection (Fig. 33a, b). A similar induction was also observed for the ET signalling gene *ERF2* (Fig. 33c), previously reported as susceptibility factor for *Verticillium* disease (Gkizi et al. 2016). Moreover, a fast and strong induction of JA and ET marker genes, *PDF1.2* and *VSP2* was detected in leaf tissue after V143 infection in primed plants compared to the non-primed plants (Fig. 34a, b). Therefore, these results demonstrated that OMG16 and FZB42 priming induced both JA and ET biosynthesis and signalling pathways in rapeseed leaves to increase the resistance against V143 infection. In line with these results, a previous study showed that *T. harzianum* TH12 induced systemic resistance via the JA/ET pathways by increasing the *ERF2*, *PDF1.2* and *AOC3* gene expression levels at 1 and 2 dai in oilseed rape and thereby established systemic resistance against *Sclerotinia sclerotiorum* (Alkoorane et al. 2017).

In the root system of perennial apple tree, JA activated defence related *MdERF* and *PR* protein encoding genes against *Pythium ultimum* oomycete infection acted as a positive inductor in feedback regulation of JA biosynthesis (Shin et al. 2014). In *A. thaliana*, roots were treated with *Bacillus cereus* AR156 and expression of *PDF1.2*, well known to be involved in both ET and JA defence pathways (Penninckx et al. 1998; Zimmerli et al. 2001), was activated in the leaves (Niu et al. 2011) and thereby stimulated ISR against *Pseudomonas syringae* pv. tomato DC3000 (Mathys et al. 2012). In lettuce, single FZB42 treatment was shown to increase *PDF1.2* gene expression, which again could be drastically enhanced after simultaneous application of FZB42 and the pathogen *Rhizoctonia solani*. This suggests that the plants were primed upon FZB42 treatment, which induced fast responses of ET and JA defence pathways after pathogen challenge (Chowdhury et al. 2015b). A similar effect was reported in oilseed rape where *B. amyloliquefaciens* had induced ISR through increasing JA/ET dependent of *PDF1.2* gene expression against *Botrytis cinerea* (Sarosh et al. 2009), which was in line with this study where

the expression of *PDF1.2* gene was significantly upregulated on 3 days upon single FZB42 inoculation (Fig. 23b).

In addition, the expression of the SA biosynthesis gene *ICS1* and the SA signalling gene *PR1* remarkably enhanced in leaves of VI43 infected primed plants (Fig. 35a, b). Moreover, the amount of endogenous SA was elevated up to 2.6-fold in shoots of VI43 infected primed plants shortly after infection (1 dai) (Fig. 37b), which indicates that both SA biosynthesis and signalling pathways induced in leaves after priming the rapeseed roots.

Taken together, these data indicated that priming the rapeseed roots with beneficial OMG16 and FZB42 microbes can lead to faster and stronger induction of plant defence hormone biosynthesis and signalling separately in roots, stems and leaves. Moreover, a root-borne mobile signal transduces from root to stem to leaf through JA, ET and SA phytohormones to enhance the defence system in response to VI43 infection. Chowdhury et al. (2015b) demonstrated that FZB42 enhanced plant defence responses against *R. solani* by increasing the expression of *PDF1.2*. FZB42 possesses the ability to promote ISR activities in *A. thaliana* seedlings by producing surfactin and microbial VOCs (Ryu et al. 2003). Similarly, *B. amyloliquefaciens* ssp. *plantarum* UCMB5113 rhizobacterium enhanced plant defence priming and conferred resistance to airborne pathogens without any direct interaction (Sarosh et al. 2009). In a similar study, rhizobacterium *P. alvei* K165 triggered ISR to protect *A. thaliana* from *V. dahliae* infestation in a SA jasmonate-dependent defence pathways by increasing *PR1* and *PDF1.2* expression in leaves (Gkizi et al. 2016). On the other hand, transcriptomic analysis of *Trichoderma atroviride* T11 showed increased expression levels of genes involved in catalytic, hydrolytic and transporter activities, and secondary metabolism in response to *V. dahliae* infection performed on *in vitro* grown fungal culture (Morán-Diez et al. 2019). Therefore, the orchestrate transcriptional reprogramming of JA, ET and SA pathways upon priming induced rapeseed defence and restricted *V. longisporum* proliferation.

## 5. Conclusion

This study has demonstrated that *T. harzianum* OMG16 and *B. velezensis* FZB42 acted synergistically to induce the JA and ET hormone signal transduction pathways in rapeseed, which are crucial for activating ISR. Pre-treatment of roots with both OMG16 and FZB42 restricts V143 infection in roots and systemically transduces fast, strong and long-lasting signals based on the JA and ET hormonal pathways (schematically summarized in Fig. 39). Due to the importance of early root development for field performance of oilseed rape (Koscielny and Gulden, 2012; Louvieux et al. 2020) and the continuously declining availability of chemical plant protection agents, these results may offer a perspective for the development of alternative and sustainable approaches to enhance the tolerance of rapeseed cultures against fungal infections. The results also suggest that cultivar-dependent differences in the responsiveness of host plants with respect to inoculant effects need to be considered in this context. This may, at least partially, explain the reported variability of plant responses to beneficial microbes frequently observed under field conditions.

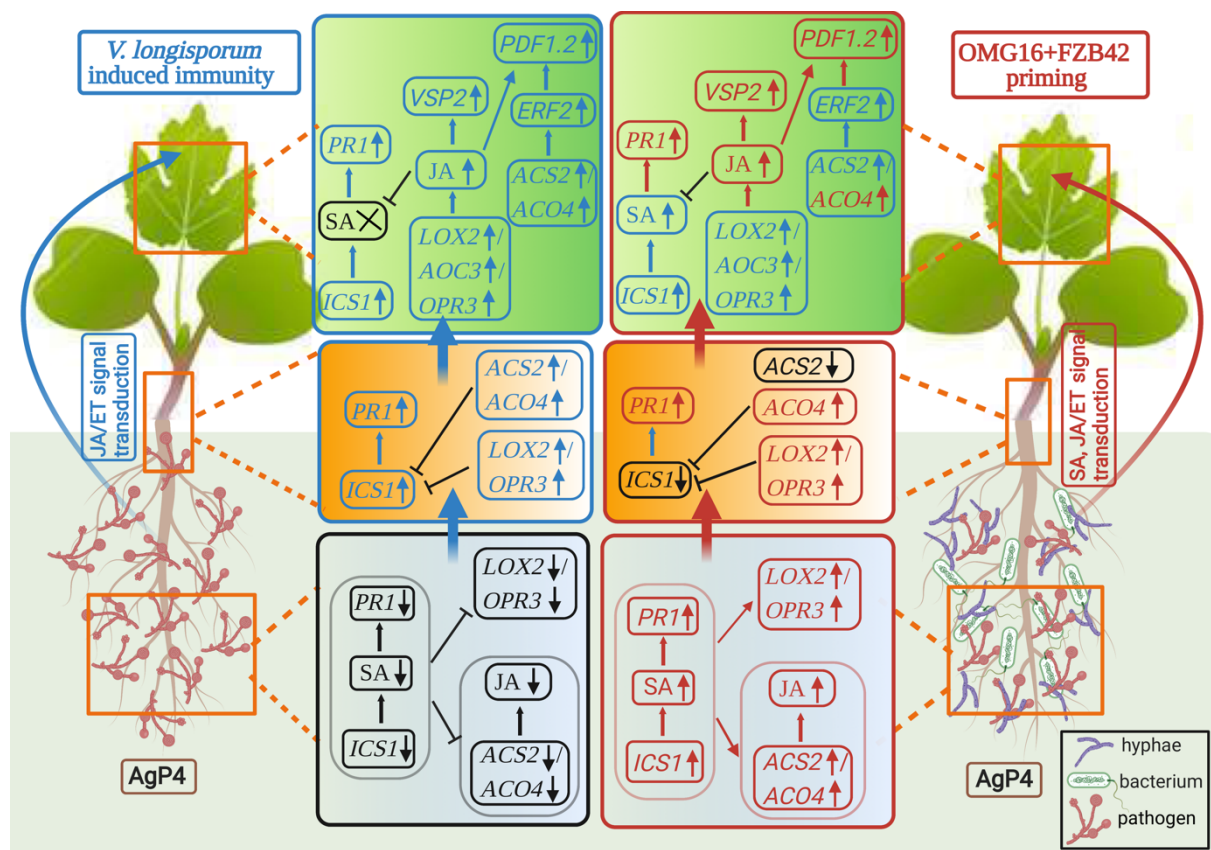


**Fig. 39.** Schematic representation of molecular mechanisms involved in rapeseed defence signal transduction from root to stem to leaf tissues through crosstalk among the SA, ET and JA hormonal pathways in response to *Verticillium*-rapeseed interaction and *Trichoderma*-*Bacillus*-rapeseed priming, followed by *Verticillium* infection. Red colour represents faster and stronger while blue represents slower and weaker responses.

Moreover, black colour represents down-regulation or suppression. Arrows indicate positive regulation (activation), blunt-ended lines indicate negative regulation (repression). While upward arrows (↑) indicate upregulation, downward arrows (↓) indicate downregulation. In the non-primed AgP4 rapeseed cultivar, V143 hyphae intercellularly colonized the root cells and penetrated the vascular system to block the flow of xylem sap. OMG16 and FZB42 primed AgP4 plants, restricted the entry of V143 into the roots. In V143 infected non-primed plants, SA biosynthesis and signalling was downregulated in roots compared to the untreated controls. SA acted antagonistically with JA and ET biosynthesis pathways and suppressed their biosynthesis. In stems, JA/ET biosynthesis pathways were antagonistic to SA biosynthesis while in leaves endogenous JA blocked SA production but acted synergistically with ET pathway to activate JA/ET signalling by inducing the expression of JA marker gene *VSP2* and JA/ET responsive gene *PDF1.2*. Evidently, weaker and slower JA/ET signal transduced from roots to the leaves in V143 infected non-primed plants. On the other hand, in OMG16 and FZB42 primed plants, SA biosynthesis and signalling were upregulated in roots after V143 infection compared to the non-primed plants. Activated SA simultaneously triggered both JA and ET biosynthetic pathways. In stems of primed plants, both JA and ET acted antagonistically with SA biosynthesis pathway. Similarly, in leaves elevated amounts of JA suppressed SA production. Strong JA signal induced the expression of JA marker gene *VSP2* as well as the JA/ET marker gene *PDF1.2* in leaves of primed plants. In OMG16 and FZB42 primed plants, expression of the JA and ET marker genes was stronger and faster after V143 infection than in the non-primed plants. Here, remarkably intense SA, JA and ET signals systematically transduced from root to the upper parts of the primed plants.

## 6. References

- Adams, D. O., and Yang, S. F. 1979. Ethylene biosynthesis: Identification of 1-aminocyclopropane-1-carboxylic acid as an intermediate in the conversion of methionine to ethylene. *Proc. Natl. Acad. Sci. U.S.A.* 76:170-174.
- Adams, D. O., and Yang, S. F. 1977. Methionine metabolism in apple tissue: implication of S-adenosylmethionine as an intermediate in the conversion of methionine to ethylene. *Plant Physiol.* 60:892-896.
- Alfiky, A.; Weisskopf, L. 2021. Deciphering *Trichoderma*-plant-pathogen interactions for better development of biocontrol applications. *J. Fungi* 7:61.
- Alizadeh, H., Behboudi, K., Ahmadzadeh, M., Javan-Nikkhah, M., Zamioudis, C., Pieterse, C. M. J., and Bakker P. A. H. M. 2013. Induced systemic resistance in cucumber and *Arabidopsis thaliana* by the combination of *Trichoderma harzianum* Tr6 and *Pseudomonas* sp. Ps14. *Biol. Control* 65:14-23.
- Alkooranee, J. T., Aledan, T. R., Ali, A. K., Lu, G., Zhang, X., Wu, J., Fu, C., and Li, M. 2017. Detecting the hormonal pathways in oilseed rape behind induced systemic resistance by *Trichoderma harzianum* TH12 to *Sclerotinia sclerotiorum*. *PLoS One* 12:e0168850.
- Alkooranee, J. T., Aledan, T. R., Xiang, J., Lu, G., and Li, M. 2015. Induced systemic resistance in two genotypes of *Brassica napus* (AACC) and *Raphanus oleracea* (RRCC) by *Trichoderma* isolates against *Sclerotinia sclerotiorum*. *Am. J. Plant Sci.* 6:1662-1674.
- Alonso-Ramírez, A., Poveda, J., Martín, I., Hermosa, R., Monte, E. and Nicolás, C. 2015. *Trichoderma harzianum* root colonization in *Arabidopsis*. *Bio-protocol* 5:e1512.
- Alonso-Ramírez, A., Poveda, J., Martín, I., Hermosa, R., Monte, E., and Nicolás, C. 2014. Salicylic acid prevents *Trichoderma harzianum* from entering the vascular system of roots. *Mol. Plant Pathol.* 15:823-831.
- Alonso, J. M., Hirayama, T., Roman, G., Nourizadeh, S., and Ecker, J. R. 1999. EIN2, a bifunctional transducer of ethylene and stress responses in *Arabidopsis*. *Science* 284, 2148-2152.
- An, F., Zhao, Q., Ji, Y., Li, W., Jiang, Z., Yu, X., Zhang, C., Han, Y., He, W., Liu, Y., Zhang, S., Ecker, J. R., and Guo, H. 2010. Ethylene-induced stabilization of ETHYLENE INSENSITIVE3 and EIN3-LIKE1 is mediated by proteasomal degradation of EIN3 binding F-box 1 and 2 that requires EIN2 in *Arabidopsis*. *Plant Cell.* 22:2384-2401.
- An, H., Qi, X., Gaynor, M. L., Hao, Y., Gebken, S. C., Mabry, M. E., McAlvay, A. C., Teakle, G. R., Conant, G. C., Barker, M. S., Fu, T., Yi, B., and Pires, J. C. 2019. Transcriptome

- and organellar sequencing highlights the complex origin and diversification of allotetraploid *Brassica napus*. *Nat. Commun.* 10:2878.
- Angel, L. P. L., Yusof, M. T., Ismail, I. S., Ping, B. T. Y., Azni, I. N. A. M., Kamarudin, N. H. J., and Sundram, S. 2016. An *in vitro* study of the antifungal activity of *Trichoderma virens* 7b and a profile of its non-polar antifungal components released against *Ganoderma boninense*. *J. Microbiol.* 54:732-744.
- Attaran, E., and He, S. Y. 2012. The long-sought-after salicylic acid receptors. *Mol. Plant* 5:971-973.
- Bae, Y. S., and Knudsen, G. R. 2000. Cotransformation of *Trichoderma harzianum* with beta-glucuronidase and green fluorescent protein genes provides a useful tool for monitoring fungal growth and activity in natural soils. *Appl. Environ. Microbiol.* 66:810-815.
- Behrens, F. H., Schenke, D., Hossain, R., Ye, W., Schemmel, M., Bergmann, T., Häder, C., Zhao, Y., Ladewig, L., Zhu, W., and Cai, D. 2019. Suppression of abscisic acid biosynthesis at the early infection stage of *Verticillium longisporum* in oilseed rape (*Brassica napus*). *Mol. Plant Pathol.* 20:1645-1661.
- Bent, A. F., Innes, R. W., Ecker, J. R., and Staskawicz, B. J. 1992. Disease development in ethylene-insensitive *Arabidopsis thaliana* infected with virulent and avirulent *Pseudomonas* and *Xanthomonas* pathogens. *Mol. Plant Microbe Interact.* 5:372-378.
- Berendsen, R. L., Pieterse, C. M., and Bakker, P. A. 2012. The rhizosphere microbiome and plant health. *Trends Plant Sci.* 17:478-486.
- Berg, G., Rybakova, D., Grube, M., and Köberl, M. 2016. The plant microbiome explored: implications for experimental botany. *J. Exp. Bot.* 67:995-1002.
- Boller, T., Hener, R. C., and Kende, H. 1979. Assay for and enzymatic formation of an ethylene precursor, 1-aminocyclopropane-1-carboxylic acid. *Planta* 145:293-303.
- Borriss, R., Chen, X. H., Rueckert, C., Blom, J., Becker, A., Baumgarth, B., Fan, B., Pukall, R., Schumann, P., Spröer, C., Junge, H., Vater, J., Pühler, A., and Klenk, H. P. 2011. Relationship of *Bacillus amyloliquefaciens* clades associated with strains DSM 7<sup>T</sup> and FZB42<sup>T</sup>: a proposal for *Bacillus amyloliquefaciens* subsp. *amyloliquefaciens* subsp. nov. and *Bacillus amyloliquefaciens* subsp. *plantarum* subsp. nov. based on complete genome sequence comparisons. *Int. J. Syst. Evol. Microbiol.* 61:1786-1801.
- Breithaupt, C., Kurzbauer, R., Lilie, H., Schaller, A., Strassner, J., Huber, R., Macheroux, P., and Clausen, T. 2006. Crystal structure of 12-oxophytodienoate reductase 3 from

- tomato: self-inhibition by dimerization. *Proc. Natl. Acad. Sci. U. S. A.* 103:14337-14342.
- Brotman, Y., Landau, U., Cuadros-Inostroza, A. Â., Takayuki, T., Fernie, A. R., Chet, I., Viterbo, A., and Willmitzer, L. 2013. *Trichoderma*-plant root colonization: escaping early plant defence responses and activation of the antioxidant machinery for saline stress tolerance. *PLoS Pathog.* 9:e1003221.
- Bustin, S. A., Benes, V., Garson, J. A., Hellems, J., Huggett, J., Kubista, M., Mueller, R., Nolan, T., Pfaffl, M. W., Shipley, G. L., Vandesompele, J., and Wittwer, C. T. 2009. The MIQE guidelines: minimum information for publication of quantitative real-time PCR experiments. *Clin. Chem.* 55:611-622.
- Caarls, L., Pieterse, C. M. J., and Van Wees, S. C. M. 2015. How salicylic acid takes transcriptional control over jasmonic acid signaling. *Front. Plant Sci.* 6:170.
- Caldelari, D., Wang, G., Farmer, E. E., and Dong, X. 2011. *Arabidopsis* lox3 lox4 double mutants are male sterile and defective in global proliferative arrest. *Plant Mol. Biol.* 75:25-33.
- Cao, H., Bowling, S. A., Gordon, A. S., and Dong, X. 1994. Characterization of an *Arabidopsis* mutant that is nonresponsive to inducers of systemic acquired resistance. *Plant Cell* 6:1583-1592.
- Carreras-Villaseñor, N., Sánchez-Arreguín, J. A., and Herrera-Estrella, A. H. 2012. *Trichoderma*: sensing the environment for survival and dispersal. *Microbiology* 158:3-16.
- Carro-Huerta, G., Compant, S., Gorfer, M., Cardoza, R. E., Schmoll, M., Gutiérrez, S., and Casquero, P. A. 2020. Colonization of *Vitis vinifera* L. by the endophyte *Trichoderma* sp. Strain T154: biocontrol activity against *Phaeoacremonium minimum*. *Front. Plant Sci.* 11:1170.
- Chacón, M. R., Rodríguez-Galán, O., Benítez, T., Sousa, S., Rey, M., Llobell, A., and Delgado-Jarana, J. 2007. Microscopic and transcriptome analyses of early colonization of tomato roots by *Trichoderma harzianum*. *Int. Microbiol.* 10:19-27.
- Chalhoub, B., Denoeud, F., Liu, S., Parkin, I. A., Tang, H., Wang, X., Chiquet, J., Belcram, H., Tong, C., Samans, B., Corréa, M., Da Silva, C., Just, J., Falentin, C., Koh, C. S., Le Clainche, I., Bernard, M., Bento, P., Noel, B., Labadie, K., ... Wincker, P. 2014. Plant genetics. Early allopolyploid evolution in the post-neolithic *Brassica napus* oilseed genome. *Science* 345:950-953.



- Chanchaichaovivat, A., Panijpana, B., and Ruenwongsaab, P. 2008. Putative modes of action of *Pichia guilliermondii* strain R13 in controlling chilli anthracnose after harvest. *Biol. Control* 47: 207-215.
- Chang, C. 2016. Q&A: How do plants respond to ethylene and what is its importance? *BMC Biol.* 14:7.
- Chang, C., Kwok, S. F., Bleecker, A. B., and Meyerowitz, E. M. 1993. Arabidopsis ethylene response gene ETR1: similarity of product to two-component regulators. *Science.* 262:539-544.
- Chauvin, A., Lenglet, A., Wolfender, J.-L., and Farmer, E. E. 2016. Paired hierarchical organization of 13-lipoxygenases in *Arabidopsis*. *Plants.* 5:16.
- Chauvin, A., Caldelari, D., Wolfender, J.-L., and Farmer, E. E. 2013. Four 13-lipoxygenases contribute to rapid jasmonate synthesis in wounded *Arabidopsis thaliana* leaves: a role for lipoxygenase 6 in responses to long-distance wound signals. *New Phytol.* 197:566-575.
- Chen, X. H., Scholz, R., Borriss, M., Junge, H., Mögel, G., Kunz, S., and Borriss, R. 2009. Difficidin and bacilysin produced by plant-associated *Bacillus amyloliquefaciens* are efficient in controlling fire blight disease. *J. Biotechnol.* 140:38-44.
- Chen, X.-H., Vater, J., Piel, J., Franke, P., Scholz, R., Schneider, K., Koumoutsi, A., Hitzeroth, G., Grammel, N., Strittmatter, A.W., Gottschalk, G., Süßmuth, R. D., and Borriss, R. 2006. Structural and functional characterization of three polyketide synthase gene clusters in *Bacillus amyloliquefaciens* FZB42. *J. Bacteriol.* 188:4024-4036.
- Chen, X., Koumoutsi, A., Scholz, R., Eisenreich, A., Schneider, K., Heinemeyer, I., Morgenstern, B., Voss, B., Hess, W. R., Reva, O., Junge, H., Voigt, B., Jungblut, P. R., Vater, J., Süßmuth, R., Liesegang, H., Strittmatter, A., Gottschalk, G., and Borriss, R. 2007. Comparative analysis of the complete genome sequence of the plant growth-promoting bacterium *Bacillus amyloliquefaciens* FZB42. *Nat. Biotechnol.* 25:1007-1014.
- Cheong, J. J., and Choi, Y. D. 2003. Methyl jasmonate as a vital substance in plants. *Trends Genet.* 19:409-413
- Chini, A., Fonseca, S., Fernandez, G., Adie, B., Chico, J. M., Lorenzo, O., Garcia-Casado, G., Lopez-Vidriero, I., Lozano, F. M., Ponce, M. R., Micol, J. L., and Solano, R. 2007. The JAZ family of repressors is the missing link in jasmonate signalling. *Nature* 448:666-671.

- Choudhary, D. K., Prakash, A., and Johri, B. N. 2007. Induced systemic resistance (ISR) in plants: mechanism of action. *Indian J. Microbiol.* 47:289-297.
- Chowdhury, S. P., Hartmann, A., Gao, X., and Borriss, R. 2015a. Biocontrol mechanism by root-associated *Bacillus amyloliquefaciens* FZB42 - a review. *Front. Microbiol.* 6:780.
- Chowdhury, S. P., Uhl, J., Grosch, R., Alquéres, S., Pittroff, S., Dietel, K., Schmitt, K. P., Borriss, R., and Hartmann, A. 2015b. Cyclic lipopeptides of *Bacillus amyloliquefaciens* subsp. *Plantarum* colonizing the lettuce rhizosphere enhance plant defense responses toward the bottom rot pathogen *Rhizoctonia solani*. *Mol. Plant Microbe Interact.* 28:984-995.
- Chung, H. S., Niu, Y., Browse, J., and Howe, G.A. 2009. Top hits in contemporary JAZ: an update on jasmonate signaling. *Phytochemistry* 70:1547-1559.
- Coleman-Derr, D., Desgarenes, D., Fonseca-Garcia, C., Gross, S., Clingenpeel, S., Woyke, T., North, G., Visel, A., Partida-Martinez, L. P., and Tringe, S. G. 2016. Plant compartment and biogeography affect microbiome composition in cultivated and native *Agave* species. *New Phytol.* 209:798-811.
- Conn, V. M., Walker, A. R., and Franco, C. M. 2008. Endophytic actinobacteria induce defense pathways in *Arabidopsis thaliana*. *Mol. Plant Microbe Interact.* 21:208-218.
- Contreras-Cornejo, H. A., Macías-Rodríguez, L., Beltrán-Peña, E., Herrera-Estrella, A., and López-Bucio, J. 2011. Trichoderma-induced plant immunity likely involves both hormonal- and camalexin-dependent mechanisms in *Arabidopsis thaliana* and confers resistance against necrotrophic fungi *Botrytis cinerea*. *Plant Signal. Behav.* 6:1554-1563.
- Coppola, M., Cascone, P., Di Lelio, I., Woo, S. L., Lorito, M., Rao, R., Pennacchio, F., Guerrieri, E., and Digilio, M. C. 2019. *Trichoderma atroviride* P1 colonization of tomato plants enhances both direct and indirect defense barriers against insects. *Front. Physiol.* 10:813.
- Cruz, C. M., Martínez, C., Buchala, A., Métraux, J.-P., and León, J. 2004. Gene-specific involvement of beta-oxidation in wound-activated responses in *Arabidopsis*. *Plant Physiol.* 135:85-94.
- Dave, A., Hernández, M. L., He, Z., Andriotis, V. M., Vaistij, F. E., Larson, T. R., and Graham, I. A. 2011. 12-oxo-phytodienoic acid accumulation during seed development represses seed germination in *Arabidopsis*. *Plant Cell.* 23:583-599.

- Delaney, T. P., Friedrich, L., and Ryals, J. A. 1995. Arabidopsis signal transduction mutant defective in chemically and biologically induced disease resistance. *Proc. Natl. Acad. Sci. U.S.A.* 92:6602-6606.
- De Lucca, A. J., Jacks, T. J., Takemoto, J. Y., Vinjard, B., Peter, J., Navarro, E., and Walsh, T. J. 1999. Fungal lethality, binding, and cytotoxicity of syringomycin-E. *Antimicrob. Agents Chemother.* 43:371-373.
- De Palma, M., Salzano, M., Villano, C., Aversano, R., Lorito, M., Ruocco, M., Docimo, T., Piccinelli, A.L., D'Agostino, N., and Tucci, M. 2019. Transcriptome reprogramming, epigenetic modifications and alternative splicing orchestrate the tomato root response to the beneficial fungus *Trichoderma harzianum*. *Hort. Res.* 6:5.
- De Vleeschauwer, D., Xu, J., and Höfte, M. 2014. Making sense of hormone-mediated defense networking: from rice to Arabidopsis. *Front. Plant Sci.* 5:611.
- De Vos, M., Van Oosten, V. R., Van Poecke, R. M., Van Pelt, J. A., Pozo, M. J., Mueller, M. J., Buchala, A. J., Métraux, J. P., Van Loon, L. C., Dicke, M., and Pieterse, C. M. 2005. Signal signature and transcriptome changes of Arabidopsis during pathogen and insect attack. *Mol Plant Microbe Interact* 18:923-937.
- Dempsey, D. A., Vlot, A. C., Wildermuth, M. C., and Klessig, D. F. 2011. Salicylic acid biosynthesis and metabolism. *Arabidopsis Book* 9:e0156.
- Depotter, J. R. L., Deketelaere, S., Inderbitzin, P., Tiedemann, A. V., Höfte, M., Subbarao, K. V., Wood, T. A., and Thomma, B. P. H. J. 2016. *Verticillium longisporum*, the invisible threat to oilseed rape and other brassicaceous plant hosts. *Mol. Plant Pathol.* 17:1004-1016.
- Dhar, N., Chen, J.-Y., Subbarao, K. V., and Klosterman, S. J. 2020. Hormone signaling and its interplay with development and defense responses in *Verticillium*-plant interactions. *Front. Plant Sci.* 11:584997.
- Ding, P., and Ding, Y. 2020. Stories of salicylic acid: a plant defense hormone. *Trends Plant Sci.* 25:549-565.
- Doornbos, R. F., van Loon, L. C., and Bakker, P. A. 2012. Impact of root exudates and plant defense signaling on bacterial communities in the rhizosphere. A review. *Agron. Sustain. Dev.* 32:227-243.
- Dubois, M., Van den Broeck, L., and Inzé, D. 2018. The pivotal role of ethylene in plant growth. *Trends Plant Sci.* 23:311-323.

- Dumur, T., Duncan, S., Graumann, K., Desset, S., Randall, R. S., Scheid, O. M., Prodanov, D., Tatout, C., and Baroux, C. 2019. Probing the 3D architecture of the plant nucleus with microscopy approaches: challenges and solutions. *Nucleus* 10:181-212.
- Dunker, S., Keunecke, H., Steinbach, P., and Tiedemann, A. V. 2008. Impact of *Verticillium longisporum* on yield and morphology of winter oilseed rape (*Brassica napus*) in relation to systemic spread in the plant. *J. Phytopathol.* 156:698-707.
- Dyrka, W., Lamacchia, M., Durrens, P., Kobe, B., Daskalov, A., Paoletti, M., Sherman, D. J., and Saupe, S. J. 2014. Diversity and variability of NOD-like receptors in fungi. *Genome Biol. Evol.* 6:3137-3158.
- Eckert, M., Maguire, K., Urban, M., Foster, S., Fitt, B., Lucas, J., and Hammond-Kosack, K. 2005. Agrobacterium tumefaciens-mediated transformation of *Leptosphaeria* spp. and *Oculimacula* spp. with the reef coral gene DsRed and the jellyfish gene gfp. *FEMS Microbiol. Lett.* 253:67-74.
- European Commission. (2022, April 28). Oilseeds and protein crops-market situation. Committee for the common organisation of agricultural markets. <https://circabc.europa.eu/sd/a/215a681a-5f50-4a4b-a953-e8fc6336819c/oilseeds-market%20situation.pdf>.
- Eynck, C., Koopmann, B., Karlovsky, P., and von Tiedemann, A. 2009. Internal resistance in winter oilseed rape inhibits systemic spread of the vascular pathogen *Verticillium longisporum*. *Phytopathology* 99:802-811.
- Eynck, C., Koopmann, B., Grunewaldt-Stoecker, G., Karlovsky, P., and Tiedemann, A. 2007. Differential interactions of *Verticillium longisporum* and *V. dahliae* with *Brassica napus* detected with molecular and histological techniques. *Eur. J. Plant Pathol.* 118:259-274.
- Fan, B., Wang, C., Song, X., Ding, X., Wu, L., Wu, H., Gao, X., and Borriss, R. 2018. *Bacillus velezensis* FZB42 in 2018: the gram-positive model strain for plant growth promotion and biocontrol. *Front. Microbiol.* 9:2491.
- Fan, B., Borriss, R., Bleiss, W., and Wu, X. 2012. Gram-positive rhizobacterium *Bacillus amyloliquefaciens* FZB42 colonizes three types of plants in different patterns. *J. Microbiol.* 50:38-44.
- Fan, B., Chen, X. H., Budiharjo, A., Vater, J., and Borriss, R. 2011. Efficient colonization of plant roots by the plant growth promoting bacterium *Bacillus amyloliquefaciens* FZB42, engineered to express green fluorescent protein. *J. Biotechnol.* 151:303-311.

- Farmer, E. E., Alme´ras, E., and Krishnamurthy, V. 2003. Jasmonates and related oxylipins in plant responses to pathogenesis and herbivory. *Curr. Opin. Plant Biol.* 6:372-378.
- Feng, Y., Cui, R., Wang, S., He, M., Hua, Y., Shi, L., Ye, X., and Xu, F. 2020. Transcription factor BnaA9.WRKY47 contributes to the adaptation of *Brassica napus* to low boron stress by up-regulating the boric acid channel gene BnaA3.NIP5;1. *Plant Biotechnol. J.* 18:1241-1254.
- Floerl, S., Druebert, C., Majcherczyk, A., Karlovsky, P., Kues, U., and Polle, A. 2008. Defense reactions in the apoplastic proteome of oilseed rape (*Brassica napus* var. *napus*) attenuate *Verticillium longisporum* growth but not disease symptoms. *BMC Plant Biol.* 8:129.
- Fogliano, V., Ballio, A., Gallo, M., Woo, S., Scala, F., and Lorito, M. 2002. Pseudomonas lipodepsipeptides and fungal cell wall-degrading enzymes act synergistically in biological control. *Mol. Plant Microbe Interact.* 15:323-333.
- Fonseca, S., Chini, A., Hamberg, M., Adie, B., Porzel, A., Kramell, R., Miersch, O., Wasternack, C., and Solano, R. 2009. (+)-7-iso-Jasmonoyl-L-isoleucine is the endogenous bioactive jasmonate. *Nat. Chem. Biol.* 5:344-350.
- Fradin, E. F., Zhang, Z., Juarez Ayala, J. C., Castroverde, C. D., Nazar, R. N., Robb, J., Liu, C. M., and Thomma, B. P. 2009. Genetic dissection of *Verticillium* wilt resistance mediated by tomato Ve1. *Plant Physiol.* 150:320-332.
- Frey-Klett, P., Burlinson, P., Deveau, A., Barret, M., Tarkka, M., and Sarniguet, A. 2011. Bacterial-fungal interactions: hyphens between agricultural, clinical, environmental, and food microbiologists. *Microbiol. Mol. Biol. Rev.* 75:583-609.
- Frey-Klett, P., Garbaye, J., and Tarkka, M. 2007. The mycorrhiza helper bacteria revisited. *New Phytol.* 176:22-36.
- Fu, Z. Q., Yan, S., Saleh, A., Wang, W., Ruble, J., Oka, N., Mohan, R., Spoel, S. H., Tada, Y., Zheng, N., and Dong, X. 2012. NPR3 and NPR4 are receptors for the immune signal salicylic acid in plants. *Nature* 486:228-232.
- Gao, X., Wheeler, T., Li, Z., Kenerley, C. M., He, P., and Shan, L. 2011. Silencing GhNDR1 and GhMKK2 compromises cotton resistance to *Verticillium* wilt. *Plant J.* 66:293-305.
- Garber, R. H., and Houston, B. R. 1966. Penetration and development of *Verticillium alboatrum* in the cotton plant. *Phytopathology* 56:1121-1126.
- Garcion, C., Lohmann, A., Lamodire, E., Catinot, J., Buchala, A., Doermann, P., and Metraux, J. P. 2008. Characterization and biological function of the ISOCHORISMATE SYNTHASE2 gene of *Arabidopsis*. *Plant Physiol.* 147:1279-1287.

- Gatz, C. 2013. From pioneers to team players: TGA transcription factors provide a molecular link between different stress pathways. *Mol. Plant-Microbe Interact.* 26:151-159.
- Geistlinger, J., Zwanzig, J., Heckendorff, S., and Schellenberg, I. 2015. SSR markers for *Trichoderma virens*: their evaluation and application to identify and quantify root-endophytic strains. *Diversity* 7:360-384.
- Gfeller, A., Dubugnon, L., Liechti, R., and Farmer, E. E. 2010. Jasmonate biochemical pathway. *Sci. Signal.* 3:cm3
- Gimenez-Ibanez, S., Boter, M., Ortigosa, A., García-Casado, G., Chini, A., Lewsey, M. G., Ecker, J. R., Ntoukakis, V., and Solano, R. 2017. JAZ2 controls stomata dynamics during bacterial invasion. *New Phytol.* 213:1378-1392.
- Gkizi, D., Lehmann, S., L'Haridon, F., Serrano, M., Paplomatas, E. J., Métraux, J.-P., and Tjamos, S. E. 2016. The innate immune signaling system as a regulator of disease resistance and induced systemic resistance activity against *Verticillium dahlia*. *Mol. Plant Microbe Interact.* 29:313-323.
- Glazebrook, J. 2005. Contrasting mechanisms of defense against biotrophic and necrotrophic pathogens. *Annu. Rev. Phytopathol.* 43:205-227.
- Gu, Q., Yang, Y., Yuan, Q., Shi, G., Wu, L., Lou, Z., Huo, R., Wu, H., Borriss, R., and Gao, X. 2017. Bacillomycin D produced by *Bacillus amyloliquefaciens* is involved in the antagonistic interaction with the plant pathogenic fungus *Fusarium graminearum*. *Appl. Environ. Microbiol.* 83:e01075-17.
- Guillaume, R. G., and Sauter, M. 2008. Ethylene biosynthesis and signaling in rice. *Plant Sci.* 175:32-42.
- Guo, J., Lu, C., Zhao, F., Gao, S., and Wang, B. 2020. Improved reproductive growth of euhalophyte *Suaeda salsa* under salinity is correlated with altered phytohormone biosynthesis and signal transduction. *Funct. Plant Biol.* 47:170-183.
- Habora, M. E. E., Eltayeb, A. E., Oka, M., Tsujimoto, H., and Tanaka, K. 2013. Cloning of allene oxide cyclase gene from *Leymus mollis* and analysis of its expression in wheat–*Leymus* chromosome addition lines. *Breed. Sci.* 63:68-76.
- Haddadi, P., Larkan, N. J., and Borhan, M. H. 2019. Dissecting *R* gene and host genetic background effect on the *Brassica napus* defense response to *Leptosphaeria maculans*. *Sci Rep.* 9:6947.
- Hamilton, A. J., Bouzayen, M., and Grierson, D. 1991. Identification of a tomato gene for the ethylene-forming enzyme by expression in yeast. *Proc. Natl. Acad. Sci. U.S.A.* 88:434-7437.

- Han, Q., Wu, F., Wang, X., Qi, H., Shi, L., Ren, A., Liu, Q., Zhao, M., and Tang, C. 2015. The bacterial lipopeptide iturins induce *Verticillium dahliae* cell death by affecting fungal signalling pathways and mediate plant defence responses involved in pathogen-associated molecular pattern-triggered immunity. *Environ. Microbiol.* 17:1166-1188.
- Harman, G. E., Herrera-Estrella, A. H., Horwitz, B. A., and Lorito, M. 2012. Special issue: *Trichoderma* - from basic biology to biotechnology. *Microbiology* 158:1-2.
- Harman, G. E., Howell, C. R., Viterbo, A., Chet, I., and Lorito, M. 2004. *Trichoderma* species -opportunistic, avirulent plant symbionts. *Nat. Rev. Microbiol.* 2:43-56.
- Harothe, S., Feussner, K., Kelly, A. A., Zienkiewicz, K., Shaikhqasem, A., Herrfurth, C., and Feussner, I. 2019. The glycosyltransferase UGT76E1 significantly contributes to 12-O-glucopyranosyl-jasmonic acid formation in wounded *Arabidopsis thaliana* leaves. *J. Biol. Chem.* 294:9858-9872.
- Hartmann, M., and Zeier, J. 2019. N-Hydroxypipicolinic acid and salicylic acid: a metabolic duo for systemic acquired resistance. *Curr. Opin. Plant Biol.* 50:44-57.
- Hassan, N., Elsharkawy, M. M., Shivanna, M. B., Meera, M. S., and Hyakumachi, M. 2014. Elevated expression of hydrolases, oxidase, and lyase in susceptible and resistant cucumber cultivars systemically induced with plant growth-promoting fungi against anthracnose. *Acta Agric. Scand. B Soil Plant Sci.* 64:155-164.
- Hatzfeld, Y., Maruyama, A., Schmidt, A., Noji, M., Ishizawa, K., and Saito, K. 2000.  $\beta$ -Cyanoalanine synthase is a mitochondrial cysteine synthase-like protein in spinach and *Arabidopsis*. *Plant Physiol.* 123:1163-1172.
- He, P., Warren, R. F., Zhao, T., Shan, L., Zhu, L., Tang, X., and Zhou, J. M. 2001. Overexpression of Pti5 in tomato potentiates pathogen-induced defense gene expression and enhances disease resistance to *Pseudomonas syringae* pv. tomato. *Mol. Plant Microbe Interact.* 14:1453-1457.
- He, X., Jiang, J., Wang, C. Q., and Dehesh, K. 2017. ORA59 and EIN3 interaction couples jasmonate-ethylene synergistic action to antagonistic salicylic acid regulation of PDF expression. *J. Integr. Plant Biol.* 59:275-287.
- Heale, J. B., and Karapapa, V. K. 1999. The *Verticillium* threat to Canada's major oilseed crop: canola. *Can. J. Plant. Pathol.* 21:1-7.
- Heil, M., and Bostock, R. M. 2002. Induced systemic resistance (ISR) against pathogens in the context of induced plant defences. *Ann. Bot.* 89:503-512.
- Hermosa, R., Viterbo, A., Chet, I., and Monte, E. 2012. Plant-beneficial effects of *Trichoderma* and of its genes. *Microbiology* 158:17-25.

- Hillmer, R. A., Tsuda, K., Rallapalli, G., Asai, S., Truman, W., Papke, M. D., Sakakibara, H., Jones, J. D. G., Myers, C. L., and Katagiri, F. 2017. The highly buffered *Arabidopsis* immune signaling network conceals the functions of its components. *PLoS Genet.* 13:e1006639.
- Honda, Y., Tanigawa, E., Tsukihara, T., Nguyen, D. X., Kawabe, H., Sakatoku, N., Watari, J., Sato, H., Yano, S., Tachiki, T., Irie, T., Watanabe, T., and Watanabe, T. 2019. Stable and transient transformation, and a promoter assay in the selective lignin-degrading fungus, *Ceriporiopsis subvermispota*. *AMB Expr.* 9:92.
- Hossain, M. M., Sultana, F., and Hyakumachi, M. 2017. Role of ethylene signalling in growth and systemic resistance induction by the plant growth promoting fungus *Penicillium viridicatum* in *Arabidopsis*. *J. Phytopathol.* 165:432-441.
- Hoyos-Carvajal, L., Orduz, S., and Bisset, J. 2009. Growth stimulation in bean (*Phaseolus vulgaris* L.) by *Trichoderma*. *Biol. Control* 51:409-416.
- Huang, W., Wang, Y., Li, X., and Zhang Y. 2020. Biosynthesis and regulation of salicylic Acid and N-hydroxypipicolinic acid in plant immunity. *Mol. Plant.* 13:31-41.
- Illescas, M., Pedrero-Méndez, A., Pitorini-Bovolini, M., Hermosa, R., and Monte, E. 2021. Phytohormone production profiles in *Trichoderma* species and their relationship to wheat plant responses to water stress. *Pathogens* 10:991.
- Ipcho, S., Sundelin, T., Erbs, G., Kistler, H. C., Newman, M. A., and Olsson, S. 2016. Fungal innate immunity induced by bacterial microbe-associated molecular patterns (MAMPs). *G3* 6:1585-1595.
- Ishiguro, S., Kawai-Oda, A., Ueda, J., Nishida, I., and Okada, K. 2001. The DEFECTIVE IN ANTHHER DEHISCENCE gene encodes a novel phospholipase A1 catalyzing the initial step of jasmonic acid biosynthesis, which synchronizes pollen maturation, anther dehiscence, and flower opening in *Arabidopsis*. *Plant Cell* 13:2191-2209.
- Iven, T., Koenig, S., Singh, S., Braus-Stronmeyer, S. A., Bischoff, M., Tietze, L. F., Braus, G. H., Lipka, V., Feussner, I., and Droege-Laser, W. 2012. Transcriptional activation and production of tryptophan-derived secondary metabolites in *Arabidopsis* roots contributes to the defense against the fungal vascular pathogen *Verticillium longisporum*. *Mol. Plant* 5:1389-1402.
- Jacquard, C., Mazeyrat-Gourbeyre, F., Devaux, P., Boutilier, k., Baillieul, F., and Cle'ment, C. 2009. Microspore embryogenesis in barley: anther pre-treatment stimulates plant defence gene expression. *Planta* 229:393-402.



- Jiang, K., and Asami, T. 2018. Chemical regulators of plant hormones and their applications in basic research and agriculture. *Biosci., Biotechnol., Biochem.* 82:1265-1300.
- Jogaiah, S., Abdelrahman, M., Tran, L. S. P., and Shin-ichi, I. 2013. Characterization of rhizosphere fungi that mediate resistance in tomato against bacterial wilt disease. *J. Exp. Bot.* 64:3829-3842.
- Johansson, A., Staal, J., and Dixelius, C. 2006. Early responses in the *Arabidopsis- Verticillium longisporum* pathosystem are dependent on NDR1, JA- and ET-associated signals via cytosolic NPR1 and RFO1. *Mol. Plant Microbe Interact.* 19:958-969.
- Jones, J., and Dangl, J. 2006. The plant immune system. *Nature* 444:323-329.
- Ju, C., and Chang, C. 2015. Mechanistic insights in ethylene perception and signal transduction. *Plant Physiol.* 169:85-95.
- Ju, C., Yoon, G. M., Shemansky, J. M., Lin, D. Y., Ying, Z. I., Chang, J., Garrett, W. M., Kessenbrock, M., Groth, G., Tucker, M. L., Cooper, B., Kieber, J. J., and Chang, C. 2012. CTR1 phosphorylates the central regulator EIN2 to control ethylene hormone signaling from the ER membrane to the nucleus in *Arabidopsis*. *Proc. Natl. Acad. Sci. USA.* 109:19486-19491.
- Jung, S. C., Martinez-Medina, A., Lopez-Raez, J. A., and Pozo, M. J. 2012. Mycorrhiza-Induced Resistance and priming of plant defenses. *J. Chem. Ecol.* 38:651-664.
- Kamble, A., Koopmann, B., and Tiedemann, A. V. 2013. Induced resistance to *Verticillium longisporum* in *Brassica napus* by  $\beta$ -aminobutyric acid. *Plant Pathol.* 62:552-561.
- Karapapa, V. K., Bainbridge, B. W., and Heale, J. B. 1997. Morphological and molecular characterization of *Verticillium longisporum* comb. nov., pathogenic to oilseed rape. *Mycol. Res.* 101:1281-1294.
- Karlsson, M., Atanasova, L., Jensen, D. F., and Zeilinger, S. 2017. Necrotrophic mycoparasites and their genomes. *Microbiol. Spectr.* 5:10.
- Karuppiah, V., Zhixiang, L., Liu, H., Vallikkannu, M., and Chen, J. 2021. Co-culture of Vell1-overexpressed *Trichoderma asperellum* and *Bacillus amyloliquefaciens*: An eco-friendly strategy to hydrolyze the lignocellulose biomass in soil to enrich the soil fertility, plant growth and disease resistance. *Microb. Cell Fact.* 20:57.
- Karuppiah, V., Sun, J., Li, T., Vallikkannu, M., and Chen, J. 2019a. Co-cultivation of *Trichoderma asperellum* GDFS1009 and *Bacillus amyloliquefaciens* 1841 causes differential gene expression and improvement in the wheat growth and biocontrol activity. *Front. Microbiol.* 10:1068.

- Karuppiah, V., Vallikkannu, M., Li, T., and Chen, J. 2019b. Simultaneous and sequential based co-fermentations of *Trichoderma asperellum* GDFS1009 and *Bacillus amyloliquefaciens* 1841: a strategy to enhance the gene expression and metabolites to improve the bio-control and plant growth promoting activity. *Microb. Cell Fact.*18:185.
- Kehr, J., Buhtz, A., and Giavalisco, P. 2005. Analysis of xylem sap proteins from *Brassica napus*. *BMC Plant Biol.* 5:11
- Khoshmanzar, E., Aliasgharzad, N., Neyshabouri, M. R., Khoshru, B., Arzanlou, M. and Lajayeral, B. A. 2020. Effects of *Trichoderma* isolates on tomato growth and inducing its tolerance to water-deficit stress. *Int. J. Environ. Sci. Technol.* 17:869-878.
- Kim, Y., Tsuda, K., Igarashi, D., Hillmer, R. A., Sakakibara, H., Myers, C. L., and Katagiri, F. 2014. Mechanisms underlying robustness and tunability in a plant immune signaling network. *Cell Host Microbe* 15:84-94.
- Klee, H. J. 2004. Ethylene signal transduction: moving beyond *Arabidopsis*. *Plant Physiol.* 135:660-667.
- Klessig, D. F., Choi, H. W., and Dempsey, D. A. 2018. Systemic acquired resistance and salicylic acid: past, present, and future. *Mol. Plant Microbe Interact.* 31:871-888.
- Kloepper, J. W., Leong, J., Teintze, M., and Schroth, M. N. 1980. Enhancing plant growth by siderophores produced by plant-growth-promoting rhizobacteria. *Nature* 286:885-886.
- Kodama Y. 2016. Time gating of chloroplast autofluorescence allows clearer fluorescence imaging *in planta*. *PLoS ONE* 11: e0152484.
- Köhl, J., Kolnaar, R., and Ravensberg, W. J. 2019. Mode of action of microbial biological control agents against plant diseases: relevance beyond efficacy. *Front. Plant Sci.* 10:845.
- König, S., Feussner, K., Kaefer, A., Landesfeind, M., Thurow, C., Karlovsky, P., Gatz, C., Polle, A. and Feussner, I. 2014. Soluble phenylpropanoids are involved in the defense response of *Arabidopsis* against *Verticillium longisporum*. *New Phytol.* 202:823-837.
- Koscielny, C. B, and Gulden, R. H. 2012. Seedling root length in *Brassica napus* L. is indicative of seed yield. *Can. J. Plant Pathol.* 92:1229-1237.
- Koumoutsis, A., Chen, X.-H., Henne, A., Liesegang, H., Hitzeroth, G., Franke, P., Vater, V., and Borriss R. 2004. Structural and functional characterization of gene clusters directing nonribosomal synthesis of bioactive cyclic lipopeptides in *Bacillus amyloliquefaciens* strain FZB42. *J. Bacteriol.* 186:1084-1096.

- Lam, V. B., Meyer, T., Arias, A. A., Ongena, M., Oni, F. E., and Höfte, M. 2021. *Bacillus* cyclic lipopeptides iturin and fengycin control rice blast caused by *Pyricularia oryzae* in potting and acid sulfate soils by direct antagonism and induced systemic resistance. *Microorganisms* 9:1441.
- Larrieu, A., and Vernoux, T. 2016. Q&A: How does jasmonate signaling enable plants to adapt and survive?. *BMC Biol.* 14:79.
- Laudert, D., Pfannschmidt, U., Lottspeich, F., Holländer-Czytko, H., and Weiler, E. W. 1996. Cloning, molecular and functional characterization of *Arabidopsis thaliana* allene oxide synthase (CYP 74), the first enzyme of the octadecanoid pathway to jasmonates. *Plant Mol. Biol.* 31:323-335.
- Lee, B., Farag, M. A., Park, H. B., Kloepper, J. W., Lee, S. H., and Ryu, C-M. 2012. Induced resistance by a long-chain bacterial volatile: elicitation of plant systemic defense by a C13 volatile produced by *Paenibacillus polymyxa*. *PLoS One* 7:e48744.
- Lee, D.-S., Nioche, P., Hamberg, M., and Raman, C. S. 2008. Structural insights into the evolutionary paths of oxylipin biosynthetic enzymes. *Nature.* 455:363-368.
- Lefevre, H., Bauters, L., and Gheysen, G. 2020. Salicylic acid biosynthesis in plants. *Front. Plant Sci.* 11:338.
- Leon-Reyes, A., Spoel, S. H., De Lange, E. S., Abe, H., Kobayashi, M., Tsuda, S., Millenaar, F. F., Welschen, R. A., Ritsema, T., and Pieterse, C. M. 2009. Ethylene modulates the role of NONEXPRESSOR OF PATHOGENESIS-RELATED GENES1 in cross talk between salicylate and jasmonate signaling. *Plant Physiol.* 149:1797-1809.
- Leon, J., Shulaev, V., Yalpani, N., Lawton, M.A., and Raskin, I. 1995. Benzoic acid 2-hydroxylase, a soluble oxygenase from tobacco, catalyzes salicylic acid biosynthesis. *Proc. Natl. Acad. Sci. U S A* 92:10413-10417.
- Leon, J., Yalpani, N., Raskin, I., and Lawton, M. A. 1993. Induction of benzoic acid 2-hydroxylase in virus-inoculated tobacco. *Plant Physiol.* 103:323-328.
- Leonard, M., Kühn, A., Harting, R., Maurus, I., Nagel, A., Starke, J., Kusch, H., Valerius, O., Feussner, K., Feussner, I., Kaefer, A., Landesfeind, M., Morgenstern, B., Becher, D., Hecker, M., Braus-Stromeier, S. A., Kronstad, J. W., and Braus, G. H. 2020. *Verticillium longisporum* elicits media-dependent secretome responses with capacity to distinguish between plant-related environments. *Front. Microbiol.* 11:1876.
- Li, L., Long, M., Islam, F., Farooq, M. A., Wang, J., Mwamba, T. M., Shou, J., and Zhou, W. 2019. Synergistic effects of chromium and copper on photosynthetic inhibition,

- subcellular distribution, and related gene expression in *Brassica napus* cultivars. *Environ. Sci. Pollut. Res.* 26:11827-11845.
- Li, N., Han, X., Feng, D., Yuan, D., and Huang, L.-J. 2019. Signaling crosstalk between salicylic acid and ethylene/jasmonate in plant defense: do we understand what they are whispering? *Int. J. Mol. Sci.* 20:671.
- Lieberman, M., Kunishi, A., Mapson, L. W., and Wardale, D. A. 1966. Stimulation of ethylene production in apple tissue slices by methionine. *Plant Physiol.* 41:376-382.
- Life Science Market. (2018, August 15). pBARGPE1-Hygro-EGFP Plasmid. <https://www.lifescience-market.com/plasmid-c-94/pbargpe1-hygro-egfp-plasmid-p-63825.html>
- Liu, B., Wang, W., Gao, J., Chen, F., Wang, S., Xu, Y., Tang, L., and Jia, Y. 2010. Molecular cloning and characterization of a jasmonate biosynthetic pathway gene for allene oxide cyclase from *Jatropha curcas*. *Acta Physiol. Plant* 32:531-539.
- Lopisso, D. T., Knüfer, J., Koopmann, B., and von Tiedemann, A. 2017. Growth of *Verticillium longisporum* in xylem sap of *Brassica napus* is independent from cultivar resistance but promoted by plant aging. *Phytopathology* 107:1047-1054.
- Lorito, M., Woo, S. L., Harman, G. E., and Monte, E. 2010. Translational research on *Trichoderma*: from 'omics to the field. *Annu. Rev. Phytopathol.* 48:395-417.
- Louvieaux, J., Spanoghe, M., and Hermans, C. 2020. Root morphological traits of seedlings are predictors of seed yield and quality in winter oilseed rape hybrid cultivars. *Front. Plant Sci.* 11:568009.
- Lu, K., Wei, L., Li, X., Wang, Y., Wu, J., Liu, M., Zhang, C., Chen, Z., Xiao, Z., Jian, H., Cheng, F., Zhang, K., Du, H., Cheng, X., Qu, C., Qian, W., Liu, L., Wang, R., Zou, Q., Ying, J., Xu, X., Mei, J., Liang, Y., Chai, Y.-R., Tang, Z., Wan, H., Ni, Y., He, Y., Lin, N., Fan, Y., Sun, W., Li, N.-N., Zhou, G., Zheng, H., Wang, X., Paterson, A. H., and Li, J. 2019. Whole-genome resequencing reveals *Brassica napus* origin and genetic loci involved in its improvement. *Nat. Commun.* 10:1154.
- Lu, Z., Tombolini, R., Woo, S., Zeilinger, S., Lorito, M., and Jansson, J. K. 2004. *In vivo* study of trichoderma-pathogen-plant interactions, using constitutive and inducible green fluorescent protein reporter systems. *Appl. Environ. Microbiol.* 70:3073-3081.
- Mácha, H.; Marešová, H.; Juříková, T.; Švecová, M.; Benada, O.; Škríba, A.; Baránek, M.; Novotný, C.; Palyzová, A. 2021. Killing effect of *Bacillus velezensis* FZB42 on a *Xanthomonas campestris* pv. *Campestris* (Xcc) strain newly isolated from cabbage

- Brassica oleracea* Convar. *Capitata* (L.): A metabolomic study. *Microorganisms* 9:1410.
- Maheshwari, D. K. 2011. *Bacteria in agrobiolgy: plant growth responses*. Springer Verlag Berlin Heidelberg. Pp 53.
- Malinich, E. A., Wang, K., Mukherjee, P. K., Kolomiets, M., and Kenerley, C. M. 2019. Differential expression analysis of *Trichoderma virens* RNA reveals a dynamic transcriptome during colonization of *Zea mays* roots. *BMC Genom.* 20:280.
- Mamun, M. A., Islam, M. T., Lee, B. R., La, V. H., Bae, D. W., and Kim, T. H. 2020. Genotypic variation in resistance gene-mediated calcium signaling and hormonal signaling involved in effector-triggered immunity or disease susceptibility in the *Xanthomonas campestris* pv. *Campestris-Brassica napus* Pathosystem. *Plants* 9:303.
- Martinez-Medina, A., Flors, V., Heil, M., Mauch-Mani, B., Pieterse, C., Pozo, M. J., Ton, J., van Dam, N. M., and Conrath, U. 2016. Recognizing plant defense priming. *Trends Plant Sci.* 21:818-822.
- Mastouri, F., Björkman, T., and Harman, G. E. 2010. Seed treatment with *Trichoderma harzianum* alleviates biotic, abiotic, and physiological stresses in germinating seeds and seedlings. *Phytopathology* 100:1213-1221.
- Mathys, J., De Cremer, K., Timmermans, P., Van Kerckhove, S., Lievens, B., Vanhaecke, M., Cammue, B. P., and De Coninck, B. 2012. Genome-wide characterization of ISR induced in *Arabidopsis thaliana* by *Trichoderma hamatum* T382 against *Botrytis cinerea* infection. *Front. Plant Sci.* 3:108.
- Mendes, R., Kruijt, M., de Bruijn, I., Dekkers, E., van der Voort, M., Schneider, J. H., Piceno, Y. M., DeSantis, T. Z., Andersen, G. L., Bakker, P. A., and Raaijmakers, J. M. 2011. Deciphering the rhizosphere microbiome for disease-suppressive bacteria. *Science* 332:1097-1100.
- Meng, X., Miao, Y., Liu, Q., Ma, L., Guo, K., Liu, D., Ran, W., and Shen, Q. 2019. TgSWO from *Trichoderma guizhouense* NJAU4742 promotes growth in cucumber plants by modifying the root morphology and the cell wall architecture. *Microb. Cell Fact.* 18:148.
- Mikkelsen, L., Sarrocco, S., Lübeck, M., and Jensen, D. F. 2003. Expression of the red fluorescent protein DsRed-Express in filamentous ascomycete fungi. *FEMS Microbiol. Lett.* 223:135-139.

- Mine, A., Nobori, T., Salazar-Rondon, M. C., Winkelmüller, T. M., Anver, S., Becker, D., and Tsuda, K. 2017. An incoherent feed-forward loop mediates robustness and tunability in a plant immune network. *EMBO Rep.* 18:464-476.
- Moradtalab, N., Ahmed, A., Geistlinger, J., Walker, F., Höglinger, B., Ludewig, U., and Neumann, G. 2020. Synergisms of microbial consortia, N forms, and micronutrients alleviate oxidative damage and stimulate hormonal cold stress adaptations in maize. *Front. Plant Sci.* 11:396.
- Moradtalab, N., Weinmann, M., Walker, F., Höglinger, B., Ludewig, U., and Neumann, G. 2018. Silicon improves chilling tolerance during early growth of maize by effects on micronutrient homeostasis and hormonal balances. *Front. Plant Sci.* 9:420.
- Morán-Diez, M. E., Carrero-Carrón, I., Rubio, M. B., Jiménez-Díaz, R. M., Monte, E., and Hermosa, R. 2019. Transcriptomic analysis of *Trichoderma atroviride* overgrowing plant-wilting *Verticillium dahliae* reveals the role of a new M14 metallocarboxypeptidase CPA1 in Biocontrol. *Front. Microbiol.* 10:1120.
- Mou, Z., Fan, W., and Dong, X. 2003. Inducers of plant systemic acquired resistance regulate NPR1 function through redox changes. *Cell* 113:935-944.
- Mpanga, I. K., Nkebiwe, P. M., Kuhlmann, K., Cozzolino, V., Piccolo, A., Geistlinger, G., Berger, N., Ludewig, U., and Neumann, G. 2019a. The form of N supply determines plant growth promotion by P-solubilizing microorganisms in maize. *Microorganisms* 7:38.
- Mpanga, I. K., Gomez-Genao, N., Moradtalab, N., Wanke, D., Chrobaczek, V., Ahmed, A., Windisch, S., Geistlinger, J., Hafiz, F. B., Walker, F., Ludewig, U., and Neumann, G. 2019b. The role of N form supply for PGPM-host plant interactions in maize. *J. Plant Nutr. Soil Sci.* 182:908-920.
- Mpanga, I. K., Dapaah, H. K., Geistlinger, J., Ludewig, U., and Neumann, G. 2018. Soil type-dependent interactions of P-solubilizing microorganisms with organic and inorganic fertilizers mediate plant growth promotion in tomato. *Agronomy* 8:213.
- Müller, S., Galliardt, H., Schneider, J., Barisas, B. G., and Seidel, T. 2013. Quantification of Förster resonance energy transfer by monitoring sensitized emission in living plant cells. *Front. Plant Sci.* 4:413.
- Mukherjee, P. K., Horwitz, B. A., Herrera-Estrella, A., Schmoll, M., and Kenerley, C. M. 2013. *Trichoderma* research in the genome era. *Annu. Rev. Phytopathol.* 51:105-129.
- Mur, L. A. J., Kenton, P., Atzorn, R., Miersch, O., and Wasternack, C. 2006. The outcomes of concentration-specific interactions between salicylate and jasmonate signaling include

- synergy, antagonism and oxidative stress leading to cell death. *Plant Physiol.* 140:249-262.
- Murr, D. P., and Yang, S. F. 1975. Conversion of 5'-methylthioadenosine to methionine by apple tissue. *Phytochemistry* 14:1291-1292.
- Muslim, A., Hyakumachi, M., Kageyama, K., and Suwandi, S. 2019. Induction of systemic resistance in cucumber by hypovirulent binucleate *Rhizoctonia* against anthracnose caused by *Colletotrichum orbiculare*. *Trop. Life Sci. Res.* 30:109.
- Nakano, T., Suzuki, K., Fujimura, T., and Shinshi, H. 2006. Genome-wide analysis of the ERF gene family in *Arabidopsis* and rice. *Plant Physiol.* 140:411-432.
- Nawrath, C., and Metraux, J. P. 1999. Salicylic acid induction-deficient mutants of *Arabidopsis* express PR-2 and PR-5 and accumulate high levels of camalexin after pathogen inoculation. *Plant Cell* 11:1393-1404.
- Naznin, H. A., Kiyohara, D., Kimura, M., Miyazawa, M., Shimizu, M., and Hyakumachi, M. 2014. Systemic resistance induced by volatile organic compounds emitted by plant growth-promoting fungi in *Arabidopsis thaliana*. *PLoS One* 9:e86882.
- Netzker, T., Fischer, J., Weber, J., Mattern, D. J., König, C. C., Valiante, V., Schroeckh, V., and Brakhage, A. A. 2015. Microbial communication leading to the activation of silent fungal secondary metabolite gene clusters. *Front. Microbiol.* 6:299.
- Niu, D., Wang, X., Wang, Y., Song, X., Wang, J., Guo, J., and Zhao, H. 2016. *Bacillus cereus* AR156 activates PAMP-triggered immunity and induces a systemic acquired resistance through a NPR1-and SA-dependent signaling pathway. *Biochem. Biophys. Res. Commun.* 469:120-125.
- Nogueira-Lopez, G., Greenwood, D. R., Middleditch, M., Winefield, C., Eaton, C., Steyaert, J. M., and Mendoza-Mendoza, A. 2018. The apoplastic secretome of *Trichoderma virens* during interaction with maize roots shows an inhibition of plant defence and scavenging oxidative stress secreted proteins. *Front. Plant Sci.* 9:409.
- Novakazi, F., Inderbitzin, P., Sandoya, G., Hayes, R. J., von Tiedemann, A., and Subbarao, K. V. 2015. The three lineages of the diploid hybrid *Verticillium longisporum* differ in virulence and pathogenicity. *Phytopathology* 105:662-673.
- Obermeier, C., Hossain, M. A., Snowdon, R., Knüfer, J., Tiedemann, A. V., and Friedt, W. 2013. Genetic analysis of phenylpropanoid metabolites associated with resistance against *Verticillium longisporum* in *Brassica napus*. *Mol. Breed.* 31:347-361.
- Oldroyd, G. E., Harrison, M. J., and Paszkowski, U. 2009. Reprogramming plant cells for endosymbiosis. *Science* 324:753-754.

- Ogata, T., Kida, Y., Arai, T., Kishi, Y., Manago, Y., Murai, M., and Matsushita, Y. 2012. Overexpression of tobacco ethylene response factor *NtERF3* gene and its homologues from tobacco and rice induces hypersensitive response-like cell death in tobacco. *J. Gen. Plant Pathol.* 78:8-17.
- Otto, M., Naumann, C., Brandt, W., Wasternack, C., and Hause, B. 2016. Activity Regulation by Heteromerization of *Arabidopsis* Allene Oxide Cyclase Family Members. *Plants* 5:3.
- Palyzová, A., Svobodová, K., Sokolová, L. Novák, J., and Novotný, C. 2019. Metabolic profiling of *Fusarium oxysporum* f. sp. *conglutinans* race 2 in dual cultures with biocontrol agents *Bacillus amyloliquefaciens*, *Pseudomonas aeruginosa*, and *Trichoderma harzianum*. *Folia Microbiol.* 64:779-787.
- Paoletti, M., and Saupe, S. J. 2009. Fungal incompatibility: evolutionary origin in pathogen defense?. *Bioessays* 31:1201-1210.
- Pattyn, J., Vaughan-Hirsch, J., and Van de Poel, B. 2021. The regulation of ethylene biosynthesis: a complex multilevel control circuitry. *New Phytol.* 229:770-782.
- Pauwels, L., and Goossens, A. 2011. The JAZ proteins: a crucial interface in the jasmonate signaling cascade. *Plant Cell.* 23:3089-3100.
- Pauwels, L., Barbero, G. F., Geerinck, J., Tilleman, S., Grunewald, W., Pérez, A. C., Chico, J. M., Bossche, R. V., Sewell, J., Gil, E., García-Casado, G., Witters, E., Inzé, D., Long, J. A., De Jaeger, g., Solano R., and Goossens, A. 2010. NINJA connects the co-repressor TOPLESS to jasmonate signalling. *Nature* 464:788-791.
- Pauwels, L., Inze', D., and Goossens, A. 2009. Jasmonate-inducible gene: what does it mean? *Trends Plant Sci.* 14:87-91.
- Pelagio-Flores, R., Esparza-Reynoso, S., Garnica-Vergara, A., López-Bucio, J., and Herrera-Estrella, A. 2017. *Trichoderma*-induced acidification is an early trigger for changes in *Arabidopsis* root growth and determines fungal phytostimulation. *Front. Plant Sci.* 8:822.
- Penninckx, I. A., Thomma, B. P., Buchala, A., Métraux, J. P., and Broekaert, W. F. 1998. Concomitant activation of jasmonate and ethylene response pathways is required for induction of a plant defensin gene in *Arabidopsis*. *Plant Cell.* 10:2103-2113.
- Perazzolli, M., Dagostin, S., Ferrari, A., Elad, Y., and Pertot, I. 2008. Induction of systemic resistance against *Plasmopara viticola* in grapevine by *Trichoderma harzianum* T39 and benzothiadiazole. *Biol. Control* 47:228-234.



- Pfaffl, M. W. 2001. A new mathematical model for relative quantification in real-time RT-PCR. *Nucleic Acids Res.* 29:e45.
- Pieterse, C. M. J., Zamioudis, C., Berendsen, R. L., Weller, D. M., Van Wees, S. C. M., and Bakker, P. A. H. M. 2014. Induced systemic resistance by beneficial microbes. *Annu. Rev. Phytopathol.* 52:347-375.
- Pieterse, C. M. J., Van der Does, D., Zamioudis, C., Leon-Reyes, A., and Van Wees, S. C. M. 2012. Hormonal modulation of plant immunity. *Annu. Rev. Cell Dev. Biol.* 28:489-521.
- Pieterse, C. M. J., Van Wees, S. C. M., Ton, J., Van Pelt, J. A., and Van Loon, L. C. 2002. Signalling in rhizobacteria-induced systemic resistance in *Arabidopsis thaliana*. *Plant Biol.* 4:535-544.
- Pieterse, C. M. J., Van Wees, S. C. M., van Pelt, J. A., Knoester, M., Laan, R., Gerrits, H., Weisbeek, P. J., and van Loon L. C. 1998. A novel signaling pathway controlling induced systemic resistance in *Arabidopsis*. *Plant Cell* 10:1571-1580.
- Poveda, J., Hermosa, R., Monte, E., and Nicolás C. 2019. *Trichoderma harzianum* favours the access of arbuscular mycorrhizal fungi to non-host Brassicaceae roots and increases plant productivity. *Sci. Rep.* 9:11650.
- Pozo, M. J., Van Der Ent, S., Van Loon, L. C., and Pieterse, C. 2008. Transcription factor MYC2 is involved in priming for enhanced defense during rhizobacteria-induced systemic resistance in *Arabidopsis thaliana*. *New Phytol.* 180:511-523.
- Pré, M., Atallah, M., Champion, A., De Vos, M., Pieterse, C. M. J., and Memelink, J. 2008. The AP2/ERF domain transcription factor ORA59 integrates jasmonic acid and ethylene signals in plant defense. *Plant Physiol.* 47:1347-1357.
- Qiao, H., Shen, Z., Huang, S. C., Schmitz, R. J., Urich, M. A., Briggs, S. P., and Ecker, J. R. 2012. Processing and subcellular trafficking of ER-tethered EIN2 control response to ethylene gas. *Science* 338:390-393.
- R Development Core Team. 2019. A language and environment for statistical computing. R foundation for statistical computing, Vienna, Austria.
- Rabbee, M. F., Ali, M. S., Choi, J., Hwang, B. S., Jeong, S. C., and Baek, K. H. 2019. *Bacillus velezensis*: a valuable member of bioactive molecules within plant microbiomes. *Molecules* 24:1046.
- Ralhan, A., Schottle, S., Thurow, C., Iven, T., Feussner, I., Polle, A., and Gatz, C. 2012. The vascular pathogen *Verticillium longisporum* requires a jasmonic acid-independent

- COII function in roots to elicit disease symptoms in *Arabidopsis* shoots. *Plant Physiol.* 159:1192-1203.
- Ratzinger, A., Riediger, N., von Tiedemann, A., and Karlovsky, P. 2009. Salicylic acid and salicylic acid glucoside in xylem sap of *Brassica napus* infected with *Verticillium longisporum*. *J. Plant Res.* 12:571-579.
- Rekhter, D., Lüdke, D., Ding, Y., Feussner, K., Zienkiewicz, K., Lipka, V., Wiermer, M., Zhang, Y., and Feussner, I. 2019. Isochorismate-derived biosynthesis of the plant stress hormone salicylic acid. *Science* 365:498-502.
- Ribnicky, D. M., Shulaev, V., and Raskin, I. 1998. Intermediates of salicylic acid biosynthesis in tobacco. *Plant Physiol.* 118:565-572.
- Richmond, T.A., and Bleecker, A.B. 1999. A defect in b-oxidation causes abnormal inflorescence development in *Arabidopsis*. *Plant Cell* 11:1911-1923.
- Rodriguez, M. C., Petersen, M., and Mundy, J. 2010. Mitogen-activated protein kinase signaling in plants. *Annu. Rev. Plant Biol.* 61:621-649.
- Rodriguez, R. J., White, J. F., Jr, Arnold, A. E., and Redman, R. S. 2009. Fungal endophytes: diversity and functional roles. *New Phytol.* 182:314-330.
- Romera, F. J., García, M. J., Lucena, C., Martínez-Medina, A., Aparicio, M. A., Ramos, J., Alcántara, E., Angulo, M., and Pérez-Vicente, R. 2019. Induced Systemic Resistance (ISR) and Fe deficiency responses in dicot plants. *Front. Plant Sci.* 10:287.
- Rowe, R. C., and Powelson, M. L. 2002. Potato early dying: management challenges in a changing production environment. *Plant Dis.* 86:1184-1193.
- Rozen, S., and Skaletsky, H. 2000. Primer3 on the WWW for general users and for biologist programmers. *Methods Mol. Biol.* 132:365-386.
- Rybakova, D., Mancinelli, R., Wikström, M., Birch-Jensen, A.-S., Postma, J., Ehlers, R.-U., Goertz, S., and Berg, G. 2017. The structure of the *Brassica napus* seed microbiome is cultivar-dependent and affects the interactions of symbionts and pathogens. *Microbiome* 5:104.
- Ryder, L. S., Harris, B. D., Soanes, D. M., Kershaw, M. J., Talbot, N. J., and Thornton, C. R. 2012. Saprotrophic competitiveness and biocontrol fitness of a genetically modified strain of the plant-growth-promoting fungus *Trichoderma hamatum* GD12. *Microbiology* 158:84-97.
- Ryu, C. M., Farag, M. A., Hu, C. H., Reddy, M. S., Wei, H. X., Paré, P. W., and Kloepper, J. W. 2003. Bacterial volatiles promote growth in *Arabidopsis*. *Proc. Natl. Acad. Sci. U.S.A.* 100:4927-4932.

- Salas-Marina, M. A., Silva-Flores, M. A., Uresti-Rivera, E. E., Castro-Longoria, E., Herrera-Estrella, A., and Casas-Flores, S. 2011. Colonization of *Arabidopsis* roots by *Trichoderma atroviride* promotes growth and enhances systemic disease resistance through jasmonic acid/ethylene and salicylic acid pathways. *Eur. J. Plant Pathol.* 131:15-26.
- Saleh, A., Withers, J., Mohan, R., Marqués, J., Gu, Y., Yan, S., Zavaliev, R., Nomoto, M., Tada, Y., and Dong, X. 2015. Posttranslational modifications of the master transcriptional regulator NPR1 enable dynamic but tight control of plant immune responses. *Cell Host Microbe* 18:169-182.
- Salvioli, A., Ghignone, S., Novero, M., Navazio, L., Venice, F., Bagnaresi, P., and Bonfante, P. 2016. Symbiosis with an endobacterium increases the fitness of a mycorrhizal fungus, raising its bioenergetic potential. *ISME J.* 10:130-144.
- Samolski, I., Rincón, A. M., Pinzón, L. M., Viterbo, A., and Monte, E. 2012. The *qid74* gene from *Trichoderma harzianum* has a role in root architecture and plant biofertilization. *Microbiology* 158:129-138.
- Sangwan, S., and Prasanna, R. 2022. Mycorrhizae helper bacteria: unlocking their potential as bioenhancers of plant-arbuscular mycorrhizal fungal associations. *Microb. Ecol.* 84:1-10.
- Sarosh, B. R., Danielsson, J., and Meijer, J. 2009. Transcript profiling of oilseed rape (*Brassica napus*) primed for biocontrol differentiate genes involved in microbial interactions with beneficial *Bacillus amyloliquefaciens* from pathogenic *Botrytis cinerea*. *Plant Mol. Biol.* 70:31-45.
- Šašek, V., Nováková, M., Jindřichová, B., Bóka, K., Valentová, O., and Burketová, L. 2012. Recognition of avirulence gene *AvrLm1* from hemibiotrophic ascomycete *Leptosphaeria maculans* triggers salicylic acid and ethylene signaling in *Brassica napus*. *Mol. Plant Microbe Interact.* 25:1238-1250.
- Schaller, F., Zerbe, P., Reinbothe, S., Reinbothe, C., Hofmann, E., and Pollmann, S. 2008. The allene oxide cyclase family of *Arabidopsis thaliana* - localization and cyclization. *FEBS J.* 275:2428-2441.
- Scholz, R., Vater, J., Budiharjo, A., Wang, Z., He, Y., and Dietel, K. 2014. Amylocyclicin, a novel circular bacteriocin produced by *Bacillus amyloliquefaciens* FZB42. *J. Bacteriol.* 196:1842-1852.

- Scholz, R., Molohon, K. J., Nachtigall, J., Vater, J., Markley, A. L., Süssmuth, R. D., Mitchell, D. A. and Borriss, R. 2011. Plantazolicin, a novel microcin B17/streptolysin S-like natural product from *Bacillus amyoliquefaciens* FZB42. *J. Bacteriol.* 193:215-224.
- Schroeckh, V., Scherlach, K., Nützmann, H. W., Shelest, E., Schmidt-Heck, W., Schuemann, J., Martin, K., Hertweck, C., and Brakhage, A. A. 2009. Intimate bacterial-fungal interaction triggers biosynthesis of archetypal polyketides in *Aspergillus nidulans*. *Proc. Natl. Acad. Sci. U.S.A.* 106:14558-14563.
- Schweiger, R., Padilla-Arizmendi, F., Nogueira-López, G., Rostás, M., Lawry, R., Brown, C., Hampton, J., Steyaert, J. M., Müller, C., and Mendoza-Mendoza, A. 2021. Insights into metabolic changes caused by the *Trichoderma virens*-maize root interaction. *Mol. Plant Microbe Interact.* 34:524-537.
- Segarra, G., Casanova, E., Avilés, M., and Trillas, I. 2010. *Trichoderma asperellum* strain T34 controls *Fusarium* wilt disease in tomato plants in soilless culture through competition for iron. *Microb. Ecol.* 59:141-149.
- Seo, H. S., Song, J. T., Cheong, J. J., Lee, Y. H., Lee, Y. W., Hwang, I., Lee, J. S., and Choi, Y. D. 2001. Jasmonic acid carboxyl methyltransferase: a key enzyme for jasmonate-regulated plant responses. *Proc. Natl. Acad. Sci. U. S. A.* 98:4788-4793
- Serrano, M., Wang, B., Aryal, B., Garcion, C., Abou-Mansour, E., Heck, S., Geisler, M., Mauch, F., Nawrath, C., and Metraux, J. P. 2013. Export of salicylic acid from the chloroplast requires the multidrug and toxin extrusion-like transporter EDS5. *Plant Physiol.* 162:1815-1821.
- Shen, D., Suhrkamp, I., Wang, Y., Liu, S., Menkhaus, J., Verreet, J.-A., Fan, L., and Cai, D. 2014. Identification and characterization of microRNAs in oilseed rape (*Brassica napus*) responsive to infection with the pathogenic fungus *Verticillium longisporum* using *Brassica AA* (*Brassica rapa*) and *CC* (*Brassica oleracea*) as reference genomes. *New Phytol.* 204:577-594.
- Sharma, V., Salwan, R., Sharma, P. N., and Gulati, A. 2017. Integrated translome and proteome: approach for accurate portraying of widespread multifunctional aspects of *Trichoderma*. *Front. Microbiol.* 8:1602.
- Shigenaga, A. M., Berens, M. L., Tsuda, K., and Argueso, C. T. 2017. Towards engineering of hormonal crosstalk in plant immunity. *Curr. Opin. Plant Biol.* 38:164-172.
- Shigenaga, A. M., and Argueso, C. T. 2016. No hormone to rule them all: interactions of plant hormones during the responses of plants to pathogens. *Semin. Cell Dev. Biol.* 56:174-189.

- Shim, J. S., Jung, C., Lee, S., Min, K., Lee, Y. W., Choi, Y., Lee, J. S., Song, J. T., Kim, J. K., and Choi, Y. D. 2013. AtMYB44 regulates WRKY70 expression and modulates antagonistic interaction between salicylic acid and jasmonic acid signaling. *Plant J.* 73:483-495.
- Sindhu, G. M., Murali, M., Thriveni, M. C., Anupama, N., and Amruthesh, K. N. 2018. Growth promotion and disease resistance in muskmelon induced by crude proteins of *Penicillium verruculosum* against gummy stem blight disease. *J. Crop Sci.* 10:160-167.
- Singh, U. B., Malviya, D., Singh, S., Kumar, M., Sahu, P. K., Singh, H. V., Kumar, S., Roy, M., Imran, M., Rai, J. P., Sharma, A. K., and Saxena, A. K. 2019. *Trichoderma harzianum*- and methyl jasmonate-induced resistance to *Bipolaris sorokiniana* through enhanced phenylpropanoid activities in bread wheat (*Triticum aestivum* L.). *Front. Microbiol.* 10:1697.
- Solano, R., Stepanova, A., Chao, Q., and Ecker, J. R. 1998. Nuclear events in ethylene signaling: A transcriptional cascade mediated by ETHYLENE-INSENSITIVE3 and ETHYLENE-RESPONSE-FACTOR1. *Genes Dev.* 12:3703-3714.
- Spoel, S. H., Mou, Z., Tada, Y., Spivey, N. W., Genschik, P., and Dong, X. 2009. Proteasome-mediated turnover of the transcription coactivator NPR1 plays dual roles in regulating plant immunity. *Cell* 137:860-872.
- Staswick, P. E., and Tiryaki, I. 2004. The oxylipin signal jasmonic acid is activated by an enzyme that conjugates it to isoleucine in *Arabidopsis*. *Plant Cell.* 16:2117-2127.
- Stenzel, I., Otto, M., Delker, C., Kirmse, N., Schmidt, D., Miersch, O., Hause, B., and Wasternack, C. 2012. ALLENE OXIDE CYCLASE (AOC) gene family members of *Arabidopsis thaliana*: tissue- and organ-specific promoter activities and *in vivo* heteromerization. *J. Exp. Bot.* 63:6125-6138.
- Sun, C., Shao, Y., Vahabi, K., Lu, J., Bhattacharya, S., Dong, S., Yeh, K. W., Sherameti, I., Lou, B., Baldwin, I. T., and Oelmüller, R. 2014. The beneficial fungus *Piriformospora indica* protects *Arabidopsis* from *Verticillium dahliae* infection by downregulation plant defense responses. *BMC plant biol.* 14:268-283.
- Taylor, J. T.; Harting, R.; Shalaby, S.; Kenerley, C. M.; Braus, G. H.; and Horwitz, B. A. 2022. Adhesion as a focus in *Trichoderma*-root interactions. *J. Fungi* 8:372.
- Taylor, J. T., Wang, K.-D., Horwitz, B., Kolomiets, M., and Kenerley, C. M. 2021. Early transcriptome response of *Trichoderma virens* to colonization of maize roots. *Front. Fungal Biol.* 2:718557.

- Thines, B., Katsir, L., Melotto, M., Niu, Y., Mandaokar, A., Liu, G. H., Nomura, K., He, S. Y., Howe, G. A., and Browse, J. 2007. JAZ repressor proteins are targets of the SCF<sup>COII</sup> complex during jasmonate signalling. *Nature* 448:661-665.
- Thonar, C., Lekfeldt, J. D. S., Cozzolino, V., Kundel, D., Kulhánek, M., Mosimann, C., Neumann, G., Piccolo, A., Rex, M., Symanczik, S., Walder, F., Weinmann, M., de Neergaard, A., and Mäder, P. 2017. Potential of three microbial bio-effectors to promote maize growth and nutrient acquisition from alternative phosphorous fertilizers in contrasting soils. *Chem. Biol. Technol. Agric.* 4:7.
- Tjamos, S. E., Flemetakis, E., Paplomatas, E. J., and Katinakis, P. 2005. Induction of resistance to *Verticillium dahliae* in *Arabidopsis thaliana* by the biocontrol agent K-165 and pathogenesis-related proteins gene expression. *Mol. Plant Microbe Interact.* 18:555-561.
- Torrens-Spence, M. P., Bobokalonova, A., Carballo, V., Glinkerman, C. M., Pluskal, T., Shen, A., and Weng, J.K. 2019. PBS3 and EPS1 complete salicylic acid biosynthesis from isochorismate in *Arabidopsis*. *Mol. Plant* 12:1577-1586.
- Torres, M. J., Brandan, C. P., Petroselli, G., Erra-Balsells, R., and Audisio, M. C. 2016. Antagonistic effects of *Bacillus subtilis* subsp. *subtilis* and *B. amyloliquefaciens* against *Macrophomina phaseolina*: SEM study of fungal changes and UV-MALDI-TOF MS analysis of their bioactive compounds. *Microbiol. Res.* 182:31-39.
- Tseng, Y.-H., Rouina, H., Groten, K., Rajani, P., Furch, A. C. U., Reichelt, M., Baldwin, I. T., Nataraja, K. N., Shaanker, R. U., and Oelmüller, R. 2020. An endophytic *Trichoderma* strain promotes growth of its hosts and defends against pathogen attack. *Front. Plant Sci.* 11:573670.
- Tsuda, K., Mine, A., Bethke, G., Igarashi, D., Botanga, C. J., Tsuda, Y., Glazebrook, J., Sato, M., and Katagiri, F. 2013. Dual regulation of gene expression mediated by extended MAPK activation and salicylic acid contributes to robust innate immunity in *Arabidopsis thaliana*. *PLoS Genet.* 9:e1004015.
- Tsuda, K., Sato, M., Stoddard, T., Glazebrook, J., and Katagiri, F. 2009. Network properties of robust immunity in plants. *PLoS Genet.* 5:e1000772.
- Tucci, M., Ruocco, M., De Masi, L., De Palma, M., and Lorito, M. 2011. The beneficial effect of *Trichoderma* spp. on tomato is modulated by the plant genotype. *Mol. Plant Pathol.* 12:341-354.

- Uehling, J., Deveau, A., and Paoletti, M. 2017. Do fungi have an innate immune response? An NLR-based comparison to plant and animal immune systems. *PLoS Pathog.* 13:e1006578.
- Van de Poel, B., and Van Der Straeten, D. 2014. 1-aminocyclopropane-1-carboxylic acid (ACC) in plants: more than just the precursor of ethylene!. *Front. Plant Sci.* 5:640.
- van der Fits, L., and Memelink, J. 2001. The jasmonate-inducible AP2/ERF-domain transcription factor ORCA<sub>3</sub> activates gene expression via interaction with a jasmonate-responsive promoter element. *Plant J.* 25:43-53.
- Van Loon, L. C., Bakker, P. A. H. M., and Pieterse, C. M. J. 1998. Systemic resistance induced by rhizosphere bacteria. *Annu. Rev. Phytopathol.* 36:453-483.
- Van Wees, S. C., Van der Ent, S., and Pieterse, C. M. 2008. Plant immune responses triggered by beneficial microbes. *Curr. Opin. Plant Biol.* 11:443-448.
- Vandesompele, J., De Preter, K., Pattyn, F., Poppe, B., Van Roy, N., De Paepe, A., and Speleman, F. 2002. Accurate normalization of real-time quantitative RT-PCR data by geometric averaging of multiple internal control genes. *Genome Biol.* 3:research0034.1.
- Velázquez-Robledo, R., Contreras-Cornejo, H. A., Macías-Rodríguez, L., Hernández-Morales, A., Aguirre, J., Casas-Flores, S., López-Bucio, J., and Herrera-Estrella A. 2011. Role of the 4-phosphopantetheinyl transferase of *Trichoderma virens* in secondary metabolism and induction of plant defense responses. *Mol. Plant Microbe Interact.* 24:1459-1471.
- Veronese, P., Narasimhan, M. L., Stevenson, R. A., Zhu, J. K., Weller, S. C., Subbarao, K. V. and Bressan, R. A. 2003. Identification of a locus controlling *Verticillium* disease symptom response in *Arabidopsis thaliana*. *Plant J.* 35:574-587.
- Ververidis, P., and John, P. 1991. Complete recovery in vitro of ethylene-forming activity. *Phytochemistry* 30:725-727.
- Viterbo, A., and Chet, I. 2006. TasHyd1, a new hydrophobin gene from the biocontrol agent *Trichoderma asperellum*, is involved in plant root colonization. *Mol. Plant Pathol.* 7:249-258.
- Vlot, A. C., Sales, J. H., Lenk, M., Bauer, K., Brambilla, A., Sommer, A., Chen, Y., Wenig, M. and Nayem, S. 2021. Systemic propagation of immunity in plants. *New Phytol.* 229:1234-1250.
- Vogt, T. 2010. Phenylpropanoid biosynthesis. *Mol. Plant* 3:2-20.

- Wakefield, J., Hassan, H. M., Jaspars, M., Ebel, R., and Rateb, M. E. 2017. Dual induction of new microbial secondary metabolites by fungal bacterialco-cultivation. *Front. Microbiol.* 8:1284.
- Wang, K. L., Li, H., and Ecker, J. R. 2002. Ethylene biosynthesis and signaling networks. *Plant Cell* 14 Issue suppl\_1:S131-S151.
- Wang, Z., Tan, X., Zhang, Z., Gu, S., Li, G., and Shi, H. 2012. Defense to *Sclerotinia sclerotiorum* in oilseed rape is associated with the sequential activations of salicylic acid signaling and jasmonic acid signaling. *Plant Sci.* 184:75-82.
- Wasternack, C., and Hause, B. 2013. Jasmonates: biosynthesis, perception, signal transduction and action in plant stress response, growth and development. An update to the 2007 review in *Annals of Botany*. *Ann. Bot.* 111:1021-1058.
- White, J. F., Kingsley, K. L., Verma, S. K., and Kowalski, K. P. 2018. Rhizophagy cycle: an oxidative process in plants for nutrient extraction from symbiotic microbes. *Microorganisms* 6:95.
- Wildermuth, M. C., Dewdney, J., Wu, G., and Ausubel, F. M. 2001. Isochorismate synthase is required to synthesize salicylic acid for plant defence. *Nature* 414:562-565.
- Wilhelm, S. 1955. Longevity of the *Verticillium* wilt fungus in the laboratory and field. *Phytopathology* 45:180-181.
- Wilkinson, J. Q., Lanahan, M. B., Yen, H. C., Giovannoni, J. J., and Klee, H. J. 1995. An ethylene-inducible component of signal transduction encoded by never-ripe. *Science* 270:1807-1809.
- Windisch, S., Sommermann, L., Babin, D., Chowdhury, S. P., Grosch, R., Moradtalab, N., Walker, F., Höglinger, B., El-Hasan, A., Armbruster, W., Nesme, J., Sørensen, S. J., Schellenberg, I., Geistlinger, J., Smalla, K., Rothballer, M., Ludewig, U., and Neumann, G. 2021. Impact of long-term organic and mineral fertilization on rhizosphere metabolites, root-microbial interactions and plant health of lettuce. *Front. Microbiol.* 11:597745.
- Wittstock, U. and Halkier B. A. 2002. Glucosinolate research in the *Arabidopsis* era. *Trends Plant Sci.* 7:263-270.
- Woo, S., Fogliano, V., Scala, F., and Lorito, M. 2002. Synergism between fungal enzymes and bacterial antibiotics may enhance biocontrol. *Antonie van Leeuwenhoek*, 81:353-356.
- Wu, D., Liang, Z., Yan, T., Xu, Y., Xuan, L., Tang, J., Zhou, G., Lohwasser, U., Hua, S., Wang, H., Chen, X., Wang, Q., Zhu, L., Maodzeka, A., Hussain, N., Li, Z., Li, X., Shamsi, I. H., Jilani, G., Wu, L., ... Jiang, L. 2019. Whole-genome resequencing of a worldwide



- collection of rapeseed accessions reveals the genetic basis of ecotype divergence. *Mol. Plant* 12:30-43.
- Wu, L., Huang, Z., Li, X., Ma, L., Gu, Q., Wu, H., Liu J, Borriss R, Wu Z, and Gao X. 2018. Stomatal closure and SA-, JA/ET- signaling pathways are essential for *Bacillus amyloliquefaciens* FZB42 to restrict leaf disease caused by *Phytophthora nicotianae* in *Nicotiana benthamiana*. *Front. Microbiol.* 9:847.
- Wu, Q., Wu, J., Suu, H., Dan, Z., and Yu, D. 2011. Sequence and expression divergence of the AOC gene family in soybean: insights into functional diversity for stress responses. *Biotechnol. Lett.* 33:1351-1359.
- Xu J, and Zhang S. 2015. Ethylene biosynthesis and regulation in plants. In: Wen C-K, editor. *Ethylene in plants*. Berlin: Springer. p. 1-25.
- Xu, L., Zhao, H., Ruan, W., Deng, M., Wang, F., Peng, J., Luo, J., Chen, Z., and Yi, K. 2017. ABNORMAL INFLORESCENCE MERISTEM1 functions in salicylic acid biosynthesis to maintain proper reactive oxygen species levels for root meristem activity in rice. *Plant Cell* 29:560-574.
- Xu, Y., Zhao, Y., Duan, H., Sui, N., Yuan, F., and Song, J. 2017. Transcriptomic profiling of genes in matured dimorphic seeds of euhalophyte *Suaeda salsa*. *BMC Genom.* 18:727.
- Yadav, M., Dubey, M. K., and Upadhyay, R. S. 2021. Systemic resistance in chilli pepper against Anthracnose (Caused by *Colletotrichum truncatum*) induced by *Trichoderma harzianum*, *Trichoderma asperellum* and *Paenibacillus dendritiformis*. *J. Fungi* 7:307.
- Yadeta, K. A., Valkenburg, D. J., Hanemian, M., Marco, Y., Thomma, B. P. H. J. 2014. The *Brassicaceae*-specific EWR1 gene provides resistance to vascular wilt pathogens. *PLoS One* 9:e88230.
- Yadeta, K. A., Hanemian, M., Smit, P., Hiemstra, J. A., Pereira, A., Marco, Y., and Thomma B. P. H. J. 2011. The *Arabidopsis thaliana* DNA-binding protein AHL19 mediates *Verticillium* Wilt resistance. *Mol. Plant-Microbe Interact.* 24:1582-1591.
- Yalpani, N., Leo' n, J., Lawton, M. A., and Raskin, I. 1993. Pathway of salicylic acid biosynthesis in healthy and virus-inoculated tobacco. *Plant Physiol.* 103:315-321.
- Yan, J., Zhang, C., Gu, M., Bai, Z., Zhang, W., Qi, T., Cheng, Z., Peng, W., Luo, H., Nan, F., Wang, Z., and Xie D. 2009. The *Arabidopsis* CORONATINE INSENSITIVE1 protein is a jasmonate receptor. *Plant Cell* 21:2220-2236.
- Yang, J., Duan, G., Li, C., Liu, L., Han, G., Zhang, Y., and Wang, C. 2019. The crosstalks between jasmonic acid and other plant hormone signaling highlight the involvement

- of jasmonic acid as a core component in plant response to biotic and abiotic stresses. *Front. Plant Sci.* 10:1349.
- Yang, Y., Dong, C., Li, X., Du, J., Qian, M., Sun, X., and Yang, Y. 2016. A novel Ap2/ERF transcription factor from *Stipa purpurea* leads to enhanced drought tolerance in *Arabidopsis thaliana*. *Plant Cell Rep.* 35:2227-2239.
- Yedidia, I., Benhamou, N., Kapulnik, Y., and Chet, I. 2000. Induction and accumulation of PR proteins activity during early stages of root colonization by the mycoparasite *Trichoderma harzianum* strain T-203. *Plant. Physiol. Biochem.* 38:863-873.
- Yedidia, I., Benhamou, N., and Chet, I. 1999. Induction of defense responses in cucumber plants (*Cucumis sativus* L.) by the biocontrol agent *Trichoderma harzianum*. *Appl. Environ. Microbiol.* 65:1061-1070.
- Yip, W.-K., and Yang, S. F. 1988. Cyanide metabolism in relation to ethylene production in plant tissues. *Plant Physiology* 88:473-476.
- Yu, Y., Gui, Y., Li, Z., Jiang, C., Guo, J., and Niu, D. 2022. Induced systemic resistance for improving plant immunity by beneficial microbes. *Plants* 11:386.
- Yusran, Y., Roemheld, V., and Mueller, T. 2009. Effects of *Pseudomonas* sp. “Proradix” and *Bacillus amyloliquefaciens* FZB42 on the establishment of AMF infection, nutrient acquisition and growth of tomato affected by *Fusarium oxysporum* Schlecht f.sp. *radicis-lycopersici* Jarvis and Shoemaker. eScholarship Repository, University of California. 1106.
- Zander, M., Chen, S., Imkampe, J., Thurow, C., and Gatz, C. 2012. Repression of the *arabidopsis thaliana* jasmonic acid/ethylene-induced defense pathway by tga-interacting glutaredoxins depends on their c-terminal alwl motif. *Mol. Plant* 5:831-840.
- Zhang, D., Spadaro, D., Valente, S., Garibaldi, A., and Gullino, M. L. 2011. Cloning, characterization and expression of an exo-1,3- $\beta$ -glucanase gene from the antagonistic yeast, *Pichia guilliermondii* strain M8 against grey mold on apples. *Biol. Control.* 59:284-293.
- Zhang, F., Yao, J., Ke, J., Zhang, L., Lam, V. Q., Xin, X.-F., Zhou, X. E., Chen, J., Brunzelle, J., Griffin, P. R., Zhou, M., Xu, H. E., Melcher, K., and He, S. Y. 2015. Structural basis of JAZ repression of MYC transcription factors in jasmonate signalling. *Nature* 525:269-273.

- Zhang, X., Zhu, Z., An, F., Hao, D., Li, P., Song, J., Yi, C., and Guo, H. 2014. Jasmonate-activated MYC2 represses ETHYLENE INSENSITIVE3 activity to antagonize ethylene-promoted apical hook formation in Arabidopsis. *Plant cell* 26:1105-1117.
- Zhang, Y., and Li, X. 2019. Salicylic acid: biosynthesis, perception, and contributions to plant immunity. *Curr. Opin. Plant Biol.* 50:29-36.
- Zhang, Y., Chen, F. S., Wu, X. Q., Luan, F. G., Zhang, L. P., Fang, X. M., and Ye, J. R. 2018. Isolation and characterization of two phosphate-solubilizing fungi from rhizosphere soil of moso bamboo and their functional capacities when exposed to different phosphorus sources and pH environments. *PLoS One* 13:e0199625.
- Zhao, B., Liu, Q., Wang, B., and Yuan, F. 2021. Roles of phytohormones and their signaling pathways in leaf development and stress responses. *J. Agric. Food Chem.* 69:3566-3584.
- Zhao, J., Buchwaldt, L., Rimmer, S. R., Sharpe, A., McGregor, L., Bekkaoui, D., and Hegedus, D. 2009. Patterns of differential gene expression in *Brassica napus* cultivars infected with *Sclerotinia sclerotiorum*. *Mol. Plant Pathol.* 10:635-649.
- Zhao, W., Liu, H., Zhang, L., Hu, Z., Liu, J., Hua, W., Xu, S., and Liu, J. 2019. Genome-wide identification and characterization of *FBA* gene family in polyploid crop *Brassica napus*. *Int. J. Mol. Sci.* 20:5749.
- Zhao, Y., Dong, W., Zhang, N., Ai, X., Wang, M., Huang, Z., Xiao, L., and Xia, G. 2014. A wheat allene oxide cyclase gene enhances salinity tolerance via jasmonate signaling. *Plant Physiol.* 164:1068-1076.
- Zheng, X., Koopmann, B., and von Tiedemann, A. 2019. Role of salicylic acid and components of the phenylpropanoid pathway in basal and cultivar-related resistance of oilseed rape (*Brassica napus*) to *Verticillium longisporum*. *Plants* 8:491.
- Zhou, L., Tang, K., and Guo, S. 2018. The plant growth-promoting fungus (PGPF) *Alternaria sp.* A13 markedly enhances *Salvia miltiorrhiza* root growth and active ingredient accumulation under greenhouse and field conditions. *Int. J. Mol. Sci.* 19:270.
- Zhu, Z., and Lee, B. 2015. Friends or foes: new insights in jasmonate and ethylene co-actions. *Plant Cell Physiol.* 56:414.
- Zhu, Z. 2014. Molecular basis for jasmonate and ethylene signal interactions in Arabidopsis. *J. Exp. Bot.* 65:5743-5748.
- Zhu, Z., An, F., Feng, Y., Li, P., Xue, L., A, M., Jiang, Z., Kim, J. M., To, T. K., Li, W., Zhang, X., Yu, Q., Dong, Z., Chen, W. Q., Seki, M., Zhou, J. M., and Guo, H. 2011. Derepression of ethylene-stabilized transcription factors (EIN3/EIL1) mediates

jasmonate and ethylene signaling synergy in Arabidopsis. Proc. Natl. Acad. Sci. USA. 108:12539-12544.

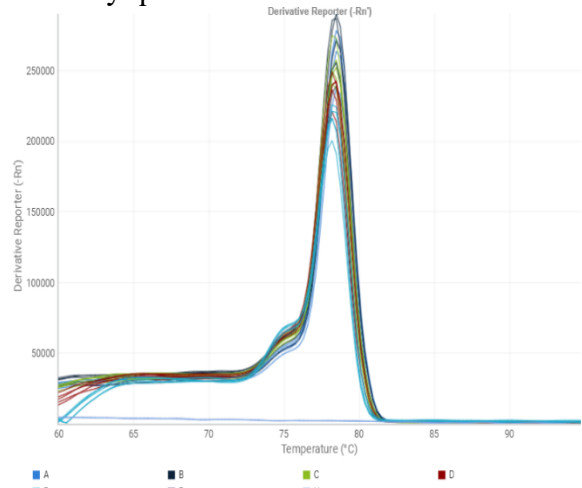
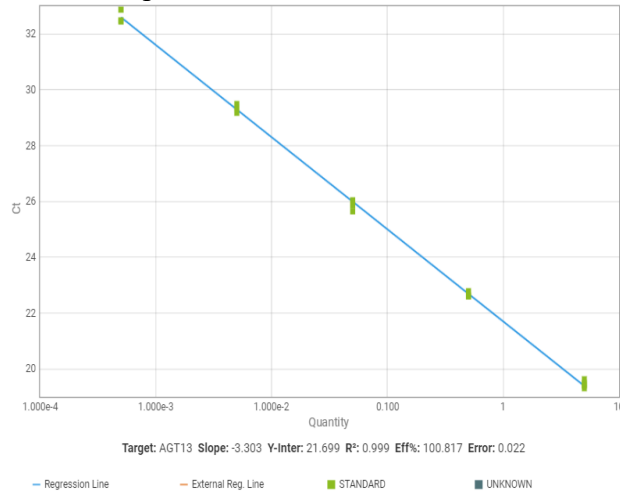
Zimmerli, L., Métraux, J. P., and Mauch-Mani, B. 2001. beta-Aminobutyric acid-induced protection of Arabidopsis against the necrotrophic fungus *Botrytis cinerea*. Plant Physiol. 126:517-523.

## 7. Appendix

GACAGAATCTTGCGGACTCTAAATATCGCCTCGAGACAAGGGCAATCCGGCCACTCTGAGAA  
CGCACAGTCTGTCACTATGGCAAATGTGGTCCGTGTTGCATACGCTGCAACGCTTTCACACC  
ATTCAGCAGACCATCCTAGCTCTGTTCTTTTCCCTAGAATCTCTCGGTGGTCGGAATTCAAGC  
CTGAAGGGCATCGATCGTGTGCTGGACCGACCCTCCTGACCATCCCTACGAGATTGGAGCT  
ACCAGGTGTCAAGTCATGCAAAGATATTGTACTGGAAGCGCAGACATCACTTCTGGAGAGAA  
TGAAGTTTGAGAGCTTCCCCTTGCTCCGTCTCCTACCGCTTGACCAGCTCTGGAGCTGCGT  
AATGTCCCTCATGATAGAGAATGAAGCGTTTTTGTATCAACGGAGATGGCAATGGTCTATTTCGG  
CCGTGGAAAAGAAGAGTTGAAGTTAGAGGAGACGGAGGGCTTACCAATGATATTCCGGTGCA  
CTATTCTTCAAAGCCAGTTGGATGTGATATAAGATACGACAGTACCATCATTCCCCACGGG  
GAGACGGAAGCTTCTTGGAACCTTTGAAAGATATTTTGAAGAGTTATGGCATGGCGATGG  
AGCCAGATCTTTTGTATGTCATTGCTTCATCTTGATGTATAGGACAGCGACTTGACAGCTTGT  
AAGAGATCAGACCTAGACTCTCATCAGATGCTAGCCTAGATGTTAGCTGCTGGGACATTACA  
CCGAAGACAGACTAGTTTCTTAAGAATATGATATACCGAATCCTCGCAACACTTGTA AAAAG  
GTTCATAACAACAGTACGTGAAGGTTATGCCACAGAGAGAAGCCAGTCTATTACGGGGGAGAC  
AAATAGTCGGTTATTTATCGAGTCTGCATACCTTTGCATCTGAGTACTTGCGGTAAAGTAGT  
AGTAGTAGTAGTAGTAGTAGTAGTAGTAGTAGTAGGCTGTATTGAAGACTAATTAATAAATT  
ATTTAACAAAGAATCATTCATATACGATAGATGGGGACATGACGCGAAGTTCTATTTCGACG  
ATAACAGGCAACCTCTACTATGGCTACACAGGTAGTTTAACACGACACTATGGGATGTGCGT  
TGAGTGTGAGCAAGTATGCAAGCTCCAGATAGTACAAGTAACCAAACCTACACTATGTAT  
CTCCTTTACGTTATATCGAAAAAAATGCAATTGAACTATAATTATTTTCTCAAGTTTGACT  
CTTGGCTCCTCGGTCAAGCAGCAATTCGACCACATCCGCTCTTCCCCTTCTGTGAAGCACAGC  
TCAGTGGTGTAAAGCTGCGAACCATTTTTCGTCTTCAATATCAGCTCCCCGGTCAAGAAGTATG  
CTGACTGAGTAGATAGATCCATTTTTTGTGCTGCATCATGAAGTGGTGTATCGCCATTTTTTATT  
CCATATGTCAGTCTTAGCTCCTCGGCCAAGAAGCAACCTAACAAATAGCTCCATTTGAATGCC  
TAGTTGCAATAAAGAGCGGCGTATTAAGAATGTCATTCGTGGCTTCGATATCAGCTCCTCGA  
TTAAGAAGTAAAGTGACGATGTCTGTCTTTGATAATGAACTGCTTCATGAAGTGGTGTATT  
GCCCTTATTGCTCTTGACTTCAATATTGGCTCCTCGGTTGAGAAGCAATTTGACGGCATCTG  
CTTGTCCATGATGCACAGCATCGTGAAGGAGTGCATTACCAGTAATTCCATCCACGGTGTCA  
ATTCTTTTATCGGCTGTGAGTAACATAGATGCGGTGCTCAGTTGACCATTTATAATGGCATA  
GTGAAGCATTTTTAGGTAACAGATTTTCATTTCCGTACCCCTTTAAA

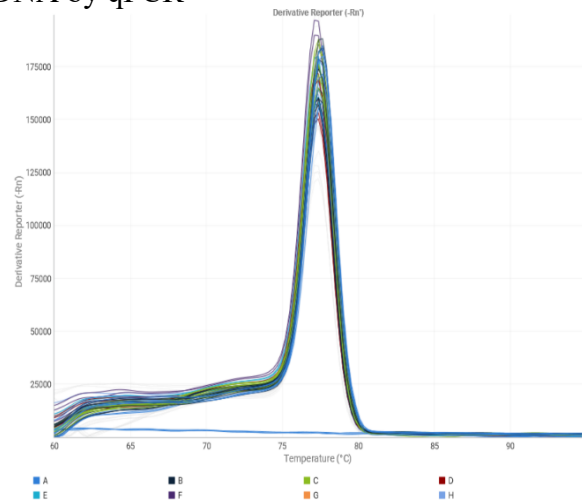
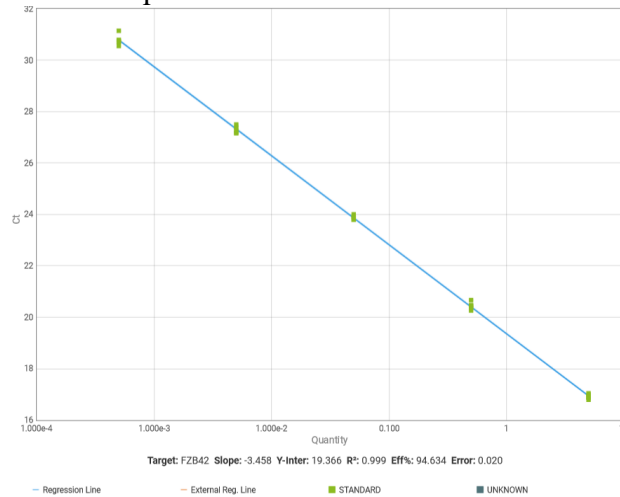
**Appendix 1.** Nucleotide sequence of the *T. harzianum* OMG16 single-locus region used as a molecular marker for quantification of OMG16 DNA in root tissues. The microsatellite locus (ATG)<sub>13</sub>, the forward (T.harz.SSRAGT13-F) and reverse primer (T.harz.SSRAGT13-R) are marked in yellow, green and blue, respectively. Locus size: 1,844 nt; amplicon size: 205 bp.

### Absolute quantification of *T. harzianum* OMG16 DNA by qPCR



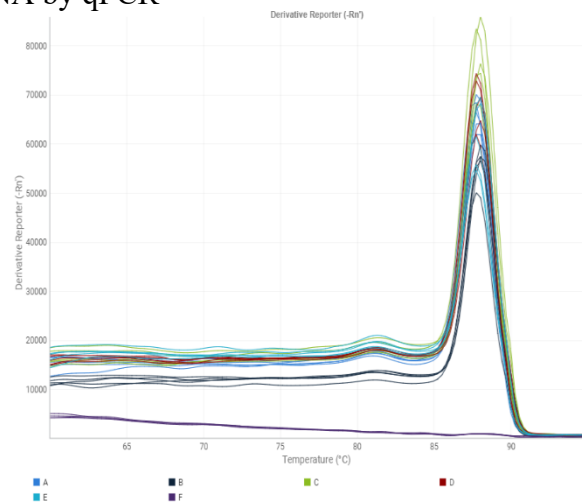
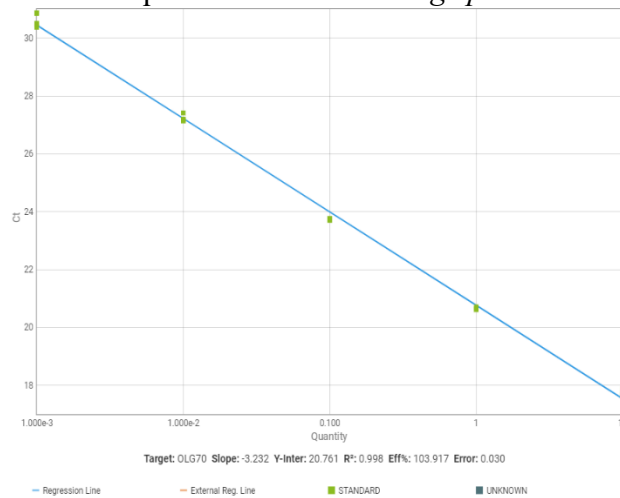
R<sup>2</sup> = 0.999; Primer efficiency = 100.8%

### Absolute quantification of *B. velezensis* FZB42 DNA by qPCR



R<sup>2</sup> = 0.999; Primer efficiency = 94.6%

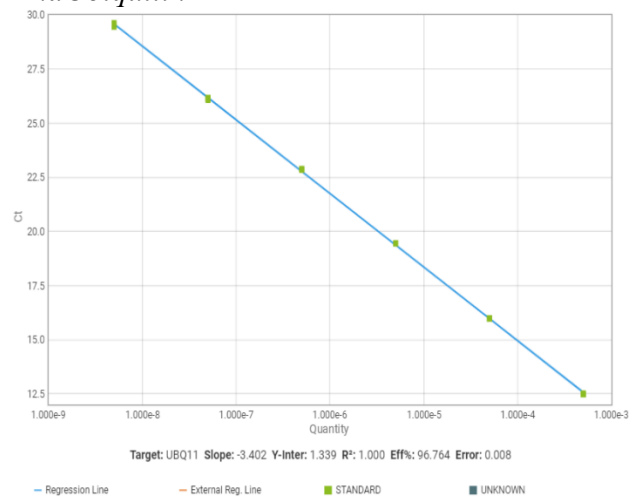
### Absolute quantification of *V. longisporum* 43 DNA by qPCR



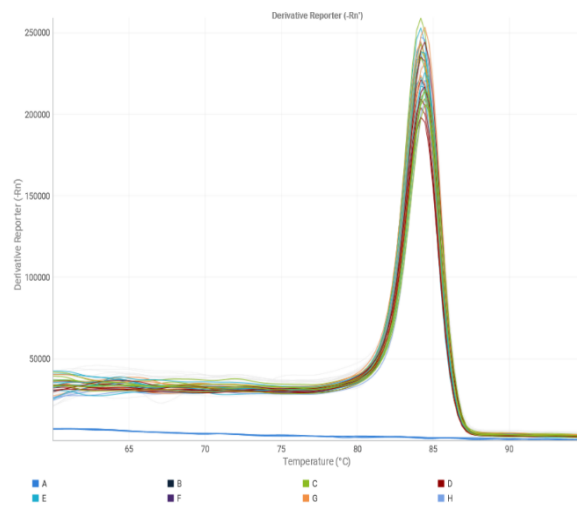
R<sup>2</sup> = 0.998; Primer efficiency = 103.9%

## Transcript analyses of *B. napus* reference genes for normalization by qRT-PCR

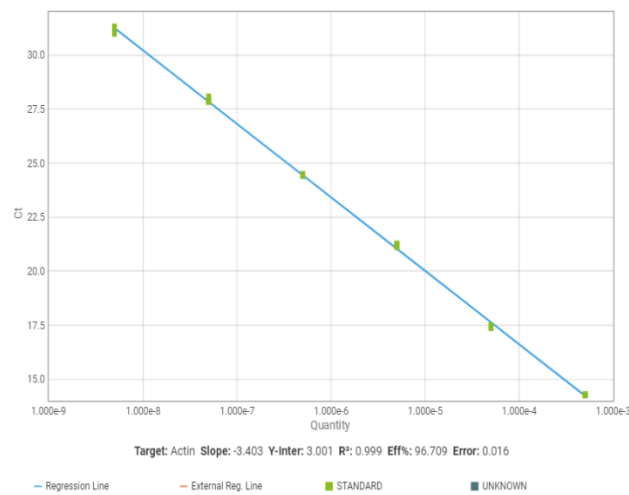
### *BnaUbiquitin11*



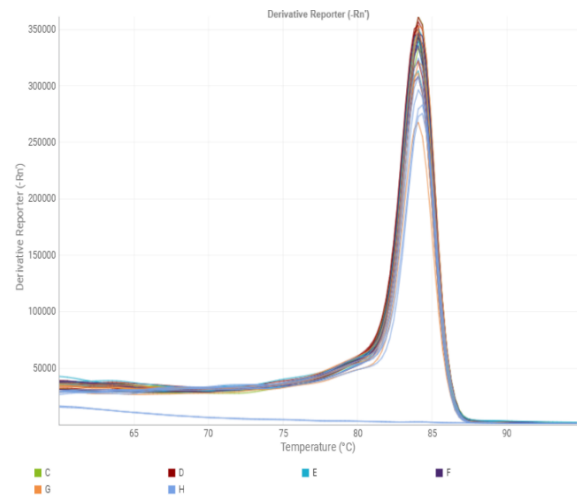
R<sup>2</sup> = 1.000; Primer efficiency = 96.8%



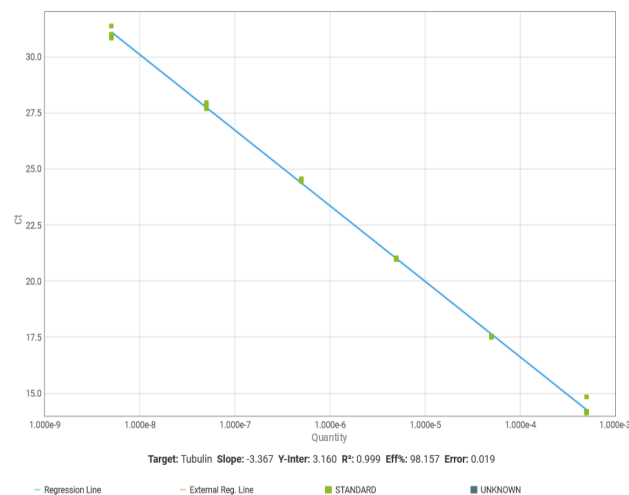
### *BnaActin*



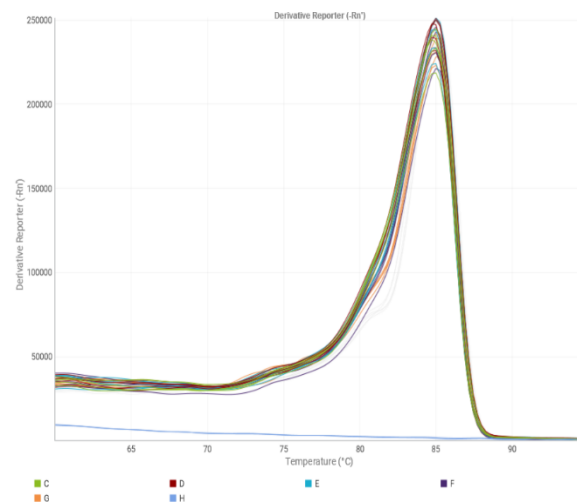
R<sup>2</sup> = 0.999; Primer efficiency = 96.7%



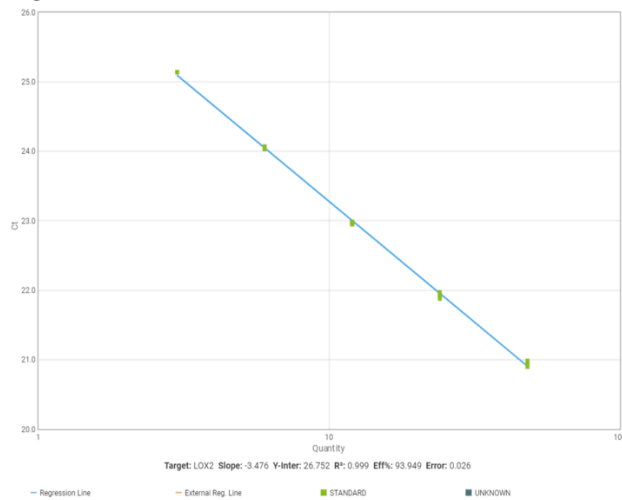
### *BnaTubulin*



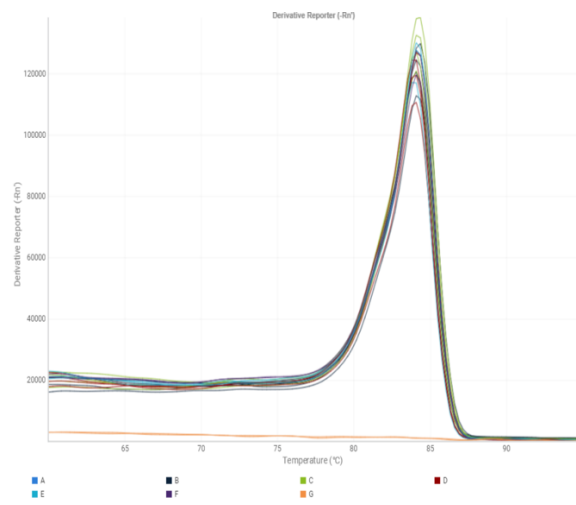
R<sup>2</sup> = 0.999; Primer efficiency = 98.2%



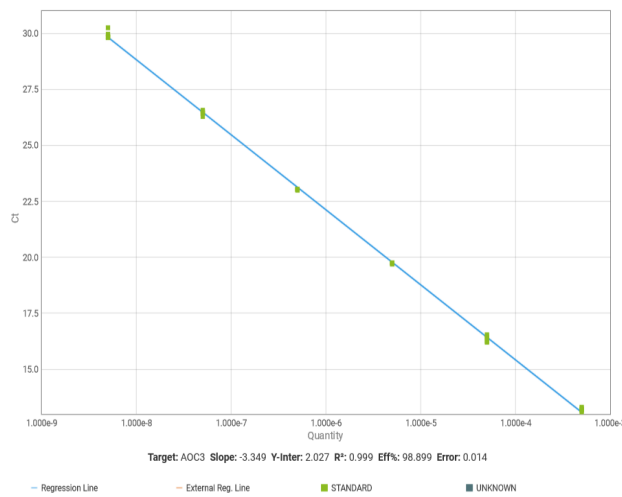
## Quantification of *B. napus* ISR genes by qRT-PCR *LOX2*



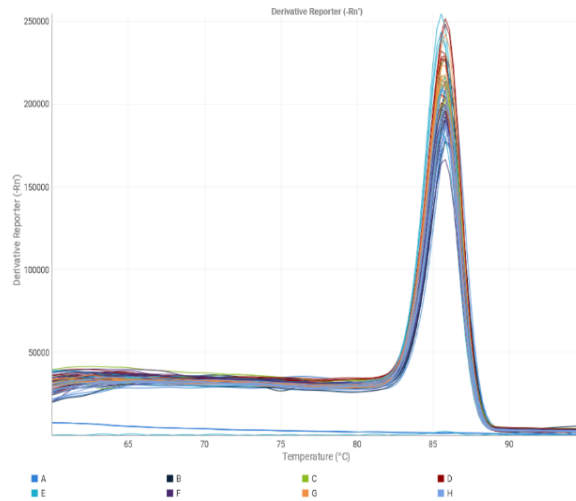
R<sup>2</sup> = 0.999; Primer efficiency = 93.9%



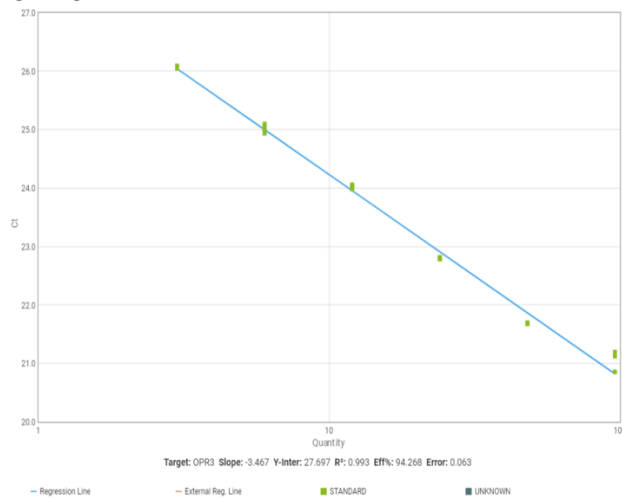
## *AOC3*



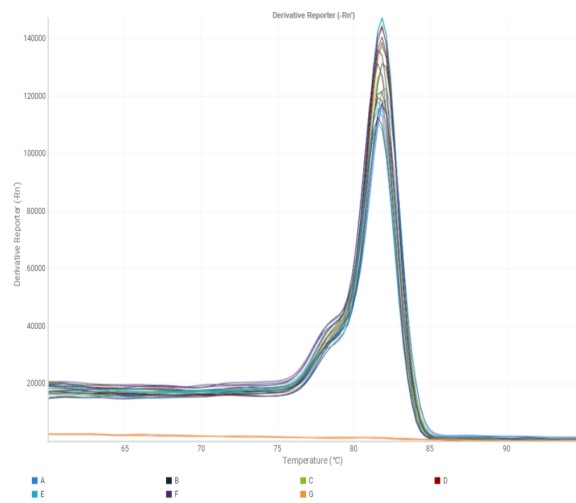
R<sup>2</sup> = 0.999; Primer efficiency = 98.9%



## *OPR3*

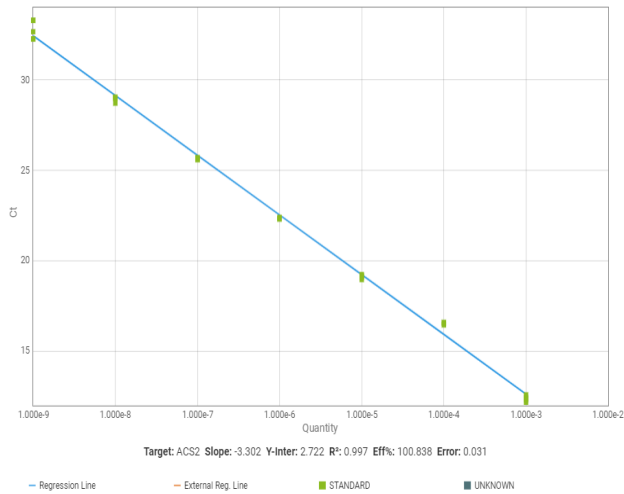


R<sup>2</sup> = 0.993; Primer efficiency = 94.3%

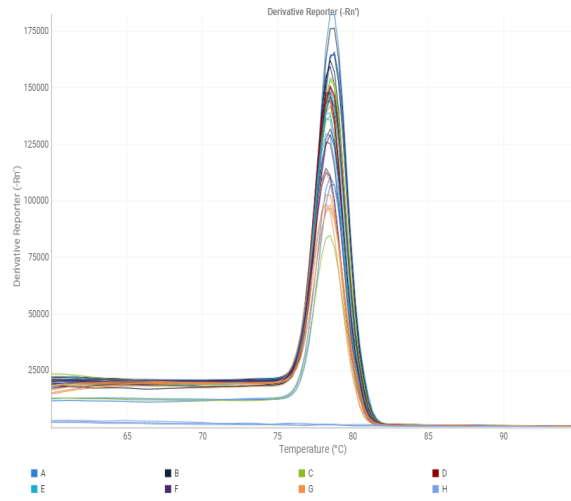




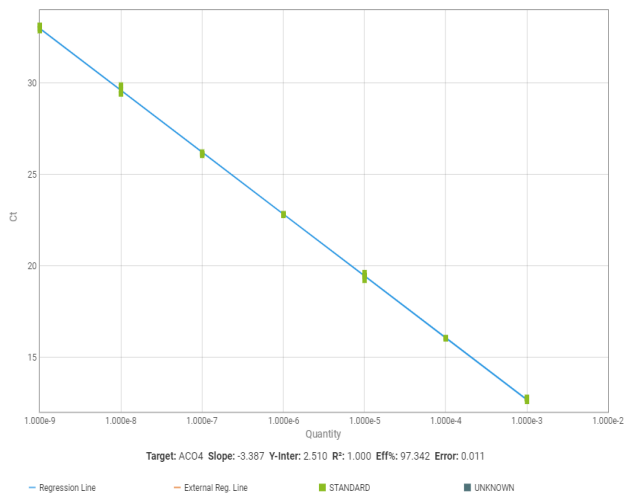
### ACS2



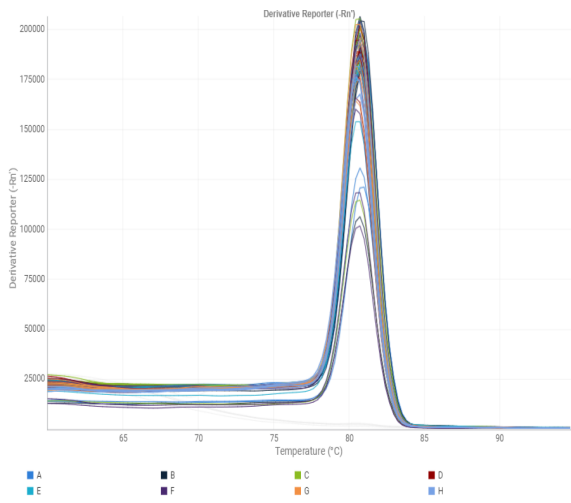
R<sup>2</sup> = 0.997; Primer efficiency = 100.8%



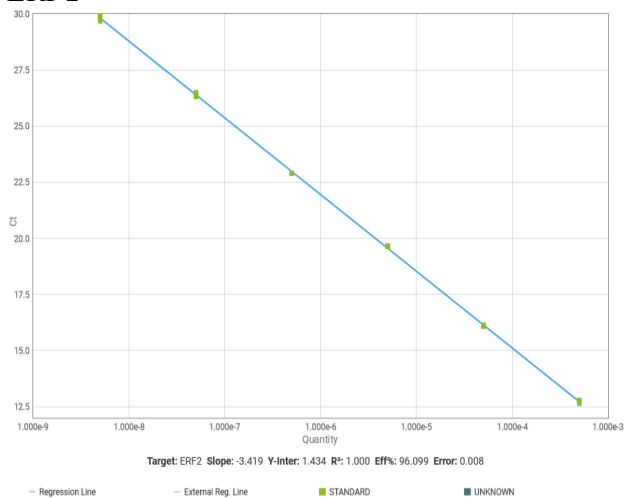
### ACO4



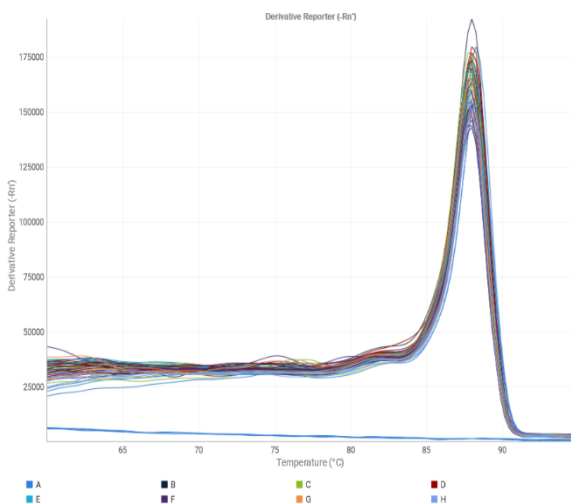
R<sup>2</sup> = 1.000; Primer efficiency = 97.3%



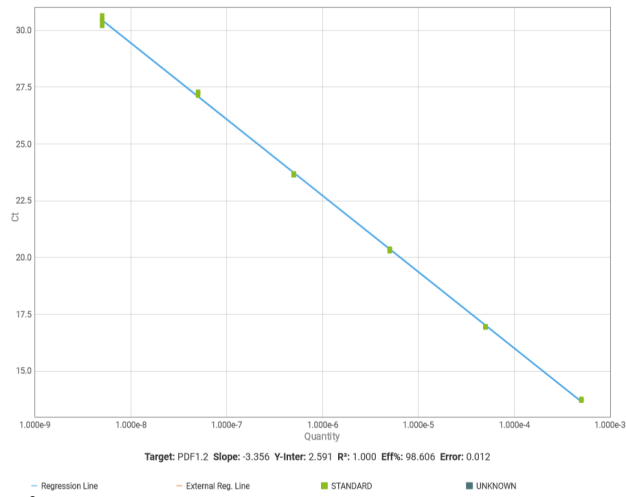
### ERF2



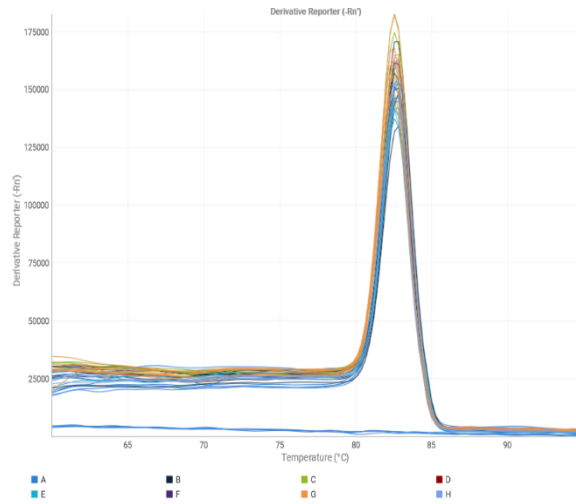
R<sup>2</sup> = 1.000; Primer efficiency = 96.1%



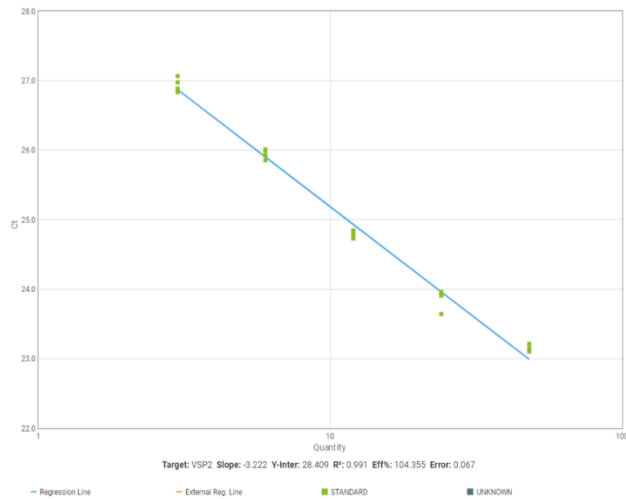
**PDF1.2**



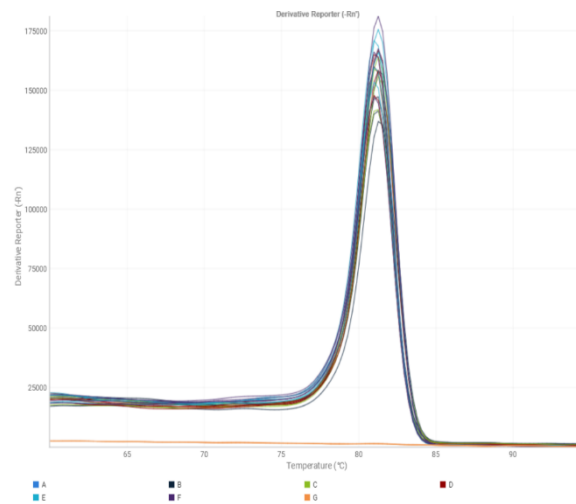
R<sup>2</sup> = 1.000; Primer efficiency = 98.6%



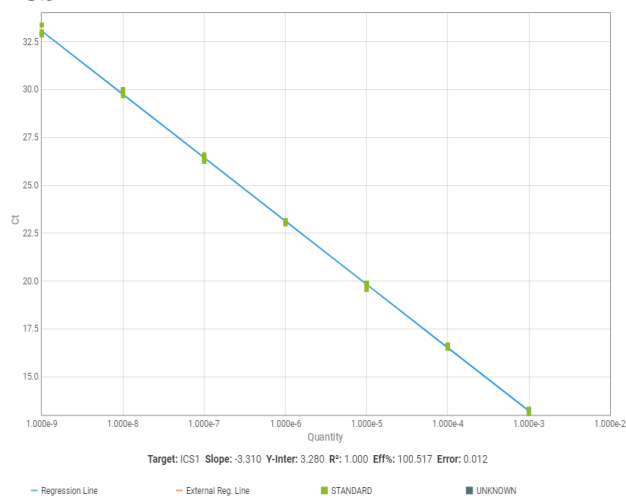
**VSP2**



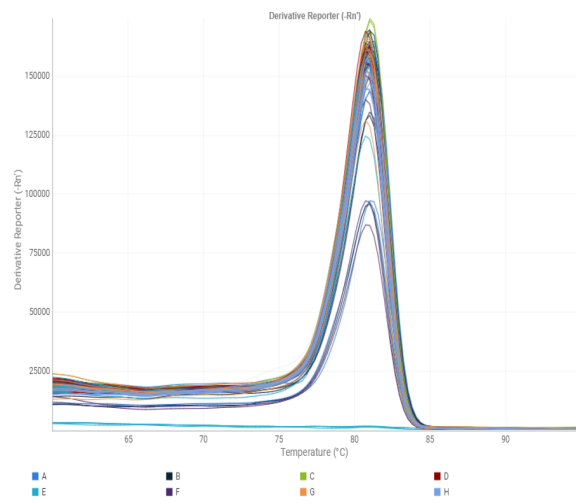
R<sup>2</sup> = 0.991; Primer efficiency = 104.4%



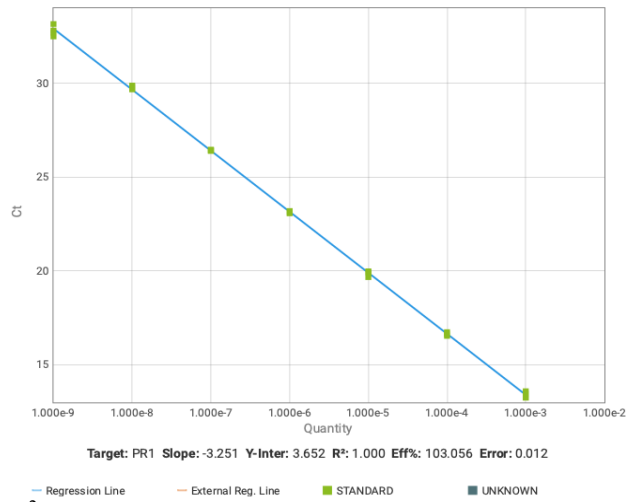
**ICSI**



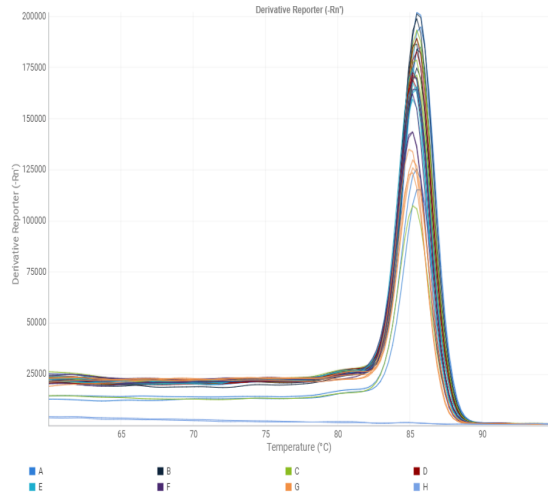
R<sup>2</sup> = 1.000; Primer efficiency = 100.5%



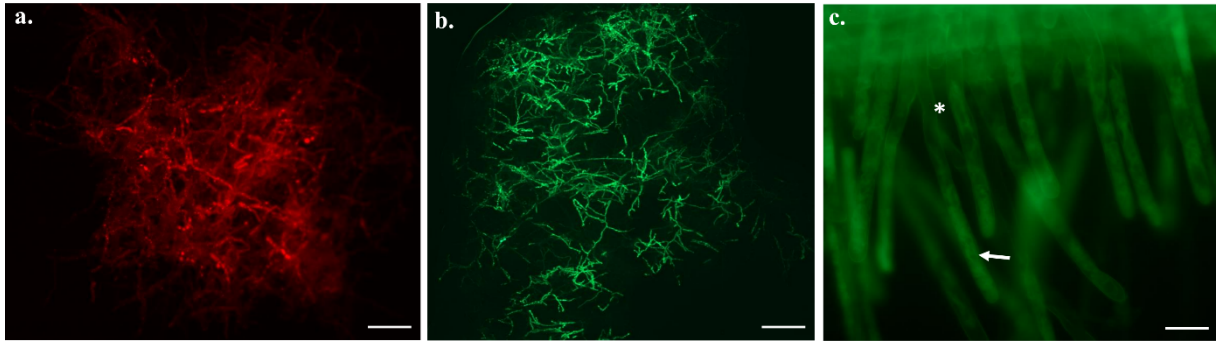
*PRI*



R<sup>2</sup> = 1.000; Primer efficiency = 103.0%



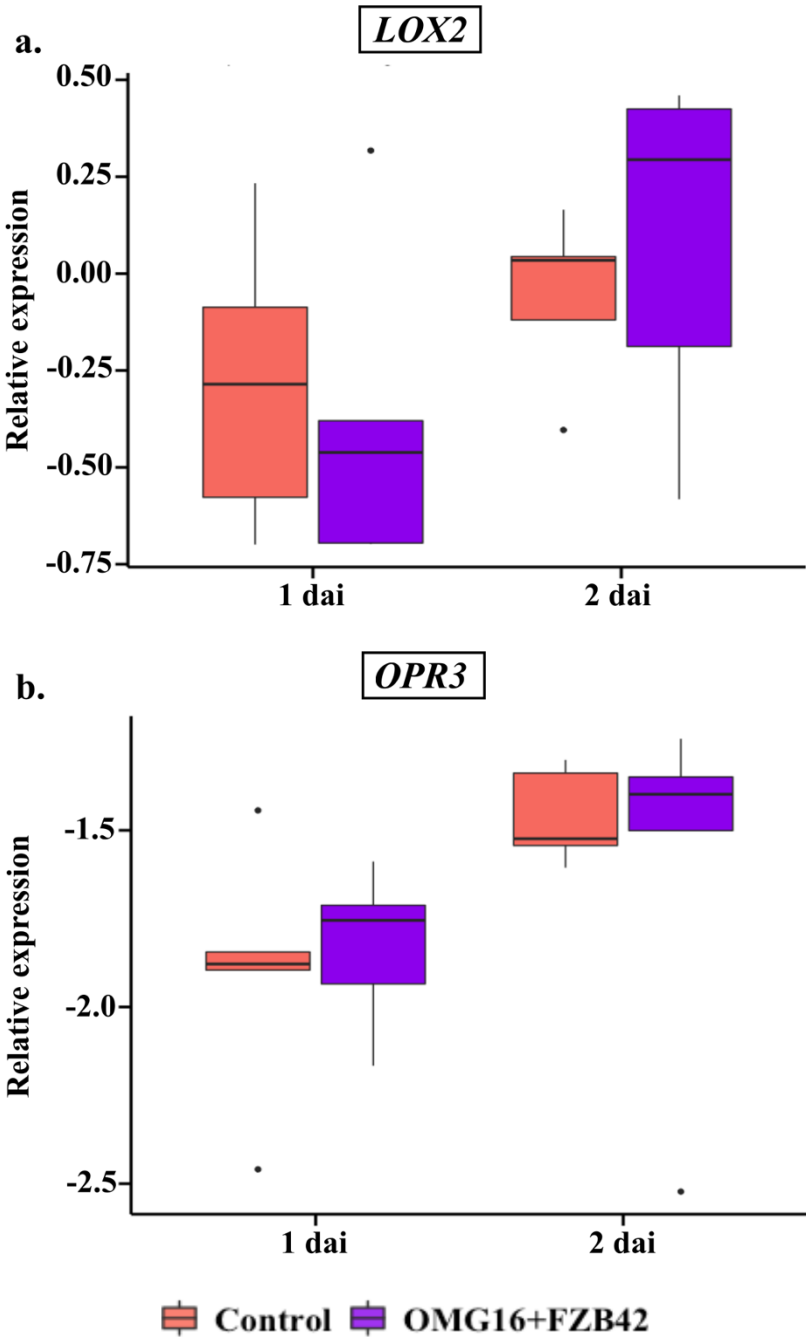
**Appendix 2.** Quality control of the primer pairs used in this study. Standard curves for calculation of primer efficiencies and melting curves (°C) of the amplified fragments are indicated.



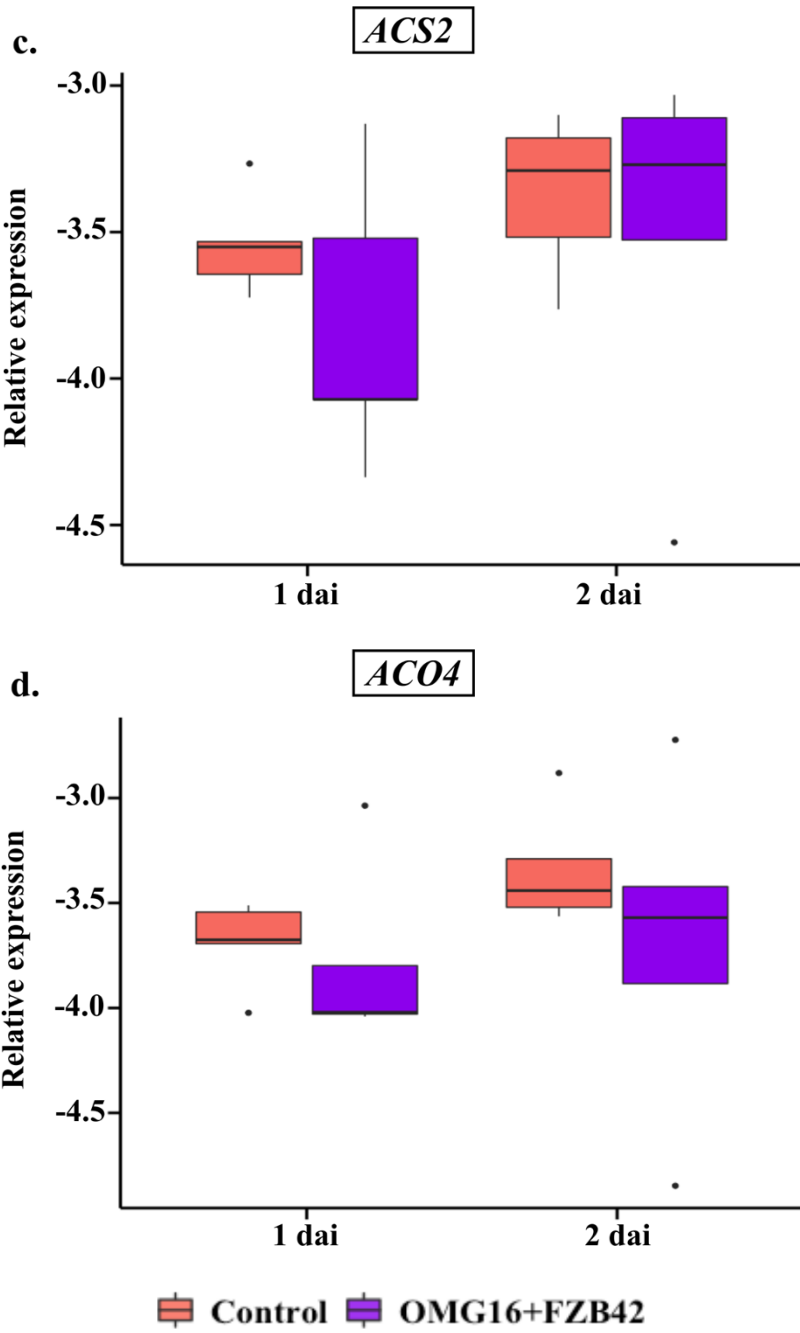
**Appendix 3.** Fluorescence microscopic images. *T. virens* hyphae expressing DsRed (a) and EGFP (b) *in vitro* on 2 days after transformation of protoplasts, colonization of rapeseed roots with OMG16 transformed with pBARGPE1-Hygro-EGFP on 7 days after inoculation (c). Arrows point to OMG16 hyphae expressing EGFP, asterisks indicate root cell walls. Scale bars, 100  $\mu\text{m}$  (a), 100  $\mu\text{m}$  (b) and 50  $\mu\text{m}$  (c).

# Expression of defence related genes upon priming in roots prior to V143 infection

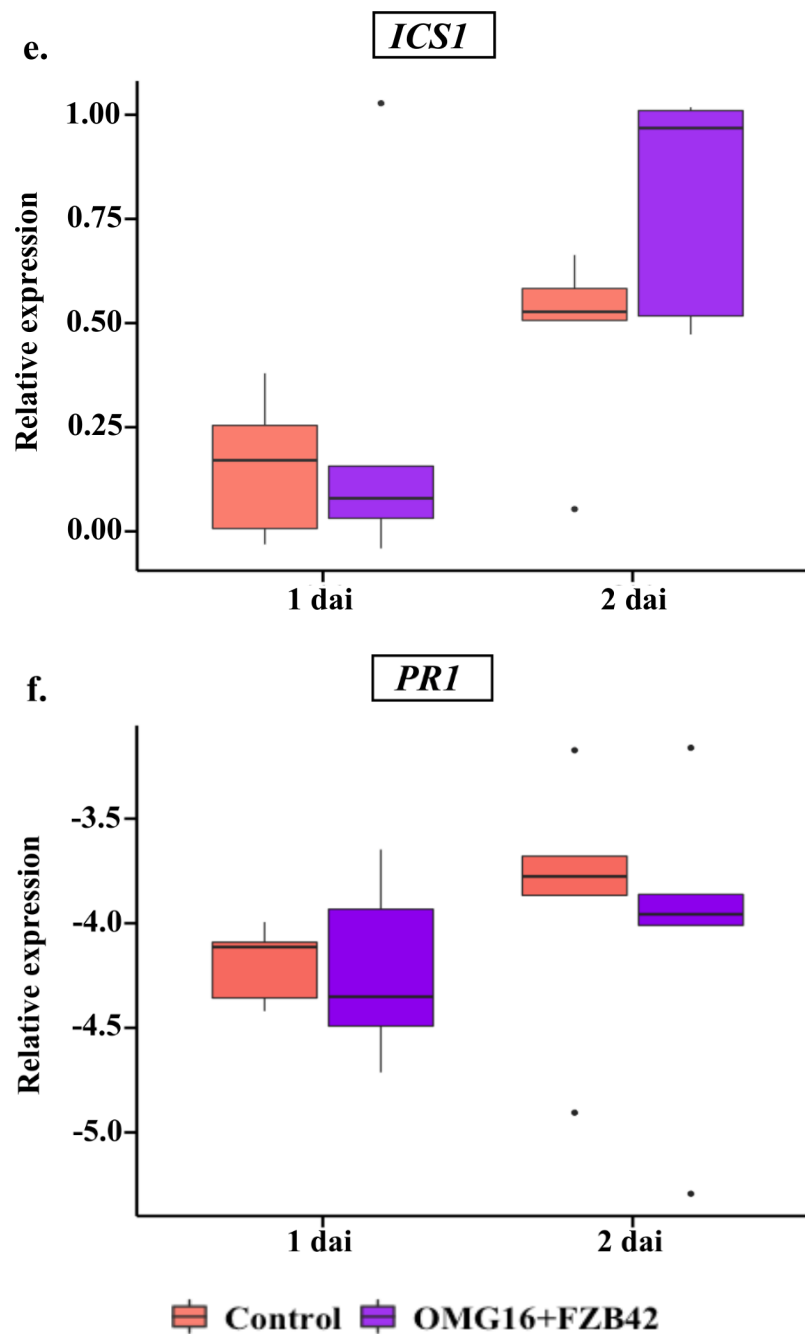
JA biosynthesis genes



ET biosynthesis genes



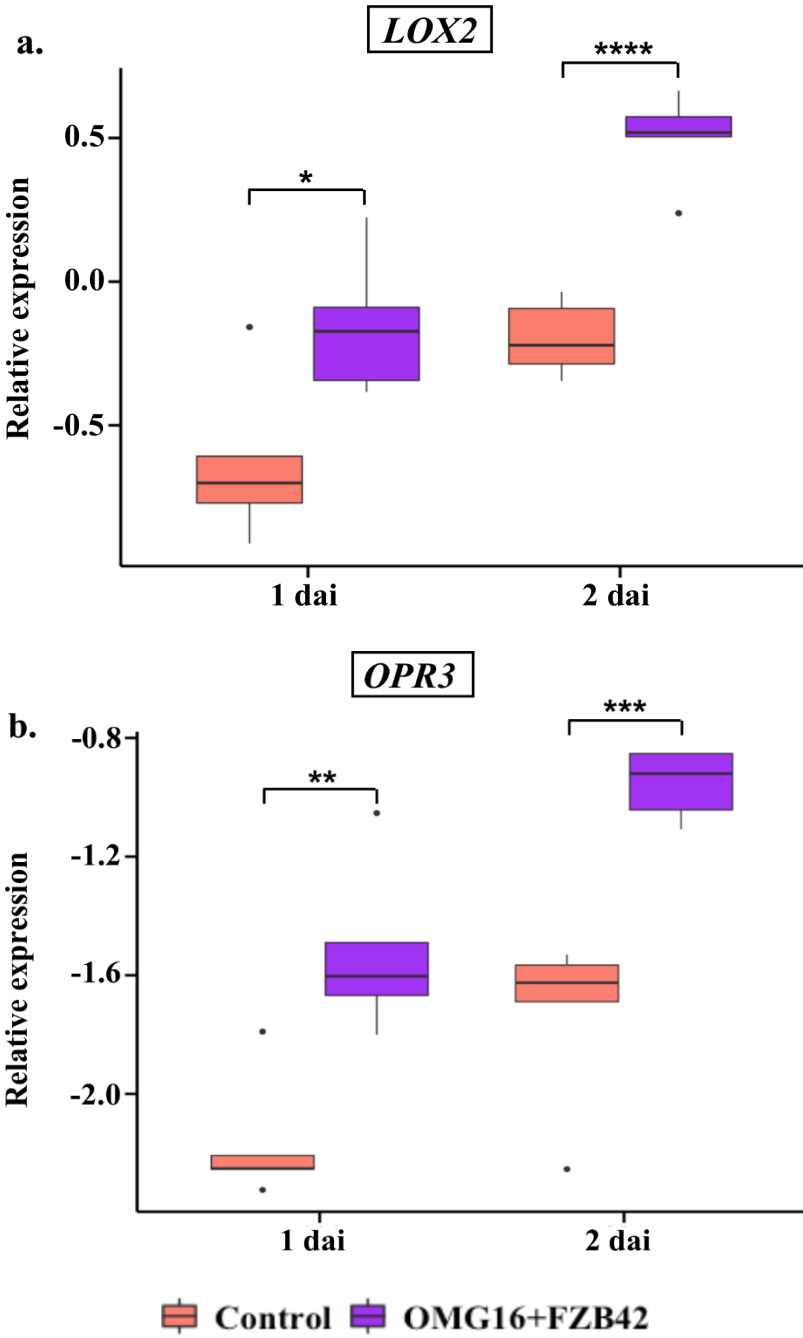
SA biosynthesis and signalling genes



**Appendix 4.** Relative expression of rapeseed defence genes *LOX2* (a), *OPR3* (b), *ACS2* (c), *ACO4* (d), *ICSI* (e) and *PR1* (f) in roots upon OMG16 plus FZB42 inoculation prior to VI43 infection. Roots of two-week-old rapeseed plantlets of the AgP4 cultivar were primed with OMG16 plus FZB42. The relative transcript abundances of the rapeseed defence genes were analysed by qRT-PCR in roots of the rapeseed plants before VI43 infection. *BnaUbiquitin11*, *BnaActin* and *BnaTubulin* were used as endogenous controls for normalization. Box and whisker plots show  $\Delta Cq$  values of five biological replicates with quadruplicate qRT-PCRs where significance of gene expression was calculated by unpaired t-test at  $P < 0.05$ . OMG16, *T. harzianum* OMG16; FZB42, *B. velezensis* FZB42; dai, days after inoculation.

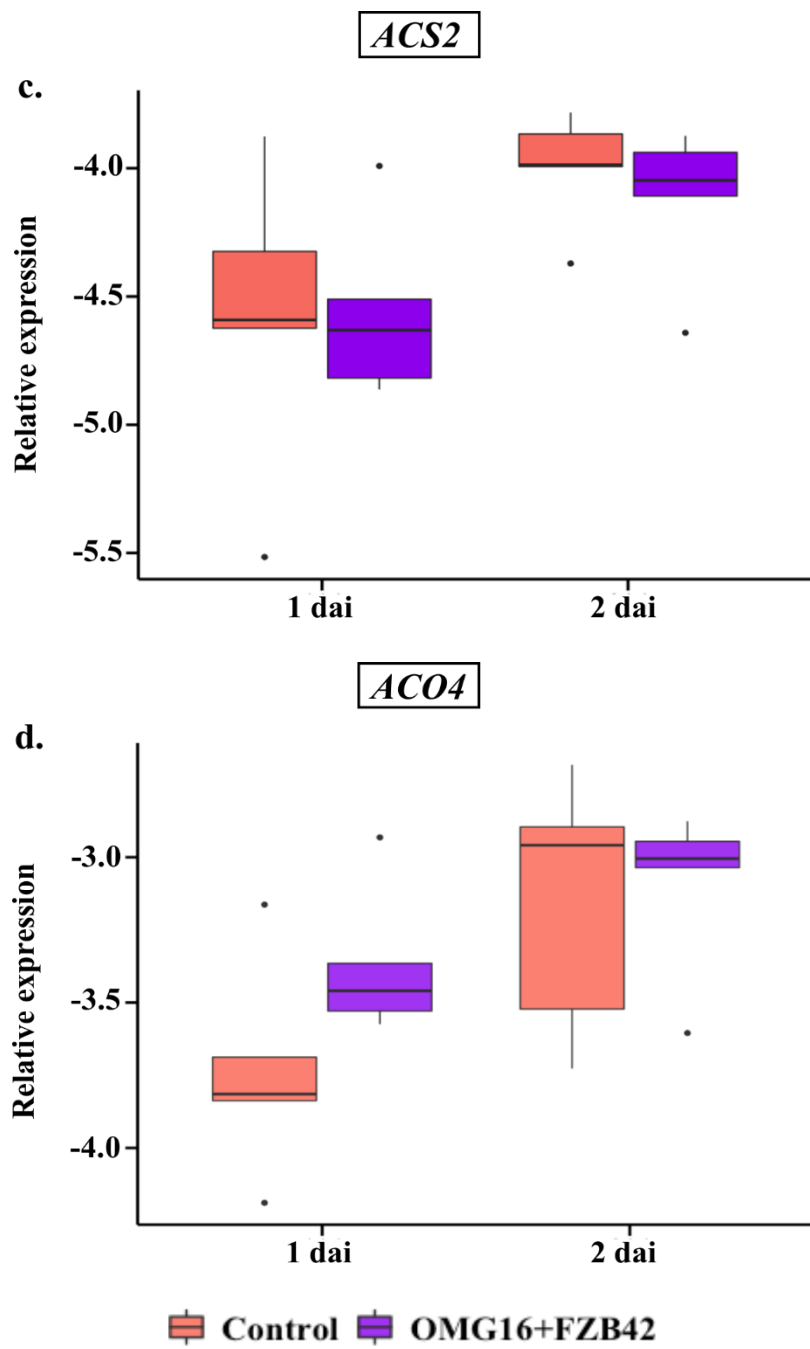
# Expression of defence related genes upon priming in stems prior to V143 infection

JA biosynthesis genes

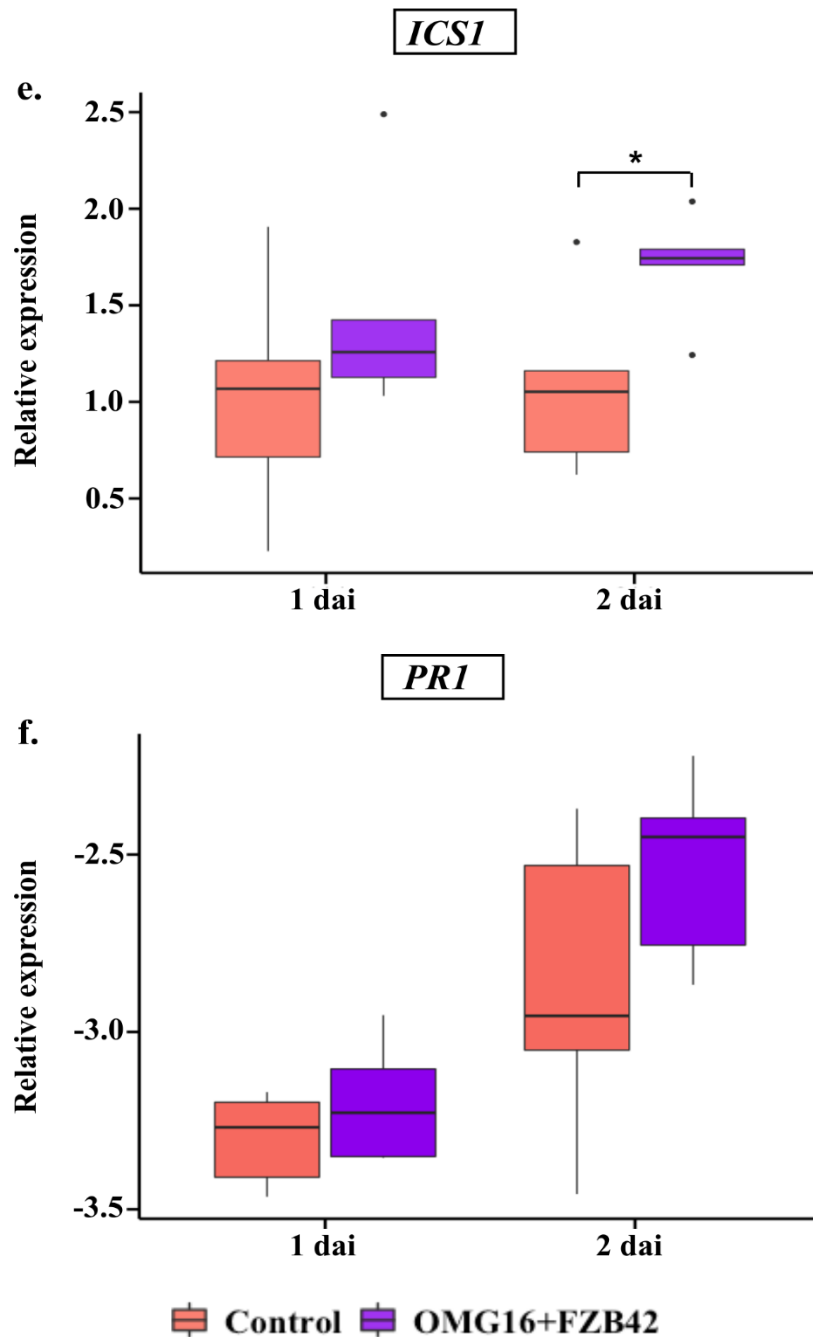




ET biosynthesis genes



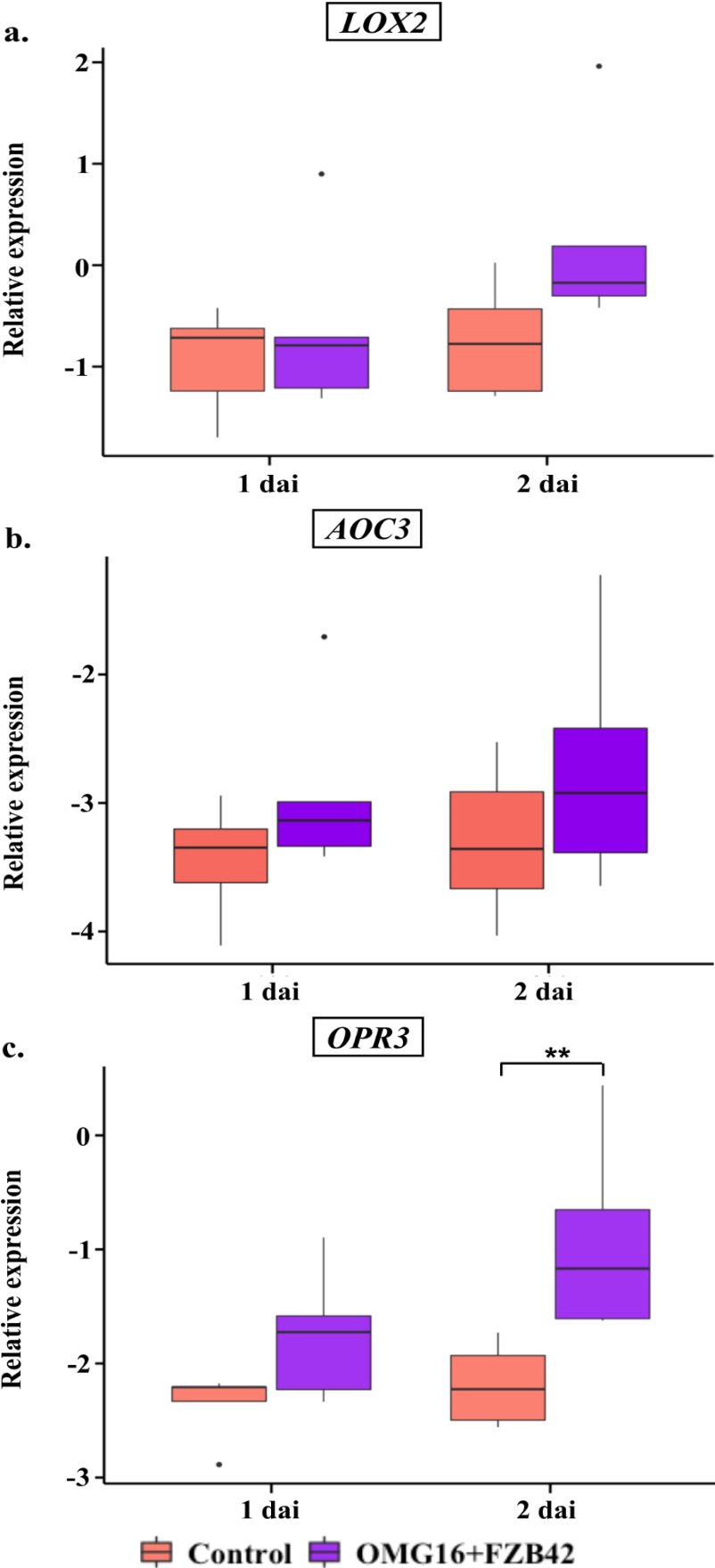
SA biosynthesis and signalling genes



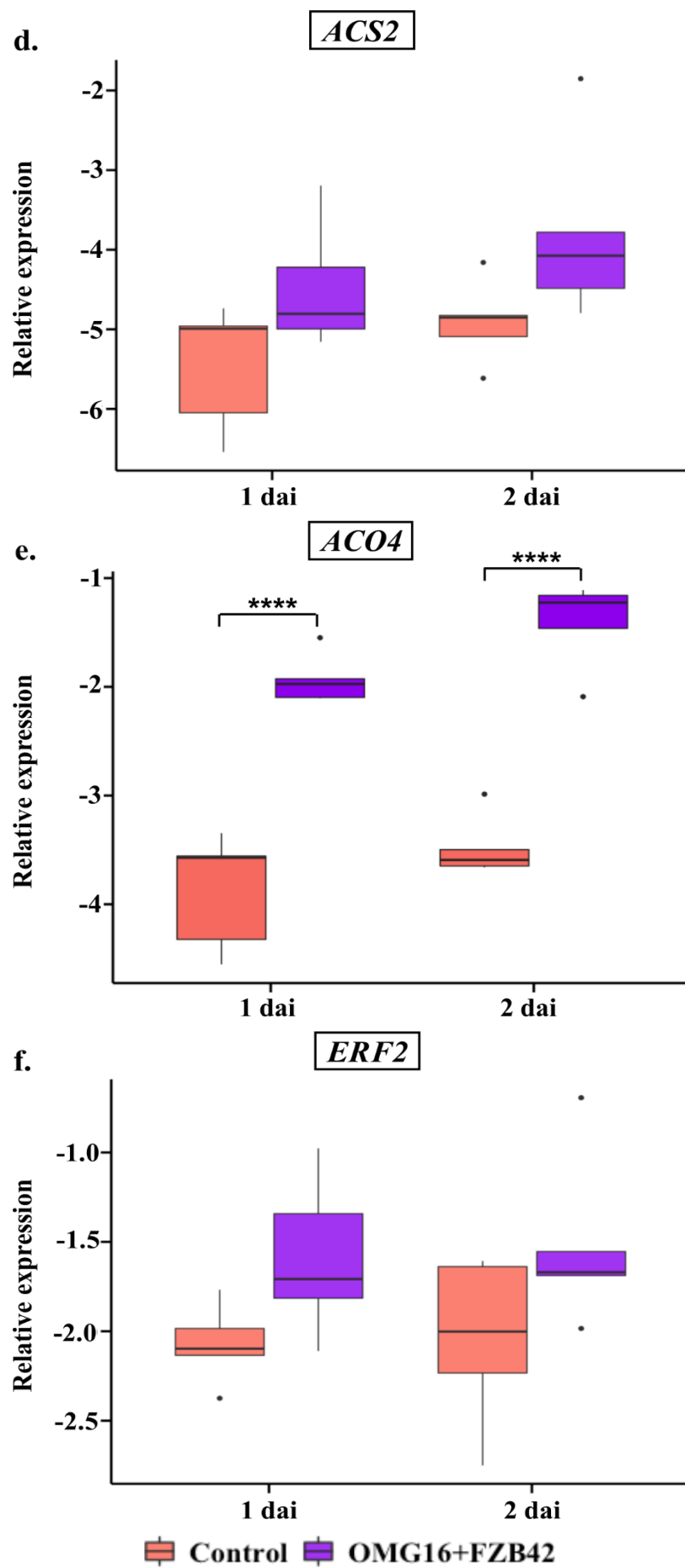
**Appendix 5.** Relative expression of rapeseed defence genes *LOX2* (a), *OPR3* (b), *ACS2* (c), *ACO4* (d), *ICSI* (e) and *PRI* (f) in stems upon OMG16 plus FZB42 inoculation prior to V143 infection. Roots of two-week-old rapeseed plantlets of the AgP4 cultivar were primed with OMG16 plus FZB42. To assess systemic responses, the relative transcript abundances of the rapeseed defence genes were analysed by qRT-PCR in stems of the same plants tested in Appendix 4 before V143 infection. *BnaUbiquitin11*, *BnaActin* and *BnaTubulin* were used as endogenous controls for normalization. Box and whisker plots show  $\Delta Cq$  values of five biological replicates with quadruplicate qRT-PCRs where significance of gene expression was calculated by unpaired t-test at  $P < 0.05$ . \*  $P < 0.05$ ; \*\*  $P < 0.01$ ; \*\*\*  $P < 0.001$ ; \*\*\*\*  $P < 0.0001$ . OMG16, *T. harzianum* OMG16; FZB42, *B. velezensis* FZB42; dai, days after inoculation.

**Expression of defence related genes upon priming in leaves prior to V143 infection**

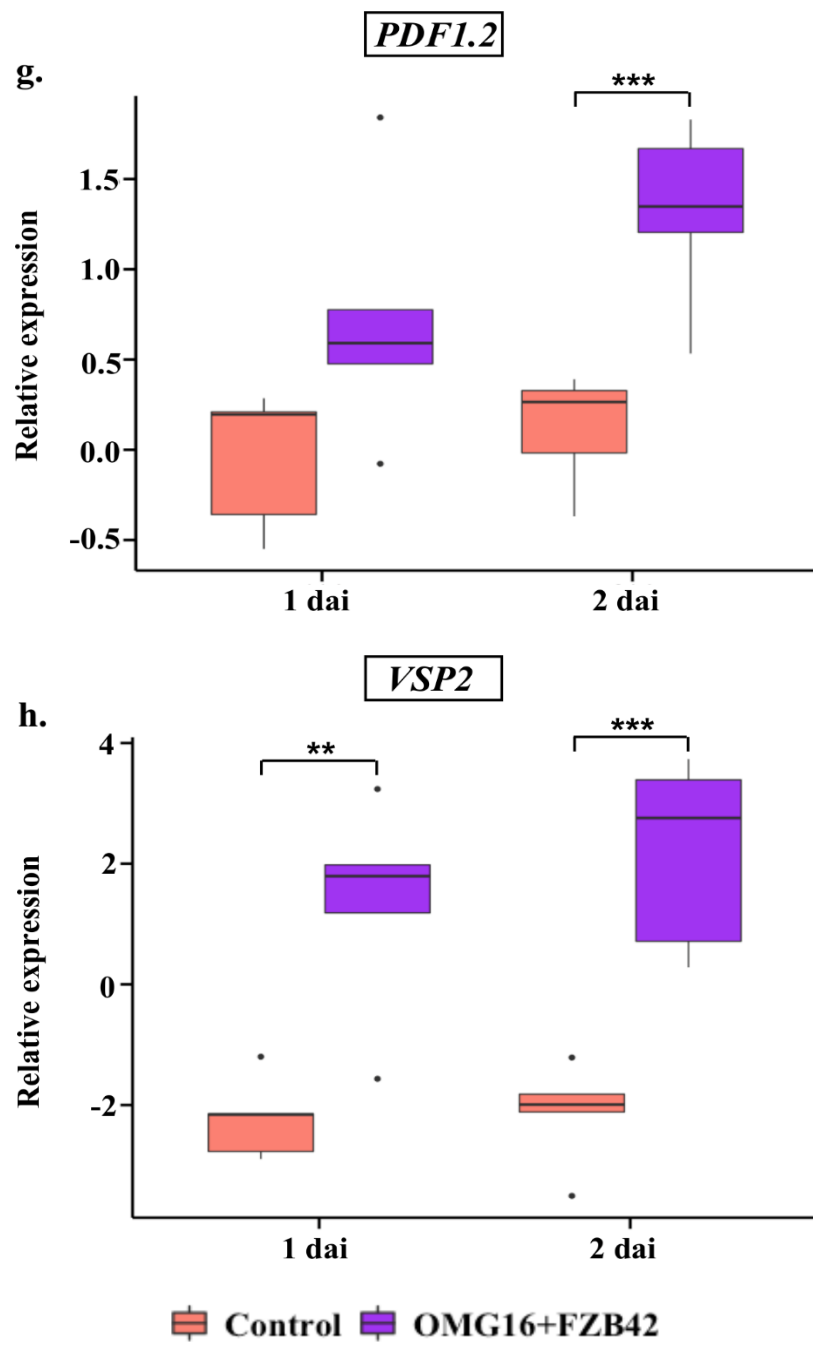
JA biosynthesis genes



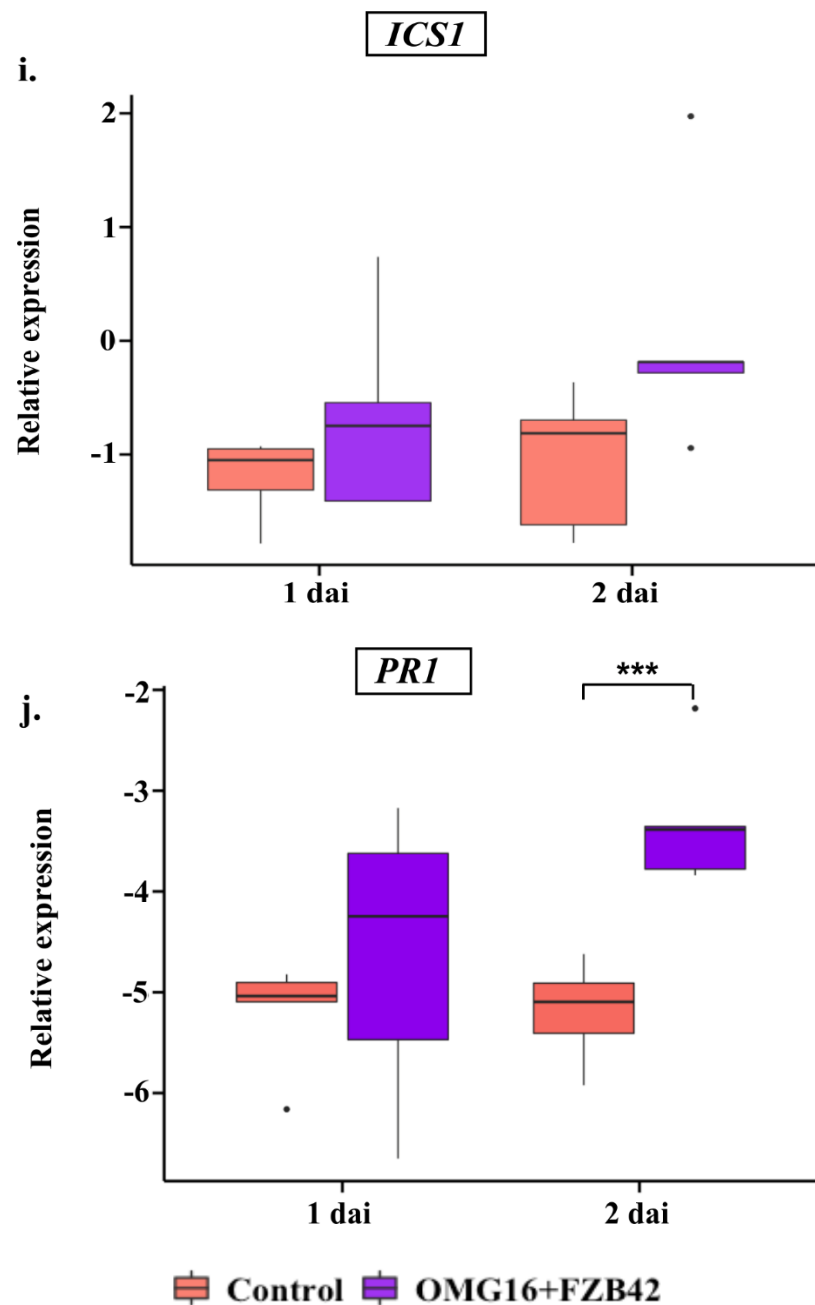
ET biosynthesis and signalling genes



JA/ET signalling genes



## SA biosynthesis and signalling genes



**Appendix 6.** Relative expression of rapeseed defence genes *LOX2* (a), *AOC3* (b), *OPR3* (c), *ACS2* (d), *ACO4* (e), *ERF2* (f), *PDF1.2* (g), *VSP2* (h), *ICS1* (i) and *PRI* (j) in leaves upon OMG16 plus FZB42 inoculation prior to VI43 infection. Roots of two-week-old rapeseed plantlets of the AgP4 cultivar were primed with OMG16 plus FZB42. To assess systemic responses, the relative transcript abundances of the rapeseed defence genes were analysed by qRT-PCR in leaves of the same plants tested in Appendix 4 before VI43 infection. *BnaUbiquitin11*, *BnaActin* and *BnaTubulin* were used as endogenous controls for normalization. Box and whisker plots show  $\Delta Cq$  values of five biological replicates with quadruplicate qRT-PCRs where significance of gene expression was calculated by unpaired t-test at  $P < 0.05$ . \*  $P < 0.05$ ; \*\*  $P < 0.01$ ; \*\*\*  $P < 0.001$ ; \*\*\*\*  $P < 0.0001$ . OMG16, *T. harzianum* OMG16; FZB42, *B. velezensis* FZB42; dai, days after inoculation.

## **Acknowledgements**

First of all, I would like to thank my research supervisor Prof. Dr. Wilfried Rozhon, Department of Agriculture, Ecotrophology, and Landscape Development, Anhalt University of Applied Sciences, Germany for his guidance, inspiration, and all the necessary facilities to attain this research work.

I would like to express my deepest sense of gratitude to Dr. Jörg Geistlinger, Department of Agriculture, Ecotrophology, and Landscape Development, Anhalt University of Applied Sciences, Germany for his constant support, constructive guidance, endless patience, co-operation during the period of research work and preparation of this manuscript.

I would also like to thank Prof. Dr. Klaus Humbeck, Institute of Biology, Plant Physiology Department, Martin-Luther-University Halle-Wittenberg, Germany for being my co-supervisor.

I specially thank to Prof. Dr. Ingo Schellenberg and Dr. Kathrin Kabrodt, Department of Agriculture, Ecotrophology, and Landscape Development, Anhalt University of Applied Sciences, Germany for providing necessary support and an excellent working environment.

I would like to thank the whole working group for the constructive cooperation and pleasant working atmosphere.

My biggest thanks go to my family for their continuous support and inspiration in every step of life.

## Curriculum Vitae

### Personal Information

**Name** Fatema Binte Hafiz  
**Date of birth** 10<sup>th</sup> February 1989  
**Place of birth** Meherpur, Bangladesh  
**Nationality** Bangladeshi  
**E-mail** fatema.hafiz@hs-anhalt.de

### Education

**2018 - present**

#### **PhD Student**

Institute of Biology, Martin Luther University, Halle-Wittenberg. Performed in Department of Agriculture, Ecotrophology, and Landscape Development, Anhalt University of Applied Sciences, Bernburg, Germany.

**Doctoral thesis:** “Root-Endophytic *Trichoderma* Fungi: Combinations with Rhizobacteria to Enhance Induced Systemic Resistance (ISR) against *Verticillium longisporum* in Rapeseed”

**04/2014 - 05/2017**

#### **Master of Science in Horticultural Science**

**University:** Technical University Munich, Germany.

**Master Thesis:** “Characterization of Malonyltransferase Activity in *planta*”

**09/2015 - 03/2016**

#### **Erasmus Exchange Semester**

**University:** Corvinus University of Budapest, Hungary.

**05/2007 - 08/2013**

#### **Bachelor of Science in Biotechnology and Genetic Engineering**

**University:** Islamic University, Kushtia, Bangladesh.

**Bachelor Thesis:** “Generation of Reactive Oxygen Species and Its Role in Ageing”

Bernburg,

Fatema Binte Hafiz



## Publications

**Hafiz, F. B.**, Moradtalab, N., Goertz, S., Rietz, S., Dietel, K., Rozhon, W., Humbeck, K., Geistlinger, J., Neumann, G., and Schellenberg, I. 2022. Synergistic effects of a root-endophytic *Trichoderma* fungus and *Bacillus* on early root colonization and defense activation against *Verticillium longisporum* in rapeseed. *Mol. Plant Microbe Interact.* 35:380-392.

**Hafiz, F. B.**, von Tucher, S., and Rozhon, W. 2022. Plant Nutrition: Physiological and Metabolic Responses, Molecular Mechanisms and Chromatin Modifications. *Int. J. Mol. Sci.* 23:4084.

Mpanga, I. K., Gomez-Genao, N., Moradtalab, N., Wanke, D., Chrobaczek, V., Ahmed, A., Windisch, S., Geistlinger, J., **Hafiz, F. B.**, Walker, F., Ludewig, U., and Neumann, G. 2019. The role of N form supply for PGPM-host plant interactions in maize. *J. Plant Nutr. Soil Sci.* 182:908-920.

## **Declaration**

### Declaration

I hereby declare that I have written this thesis independently and without external assistance other than the mentioned sources and aids being cited in this dissertation. Therefore, any extracts of external works used literally or figuratively in the present thesis are outlined and cited accordingly. I also declare that I have not applied this thesis at any other college or university in order to obtain an academic degree.

### Declaration

Erklärung Hiermit erkläre ich, dass ich die vorliegende Arbeit selbständig und ohne fremde Hilfe verfasst habe. Ich habe keine anderen als die hier angegebenen Quellen und Hilfsmittel benutzt und wörtlich oder inhaltlich entnommenen Stellen als solche kenntlich gemacht habe. Ferner erkläre ich, dass ich mich mit dieser Arbeit an keiner anderen Hochschule oder Universität um die Erlangung eines akademischen Grades beworben habe.

Bernburg,

Fatema Binte Hafiz